AD-A120 162 ARMY ENGINEER WATERWAYS EXPERIMENT STATION VICKSBURG--ETC F/G 13/2
LAKE PONTCHARTRAIN AND VICINITY HURRICANE PROTECTION PLAN. REPO--ETC(U)
JUN 82 H L BUTLER, R C BERGER, L L DAGGETT
UNCLASSIFIED WES/TR/HL-82-2-2 NL

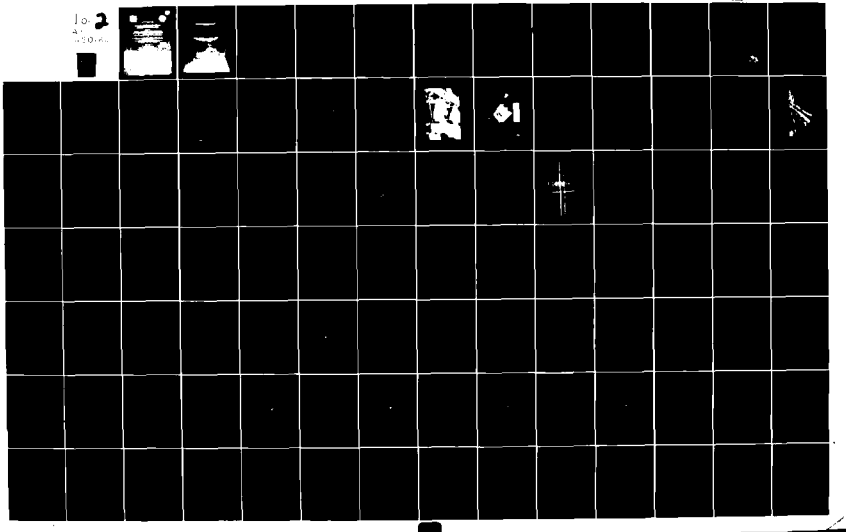

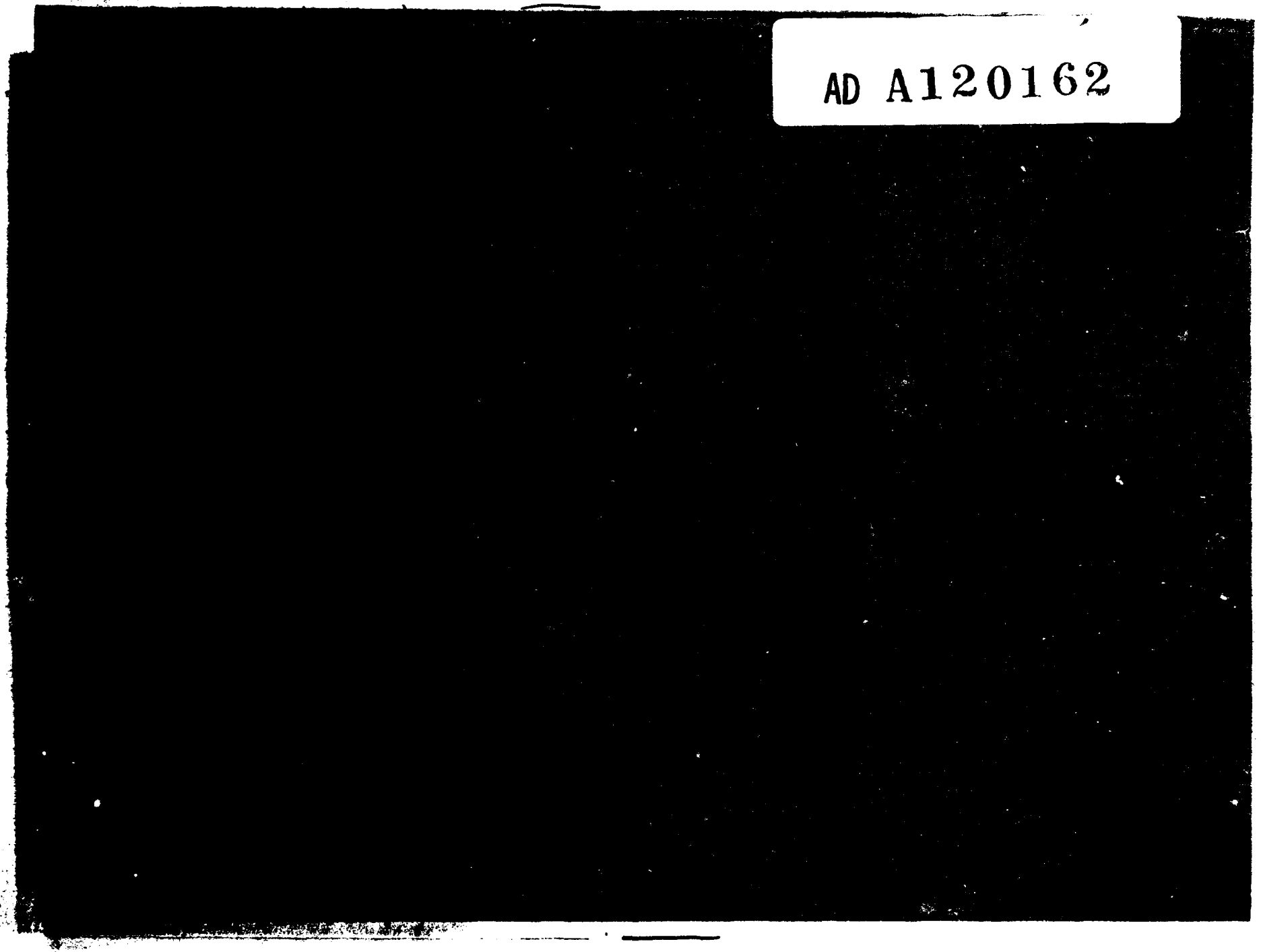

Unclassified

SECURITY CLASSIFICATION OF THIS PAGE (When Data Entered)

REPORT DOCUMENTATION PAGE

READ INSTRUCTIONS BEFORE COMPLETING FORM

1. REPORT NUMBER: Technical Report HL-82-2
2. GOVT ACCESSION NO.: AD-A120162
3. RECIPIENT'S CATALOG NUMBER:

4. TITLE (and Subtitle): LAKE PONTCHARTRAIN AND VICINITY HURRICANE PROTECTION PLAN; Report 2, PHYSICAL AND NUMERICAL MODEL INVESTIGATION OF CONTROL STRUCTURES AND THE SEABROOK LOCK; Hydraulic and Mathematical Model Investigation
5. TYPE OF REPORT & PERIOD COVERED: Report 2 of a series
6. PERFORMING ORG. REPORT NUMBER:

7. AUTHOR(s): H. Lee Butler, T. F. Berninghausen, R. C. Berger, Larry L. Daggett
8. CONTRACT OR GRANT NUMBER(s):

9. PERFORMING ORGANIZATION NAME AND ADDRESS: U. S. Army Engineer Waterways Experiment Station, Hydraulics Laboratory, P. O. Box 631, Vicksburg, Miss. 39180
10. PROGRAM ELEMENT, PROJECT, TASK AREA & WORK UNIT NUMBERS:

11. CONTROLLING OFFICE NAME AND ADDRESS: U. S. Army Engineer District, New Orleans, P. O. Box 60267, New Orleans, La. 70160
12. REPORT DATE: June 1982
13. NUMBER OF PAGES: 182

14. MONITORING AGENCY NAME & ADDRESS (if different from Controlling Office):
15. SECURITY CLASS. (of this report): Unclassified
15a. DECLASSIFICATION/DOWNGRADING SCHEDULE:

16. DISTRIBUTION STATEMENT (of this Report)

Approved for public release; distribution unlimited.

17. DISTRIBUTION STATEMENT (of the abstract entered in Block 20, if different from Report)

18. SUPPLEMENTARY NOTES

Available from National Technical Information Service, 5285 Port Royal Road, Springfield, Va. 22151

19. KEY WORDS (Continue on reverse side if necessary and identify by block number)

Chef Menteur Pass	Numerical model
Finite differences	Physical model
Hurricane barrier	The Rigolets
Inner Harbor Navigation Canal	Tidal prism
Lake Pontchartrain	

20. ABSTRACT (Continue on reverse side if necessary and identify by block number)

A comprehensive study to evaluate effects of the Lake Pontchartrain and Vicinity Hurricane Protection Plan on the tidal prism and circulation in Lake Pontchartrain, hurricane surge levels, and water quality is being conducted by the U. S. Army Engineer Waterways Experiment Station under sponsorship of the U. S. Army Engineer District, New Orleans. This report, second of a series, presents results pertinent to a detailed investigation of the three major arteries leading into the lake, namely, The Rigolets, Chef Menteur Pass, and
(Continued)

DD FORM 1 JAN 73 1473 EDITION OF 1 NOV 65 IS OBSOLETE

Unclassified

SECURITY CLASSIFICATION OF THIS PAGE (When Data Entered)

20. Abstract (Continued).

the Inner Harbor Navigation Canal.

The basic approach to simulating these passes and impact of structural alterations on the Lake Pontchartrain tidal prism can be outlined as follows:

a. Perform separate experiments with an undistorted hydraulic model of each pass with and without the proposed structure installed under steady-state conditions to quantify the hydraulic characteristics of each barrier. This is accomplished by measuring head losses across a structure for a range of water levels on the gulf side of the barrier and various flow rates.

b. Perform similar experiments with sectional numerical models (subgrids of the computational grid for the full three-lake system). The barrier effect is simulated by locally introducing the proper sill depth and by locally adjusting the flow resistance.

c. Perform similar experiments with finer scale sectional models to ensure that the computational grid resolution is adequate and that finer scale models are capable of describing the flow regime in the neighborhood of the proposed structures.

An extensive field data collection effort was undertaken to provide a data base from which known conditions could be used to calibrate and verify all of the models to be used in the study. These data are reported in the first report of this series entitled "Lake Pontchartrain and Vicinity Hurricane Protection Plan; Report 1, Collection and Analysis of Prototype Data."

A hydraulic sectional model of The Rigolets structure was built and tested in a previous study (Berger and Boland 1976) and results obtained were sufficient for the present study.

No significant problems were encountered in performing each phase of the study. Good agreement between any model and observed data was obtained. For the computational sectional model a single value of Manning's n was determined for each structure (and for each plan of operation tested for the Seabrook lock/structure complex) and found to adequately represent structure hydraulic characteristics for both flood and ebb conditions and for the entire discharge range tested. This fact permits easier implementation of a structure in a global simulation. Extreme head differences across any structure could not be maintained in either physical or numerical models, but any realistic condition could be modeled.

PREFACE

The study described herein was authorized by the U. S. Army Engineer District, New Orleans, under the general direction of Mr. F. Chatry, Chief, Engineering Division. All elements of the investigation were conducted at the U. S. Army Engineer Waterways Experiment Station (WES) during the period August 1978 to September 1981 by personnel in various divisions of the Hydraulics Laboratory under the direction of Mr. H. B. Simmons, Chief of the Hydraulics Laboratory, and Dr. R. W. Whalin, Project Manager and Chief of the Wave Dynamics Division (WDD).

The study was performed by Messrs. H. Lee Butler and T. F. Berninghausen, WDD, Dr. Larry L. Daggett, Hydraulic Analysis Division, and Mr. R. C. Berger, Estuaries Division. Numerical computations associated with this work were performed on the CYBER 176 and CRAY 1 computers located at the Air Force Weapons Laboratory, Kirtland AFB, New Mexico.

Commanders and Directors of WES during the course of the investigation and the preparation and publication of this report were COL John L. Cannon, CE, COL Nelson P. Conover, CE, and COL Tilford C. Creel, CE. Technical Director was Mr. F. R. Brown.

CONTENTS

CONVERSION FACTORS, U. S. CUSTOMARY TO METRIC (SI)
UNITS OF MEASUREMENT

U. S. customary units of measurement used in this report can be converted to metric (SI) units as follows:

Multiply	By	To Obtain
acres	4046.856	square metres
cubic feet per second	0.02831685	cubic metres per second
feet	0.3048	metres
feet per second	0.3048	metres per second
miles (U. S. statute)	1.609344	kilometres
square feet	0.09290304	square metres

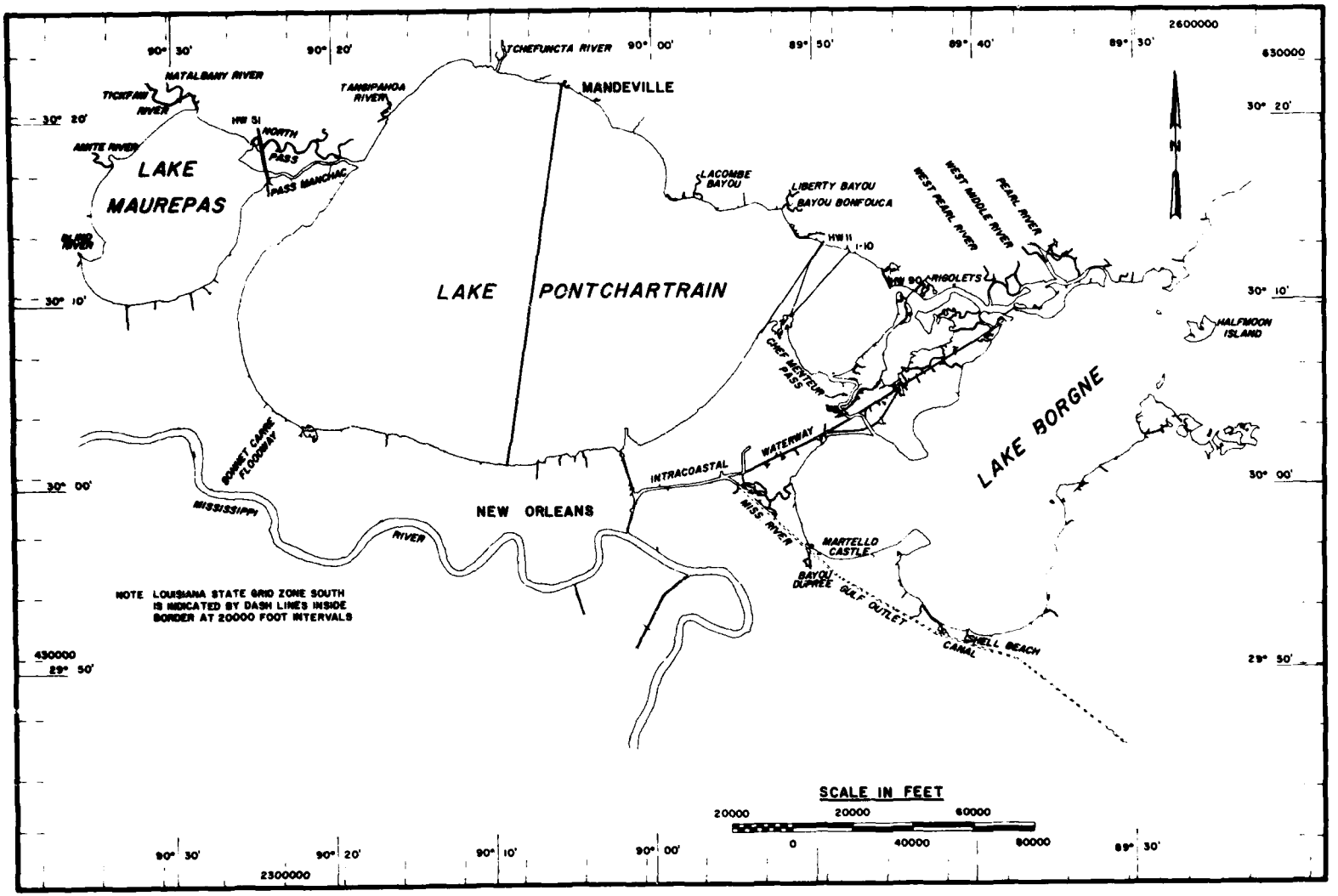

Figure 1. Vicinity map

LAKE PONTCHARTRAIN AND VICINITY HURRICANE PROTECTION PLAN
PHYSICAL AND NUMERICAL MODEL INVESTIGATION OF CONTROL STRUCTURES AND THE SEABROOK LOCK

Hydraulic and Mathematical Model Investigation

PART I: INTRODUCTION

Background

1. A comprehensive study to evaluate effects of the Lake Pontchartrain and Vicinity Hurricane Protection Plan on the tidal prism and circulation in Lake Pontchartrain, hurricane surge levels, and water quality is being conducted by the U. S. Army Engineer Waterways Experiment Station (WES) under sponsorship of the U. S. Army Engineer District, New Orleans (LMN). Results of this study are to be presented in a series of reports published under the general title "Lake Pontchartrain and Vicinity Hurricane Protection Plan." The major tool employed in the numerous investigations carried out in the course of this study is a numerical hydrodynamic model (WES Implicit Flooding Model, WIFM), developed at WES, which is capable of simulating both tidal effects and hurricane surge flooding. This report, which is the second of the series, presents results pertinent to a detailed investigation of the three major arteries leading into the lake, namely, The Rigolets, Chef Menteur Pass, and the Inner Harbor Navigation Canal.

2. One of the alternative protection plans includes a system of levees surrounding flood-prone areas to the south and east of the lake and control structures in the three passes to the lake. The key to successful modeling of the lake hydrodynamics lies in correctly simulating water flow through the passes and the impact of a hydraulic structure, i.e. a gated hurricane barrier, on that flow. Thus, the objective of this phase of the study was to calibrate and verify those parts of the Lake Pontchartrain and vicinity numerical model that represent the passes. This was accomplished by using a combination of field data,

results from undistorted physical models of the proposed barrier structures, and various numerical models of the lake and passes.

3. Lake Pontchartrain is adjacent to and just north of the city of New Orleans, Louisiana (Figure 1). The principal connections to the Gulf of Mexico are The Rigolets and Chef Menteur Passes which are natural passes, and a man-made connection through the Inner Harbor Navigation Canal (Seabrook Canal) and Mississippi River-Gulf Outlet Canal, which is a gulf-level canal. The Rigolets and Chef Menteur Passes connect Lake Pontchartrain with Lake Borgne. The Mississippi River-Gulf Outlet Canal eventually exits into the more saline Gulf of Mexico; consequently, this small canal serves as a major source of salinity for Lake Pontchartrain. In addition, Lake Maurepas is connected to the west end of Lake Pontchartrain by Pass Manchac. Lakes Maurepas, Pontchartrain, and Borgne make up the three-lake system to be modeled.

4. Gated control structures were proposed in The Rigolets and Chef Menteur Passes in concert with a planned lock and structure at the lake end of the Seabrook Canal as a part of a hurricane protection plan for the area. Figure 2 displays an enlargement of the three major passes being modeled. This plan would serve to protect areas contiguous to the shore of Lake Pontchartrain from flooding by limiting the uncontrolled entry of hurricane surges into the lake. During normal tide conditions the gates of The Rigolets and Chef Menteur control structures would remain open, allowing the passage of normal flood and ebb tidal flow. The Seabrook Lock (junction of Lake Pontchartrain and the Inner Harbor Navigation Canal) would be operated as required by navigation entering or exiting Lake Pontchartrain via the Inner Harbor Navigation Canal.

Approach

5. The basic approach to simulating the passes and impact of structural alterations on the Lake Pontchartrain tidal prism can be outlined as follows:

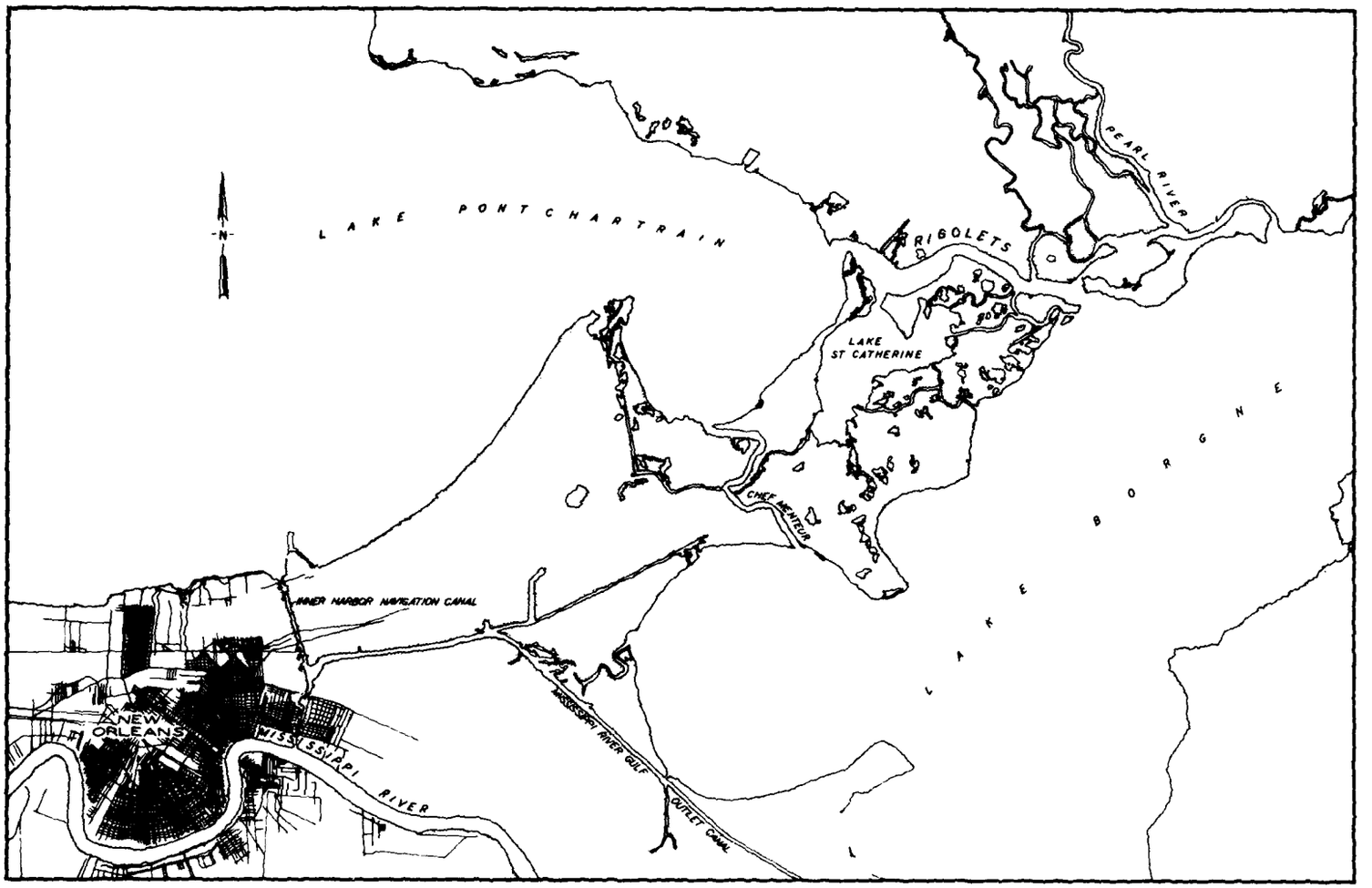

Figure 2. Site map showing The Rigolets, Chef Menteur, and Seabrook Canal

a. Perform separate experiments with an undistorted hydraulic model of each pass with and without the proposed structure installed under steady-state conditions to quantify the hydraulic characteristics of each barrier. This is accomplished by measuring head losses across a structure for a range of water levels on the gulf side of the barrier and various flow rates.

b. Perform similar experiments with sectional numerical models (subgrids of the computational grid for the full three-lake system). The barrier effect is simulated by locally introducing the proper sill depth and by locally adjusting the flow resistance. Hydrodynamic code WIFM (Butler 1980) was used for all numerical tests in this study.

c. Perform similar experiments with finer scale sectional models to ensure that the computational grid resolution is adequate and that finer scale models are capable of describing the flow regime in the neighborhood of the proposed structures.

6. An extensive field data collection effort was undertaken to provide a data base from which known conditions could be used to calibrate and verify all of the models to be potentially used in the study. The actual subset of data used in the model study is summarized in Report 1 (Outlaw 1982). These data were used in calibrating and verifying both physical and numerical sectional models. A hydraulic sectional model of The Rigolets structure was built and tested in a previous study by Berger and Boland (1976), and these results were sufficient for the present study. Since the Chef Menteur Control Structure is proposed for location in a new canal to be dredged, only plan conditions were tested.

7. Results from this investigation will provide required parameters in the global tidal prism simulations. Model adjustments made in global calibration runs will not include any variation of these parameters. The finer scale numerical models were constructed to aid in demonstrating grid insensitivity in modeling passes and to establish models which could be used in future studies involving detailed analysis of flow local to each pass.

PART II: PHYSICAL MODELS OF CONTROL STRUCTURES

Purpose and Study Approach

8. In order to quantify the hydraulic characteristics of the various proposed structures in the hurricane barrier protection plan, undistorted-scale physical models of the structures and adjacent areas were required. Undistorted-scale physical models of the Seabrook (Photo 1) and the Chef Menteur Pass (Photo 2) structures were constructed and tested. The model regions were of sufficient length to reliably produce approach and exit conditions near the structures. Experimental data acquired from these models consisted of water-surface elevations for a range of flow rates and surface-current patterns near the structures. These data provided reliable quantitative information on the head losses across these structures, and they were then used to determine the numerical model representation of the control structures.

Previous Investigations

9. Physical modeling of The Rigolets control structure was conducted in an earlier study (Berger and Boland 1976). This model (Figure 3) covered 3.2 miles* of The Rigolets Pass beginning at the Lake Pontchartrain entrance of The Rigolets. A base condition was modeled with no structure in place. A number of study plans were modeled with the final selected plan (Plan 2A-1) having only limited measurements to define improved flow conditions at the Fort Pike area. This plan was basically the same as Plan 2A (shown in Figure 3) except that the structure was relocated 250 ft closer to the center of the channel. Results from this study provided data required for calibration of the numerical representation of The Rigolets structure.

---

* A table of factors for converting U. S. customary units of measurement to metric (SI) units is presented on page 3.

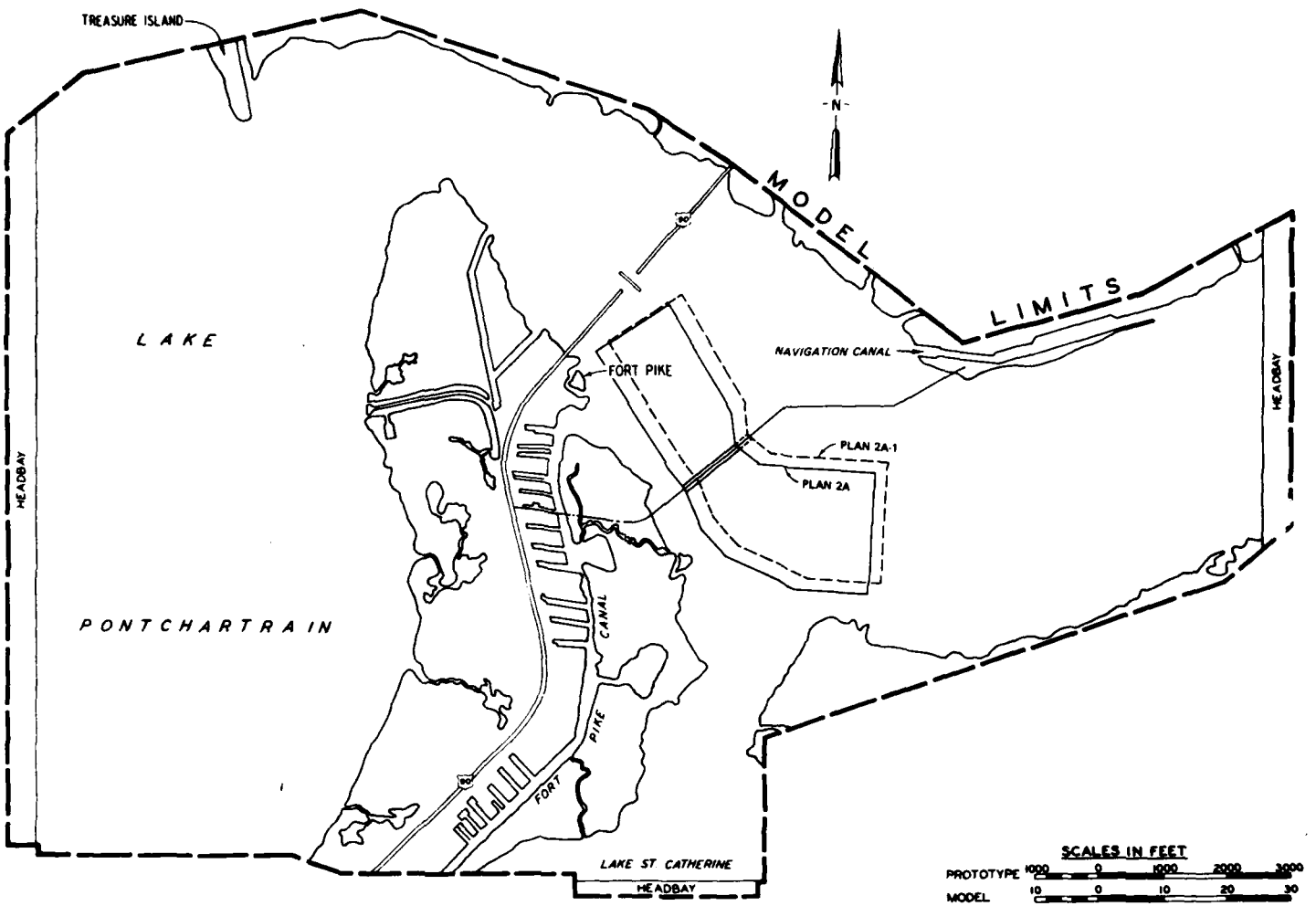

Figure 3. The Rigolets physical model with plan locations

Description

10. Testing of Seabrook and Chef Menteur Pass stuctures was performed for steady-state flows in fixed-bed, undistorted-scale models constructed within a shelter to eliminate wind effects and permit uninterrupted operation. The models were constructed of concrete, except for the structures themselves which were plastic. Linear scale ratios, model to prototype, were 1:100 horizontally and vertically. Other scale ratios were as follows: velocity 1:10, discharge 1:100,000, slope 1:1, and volume 1:1,000,000.

11. The Chef Menteur Pass model reproduced the proposed man-made channel approaches to the structure, a small portion of the natural pass, and about 390 acres of Lake Borgne (Figures 4 and 5). This model was about 120 ft long and 60 ft wide at its widest point. An assumed scoured bottom condition was used in Lake Borgne at the entrance to the proposed man-made channel. Such a condition will certainly occur in nature after construction of the structure and was considered to be much more representative of potential future prototype conditions than would an unscoured channel entrance.

12. The Seabrook model (Figure 6) reproduced about 1.5 miles of the Inner Harbor Navigation Canal and 340 acres of Lake Pontchartrain. The model was about 130 ft long and 40 ft wide at its widest point.

Appurtenances

13. Models were equipped with the necessary supply pumps and valves to allow a wide range of steady-state flow rates and water levels to be reproduced for flood and ebb directions. One pump and venturi system were used to supply and measure flow to either model. An additional pump and venturi system were used for the higher discharges on the Chef Menteur model.

14. Water-surface elevation measurements were made throughout each of these models using two types of gages. Four locations on each model were monitored using electronic water-surface elevation detectors

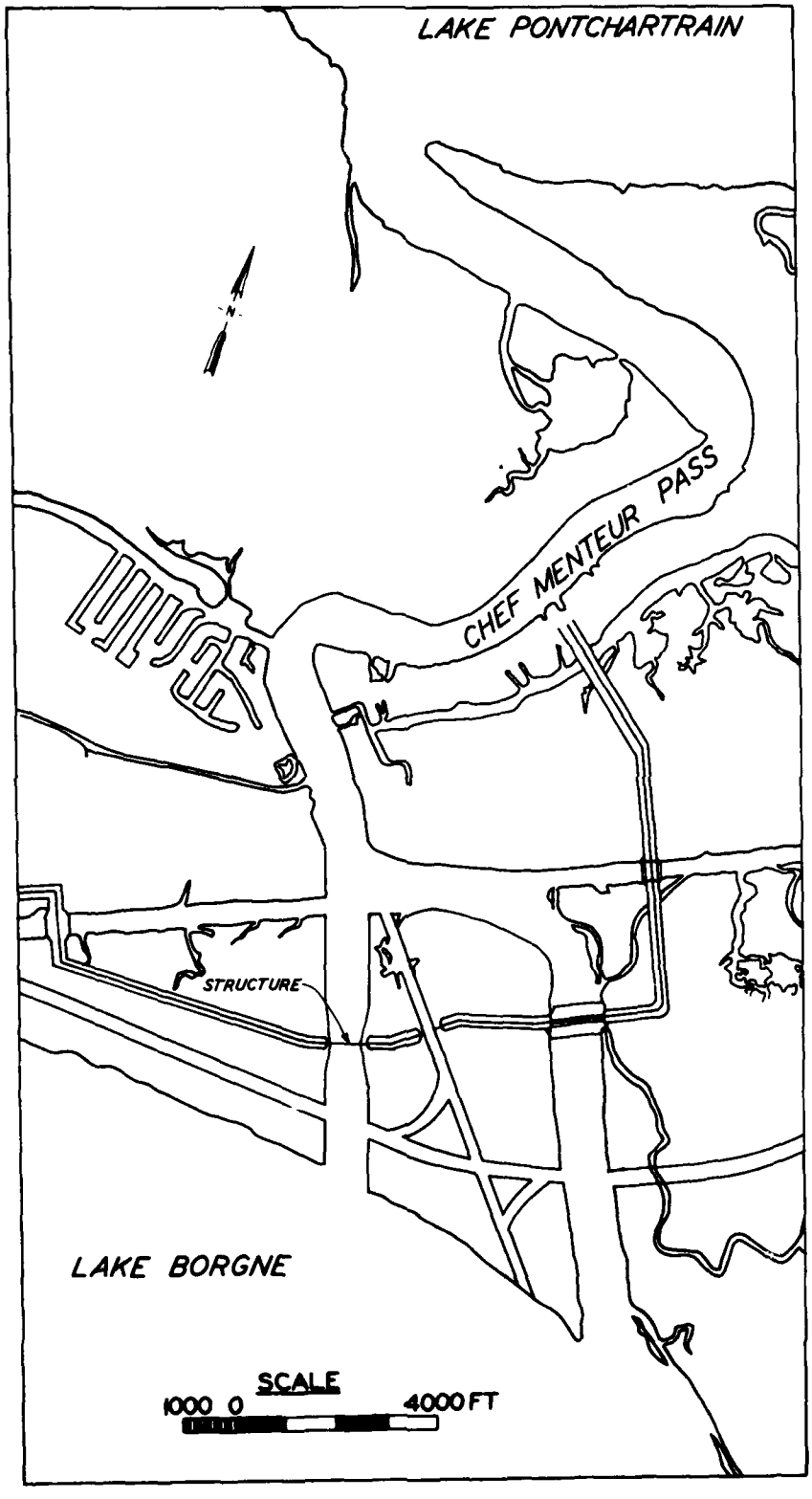

Figure 4. Chef Menteur Pass with plan location

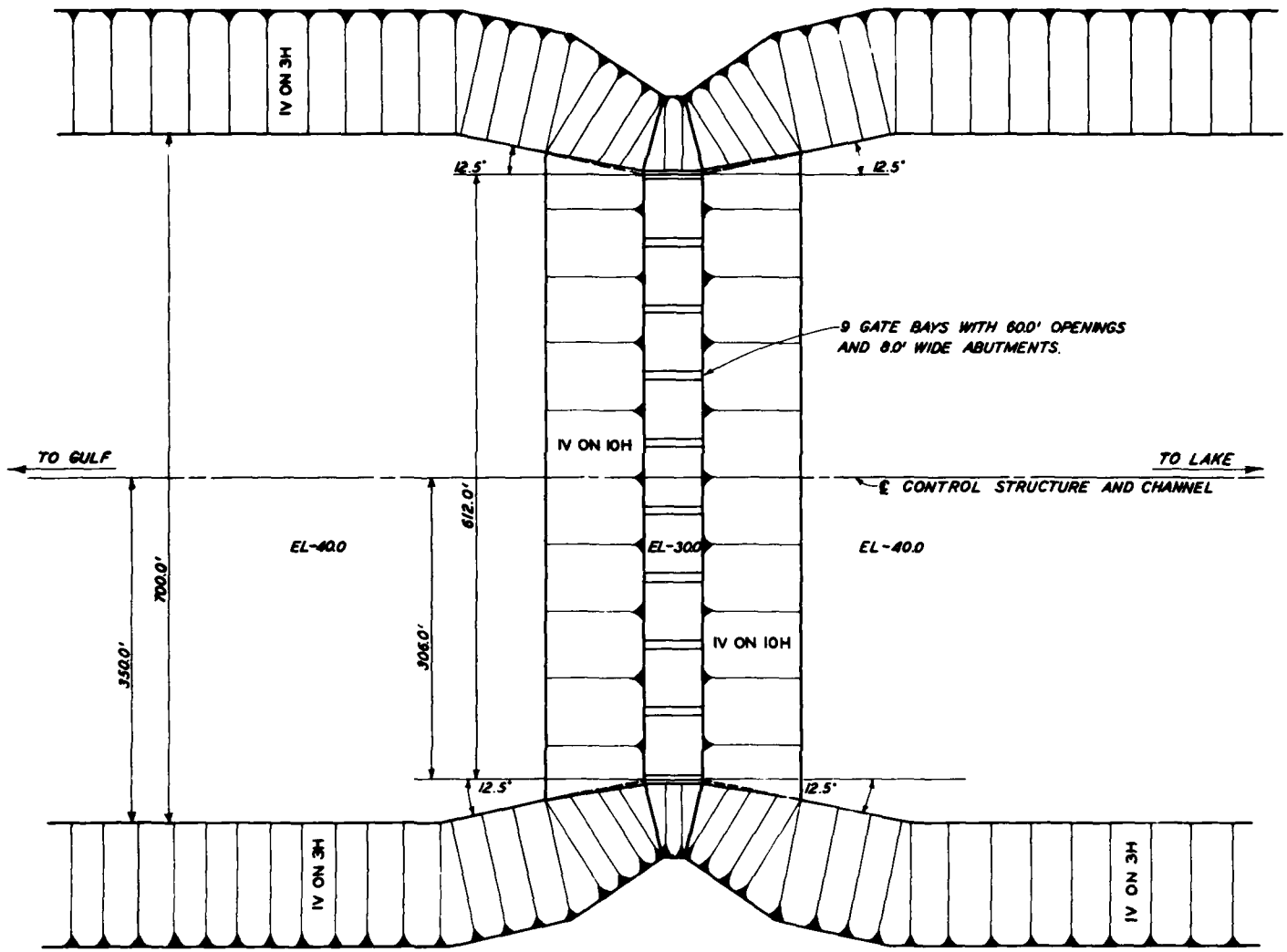

Figure 5. Chef Menteur structure

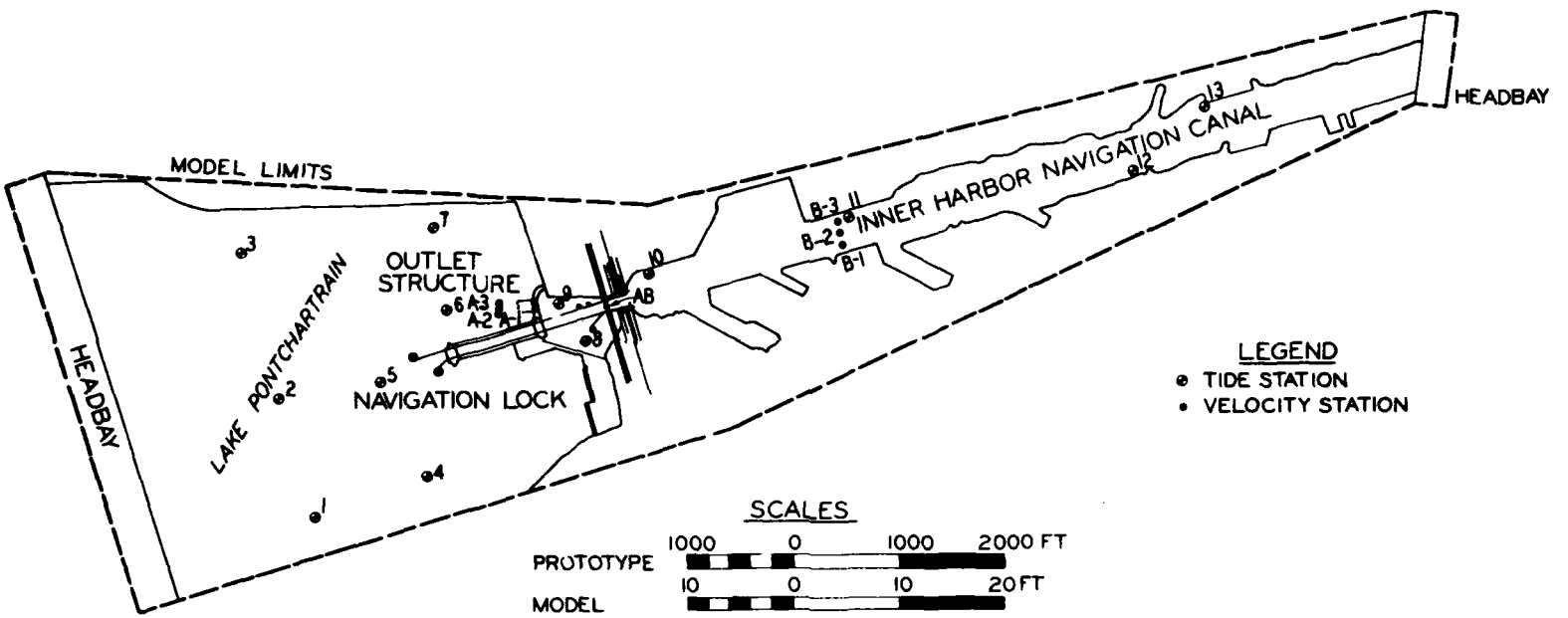

Figure 6. Seabrook physical model with plan location

(Figure 7) which employ a noncontacting capacitance probe. This detector, in conjunction with a digital readout, can detect changes in water-surface elevation of 0.0001 ft (0.01 ft prototype). The remainder of the stations were equipped with point gages. These gages with the accompanying vernier can be read directly to 0.001 ft (0.1 ft prototype).

15. Current measurements were made with miniature Price-type meters constructed of a light plastic material. These meters had five cone-shaped cups which were about 0.04 ft in diameter (4.0 ft prototype), were mounted so that the total meter diameter was about 0.09 ft (9 ft prototype), and were capable of measuring model velocities as low as about 0.03 fps (0.3 fps prototype). A meter and counter are shown in Figure 8.

Accuracy of Model Measurements

Flow measurement

16. Venturi-type flow meters used to set discharge rates are primarily subject to two error sources--the first being the sum of possible errors incurred during the calibration process and the second, the ability of the operator to set a particular manometer reading precisely. A maximum cumulative error is approximately 10 percent.

Water-surface measurement

17. The manual gage readings in these models were the average of two technicians' readings. Errors in measurement develop from two primary sources--the first being setting the gage reading to a datum ("zeroing" the gage) and the second, the actual reading of the gage (involves detection of the water surface with the gage point and reading the vernier for measurement). Errors caused by these sources were evaluated by series of runs over flow rates for four gage sites through the Chef Menteur model. An electronic and a manual gage were read at each site. Readings were made in pits that were connected to the various locations throughout the model; in this manner, disturbances in the model were effectively damped. This was the same system as was used during data collection for calibration of the structures. The electronic

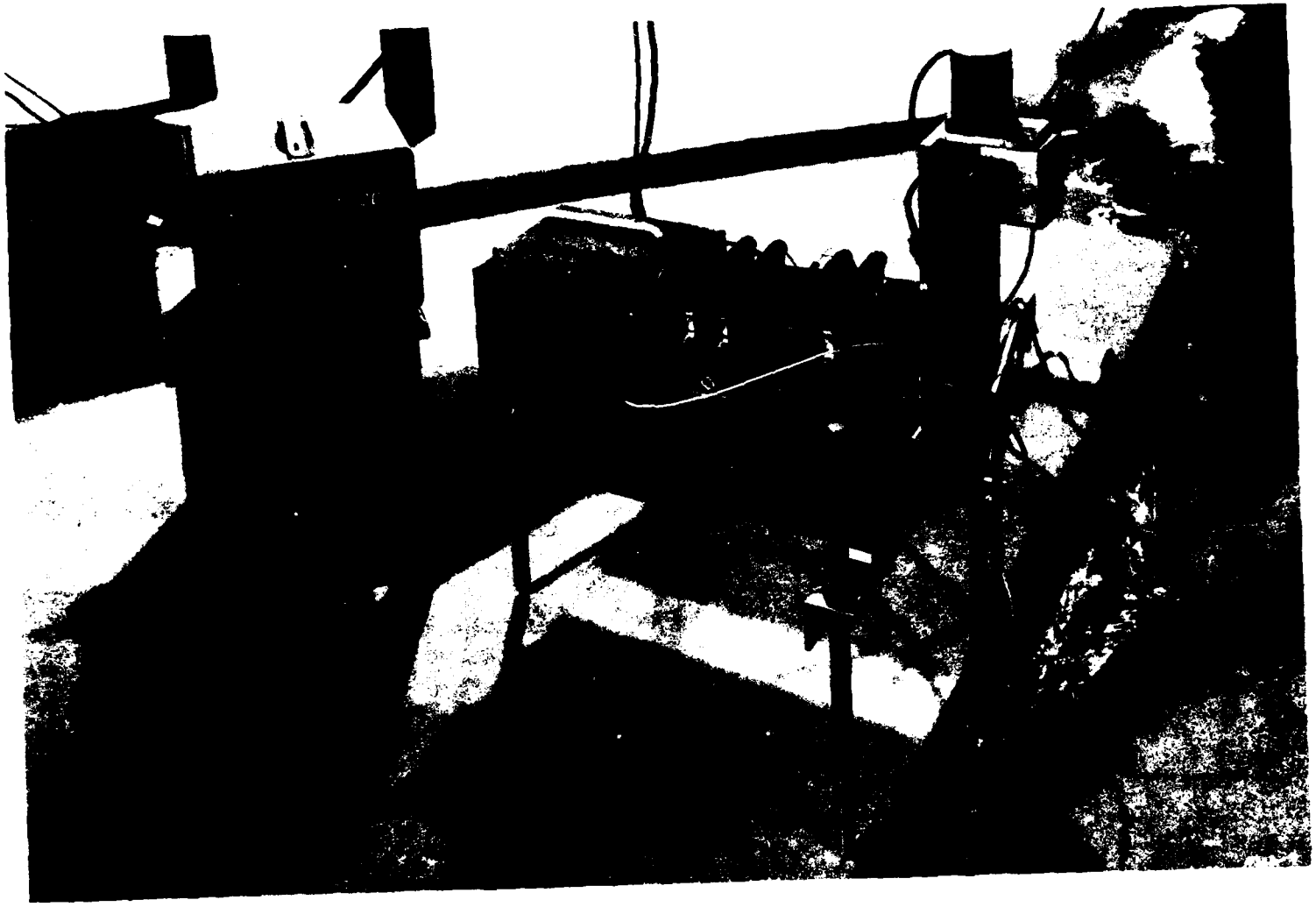

Figure 7. Electronic water-surface elevation detector

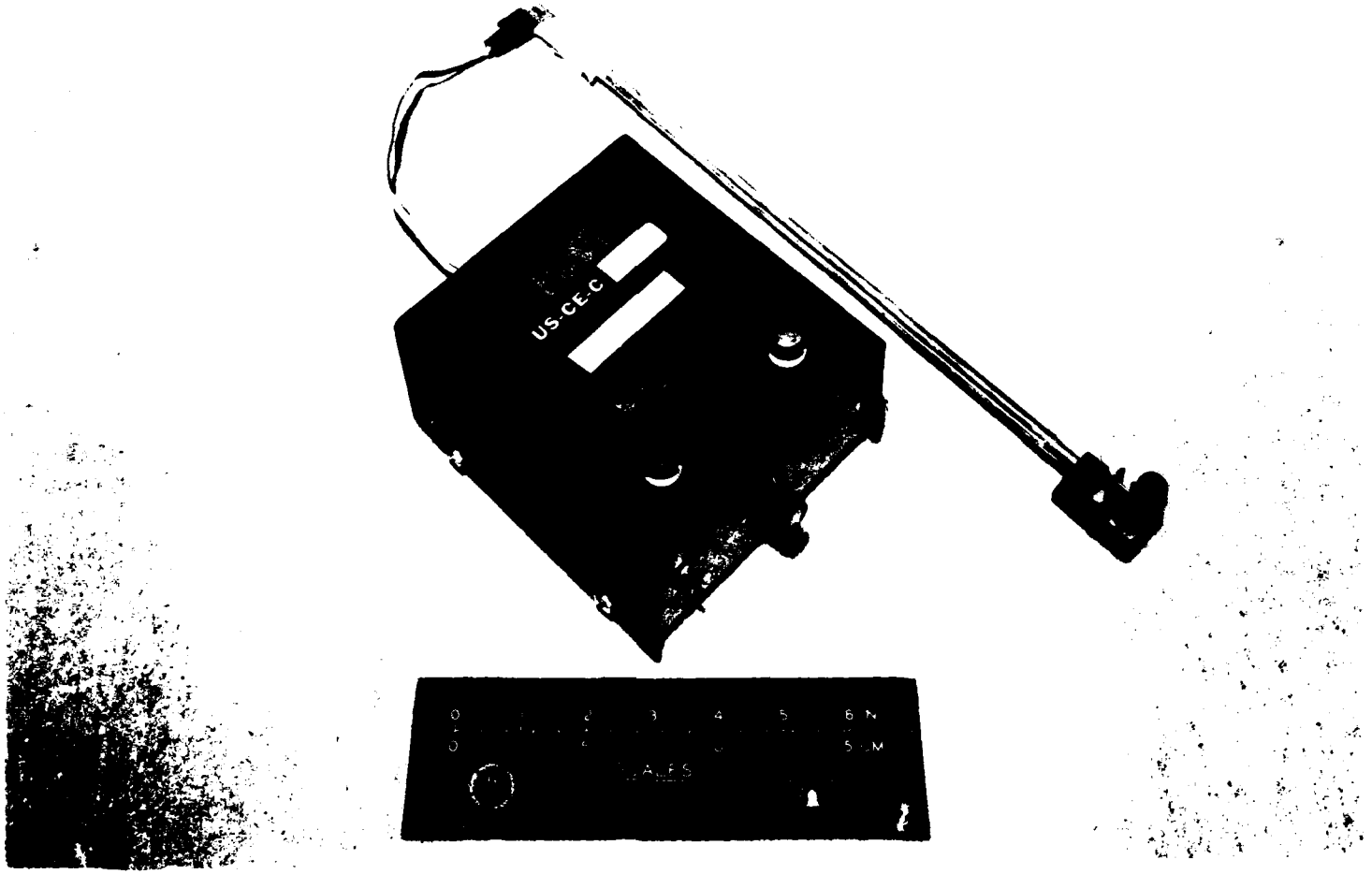

Figure 8. Velocity meter

gages were used as an aid in determining the precision of the manual gages. Results, shown in Figure 9, are for averages of two technicians' readings comparable to actual calibration data. Electronic gages were considerably more precise than manual gages. Water-surface measurements with electronic gages were displayed and subsequently recorded to 0.0001 ft (0.01 ft prototype). Normally, these gages may be confidently expected to give readings within an accuracy of ±0.0002 ft (±0.02 ft prototype).

Velocity measurement

18. Errors in measurement of model velocities may be due to a number of sources. The process of meter calibration may induce some errors due to limitations of the calibration equipment; also, generalization of the data by curve-fitting induces additional errors. The electronic counter monitors the number of light pulses in a certain length of time using a receptor that is shielded from light sources by a slit plate mounted on the shaft with the velocity meter cups. The light source remains on for a fixed length of time--30 sec in this study. The manner in which the slits are lined up with the light source and receptor when the timer is started and stopped could cause the count to be off by as much as two units, which would yield an error of about 0.1 fps (prototype). Turbulence in the model can cause readings to fluctuate and thereby not give a reliable indication of the mean velocity at a location. An evaluation of these error sources indicates that velocity measurements should be considered reliable within ±0.3 fps (prototype).

Seabrook Lock and Outlet Structure: Test Conditions and Results

Conditions

19. Testing of the Seabrook model consisted primarily of obtaining calibration data for the structure under a variety of operating conditions. The Seabrook structure consists of a navigation lock and an outlet structure (Figure 10). The outlet structure provides flow access between Lake Pontchartrain and the Inner Harbor Navigation Channel.

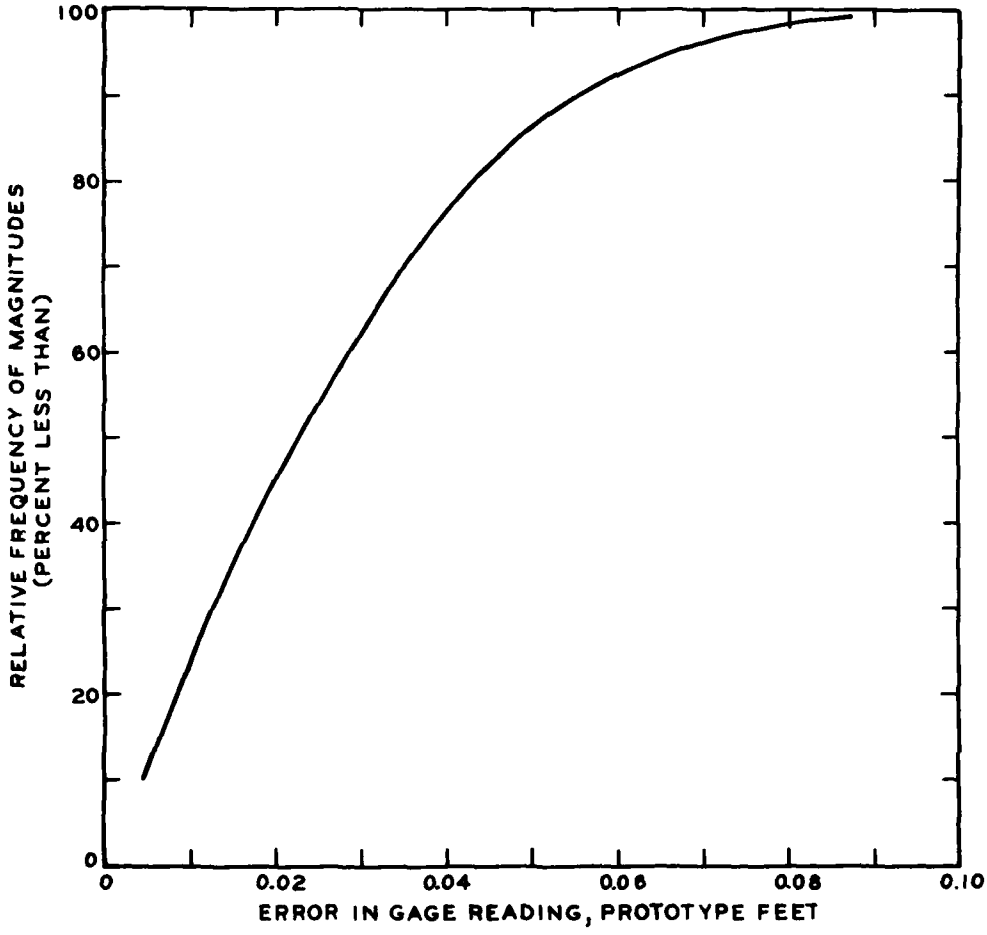

Figure 9. Precision of manual water-surface measurements

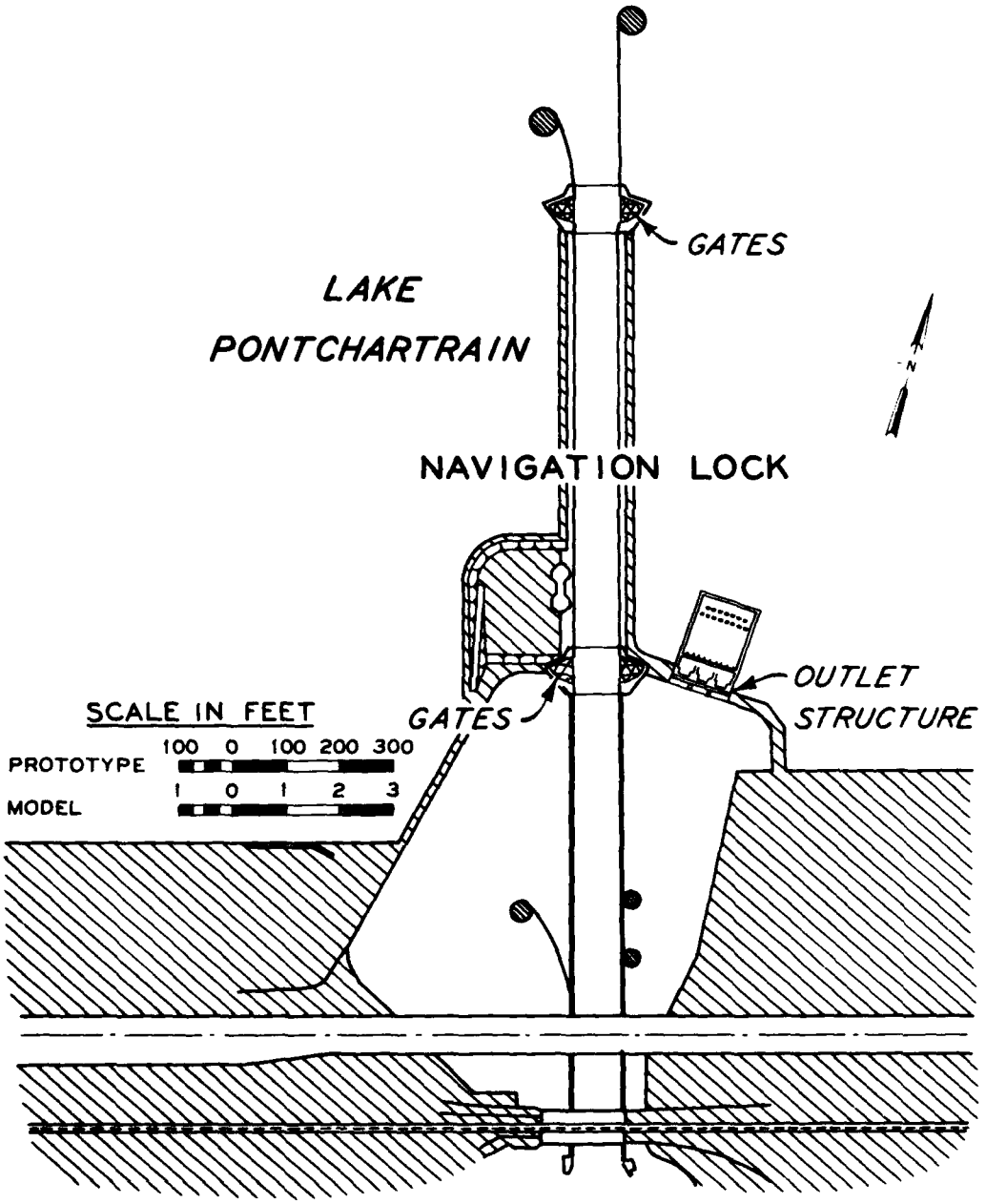

Figure 10. Seabrook Lock and structure design

Tidal flow through the Seabrook Canal is the major source of salinity for Lake Pontchartrain. The proposed outlet structure contains three gates, each of which can be opened or closed to provide an appropriate cross-sectional area to aid in regulating lake salinity. Each gate opening had a width of 32 ft with 5-ft-wide piers, and the sill elevation was -15 ft NGVD*. The navigation lock and gates totaled 946 ft in length and 84 ft in width. The sill elevation in the gate sections was -15 ft while in the lock chamber the elevation was about 1 ft deeper. A view of this structure is shown in Figure 11.

20. Operating conditions for the Seabrook structure are referred to by plan number in this report, and their designations are as follows:

Plan Designation	Navigation Lock Condition	Outlet Structure Condition
Base condition	(No structures)	
Plan 2	Gates closed	Two outside gates open
Plan 3	Gates closed	All gates open
Plan 4	Gates open	All gates open
Plan 5	Gates open	All gates closed

21. Base condition and Plans 1-4 were used to generate model data for the calibration process. Water-surface elevation data were taken at 13 stations throughout the model (gages 3, 6, 8, and 13 were electronic; the remainder were manual), as shown in Figure 6, for flow rates between 5,000 and 30,000 cfs for both flood and ebb directions. The 5,000-cfs rate served as the lower limit due to loss of equipment accuracy at lower flows and limitations imposed by scale effects. These water-surface measurements were made over a range of heights for each flow used, covering the normal range of these parameters that would occur in prototype. In the ebb direction, this meant headwater elevations between -1 and +3, while the range of headwater elevations in the flood direction was between -1 and +2. These headwater elevations

* All elevations (el) cited herein are in feet referred to the National Geodetic Vertical Datum (NGVD).

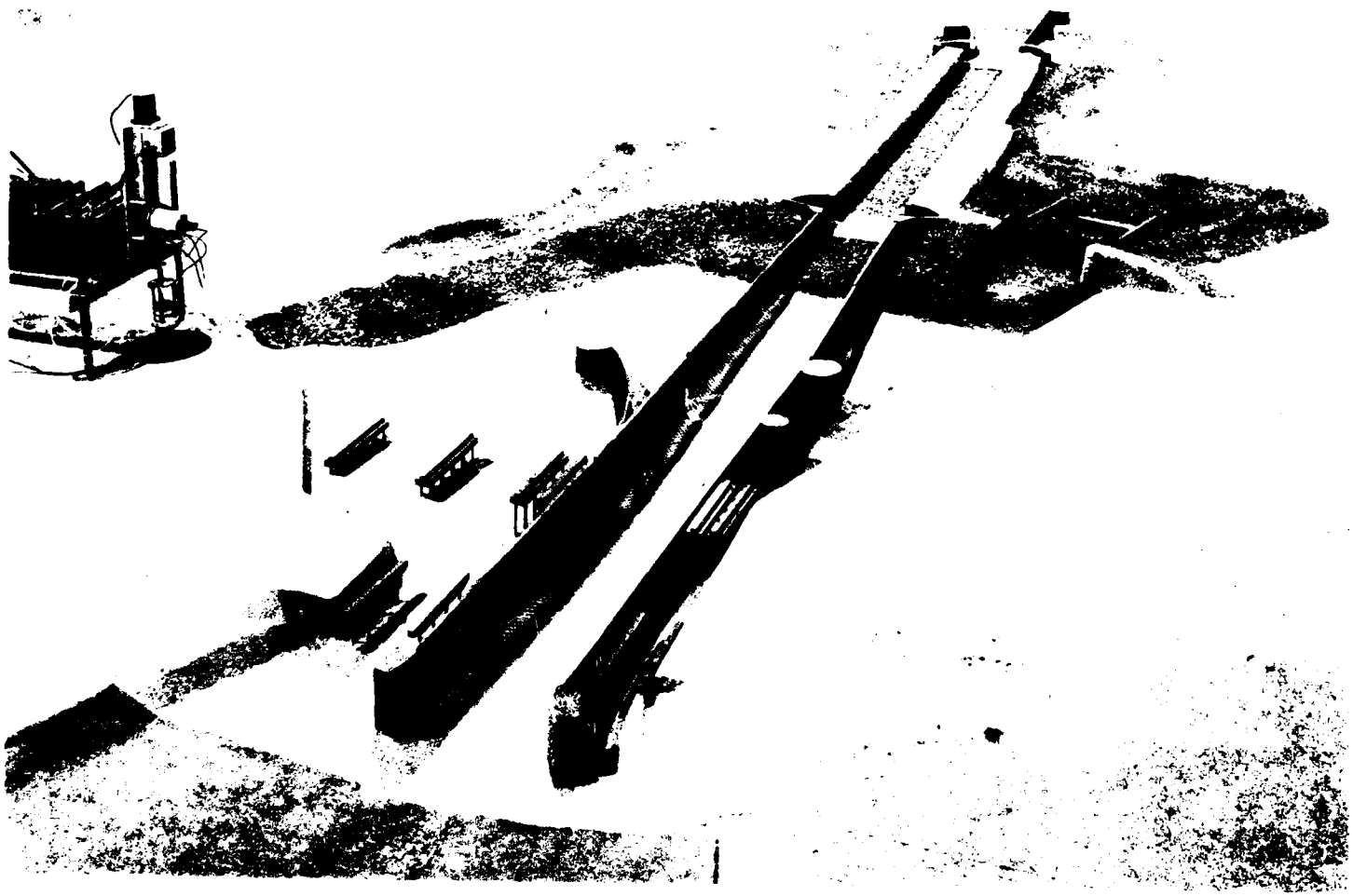

Figure 11. View of Seabrook Lock and outlet structure in physical model

were measured at sta 6 or 8 depending on the direction of flow. Water-surface data were obtained by two technicians, the final result at each gage being the average of their readings. Manual point gages were read and recorded to the nearest 0.05 ft (prototype) by interpolating readings which fell between vernier graduations. Electronic gages were read directly to 0.01 ft (prototype). The average of the two readings for each gage was rounded to the nearest 0.01 ft.

22. Velocity measurements were made at each flow rate of the +1 headwater elevation condition at seven stations for three depths (surface, middepth, and bottom). Due to the size of the velocity meter itself, the center line of the meter cups was submerged about 3 ft (prototype) for a surface reading and 5 ft above the bottom for a bottom reading.

23. Plan 5 was used to determine velocity magnitudes through the lock. Velocities were measured at nine stations (sta B1-B3, A3, plus five stations in the lock shown in Figure 12) for headwater elevations of +1 and +3 and flow rates of 5,000 and 10,000 cfs for both ebb and flood conditions. Water-surface elevations were measured at the same stations as were taken for the other operating conditions (Plans 1-4).

24. Surface current photographs were made for the base conditions by using a 3-sec exposure of confetti on the water surface. The length of each streak minus its width is proportional to the current velocity, which may then be scaled. Shortly before the end of the exposure period a strobe was flashed that created a dot near the end of each streak indicating the direction of flow. Comparison of surface velocity ascertained from these photographs and those at the same location given by velocity meter readings will not be identical since the velocity meter results were obtained about 3 ft below the water surface. Also, velocity values from the photographs result as the confetti is transported, so the velocity obtained is a spatially averaged value over the streak length. Base condition photographs were made for flow rates of 15,000 and 30,000 cfs at a headwater elevation of +1 in both ebb and flood directions. Surface current photographs of Plans 2-4 were taken under the conditions shown below for both flood and ebb directions:

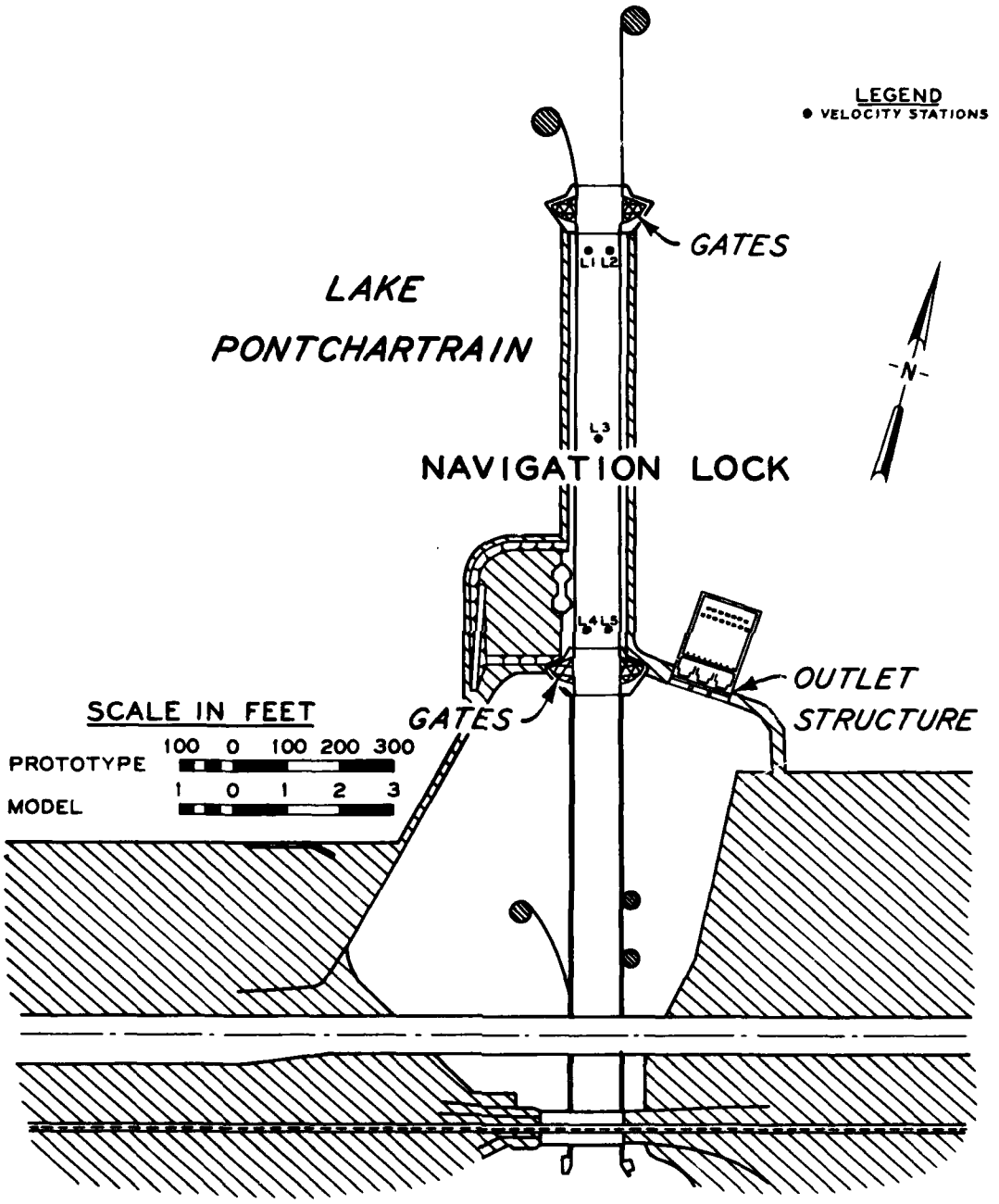

Figure 12. Additional stations for velocity measurements in the Seabrook Lock

Plan Designation	Flow Rate cfs	Headwater Elevation ft NGVD	Exposure Time sec
2	5,000	+1	3 and 9
3	5,000	+1	3 and 9
	10,000	+1	3 and 9
4	5,000	+1	3 and 9
	10,000	+1	3 and 9
	15,000	+1	3 and 9

Results for base tests

25. The primary model data (water-surface elevations and velocities for a range of discharges) were acquired for the base condition to aid in calibration of the numerical model. These data were obtained for all the conditions described previously and are shown in Tables 1-5.

26. Surface current patterns for base conditions, using a 3-sec time exposure, are shown in Photos 3-6. In the ebb direction, flow approaches the canal more rapidly along the sides of the lake than in the center. In the flood direction, the navigation canal discharges into the lake and a relatively high velocity continues in a direction traversing the lake. This relatively high-velocity stream was flowing in a direction deflected westerly from the canal entrance. East of the stream, a large clockwise gyre was present and many smaller gyres were noted west of the stream in the lake. The artificial western model boundary and particulary the headbay in Lake Pontchartrain (for introducing and extracting flow from the model) could be responsible for some of the flow patterns exhibited. Therefore, extrapolation of those details of current flow to prototype is of limited usefulness. Reliability of such flow characteristics was not required to meet the study objectives.

Results for Plan 1

27. Data obtained for calibration of the numerical model were originally planned to cover the range of normal water levels generally between -1 and +3. For the minimum flow that could be run reliably in this model (5,000 cfs prototype) a headwater condition of +3 or below headwater elevation. Water-surface elevations on the tailwater side of

the structure were not unique values corresponding to particular headwater elevations; and for the same flow rate and headwater elevation, a range of tailwater results could be established. Water-surface elevations for 5,000 cfs were taken for the minimum obtainable headwater elevation (Table 6).

Results for Plan 2

28. Water-surface elevations were taken over the complete range of planned headwater elevations, and velocity measurements were made at the +1 headwater elevation for flows of 5,000, 6,250, and 7,500 cfs and are shown in Tables 7-11. The minimum obtainable headwater for a flow of 8,750 cfs was +0.98 in the flood and +0.45 in the ebb direction. However, for a flow of 10,000 cfs, no velocities were collected as the minimum headwater was +2.08 flood and +2.20 ebb.

29. Surface current photographs were taken for a discharge of 5,000 cfs in both ebb and flood directions for a headwater elevation of about +1; results are shown in Photos 7-10. Flood flows into the lake through the outlet structure curve toward the navigation lock and flow out into the lake very nearly parallel with the lock. Two large gyres appear in these photographs. One gyre exhibits a clockwise motion above the navigation lock extending back to the outlet structures and the other gyre is counterclockwise below the navigation lock and extends to the edge of the locks protrusion into the lake. Surface flow patterns in the ebb direction show a fairly smooth flow toward the outlet structure. Most of the flow appears to be diverted toward the outlet structure gate nearest the lock.

Results for Plan 3

30. A complete set of water-surface elevations and current velocity data were obtained for flows of 5,000, 7,500, 10,000, and 12,500 cfs. Also, for a flow rate of 15,000 cfs, water-surface elevations were taken for two headwater elevations in the flood direction and three in the ebb direction. The minimum obtainable headwater at this flow rate was +1.43 in the flood and +1.21 in the ebb direction. These data are listed in Tables 12-16. Surface current photographs were made for flow rates of 5,000 and 10,000 cfs for both ebb and flood direction at a

headwater elevation of about +1; results are shown in Photos 11-18. Flow patterns were similar to those of Plan 2. However, at the higher flow in flood direction, a clockwise gyre was evident below the navigation lock.

Results for Plan 4

31. Complete sets of calibration data were taken for flow rates of 5,000, 10,000, 15,000, and 20,000 cfs. Water-surface elevation data for three headwater conditions in the flood direction and four in the ebb were taken at a flow rate of 25,000 cfs. The minimum headwater elevations obtained for this flow were +0.17 flood and +0.44 ebb. Velocity data were obtained for the +1 headwater condition for these flows. Water-surface elevation data were obtained for a flow rate of 30,000 cfs for one headwater condition in the flood direction and two headwater conditions in the ebb direction. The minimum obtainable headwater was +1.84 flood and +2.06 ebb. All of these calibration data are contained in Tables 17-22. Accurate readings of water-surface measurements on the tailwater side of the structure for flow rates of 25,000 and 30,000 cfs were difficult due to oscillations of the water surface emanating from the navigation lock. These oscillations were probably due to the unstable flow in the lock which was near critical flow conditions. Surface current photographs were obtained for 5,000, 10,000, and 15,000 cfs for both directions at a headwater condition of +1. These results were similar to previous plan results and are shown in Photos 19-30.

Results for Plan 5

32. Testing of this plan did not involve taking calibration data since this was not considered a potential operating condition. Measurement of the velocities in the lock was the actual purpose. Velocities in the lock, as well as at four stations (Figure 12) in the navigation channel, were measured for discharges of 5,000 and 10,000 cfs in both directions. Water-surface elevation data also were obtained for these conditions. Headwater elevations at which data were obtained were about +1 and +3 for 5,000 cfs and +3 for 10,000 cfs. These data are shown in Tables 23 and 24.

33. At sta L3, in the center of the lock, the maximum velocities in the flood direction were 6.2 and 5.1 fps for headwater elevations of about +1 and +3, respectively. The difference in water levels across the structure (sta 11 to 2) were 1.36 and 0.90 ft for headwater elevations of +1 and +3, respectively. In the flood direction for a flow rate of 10,000 cfs and a headwater elevation of about +3, the maximum velocity at this station was 10.8 fps while the difference in water levels across the structure was over 7 ft. In the ebb direction, the maximum velocities at this station for a discharge of 5,000 cfs were 6.7 and 5.1 fps for headwater elevations of +1 and +3, respectively. The differences in water levels across the structure were 1.21 and 1.07 ft, respectively. At a flow rate of 10,000 cfs with a headwater of +3, the maximum velocity at sta L3 was 9.4 fps and the difference in water levels was 5.28 ft. The minimum discharge for which reliable model data could be acquired was 5,000 cfs due to equipment limitations and scale effects. The discharge rate of 10,000 cfs results in velocities and water-surface elevations beyond what was considered the normal range.

Chef Menteur Pass Barrier Structure: Test Conditions and Results

Test conditions

34. Water-surface measurements were made at 16 locations (Figure 13) throughout the model. Sta 2, 3, 6, and 7 were monitored with electronic water-surface detectors; the remainder of the stations were equipped with manual point gages. Calibration data were produced by measuring water-surface elevations throughout the model for five discharges (25,000 to 125,000 cfs in 25,000-cfs increments) in both ebb and flood directions. Each discharge was run for four different headwater conditions (-1, 0, +1, and +2 ft) and measured at sta 2 or 7 depending on the direction of flow.

35. Water-surface data were obtained by two technicians, the final result at each gage being the average of their readings. Velocity measurements were made at 23 stations for three depths (surface, mid-depth, and bottom). These data were taken at three discharges (25,000,

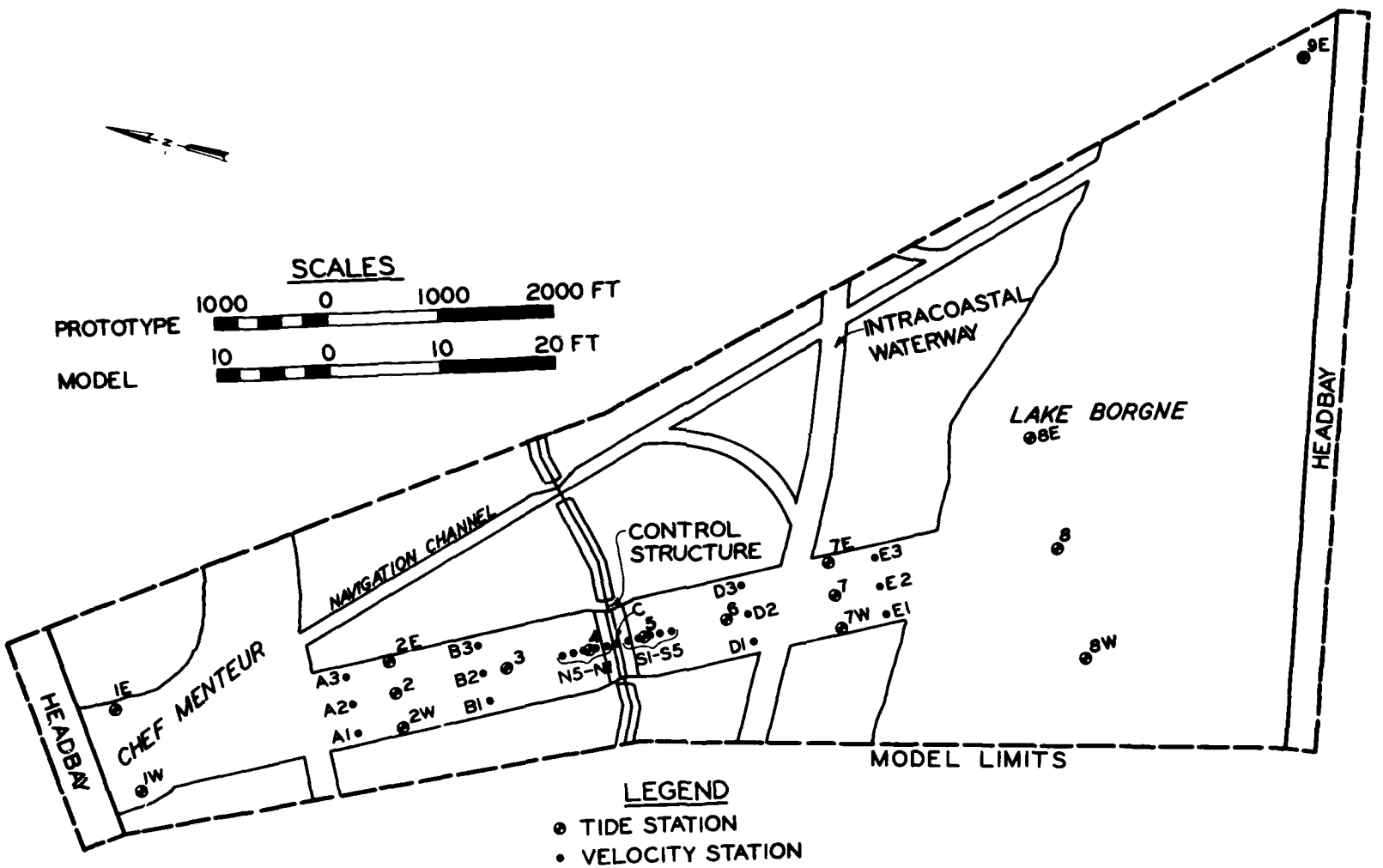

Figure 13. Model layout for Chef Menteur Pass barrier structure

75,000, and 125,000 cfs) for one headwater condition at each flow rate (+1 for 25,000 and 75,000 cfs, and +2 for 125,000 cfs) in both ebb and flood directions. Surface current photographs were made using a 3-sec exposure of confetti on the water surface for two higher discharge conditions. Testing in this model was conducted with the navigation channel and the Gulf Intracostal Waterway closed to flow. In this manner, data were obtained that truly represented head losses due solely to the proposed control structures. Treatment of the Chef Menteur navigation channel is discussed in a following section.

Results

36. Data from these model tests, which were used as calibration data for five flow rates are shown in Tables 25-29. A complete set of velocity data also is given in Tables 30-32. Velocity and water-surface elevation data that were taken together under identical conditions contain the same run numbers.

37. Velocity results for sta N1, N5, C, and S1-S5 along the center line of the channel through the structure are plotted in Plates 1-6. This information should be of aid in sizing of riprap and definition of flow patterns.

38. Surface current photographs for flows of 75,000 and 125,000 cfs are shown in Photos 31 and 32. The flow approaching the structure meanders somewhat along the approach channel. Downstream of the structure, large eddies extend along the eastern bank for about 1,000 ft for both flood flows and along the western bank for about 1,800 ft. In the ebb direction, these large eddies continued for about 1,000 ft along the western bank for both flow conditions and extend beyond the limits of these photographs on the eastern side (over 2,000 ft).

PART III: COMPUTATIONAL GRID SECTIONAL MODELS, STEADY-STATE CONDITIONS

Objective and Approach

39. The objective of the sectional modeling of the passes is to facilitate both accurate and economical modeling of the entire study area for the hurricane and tidal circulation simulations as well as to quantify the hydraulic characteristics of the proposed structures. Since the individual passes are small relative to the dimensions of the three-lake system (global model), while at the same time having both high flow rates, large depths, and meandering channel geometry, they control both the number of cells and the maximum time-step for the global model. Therefore, the balance between desired resolution and maintenance of an acceptable cost (indirectly proportional to computer time availability) for running the global model hinges on selection of grid dimensions in the vicinity of the three major passes--The Rigolets, Chef Menteur Pass, and Seabrook Canal.

40. Computational grid sectional models for both steady-state and dynamic conditions are the results of efforts to define a global grid for the three-lake system that will provide an acceptable degree of resolution and accuracy at minimum cost. Since the cost of running a model is proportional to the number of cells and the time-step, cost optimization requires that the passes models must be chosen in a fashion such that the hydrodynamics are correctly represented with a minimum number of grid cells. In order to determine that this criterion has been met, computations using several grids of each pass were compared with one another in a sensitivity study. It was found that both Chef Menteur Pass and Seabrook Canal could be modeled (with and without structure in place) by a one-dimensional system. Due to its overall size, The Rigolets was modeled in two dimensions.

41. Having determined which grids provided the required accuracy at minimum cost, a variable-spaced global grid (Figure 14) was devised such that sections covering the three major passes approximated the individual optimum grids (mapping of the global grid would not allow for

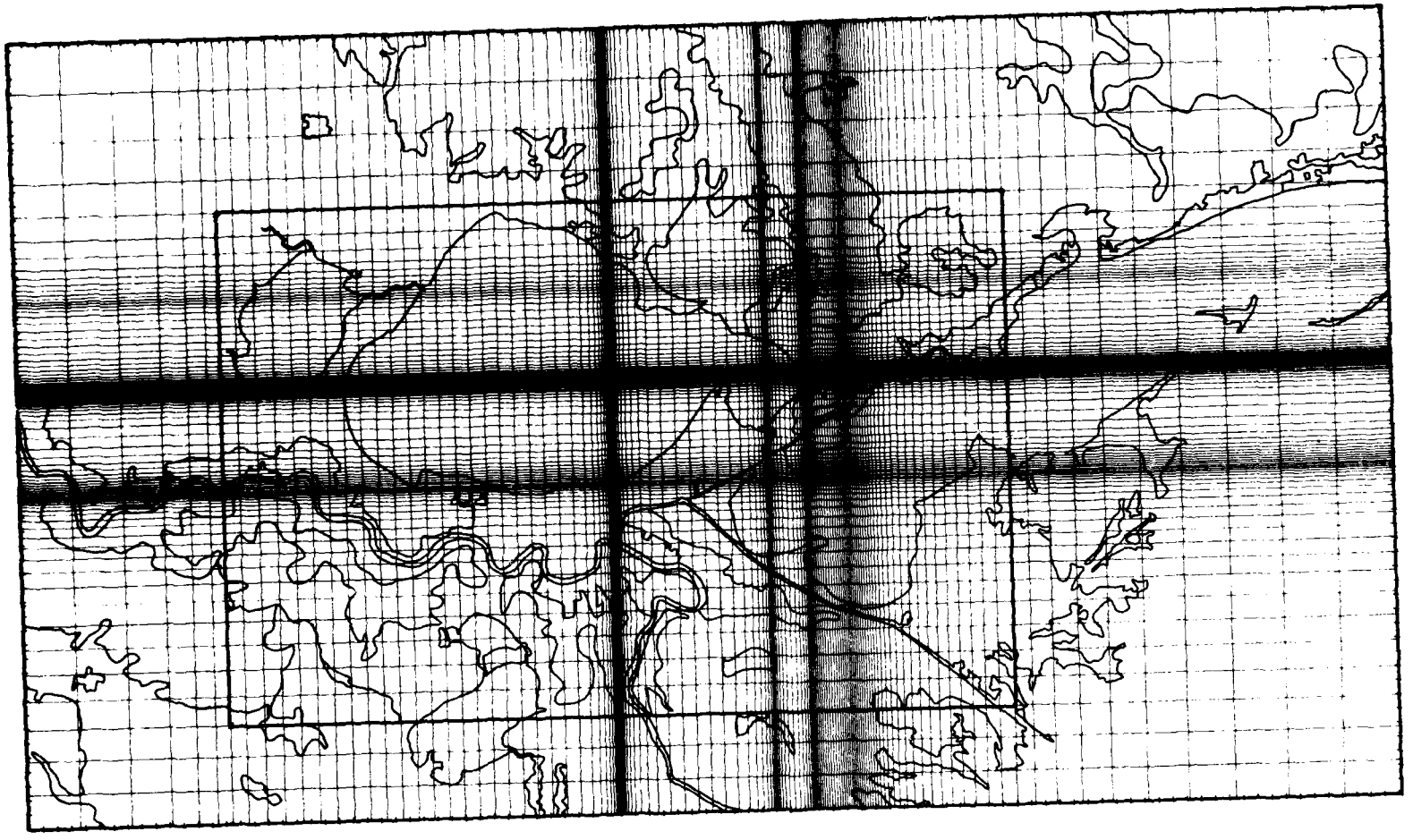

Figure 14. Embedded storm surge grid of the three-lake system depicting the tidal prism subgrid

exact duplication of the individual grids). Grid coordinates were aligned with the earth coordinate system. After constructing the global grid, portions covering the major passes were, in turn, extracted to form individual models of each pass. The sensitivity study ensured that pass models extracted from the global grid could represent the appropriate hydrodynamics; therefore these models were calibrated and verified to duplicate the physical model results (steady-state flows).

Model Descriptions

42. The steady-state model of The Rigolets Pass employs a grid (Figure 15) of 594 cells (27 by 22), with the smallest cell having a vertical (north/south) extent of about 500 ft and a horizontal (east/west) extent of about 700 ft. The numerical grid covers the same area as its physical model counterpart. The main channel has been given a full two-dimensional representation with a minimum amount of idealization. Sawmill Pass was treated as a channel of single cell width. The sandbar in midchannel, just west of the proposed structure site was represented by a submerged barrier. The grid was digitized so as to preserve the channel cross section as determined from available topographic data. The navigation channel north of the closure dam (Figure 3) is not modeled. A full description of the channel treatment follows at the end of this part.

43. The steady-state model of the Seabrook Canal uses a grid (Figure 16) of 304 cells (16 by 19), with the smallest cell having a vertical (north/south) extent of 800 ft and a horizontal (east/west) extent of 350 ft. The grid covers approximately the same area as its physical model counterpart. The channel is represented by a single column of cells. Although the actual Seabrook Canal runs 15 deg west of north and the numerical grid is aligned with north, the channel idealization has been shown to have no significant effect on computed results. The idealized channel model has been digitized so that both channel length and cross section have been preserved.

44. Chef Menteur Pass was modeled similar to the Seabrook Canal in

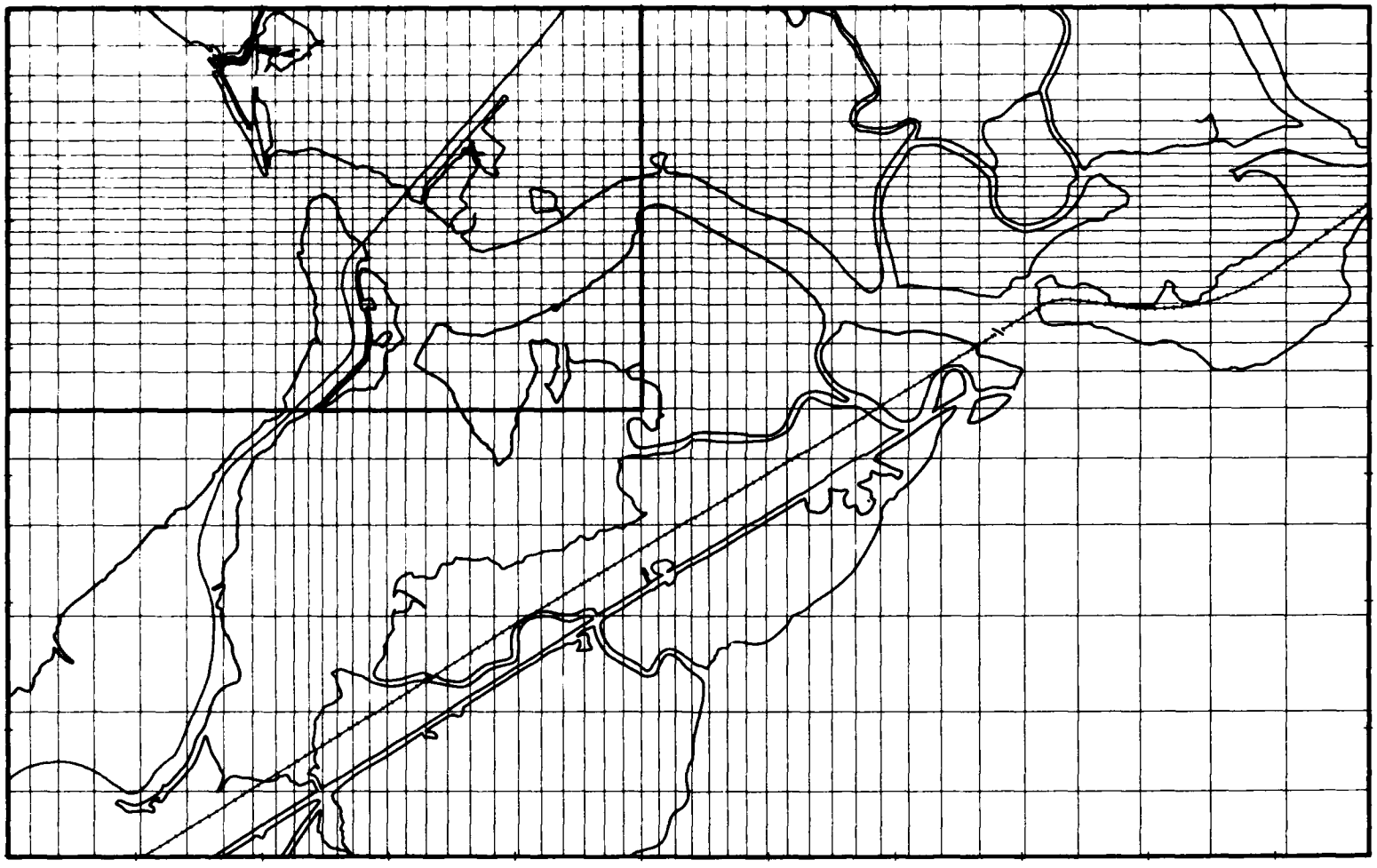

Figure 15. Sectional grid for The Rigolets computational model

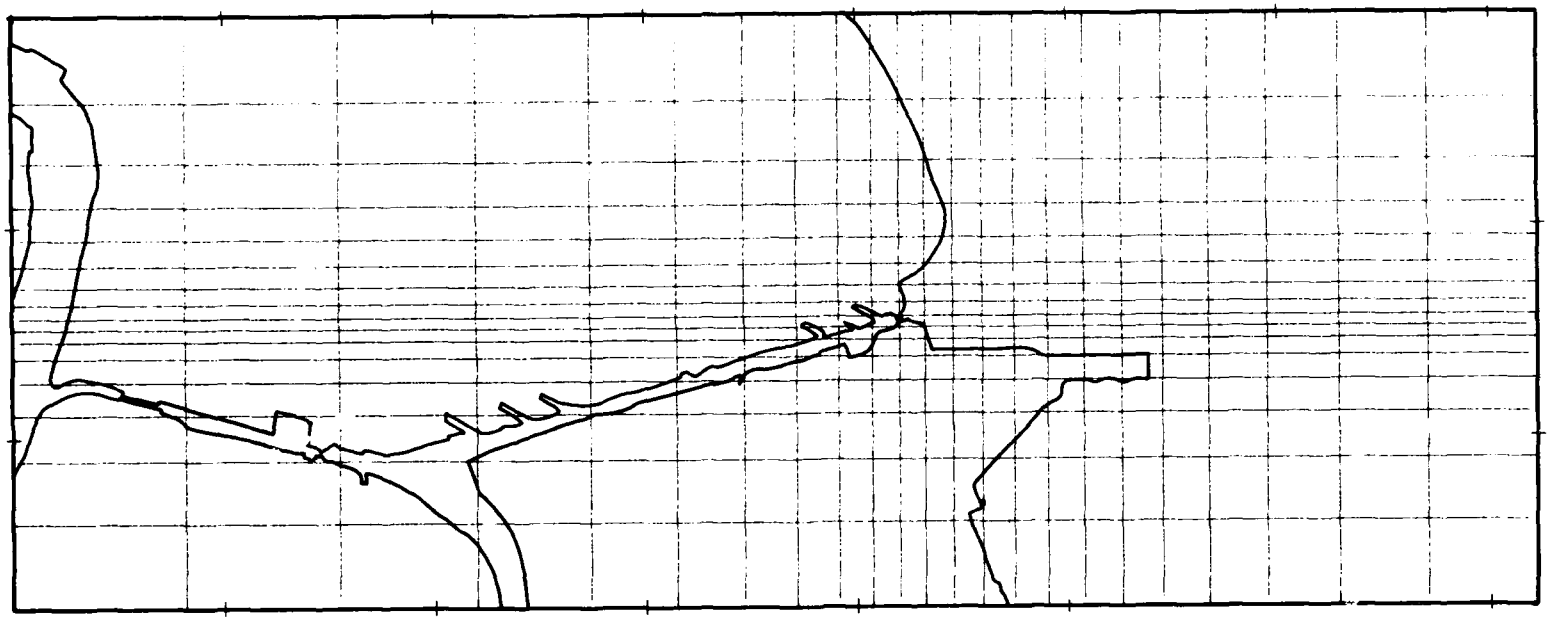

Figure 16. Sectional grid for the Seabrook Lock and structure computational model

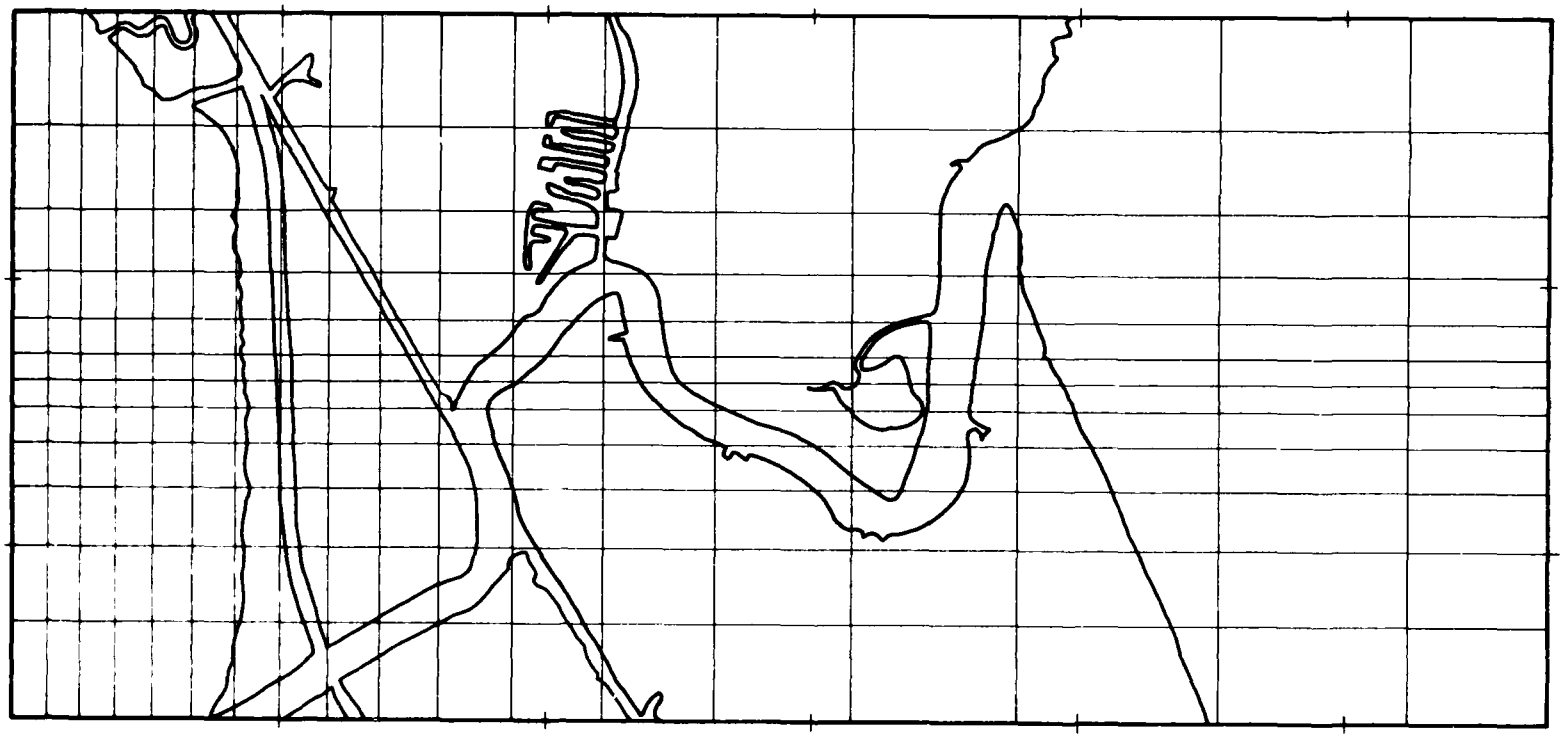

Figure 17. Sectional grid for the Chef Menteur computational model

that a single column of cells was used to represent the pass itself. The steady-state model employed a grid (Figure 17) of 204 cells (12 by 17), with the smallest cell having a vertical (north/south) extent of 800 ft and a horizontal (east/west) extent of 670 ft. The grid covers approximately the same area as its physical model counterpart. Since the physical model only covers the portion of the proposed channel that will be newly dredged, no prototype data exist for base conditions. The width of the channel was chosen to correspond to the width called for by plans for the proposed structure. The grid was digitized so that average cross sections of the channel were preserved. Since the navigation channel in the proposed plan was closed in the physical model tests its effect must be neglected in the numerical tests. The impact of closing the channel is discussed in a later section.

Numerical Model Tests

General procedure

45. The objective of the steady-state tests of the sectional pass models was to determine an appropriate numerical representation of the proposed structure for each pass. To simulate the cross-sectional restriction imposed by such structures, WIFM uses a submerged barrier of given sill depth and frictional characteristics. By varying these two parameters, the numerical model can be calibrated to reproduce the same head loss (as a function of volume transport) as that measured in the undistorted physical model of each pass/structure system.

46. Manning's equation

$$Q = \frac{1.5}{n} AR^{2/3} S^{1/2} \quad (1)$$

where

Q = discharge

A = cross-sectional area of the channel model

R = mean hydraulic radius

S = energy slope

can be used to predict a value for Manning's n for a given constriction. The energy slope is approximated by the slope of the water surface, namely, $h^*/\Delta x$, where h^* is the average head loss over a grid distance Δx.

47. The same procedures were used in testing all three of the sectional pass models. Initially, the model was calibrated (if sill depth and frictional characteristics were determined) to represent base or existing conditions (without structure in place). Having reproduced base conditions for each pass (with the exception of Chef Menteur since only the proposed channel/structure system was tested in an undistorted physical model), the appropriate structure/levee system was added to the model and tested. The tests performed were basically an iterative process in which the goal was to determine an appropriate frictional coefficient for the barrier that would allow the numerical model to reproduce the head loss experienced in the physical model for a range of water levels and flow rates.

The Rigolets model

48. Base conditions were modeled in a previous study (Berger and Boland 1976). Since the physical model was operated only in a steady-state mode and did not simulate flow throughout the tidal cycle, prototype data at various instances in time were used to verify the model. All data taken in the physical model were not reported but are available from the project files stored at WES. The numerical sectional model was operated for three conditions representing assumed maximum, medium, and minimum flow conditions for both flood and ebb events. These conditions are delineated below:

	Discharge, cfs				
	Flood		Ebb		Headwater
Flow Condition	Lake Pontchartrain	Sawmill Pass	Lake Pontchartrain	Sawmill Pass	Elevation ft
Maximum	216,000	19,000	223,000	17,000	2.0
Medium	143,000	11,000	143,000	14,000	1.0
Minimum	69,000	4,000	75,000	12,000	1.0

49. The numerical sectional model was calibrated to reproduce the maximum flood condition. A uniform Manning's n of 0.025 was used throughout the channel. Boundary conditions (as specified above) were taken directly from the physical model data, namely, the eastern boundary (in The Rigolets) was held at a constant head; and discharge conditions were maintained at the western boundary in Lake Pontchartrain and at Sawmill Pass. Figure 18 displays surface elevation results from both physical and numerical models (maximum base flood conditions) for comparative analysis. Without changing any parameters describing the model, base conditions for all other flow conditions were reproduced. Figure 19 displays comparative surface elevation results for peak ebb base conditions. Complete results are given in Tables 33 and 34.

50. A number of structure/levee systems were tested in the physical model with the final selected plan (Plan 2A-1) having only limited measurements to define improved flow conditions in the Fort Pike area. This plan was basically the same as Plan 2A except that the structure was relocated 250 ft closer to the center of the channel. Since the computational sectional model does not try to accurately reproduce the geometry of the area local to the structure (the grid is too coarse) and complete measurements were taken for Plan 2A in the physical model, these measurements will be used to calibrate the numerical structure model. Either plan (Figure 3) was represented by a series of exposed barriers (levees) extending from the north and south shores of The Rigolets to the middle of the channel. A submerged barrier approximating the cross-sectional opening of the structure connects to the ends of the exposed barriers. The frictional coefficient only for the submerged barrier was varied, and the model was adjusted to reproduce heads and flow conditions observed in the physical model study. An iterative process was used to determine an average value of Manning's n that would describe the hydraulic characteristics of the structure in the sectional model for a complete range of flow conditions. Table 35 displays results for maximum, medium, and minimum discharge conditions (both flood and ebb). All results were obtained using a value of $n = 0.110$ for the structure opening.

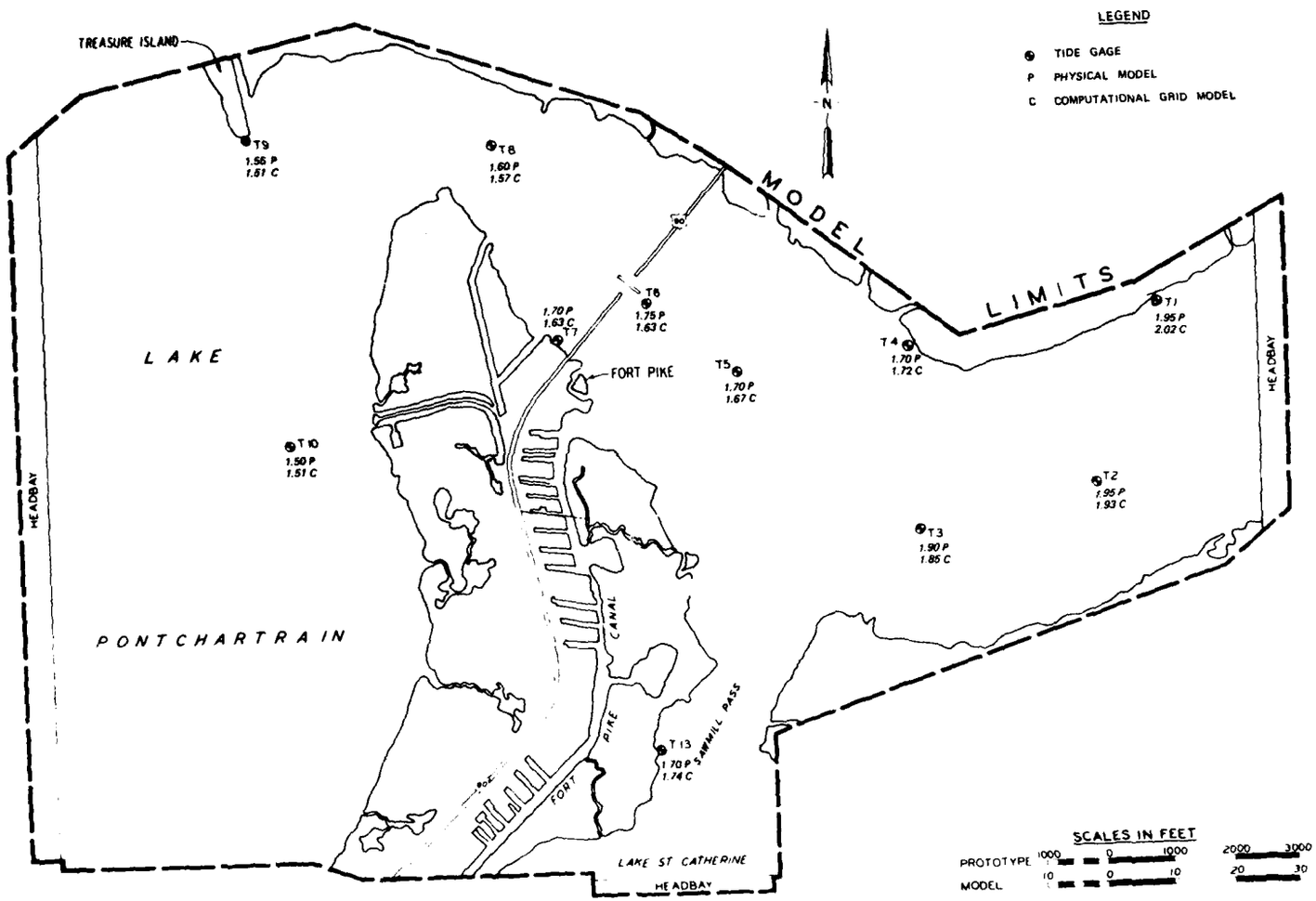

Figure 18. Surface elevation, ft NGVD, maximum flood flow; physical versus computational model for existing conditions in The Rigolets

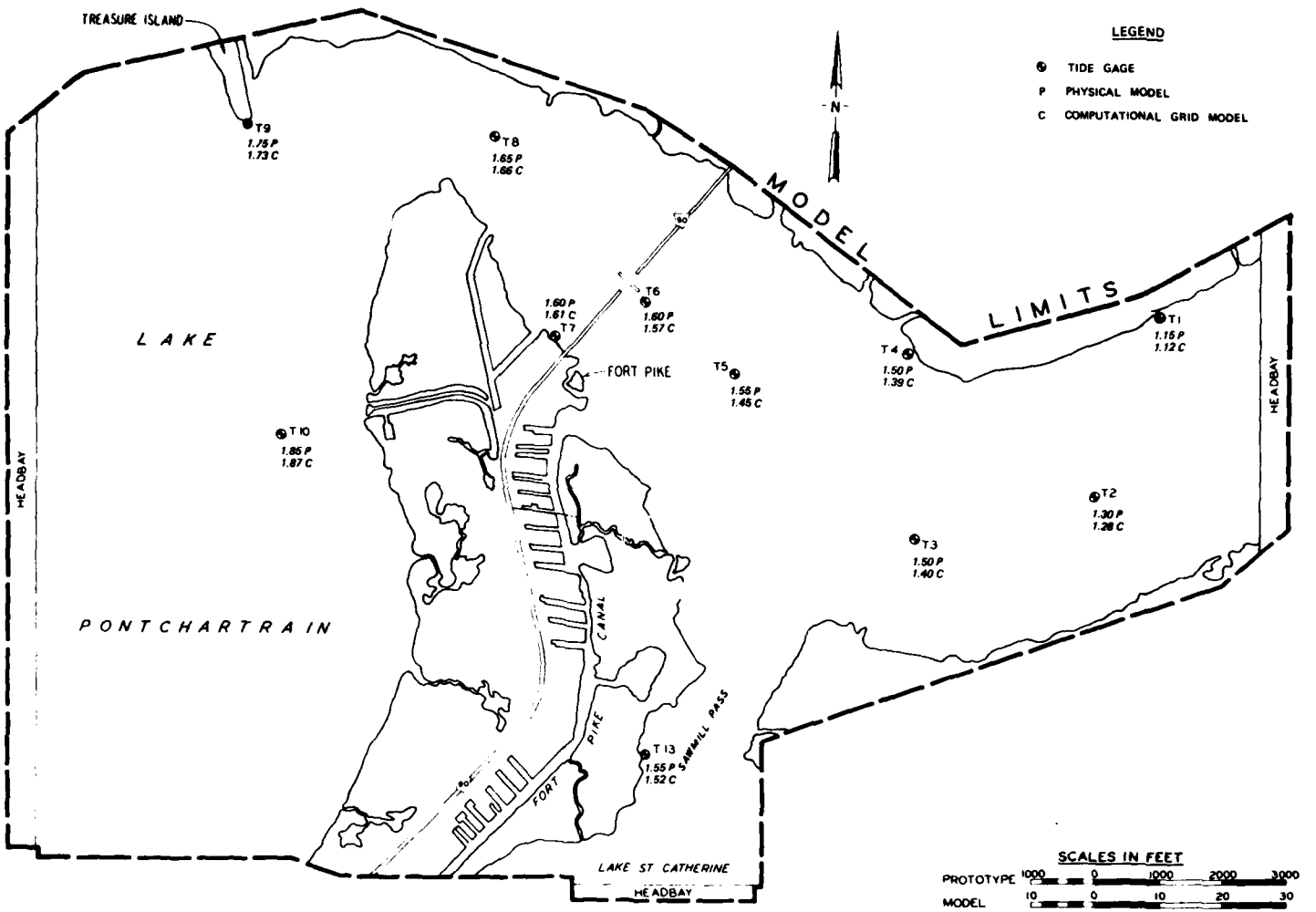

Figure 19. Surface elevation, ft NGVD, maximum ebb flow; physical versus computational model for existing conditions in The Rigolets

Seabrook Canal model

51. Base conditions tested in the physical model included five flow rates between 5,000 and 30,000 cfs for both flood and ebb directions and for various headwater elevations. Boundary conditions were taken directly from the physical model; namely, the channel boundary cell was held at a constant head (gage 13 in the physical model) and the appropriate discharge was applied at the Lake Pontchartrain open boundary.

52. Since the Seabrook Canal sectional model idealizes the canal by representing it as a one-dimensional channel, special attention was given to the constriction in the channel by the Hayne Boulevard Bridge just south of the canal's connection to Lake Pontchartrain. The frictional coefficient used in the channel and the coefficient for the submerged barrier representing the bridge constriction were varied, and the model was adjusted through an iterative process to reproduce heads and flow conditions observed in the physical model study for the 15,000-cfs discharge (run 2). If the following parameters, determined from the geometry represented in the numerical model and from physical model results, are used in Equation 1,

Parameter	Value
A	11,470 ft (353 x 32.5)
R	27.4 ft (11,470/418)
h*	0.3 ft
Δx	956 ft
Q	15,000 cfs

the resulting value of n is

$$n = \left[\frac{1.5 \times 11{,}470 \times 27.4^{2/3} \times (0.3/956)^{1/2}}{15{,}000}\right] = 0.185$$

53. Final values of Manning's n determined in the calibration of the 15,000-cfs discharge were 0.018 for the channel and 0.19 for the bridge constriction. All headwater settings with Q = 15,000 cfs for

both flood and ebb were simulated using these values for n . The various discharge conditions for run 2 in the physical model were subsequently computed. All results are presented in Tables 1-5 and indicate that the selected values for n were adequate for the model to represent the entire range of flow and head conditions.

54. The five plans tested in the physical model investigation (PART II) include various possible combinations of open/closed conditions for the lock and three structure gates. Of these alternatives, plan 4 permits the greatest discharge into Lake Pontchartrain and was thus chosen to simulate in future tests with the global three-lake model. For this report only, Plans 3 and 4 were tested in the numerical sectional model. Supercritical flow is too easily generated through the structure constriction for other plans, and thus the plans would be difficult to model with the methodology used herein.

55. Manning's Equation 1 was again employed to predict approximate values of n to represent the structure operation defined in Plans 3 and 4; these values were 0.39 and 0.24, respectively. For the structure simulations, the model produced steady-state conditions in substantially fewer computational steps if the surface elevation were defined at the Lake Pontchartrain open boundary and if discharge were used for the open-channel boundary cell. These boundary conditions were used for all testing of Plans 3 and 4. A value of $n = 0.4$ was determined by an iterative process to best represent the structure in Plan 3 for a flood discharge of 10,000 cfs; the same value appeared appropriate for an ebb discharge as well. Results are given in Table 14. No further tests with Plan 3 were made since only Plan 4 would be used in the global model. A similar procedure was used to determine a value of $n = 0.23$ to best represent a flood/ebb discharge condition of 15,000 cfs for the structure operation in Plan 4. Additional discharge conditions were then tested using this value for n and results are given in Table 17-20.

Chef Menteur Pass model

56. Since only the proposed channel/structure system was tested in the physical model, no base conditions need be simulated in the numerical sectional model. Again, a submerged barrier was used to represent the

structure. The channel width in the numerical model corresponds with the prototype width of the proposed structure. Manning's Equation 1 predicts a value of $n = 0.105$ for the barrier. Flood/ebb conditions were simulated for a discharge of 75,000 cfs; and by an iterative process, a value of $n = 0.112$ was found to best represent these conditions in the sectional model. This value of n was then used to simulate additional discharge conditions and was found to adequately represent the proposed Chef Menteur structure for the entire range of discharge conditions. Results are given in Tables 25-29.

Treatment of Navigation Channels

57. The proposed hurricane protection plans for The Rigolets and Chef Menteur Passes include shallow, narrow navigation channels connecting Lake Pontchartrain with Lake Borgne. It is infeasible to attempt to model these channels in the tidal prism computational grid by reducing the mesh size to the channel width (approximately 100 ft). The Rigolets navigation channel was included in the physical model but was closed during most plan tests. The control structure is modeled by determining a Manning's n to represent the head loss across the structure. The head loss measured in the physical model did not include the navigation channel effect, so it follows that the frictional coefficient calibrated for the structure in the numerical model does not include the channel effect.

58. The navigation channel associated with the Chef Menteur structure plan was represented in the physical model. Initial tests indicated that the resistance exhibited by the channel was significantly exaggerated due to scale effects in such a shallow channel. Calibration of the structure could not be accomplished without closing the navigation channel. Since tests were subsequently run with the channel closed, the Chef Menteur navigation channel effect cannot be simulated in the tidal prism numerical models. The impact of omitting these channel effects is discussed in the following paragraphs.

59. Keulegan (1967) developed a method of estimating water-level

fluctuations of basins in communication with seas. The method has a number of limitations but it can be used to estimate the effect of neglecting the influence of the navigation channel. The method centers on calculating a coefficient of filling or repletion for the channel in question. For the unrestricted Chef Menteur Pass the quantity

$$\phi = \frac{A_B \, K \, \sqrt{H}}{a} \qquad (2)$$

where

A_B = surface area of the basin

a = cross-sectional area of the connecting channel

H = semirange of tide in the sea

K = coefficient of repletion tabulated by Keulegan as a function of channel length (L), tidal period (T), and channel friction coefficient (n).

The maximum mean velocity expected in the channel is given by

$$V_m = 2\pi C \, \frac{A_B}{a} \, \frac{H}{T} \, \sin \tau \qquad (3)$$

where C and $\sin \tau$ are quantities depending on K. For $K < 0.3$ a constant value of $C = 0.81$ can be adopted. The quantity $\sin \tau$ varies linearly with K for small K. Nominal values were taken for the following variables:

$a = 30{,}000 \text{ ft}^2$

$H = 0.8$ ft

$T = 89{,}400$ sec

$C = 0.81$

$n = 0.025$

$\sin \tau = 1.16 \, K$

Equations 2 and 3 were solved iteratively for K and an active A_B assuming a value for V_m from measured data. The actual surface area of Lake Pontchartrain is approximately 1.8×10^{10} ft^2. Since the

change of water level in the lake is not uniform (uniformity being a method assumption), the active surface area is expected to be less than the actual surface area. These calculations resulted in a repletion coefficient for the existing Chef Menteur Pass of $K_E = 0.26$ and an active lake surface area of 0.8×10^{10} ft^2 . Equation 2 can be evaluated for the navigation channel to give a repletion coefficient of $K_{NC} = 0.008$.

60. Keulegan gives a formula for a repletion coefficient associated with a barrier cut, namely,

$$K_s = \frac{\sqrt{2gH}\ T}{2\pi H} \frac{a}{A_B} C_d$$

where C_d is a discharge coefficient for the structure. Chow (1959) relates C_d with percent of channel constriction. For the Chef Menteur structure C_d is in the range $0.8 < C_d < 0.9$. A value of $C_d = 0.85$ was assumed, giving a value for K_s of 0.22 .

61. If there is more than one connecting channel, the equivalent repletion coefficient is the sum of the individual channel coefficients. Thus, if the navigation channel is included with the Chef Menteur structure, the total repletion coefficient is $K_T = 0.228$. For small K the tidal prism or maximum rate of discharge through the connecting channel is directly proportional to K The result of omitting the navigation channel is a 3.5% error in K (0.008/0.228) and consequently a 3.5% decrease in the discharge rate through Chef Menteur Pass. Similarly, the impacts of placing the proposed structure in Chef Menteur Pass and of the structure with the navigation channel are 15.4% and 12.3% changes in K (or maximum Chef Menteur discharge rate), respectively.

62. To assess the impact of omitting the navigation channel on the tidal prism of the lake the following assumption is made, namely, the contribution to the tidal prism of any connecting channel between the lake and the gulf is proportional to the ratio of its controlling cross-sectional area to the total controlling cross-sectional area of all connecting channels with structures in place. If the total cross-sectional area of the proposed hurricane protection structure with navigation

channels is 53,100 ft^2 the following table describes the impact analysis:

Chef Menteur Pass Model

	Structure	Structure + Channel
Cross-sectional area a (ft^2)	16,200	17,500
% a_{TOTAL}	31.3	33.0
% Impact on discharge rate	-15.4	-12.3
% Impact on lake tidal prism	-4.8	-4.1

The above analysis indicates that omitting the navigation channel may have resulted in an additional 0.7% decrease in the lake tidal prism. This analysis cannot account for all the nonlinear effects involved, particularly the interaction between the Chef Menteur and Rigolets Passes, and the geometric variations in Chef Menteur itself. Nevertheless, subsequent modeling results discussed in Report 3 (Butler, in preparation) correlate with the assumptions and analysis presented here.

63. The analysis procedure applied to assess the impact of the Chef Menteur navigation channel cannot be applied with the same confidence to The Rigolets channel because of irregularity of its cross section with length. Nevertheless, since the navigation channel associated with The Rigolets structure plan is similar to that in the Chef Menteur plan (in width, depth, and length), the impact of neglecting The Rigolets navigation channel in the tidal prism model computations will be approximately the same as for the Chef Menteur navigation channel (0.7% decrease in the lake tidal prism). The actual impact of neglecting The Rigolets navigation channel will probably be less than that for Chef Menteur. Reasoning for this premise follows from expecting a larger K for The Rigolets Pass and hence a smaller error when comparing the omission of $K_{NC} = 0.008$. Thus, the total impact of adding the navigation channels into both The Rigolets and Chef Menteur plans will result in an increase in the lake tidal prism of about 2%.

PART IV: FINE SCALE NUMERICAL MODELS

Objective and Approach

64. In order to demonstrate that the numerical models of the passes and the control structures to be analyzed in this study can accurately represent the effects of the passes and structures on the flow characteristics of the lake system, fine grid models of each pass were developed and calibrated to the results of the undistorted physical models. This allowed a relatively accurate representation of the geometric characteristics of the study areas and thus tested the ability of the numerical model to reproduce the important flow characteristics with these channel descriptions. In addition, the fine scale model would allow the analysis of detailed flow patterns for particular conditions at a later date if such analysis was considered useful. In such cases the computational grid models could be used to generate the required boundary conditions for the fine scale model. These fine grid model tests involved steady-state conditions only and used the linear version of the computation scheme, except for one set of tests on The Rigolets. The linear version was used since the cost of running the model with the advective terms in the computations was relatively high, and it was demonstrated by these tests that the linear version was adequate for the purposes of this study. For a more accurate representation of the two-dimensional flow characteristics, as might be required for a near-field structural effect study, the nonlinear solution scheme would be required.

Description of Numerical Models

65. The Rigolets model area was represented with a variable-spaced computational grid in both directions with the grid spacing increasing from a minimum of 85 and 312 ft in the east/west and north/south directions, respectively. Figure 20 shows that the finer mesh was concentrated in the narrow throat of The Rigolets and at Sawmill Pass in order to properly represent the prototype geometry. A total grid of 1,520 cells

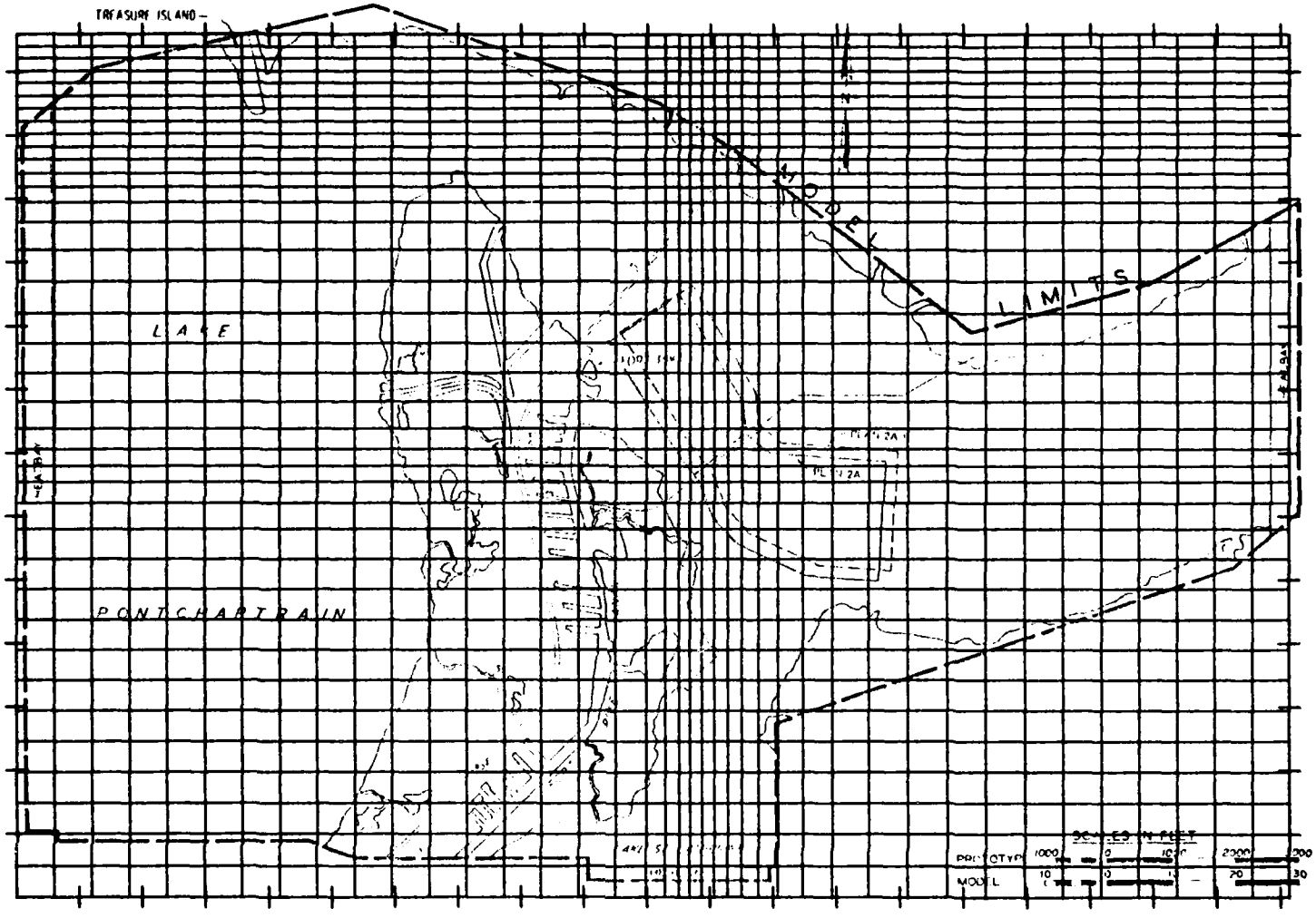

Figure 20. Fine scale model grid for The Rigolets

(40 by 38) was used. Bottom elevations were digitized from model construction maps. The control structures were represented as submerged barriers and the levees as exposed barriers along grid cell faces closely approximating the actual location of the levees and structures. Bottom elevations also were adjusted to plan conditions. Since grid spacing did not exactly match the clear opening of the gates, the bottom elevation of the submerged barrier was adjusted slightly for each plan such that total area of the clear opening would be simulated exactly. This resulted in an elevation adjustment of +1.51 ft for Plan 2A and +3.14 ft for Plan 2A-1 from the -30.0 ft design elevation. Losses due to flow passing through the structure are represented by increasing the frictional coefficient. Manning's n values of 0.120 were used for this purpose. Some smoothing of the flow across the structures was accomplished by increasing Manning's n values of the computation cells adjacent to the structures to 0.080. The navigation channel was not modeled corresponding to reasons given in the previous section.

66. The Seabrook model layout is shown in Figure 6. This is represented numerically by a variably spaced grid containing 1,885 cells with dimensions of 65 by 29. The cell spacing varies from 35 to 500 ft with the fine grid spacing concentrated at the bridge and guide wall area near the Lake Pontchartrain entrance and the lock and outlet structure area. Flow conditions were run for both a base condition with no structure and for a plan condition with a lock and gated control structure in place and fully open (Plan 4 in the physical model testing program). Guide walls and bridge piers were represented by submerged weirs to enable the additional friction due to closely spaced pilings to be included. The lock structure and tie levees are represented by exposed barriers and the gated control structure is represented by a submerged barrier. Two cell widths are used to represent the lock. Three cell widths are used to represent three gated areas. The control structure is oriented at an angle to the lock in the actual plan; however, in the numerical model, it must be oriented normal to the lock. Therefore, the flow orientation will be slightly affected. Bottom elevations for the base condition and the plan condition were obtained from model construction templates.

67. The Chef Menteur physical model layout is presented in Figure 13. This model was represented numerically with a variably spaced grid ranging from 65 to 500 ft. The resulting grid contains 1,763 cells with dimensions of 43 by 41. The finely spaced grid was concentrated in the channel particularly in the area of the structure. Barrier levees were represented as exposed barriers, and the control structure is represented as a submerged barrier. To keep the cross-sectional area of the structure equal to the clear opening of the design structure, the bottom elevation was adjusted to a -26.5 elevation. The small navigation channel is represented as a narrow channel parallel to the main channel since it was not feasible to represent this channel in its natural orientation. The interconnecting channels with the Intracoastal Waterway were blocked so that no flow will occur in the navigation channel corresponding to the conditions run in the physical model. Much of the remaining area is low marshland and can be flooded during some of the headwater conditions. Bottom elevations were obtained from physical model construction templates.

Numerical Fine Scale Test Results and Comparison with Physical Model Results

The Rigolets model

68. The fine scale numerical model results for The Rigolets were compared for both base and plan conditions with physical model results for the same flow conditions tested with the computational grid sectional model. The best comparison of results for the base condition was obtained with a uniform value of Manning's n of 0.035. Results of elevation and velocity computations for maximum flood and ebb flows are displayed in Figures 21-24 along with physical model data for comparative analysis. Complete water-surface elevation and velocity data are given in Tables 33 and 34 for all flows tested. Circulation patterns for the maximum flood and ebb flows are shown in Figures 25-28. Closeups of the structure area are included.

69. Since complete measurements of water-surface elevations and velocities were only taken for Plan 2A in the physical model, both

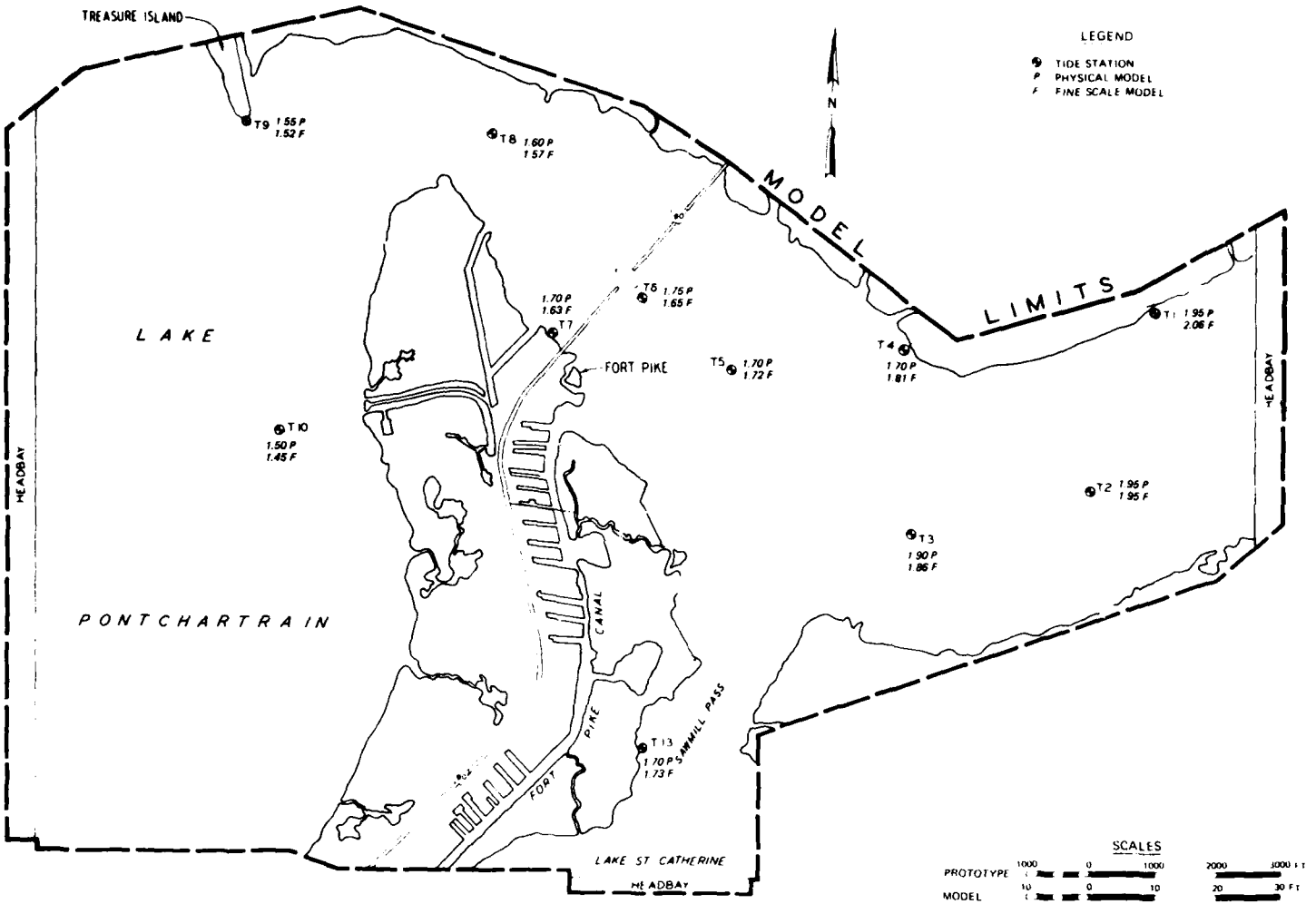

Figure 21. Surface elevation, ft NGVD, maximum flood flow; physical versus fine scale model for existing conditions in The Rigolets

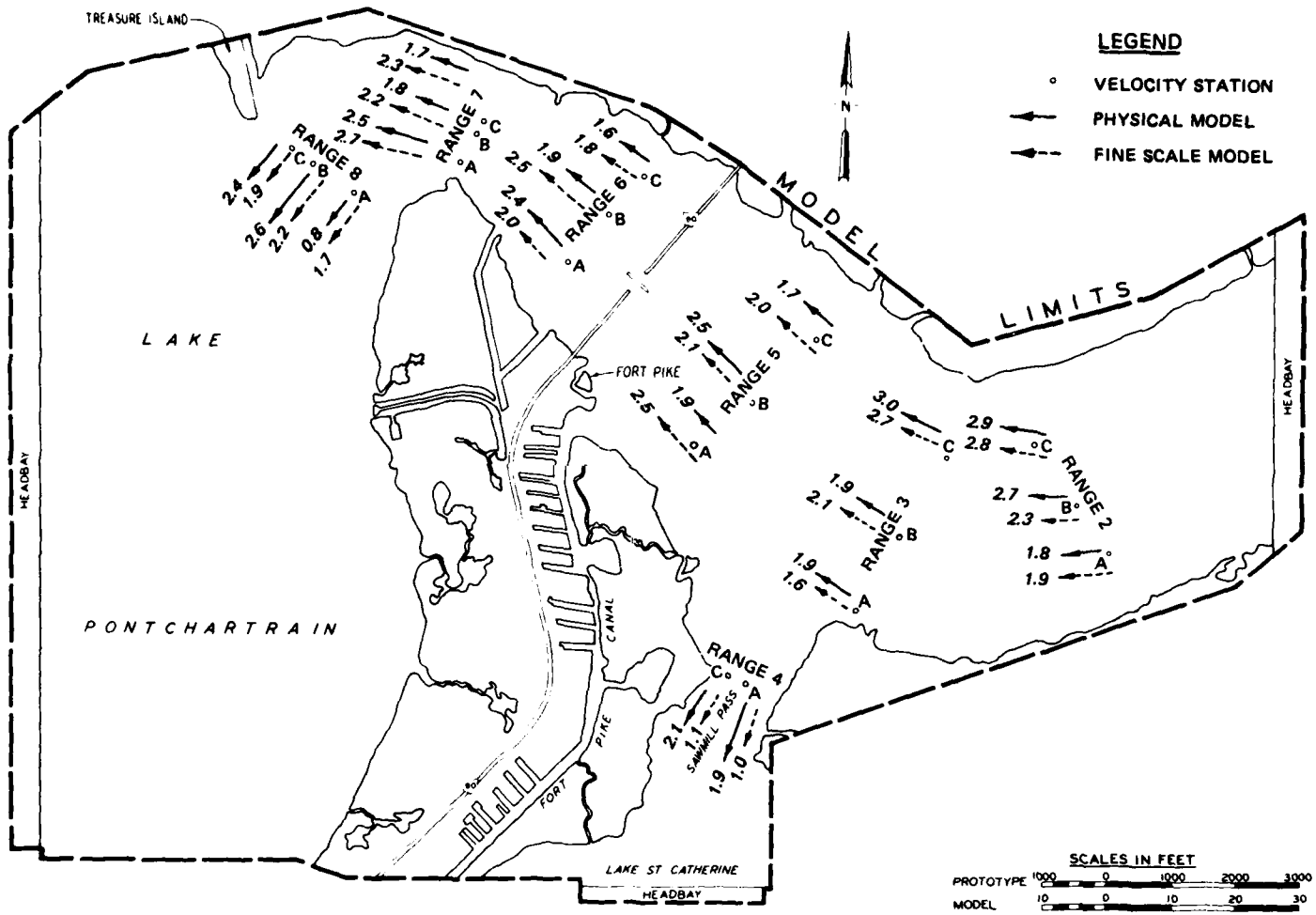

Figure 22. Velocities, fps, maximum flood flow; physical versus fine scale model for existing conditions in The Rigolets

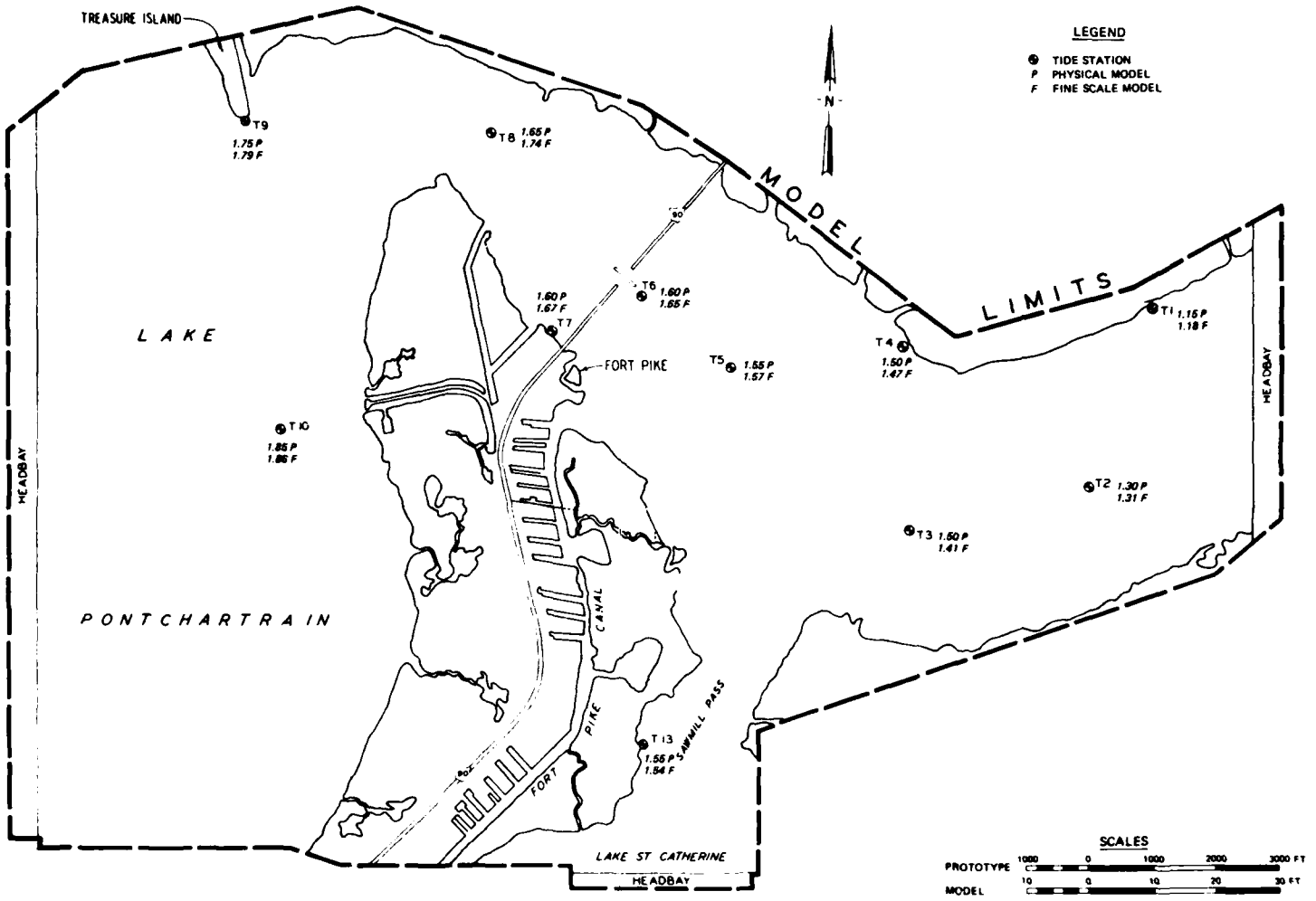

Figure 23. Surface elevation, ft NGVD, maximum ebb flow; physical versus fine scale model for existing conditions in The Rigolets

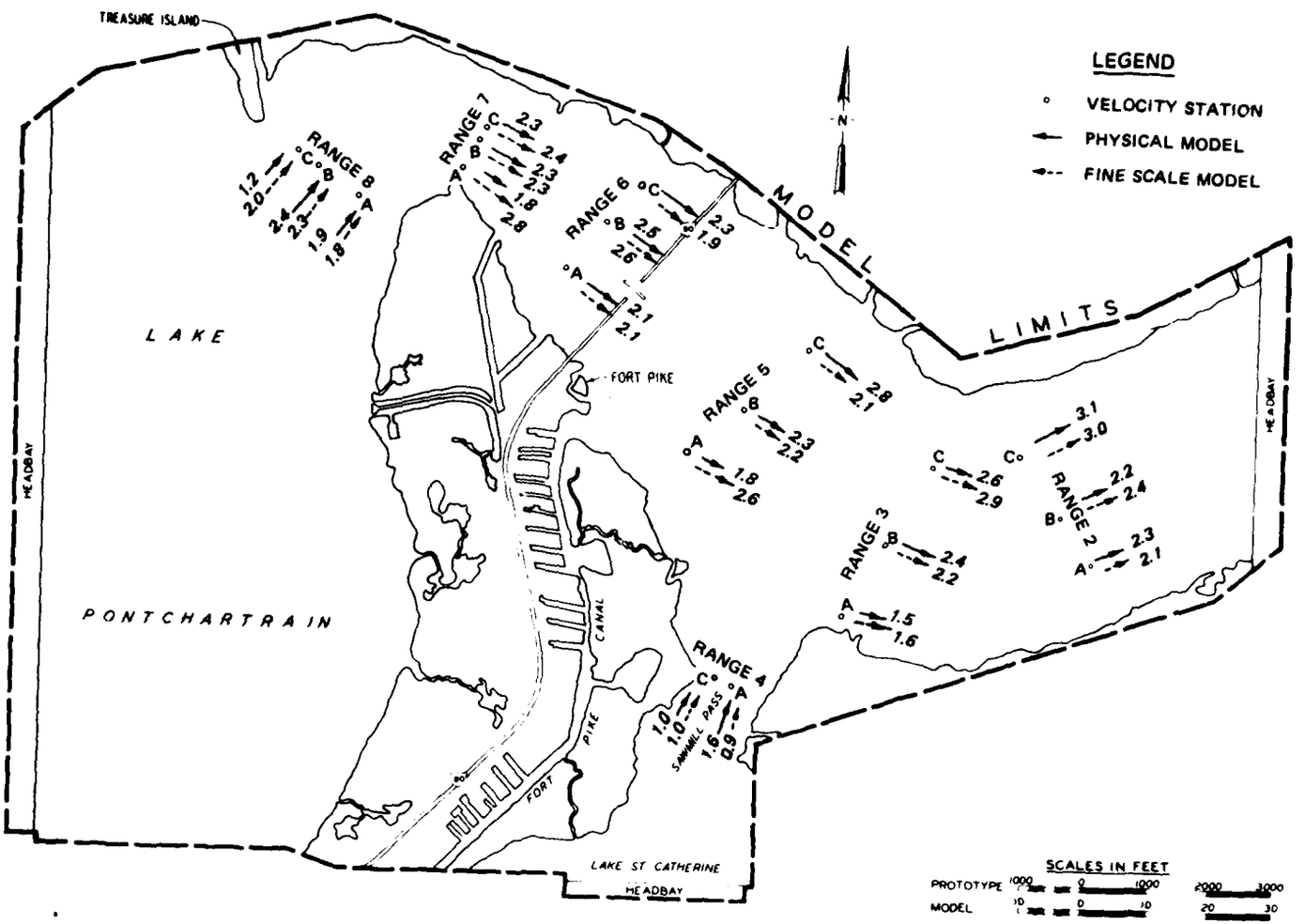

Figure 24. Velocities, fps, maximum ebb flow; physical versus fine scale model for existing conditions in The Rigolets

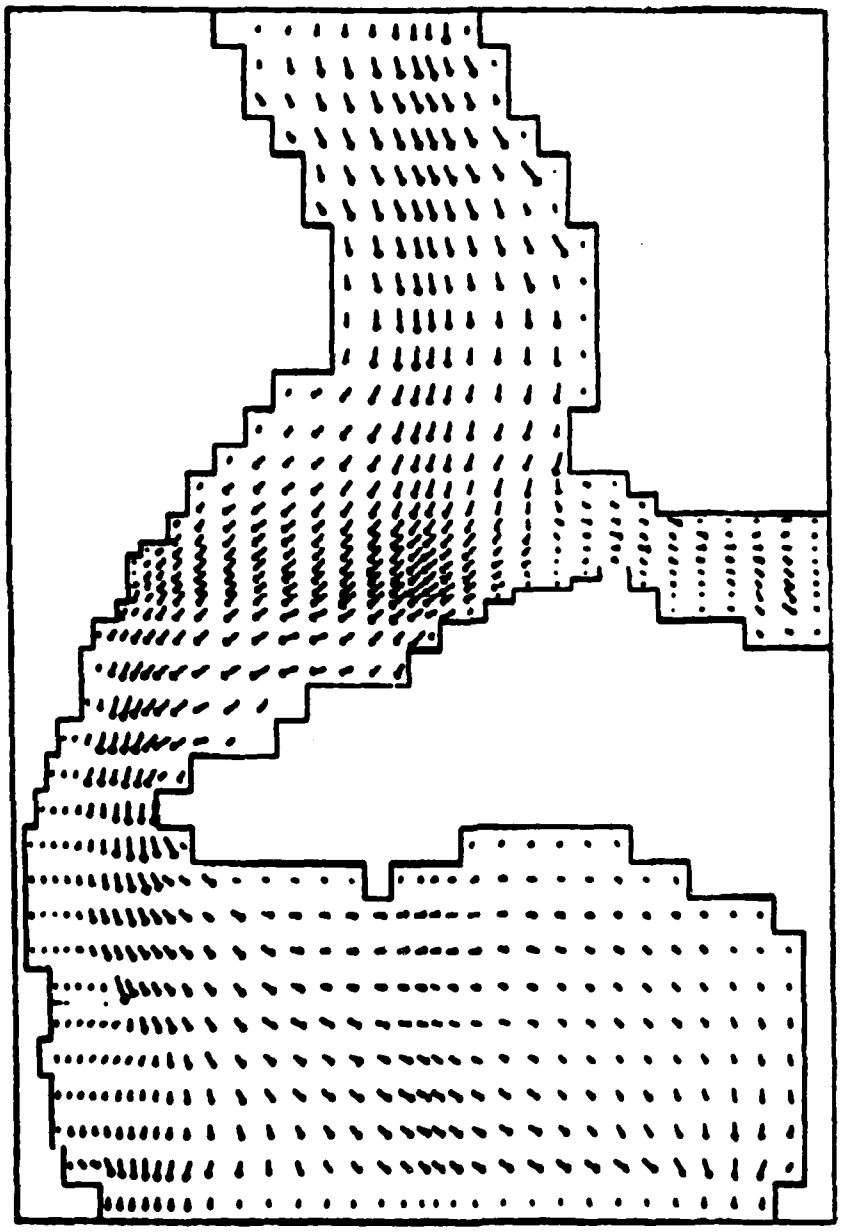

Figure 25. Circulation pattern for The Rigolets, existing conditions; maximum flood flow

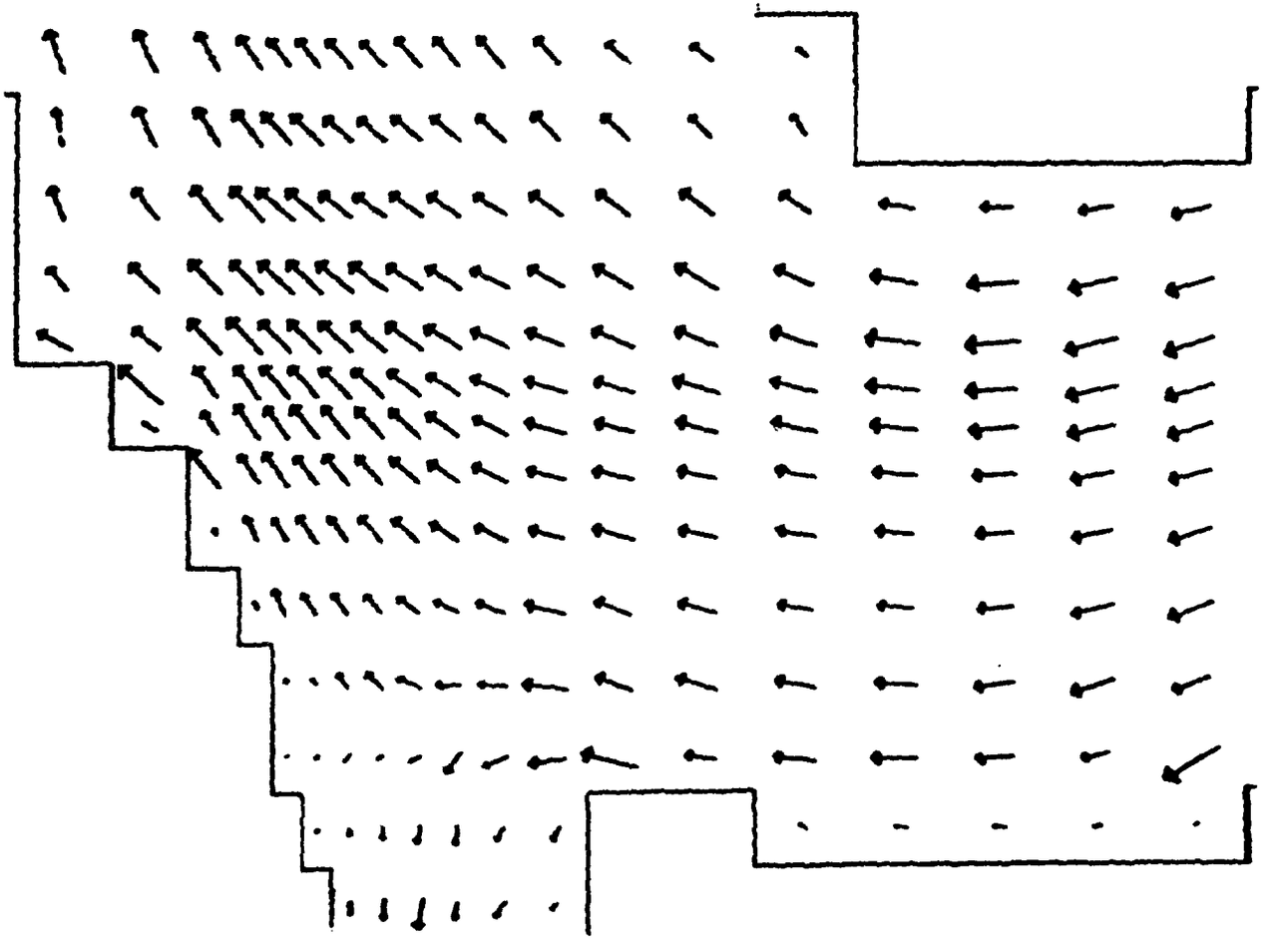

Figure 26. Enlargement of circulation pattern in the area of the proposed structure for The Rigolets, existing conditions; maximum flood flow

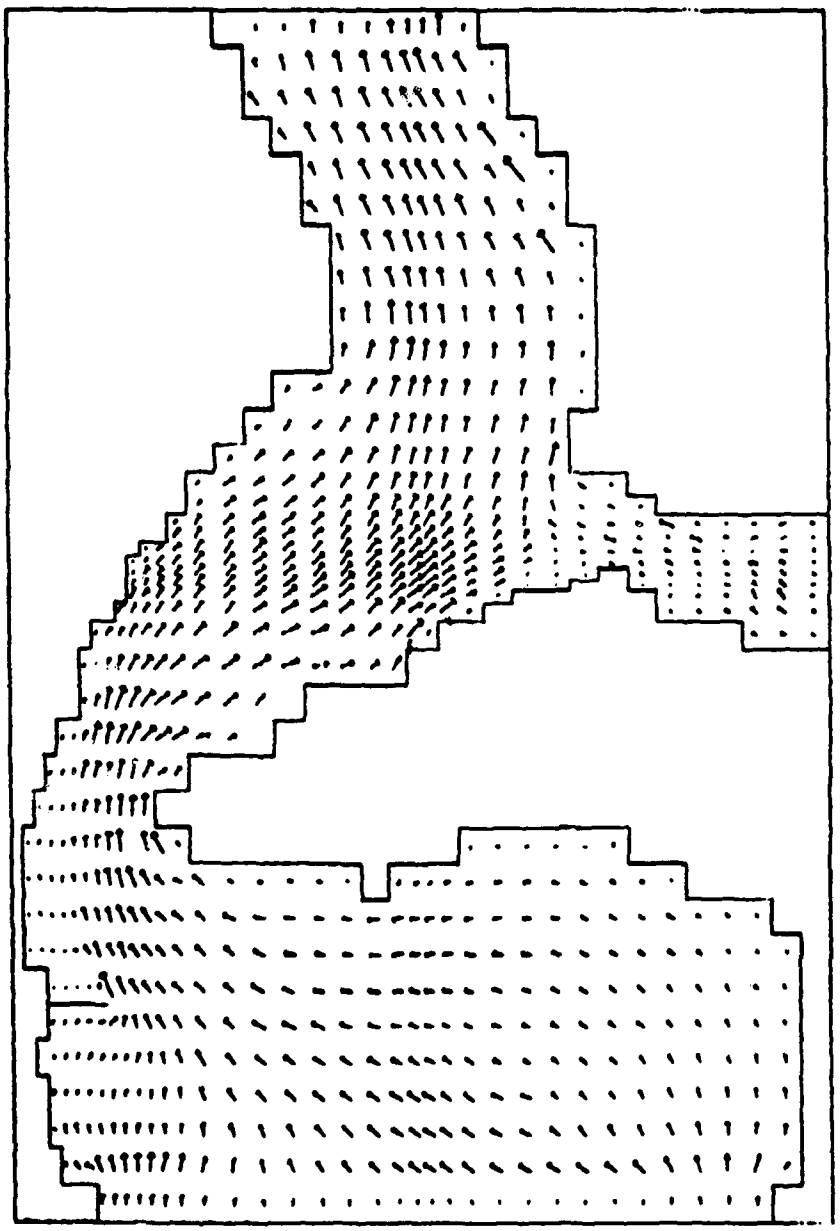

Figure 27. Circulation pattern for The Rigolets, existing conditions; maximum ebb flow

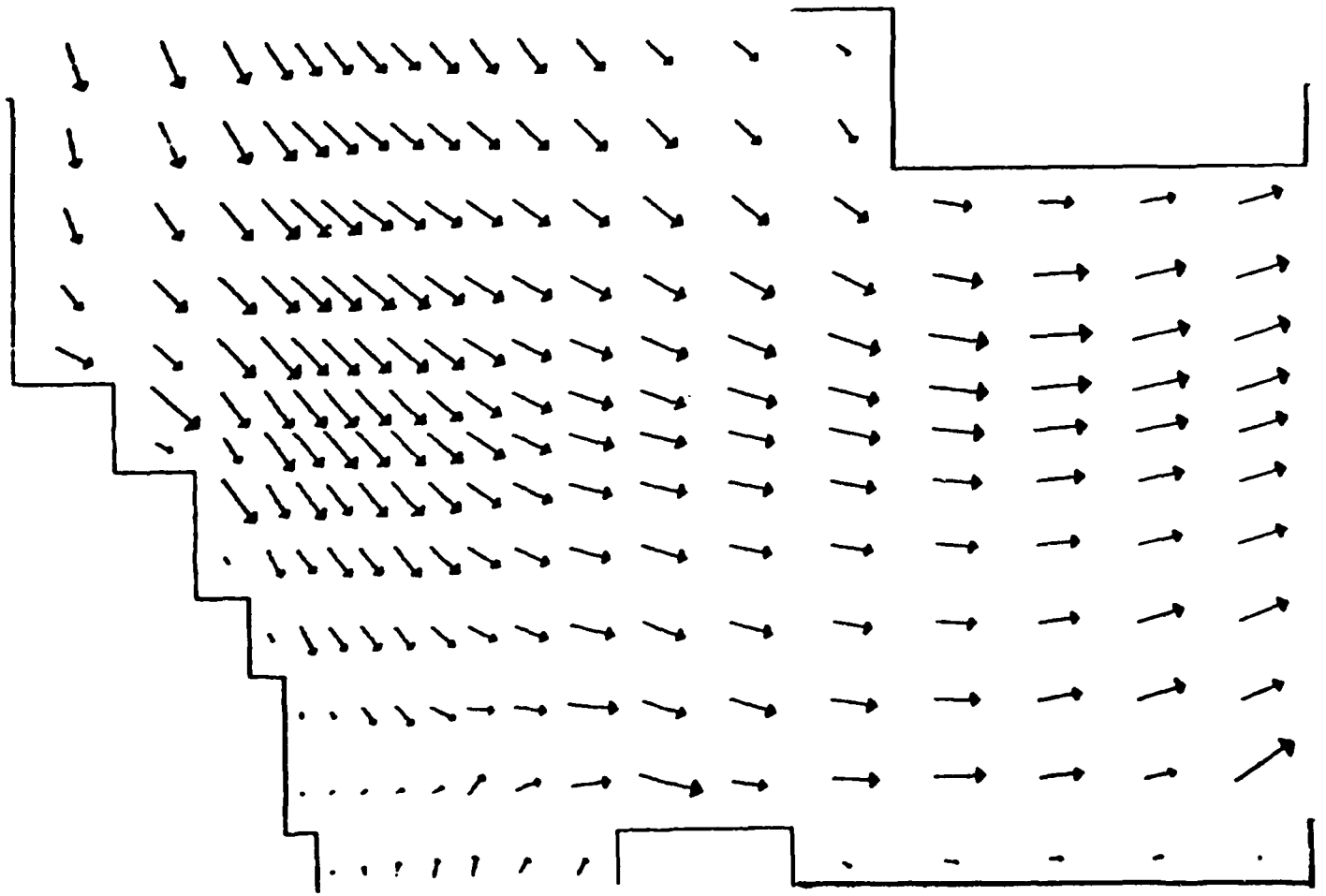

Figure 28. Enlargement of circulation pattern in the area of the proposed structure for The Rigolets, existing conditions; maximum ebb flow

Plans 2A and 2A-1 are compared with these measurements. This is reasonable since the slight shifting of the structure should only have local effects. Results of water-surface elevation and velocity computations for maximum flood and ebb flows are depicted in Figures 29-36 along with physical model measurements. Complete water-surface elevation and velocity data age given in Tables 36-38. Circulation patterns for the maximum flood and ebb flows are shown in Figures 37-44.

70. It should be noted that the velocities and water-surface elevations downstream from the structure in Plans 2A and 2A-1 are not in good agreement, particularly for flood flows. This is primarily due to the fact that the nonlinear advective terms were not used; consequently, the viscous shear flows were not simulated. As a result, the flow in the numerical model spread out behind the structure, whereas the physical model flow remained in a concentrated stream with large circulating eddies forming on either side of the structure. For the purposes of this effort (i.e., ensuring a proper numerical representation of the head losses and volume transport across the control structures), the nonlinear advective terms are not important.

71. In order to test the effects of the nonlinear advective terms on velocities and water-surface elevations and to demonstrate that a much better comparison of numerical model and physical model circulation patterns near the control structure can be obtained with the more complete set of equations, a demonstration model was run using the fully advective solution scheme. As shown in Tables 36 and 37 and Figures 45-48, use of this solution scheme results in flows that are very similar to those observed in the physical model. However, since this numerical model is much more expensive to run and the overall results of the linear version of the model are adequate for the purposes of this study, no further runs were made using the nonlinear advective terms. If detailed analyses flow patterns in the vicinity of the structures are desired, these models with the nonlinear advective terms included could be used for that purpose.

Seabrook Canal model

72. The Seabrook Lock and control structure were modeled for base

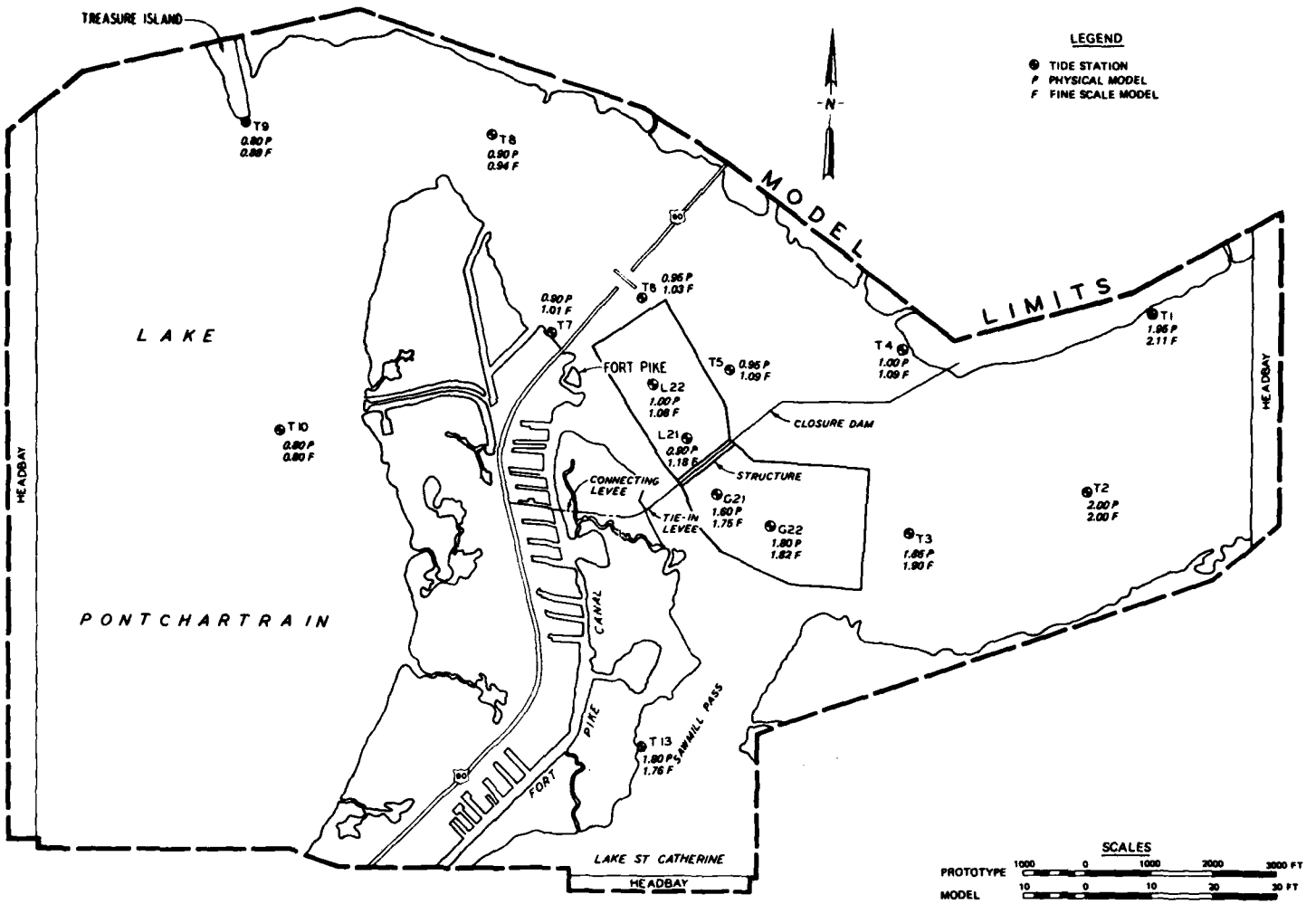

Figure 29. Surface elevation, ft NGVD, maximum flood flow; physical versus fine scale model for Plan 2A in The Rigolets

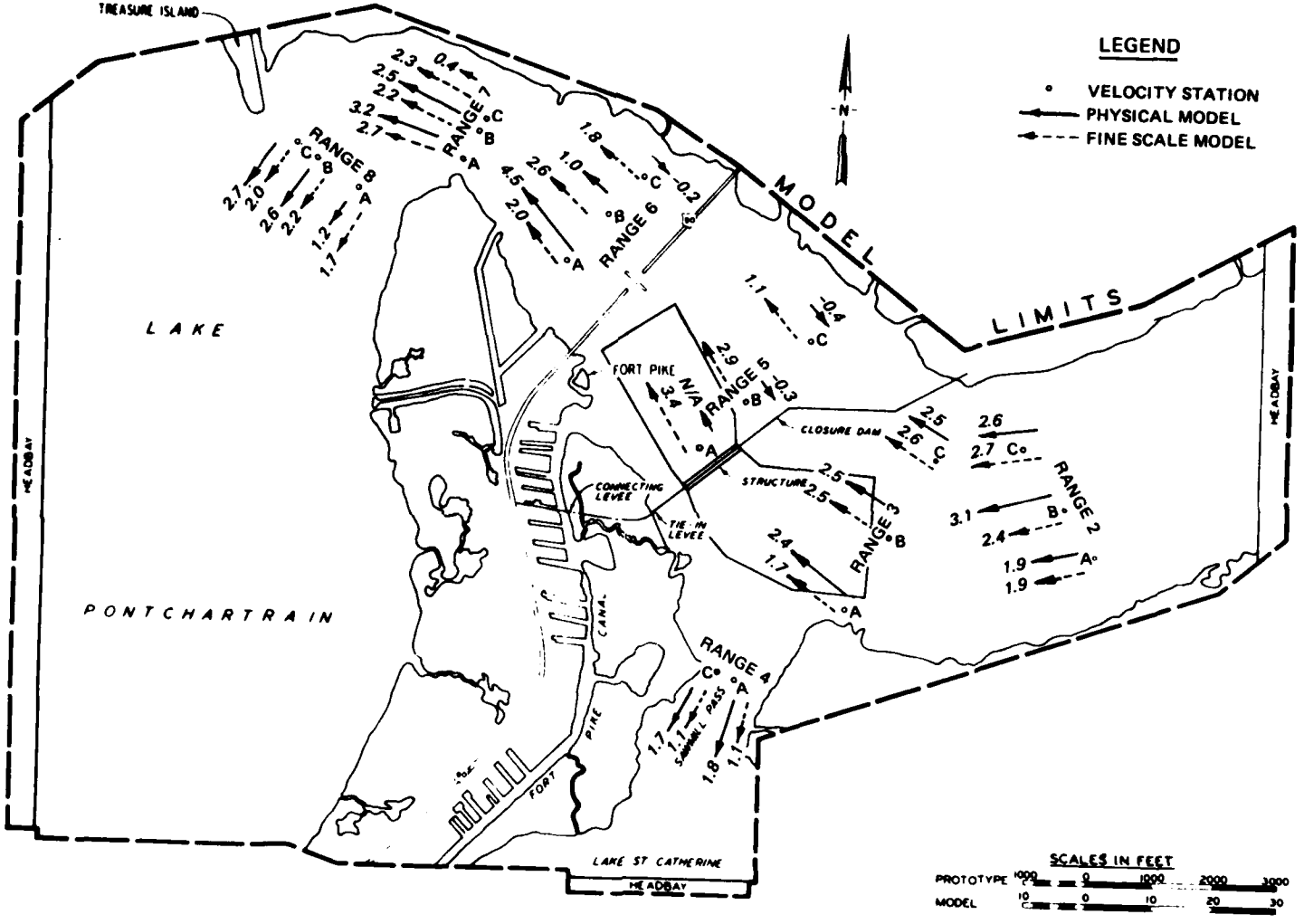

Figure 30. Velocities, fps, maximum flood flow; physical versus fine scale model for Plan 2A in The Rigolets

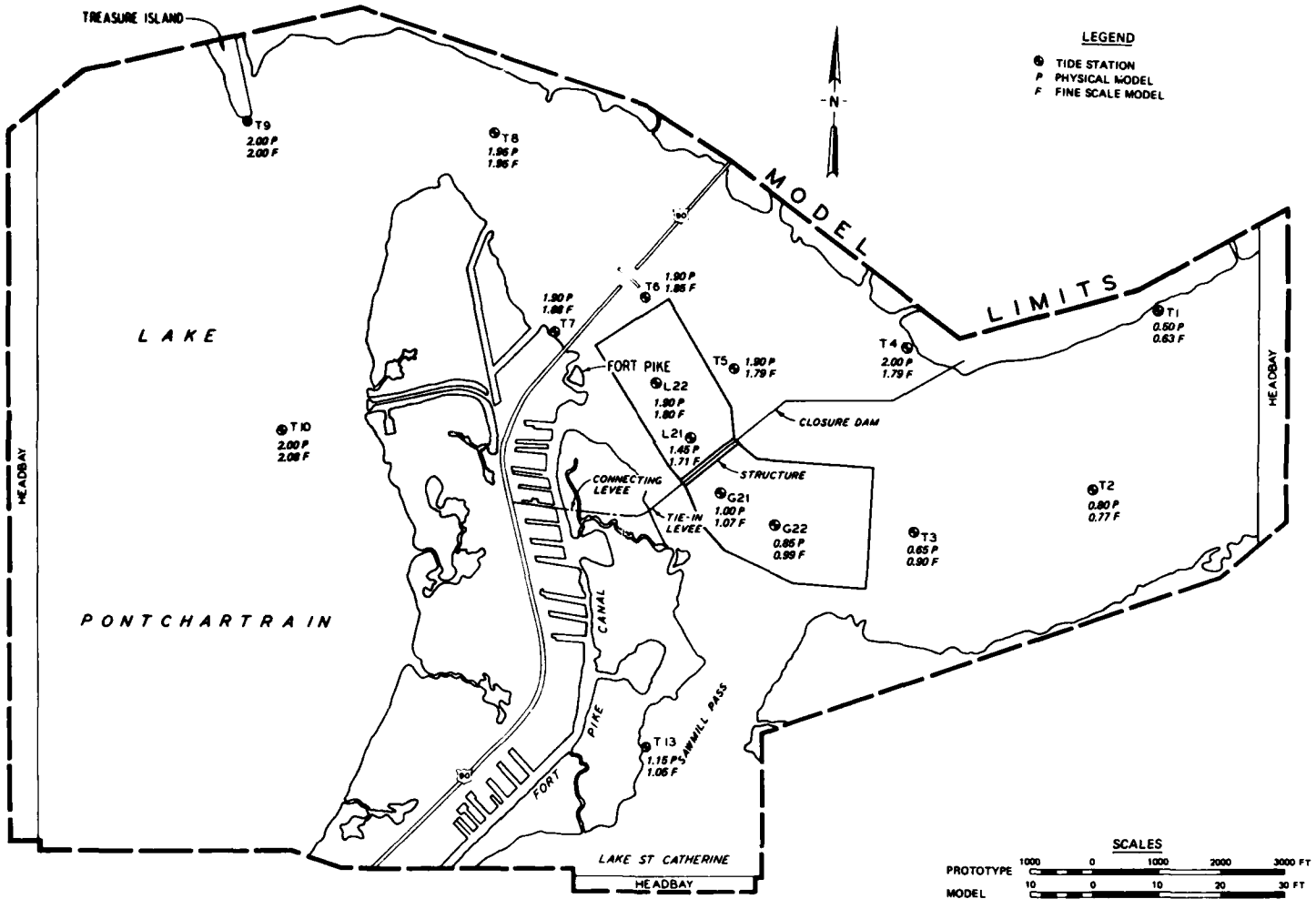

Figure 31. Surface elevation, ft NGVD, maximum ebb flow; physical versus fine scale model for Plan 2A in The Rigolets

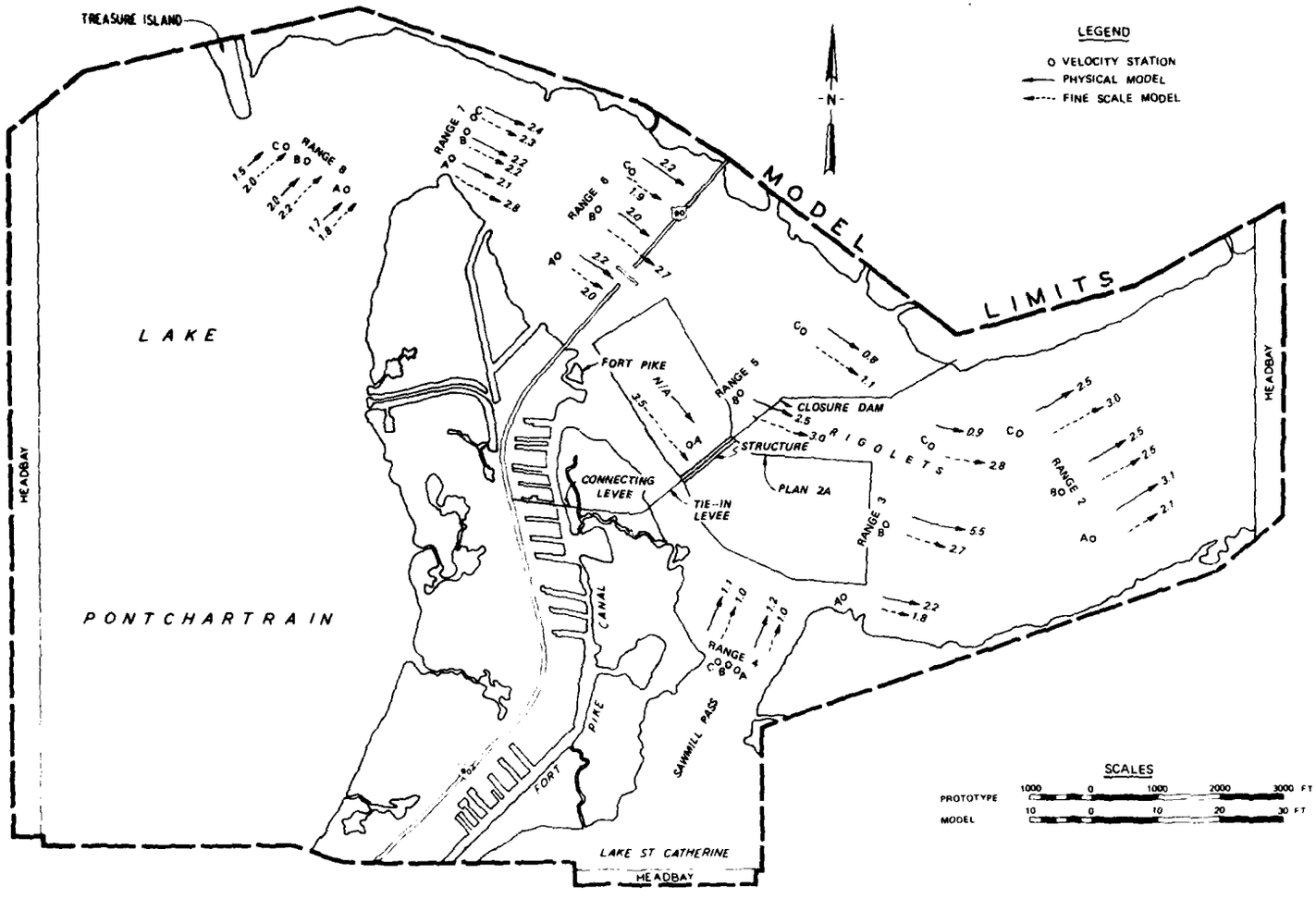

Figure 32. Velocities, fps, maximum ebb flow; physical versus fine scale model for Plan 2A in The Rigolets

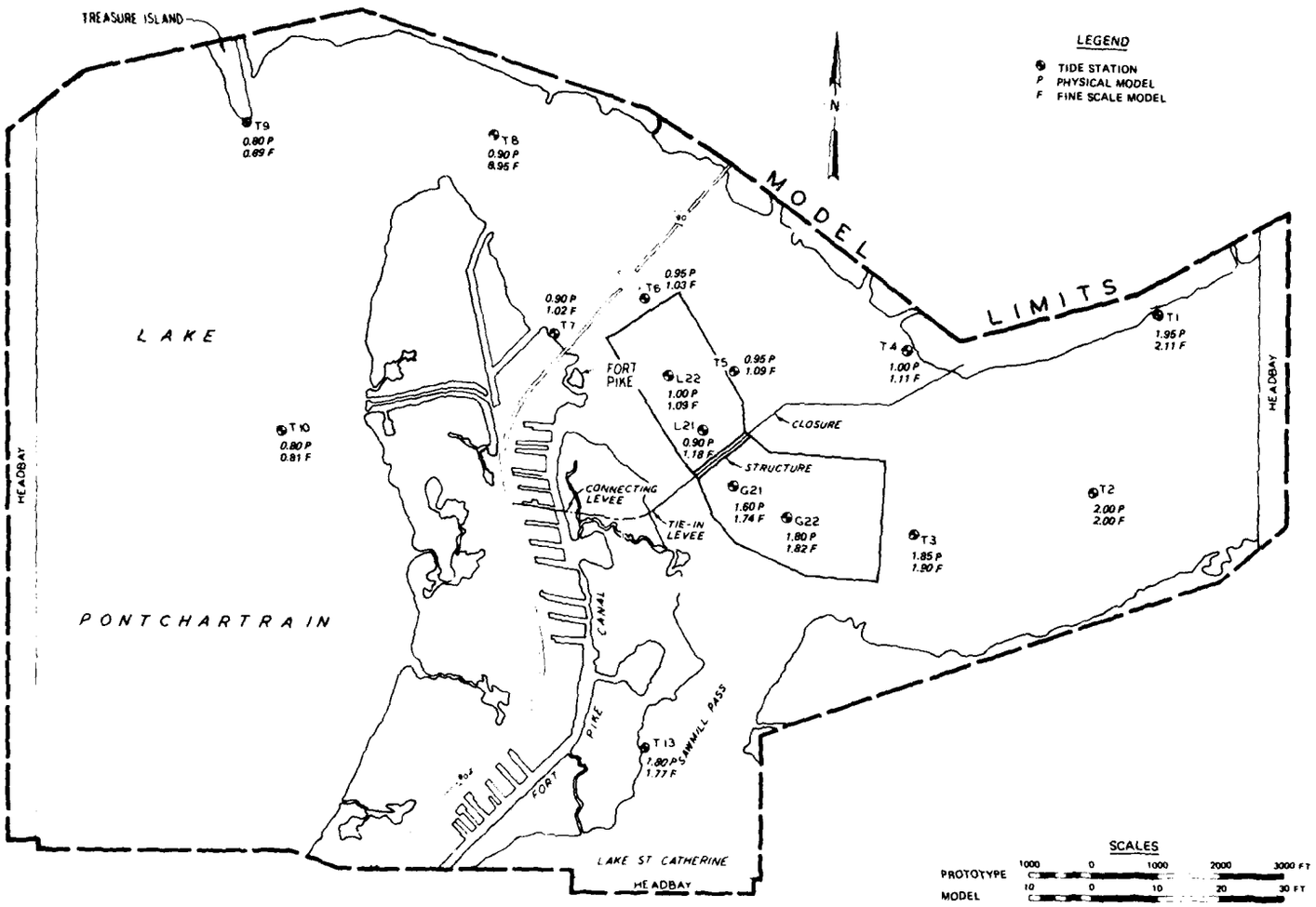

Figure 33. Surface elevation ft NGVD, maximum flood flow; physical versus fine scale model for Plan 2A-1 in The Rigolets

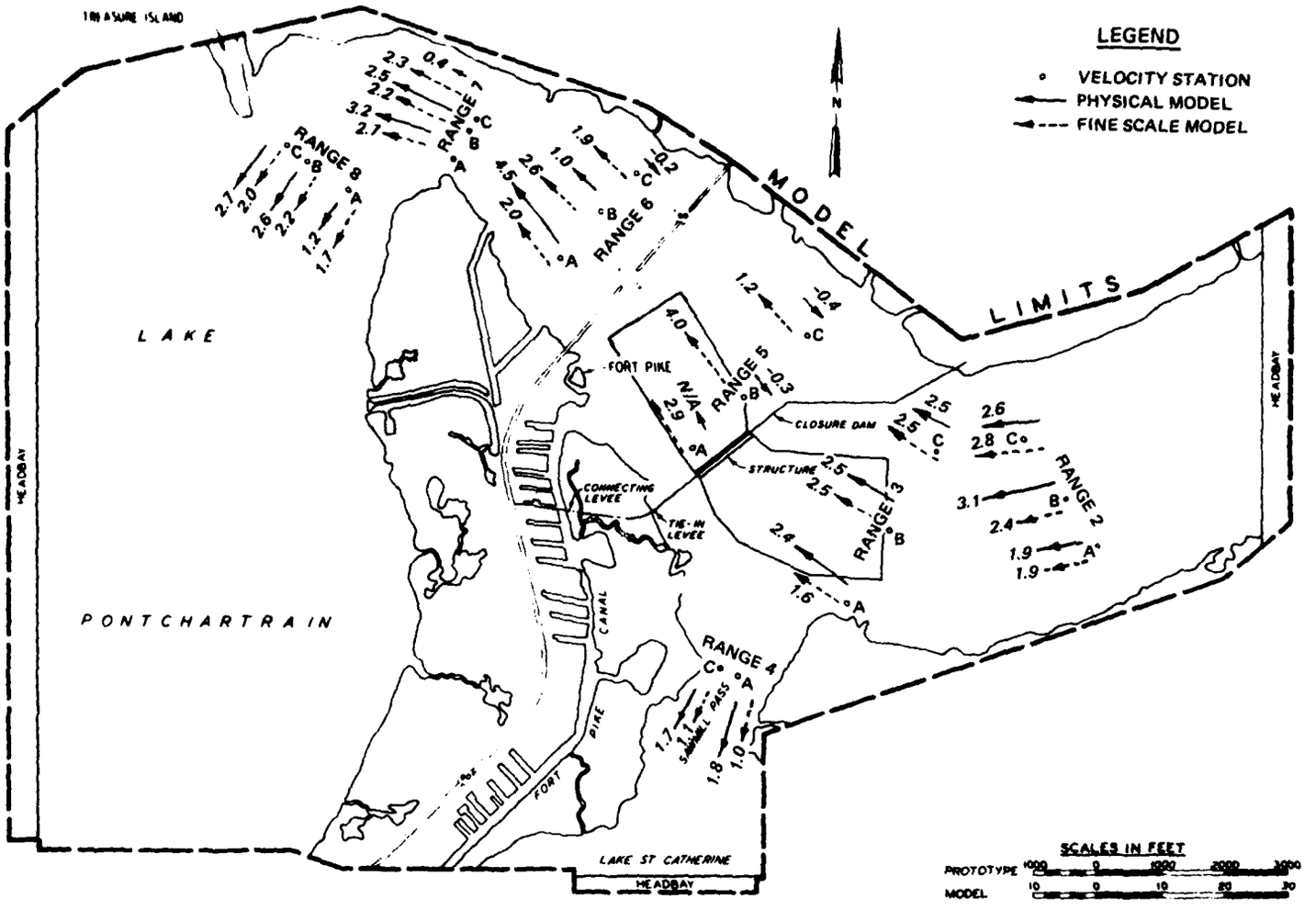

Figure 34. Velocities, fps, maximum flood flow; physical versus fine scale model for Plan 2A-1 in The Rigolets

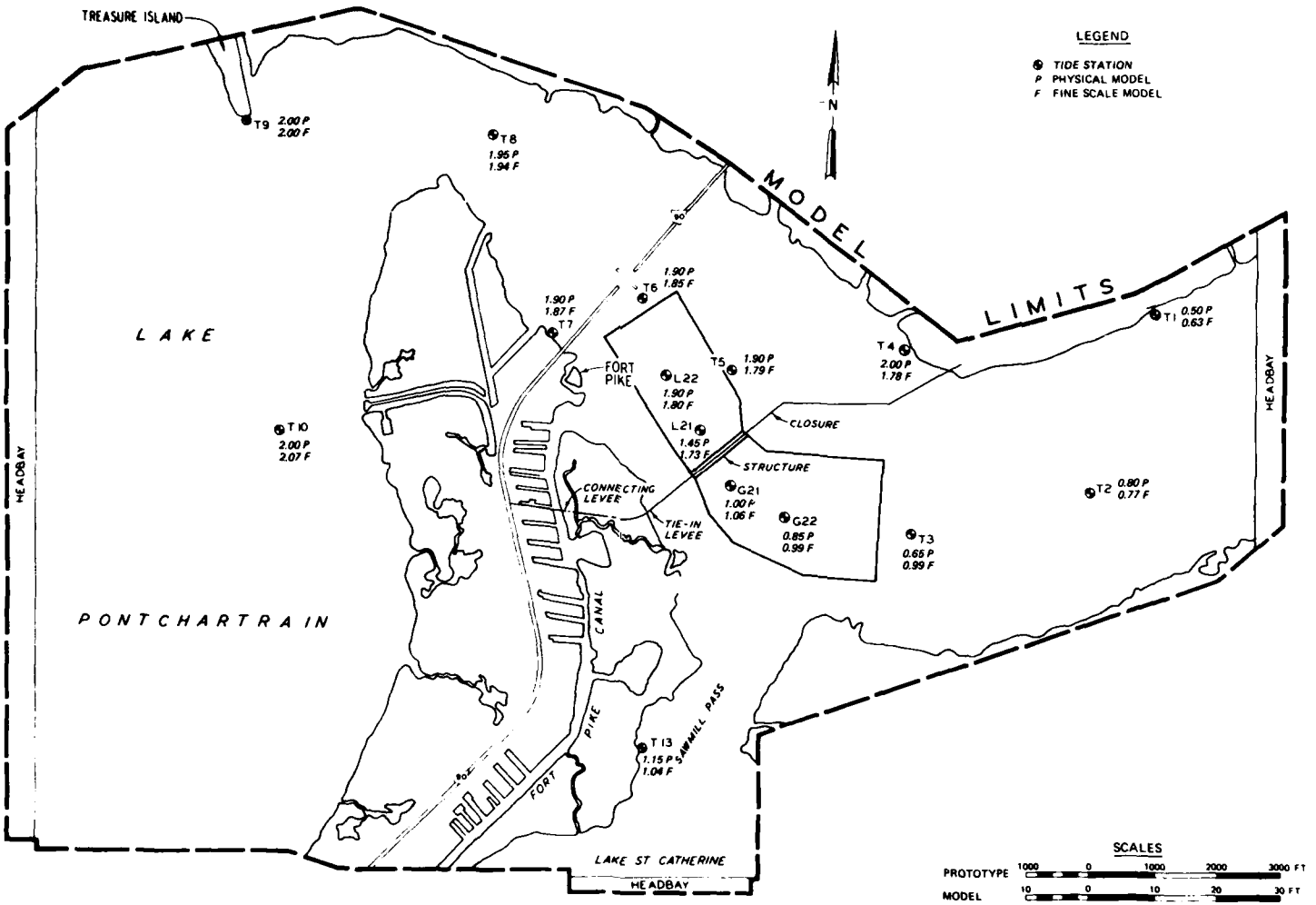

Figure 35. Surface elevation, ft NGVD, maximum ebb flow; physical versus fine scale model for Plan 2A-1 in The Rigolets

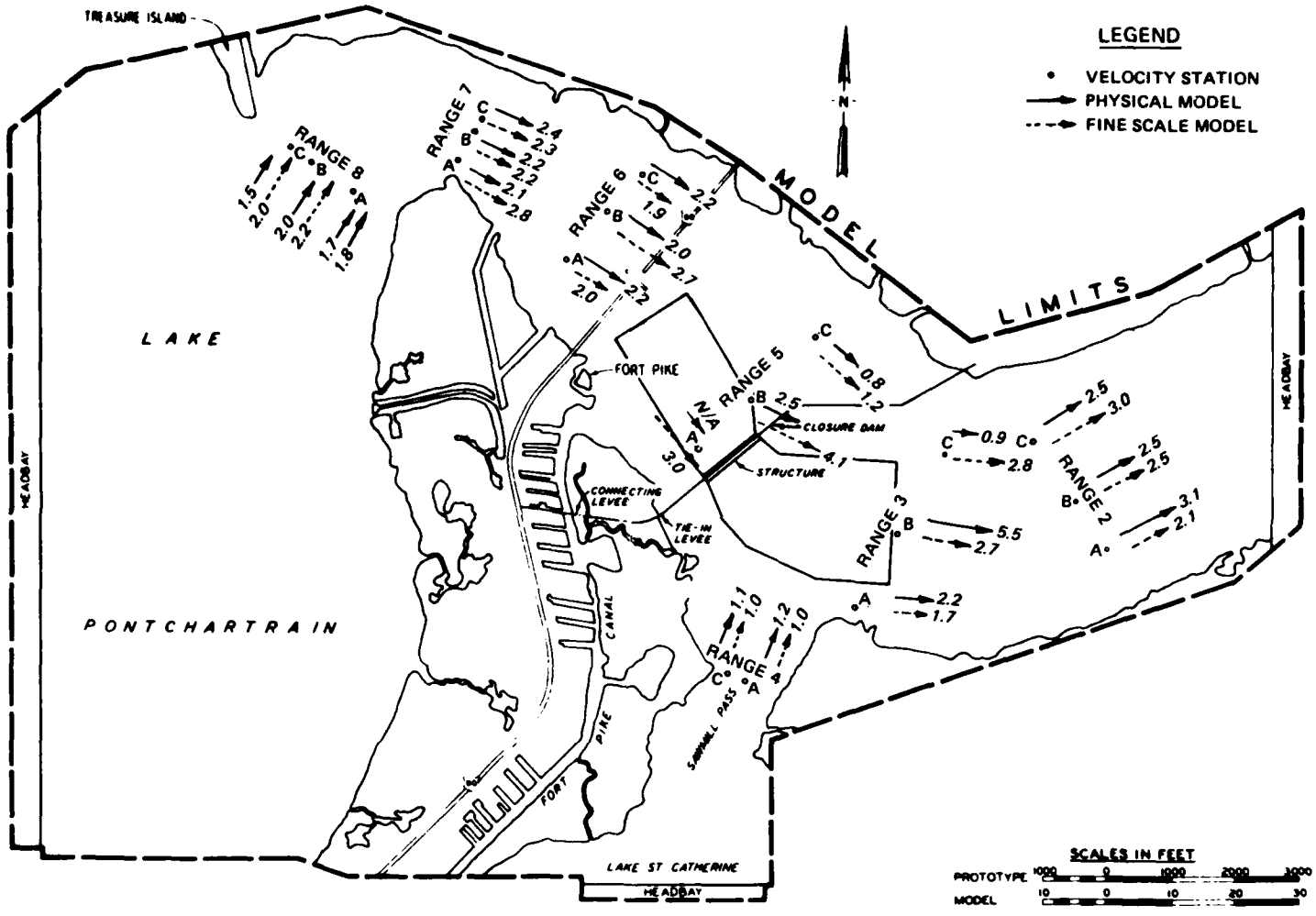

Figure 36. Velocities, fps, maximum ebb flow; physical versus fine scale model for Plan 2A-1 in The Rigolets

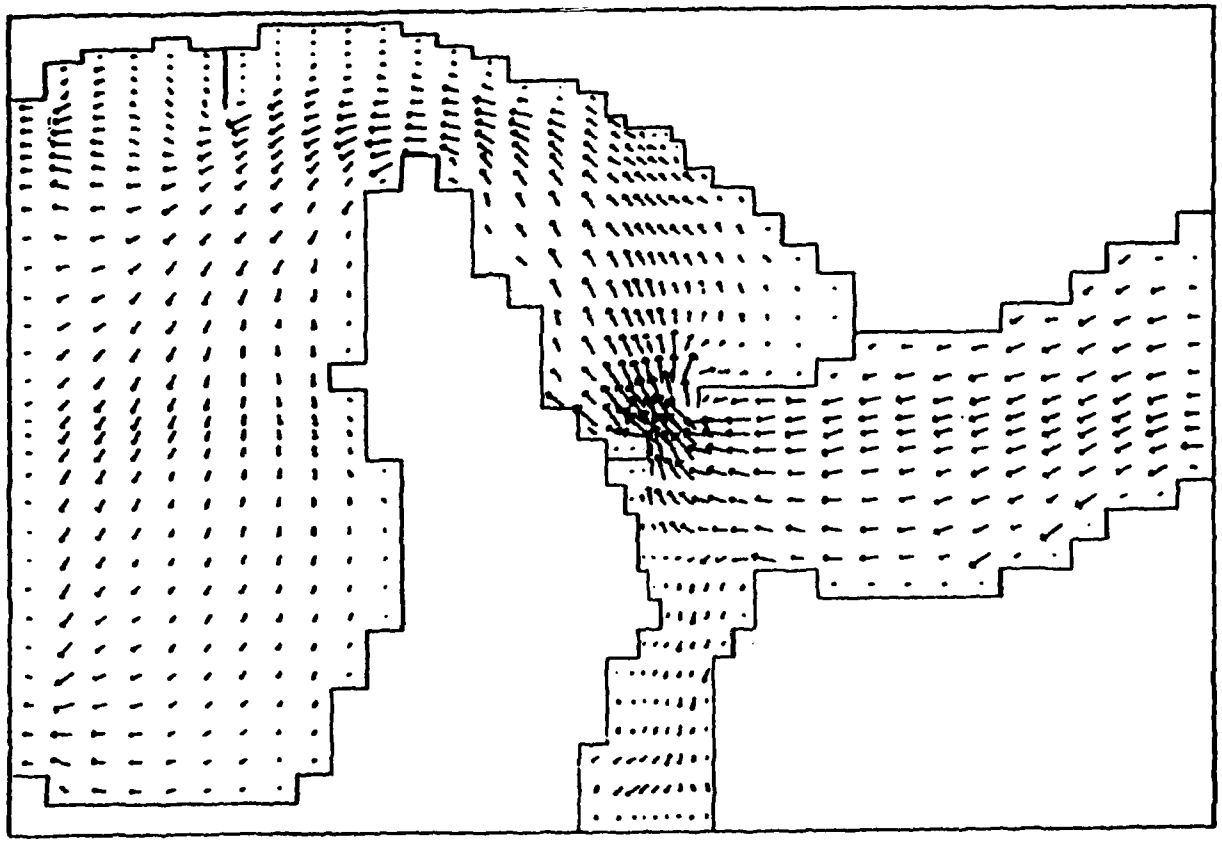

Figure 37. Circulation pattern for The Rigolets, Plan 2A; maximum flood flow

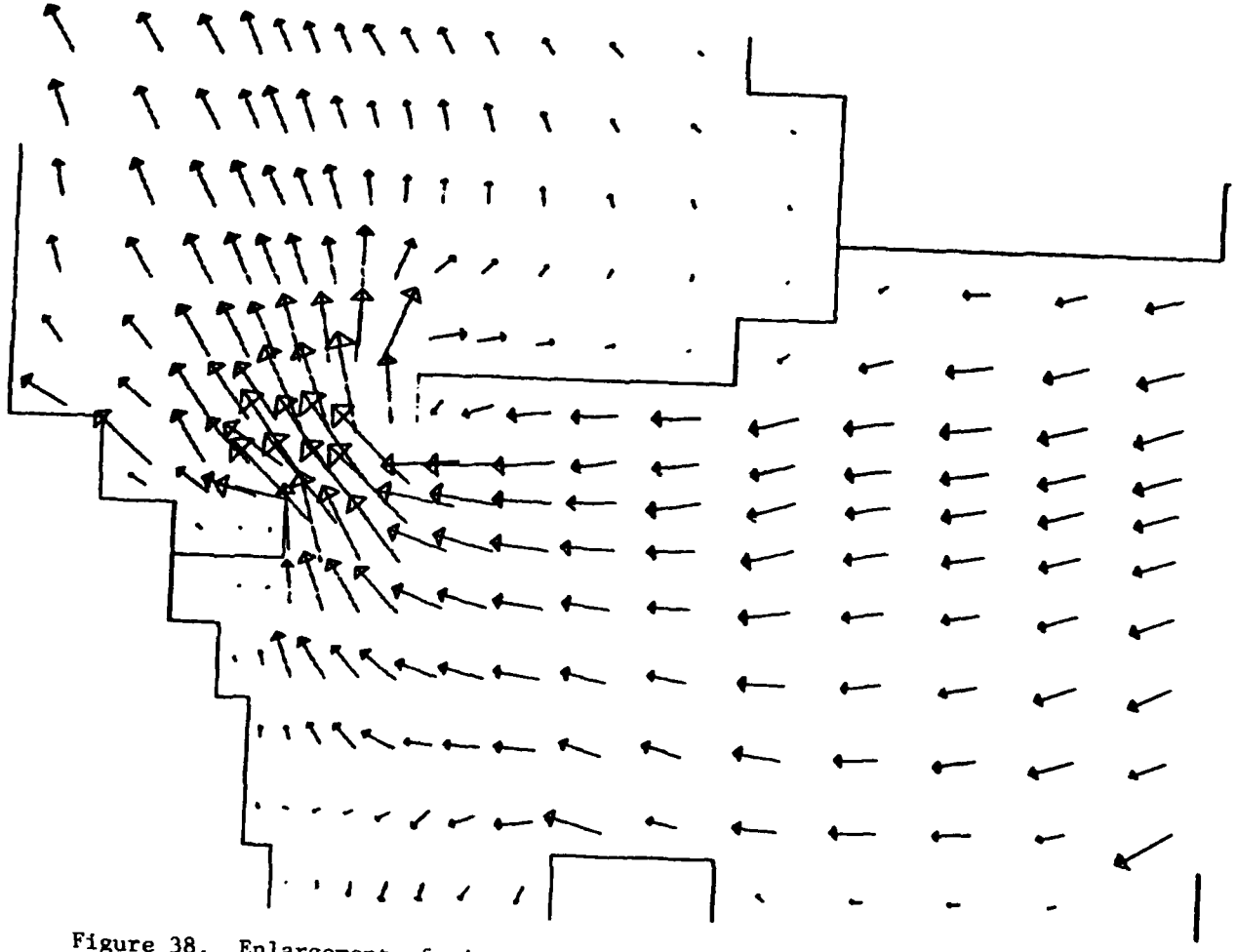

Figure 38. Enlargement of circulation pattern in the area of the proposed structure for The Rigolets, Plan 2A; maximum flood flow

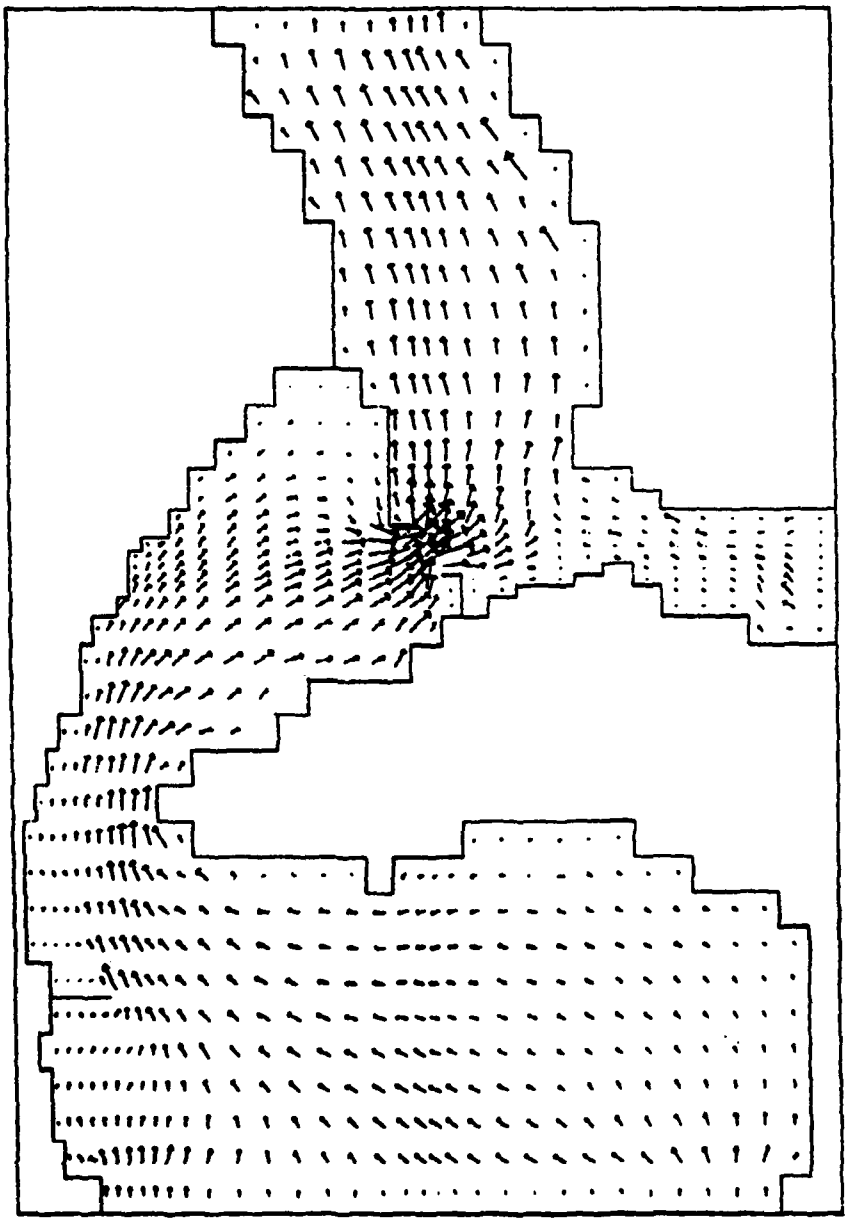

Figure 39. Circulation pattern for The Rigolets, Plan 2A; maximum ebb flow

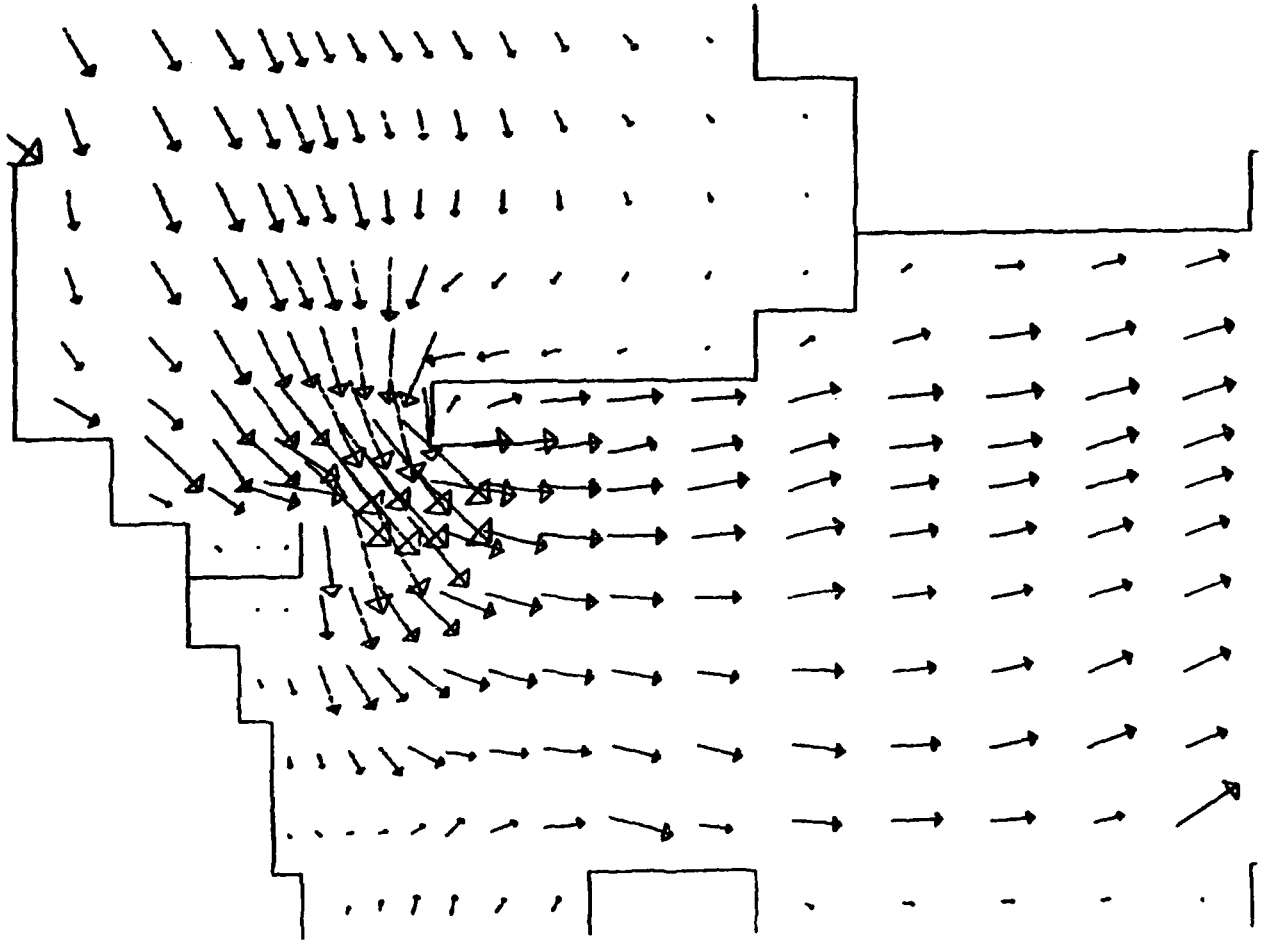

Figure 40. Enlargement of circulation pattern in the area of the proposed structure for The Rigolets, Plan 2A; maximum ebb flow

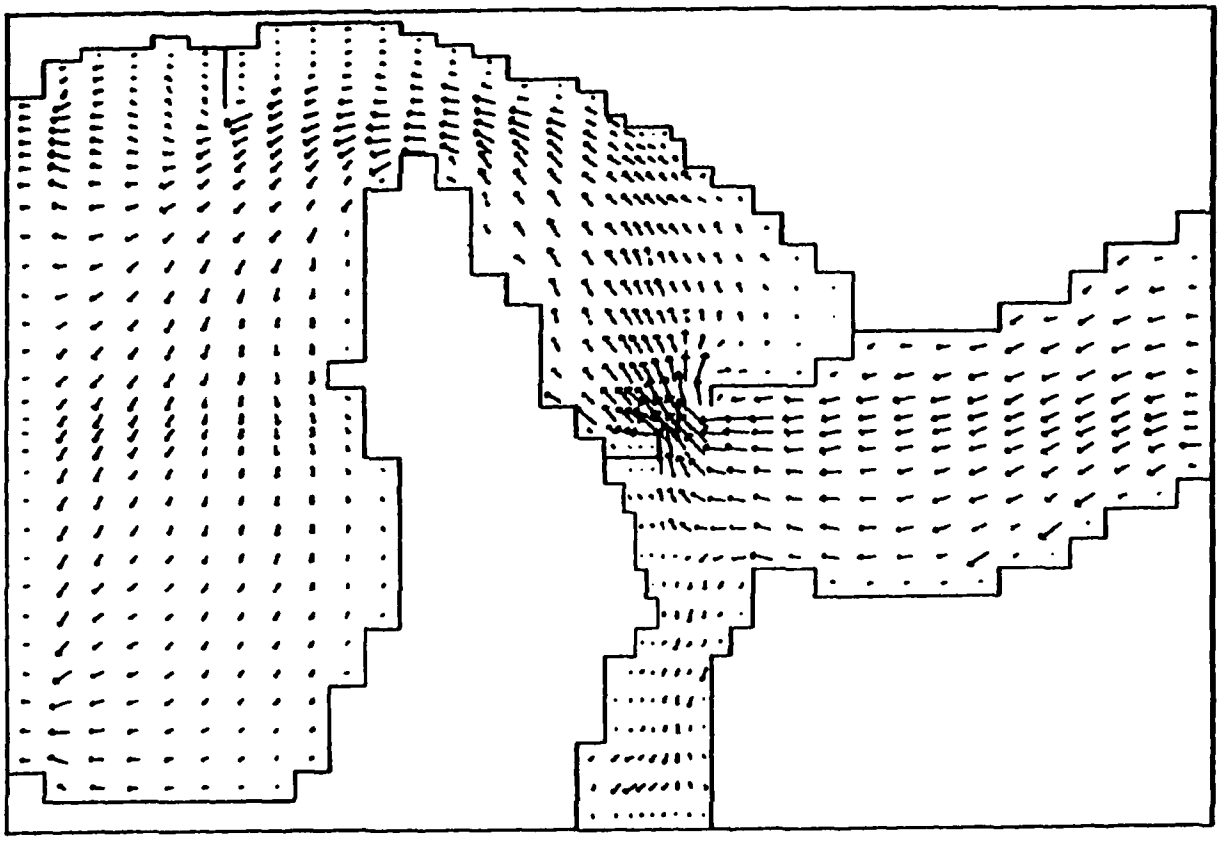

Figure 41. Circulation pattern for The Rigolets, Plan 2A-1; maximum flood flow

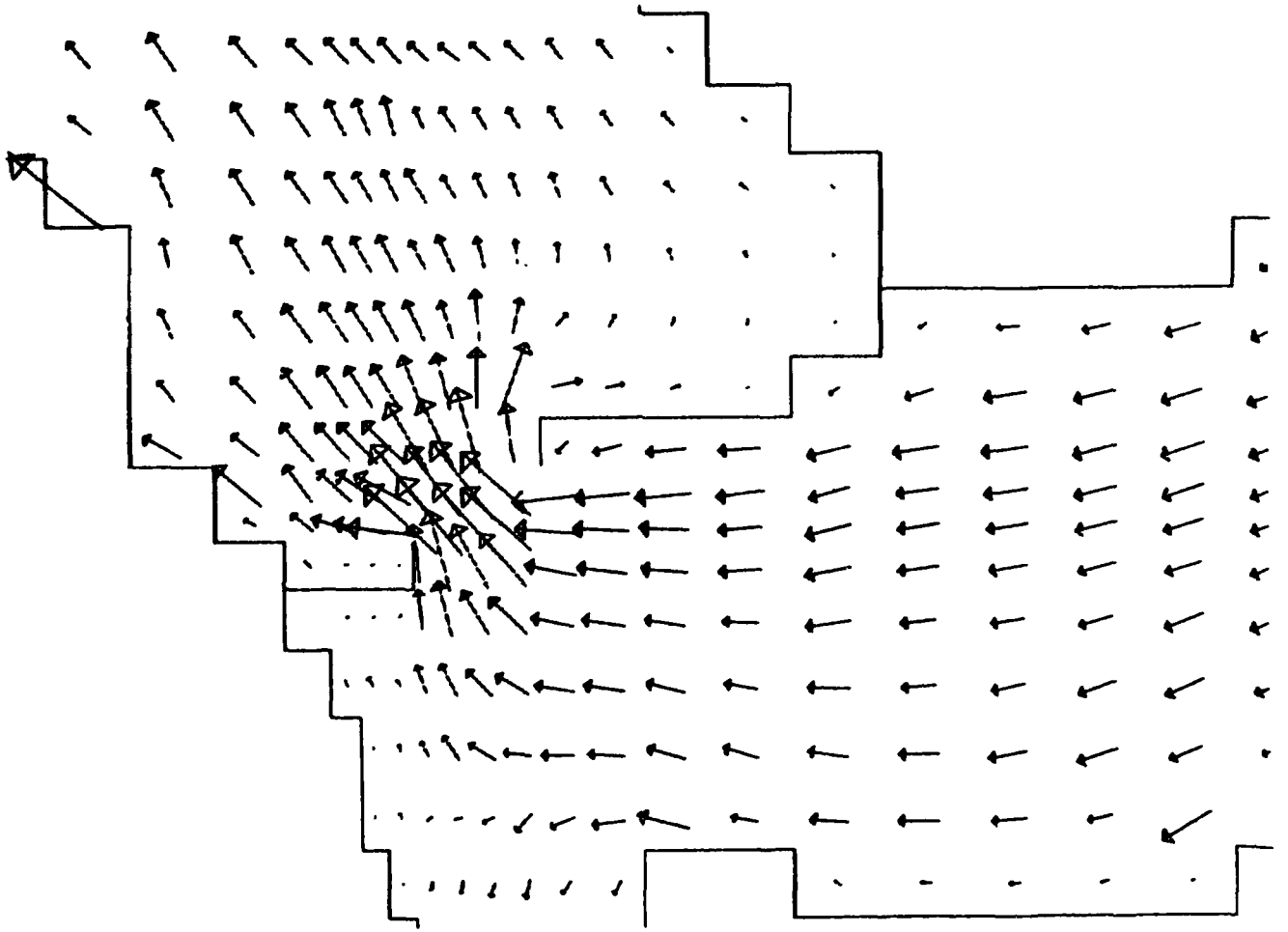

Figure 42. Enlargement of circulation pattern in the area of the proposed structure for The Rigolets, Plan 2A-1; maximum flood flow

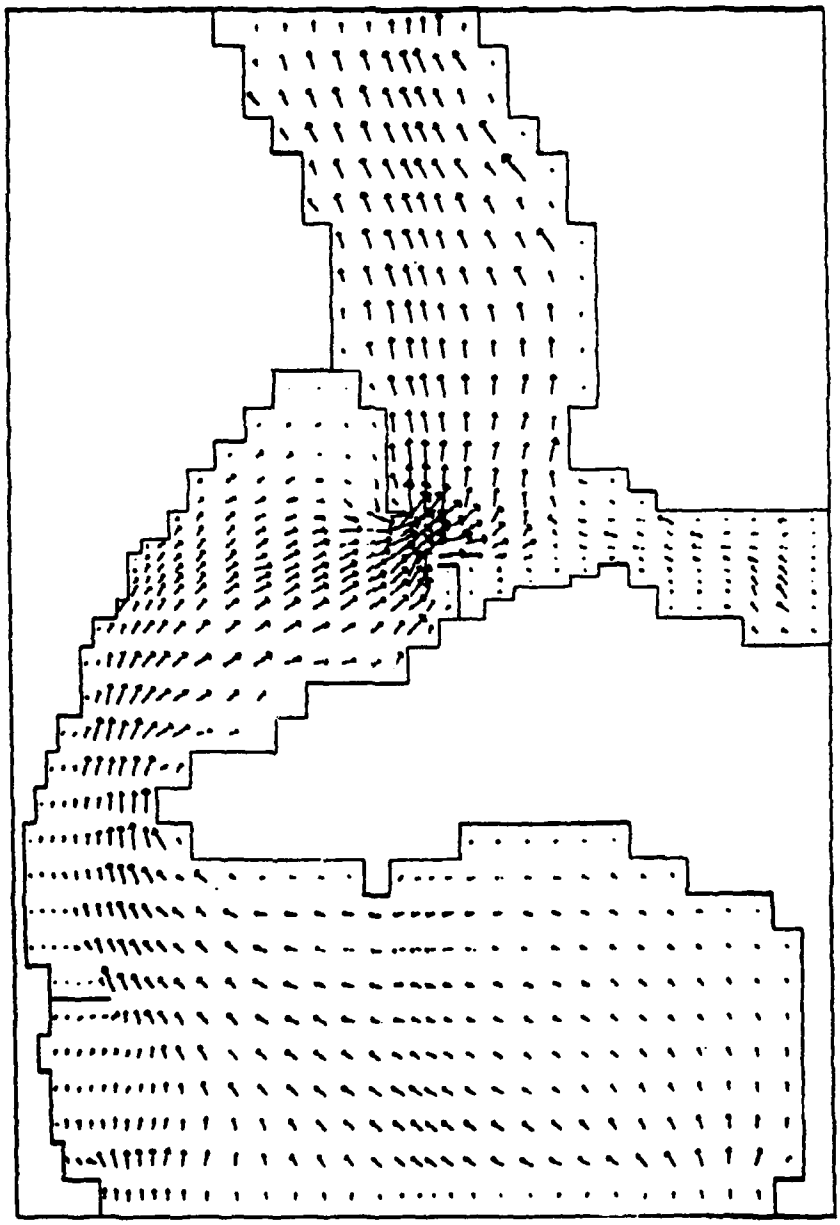

Figure 43. Circulation pattern for The Rigolets, Plan 2A-1; maximum ebb flow

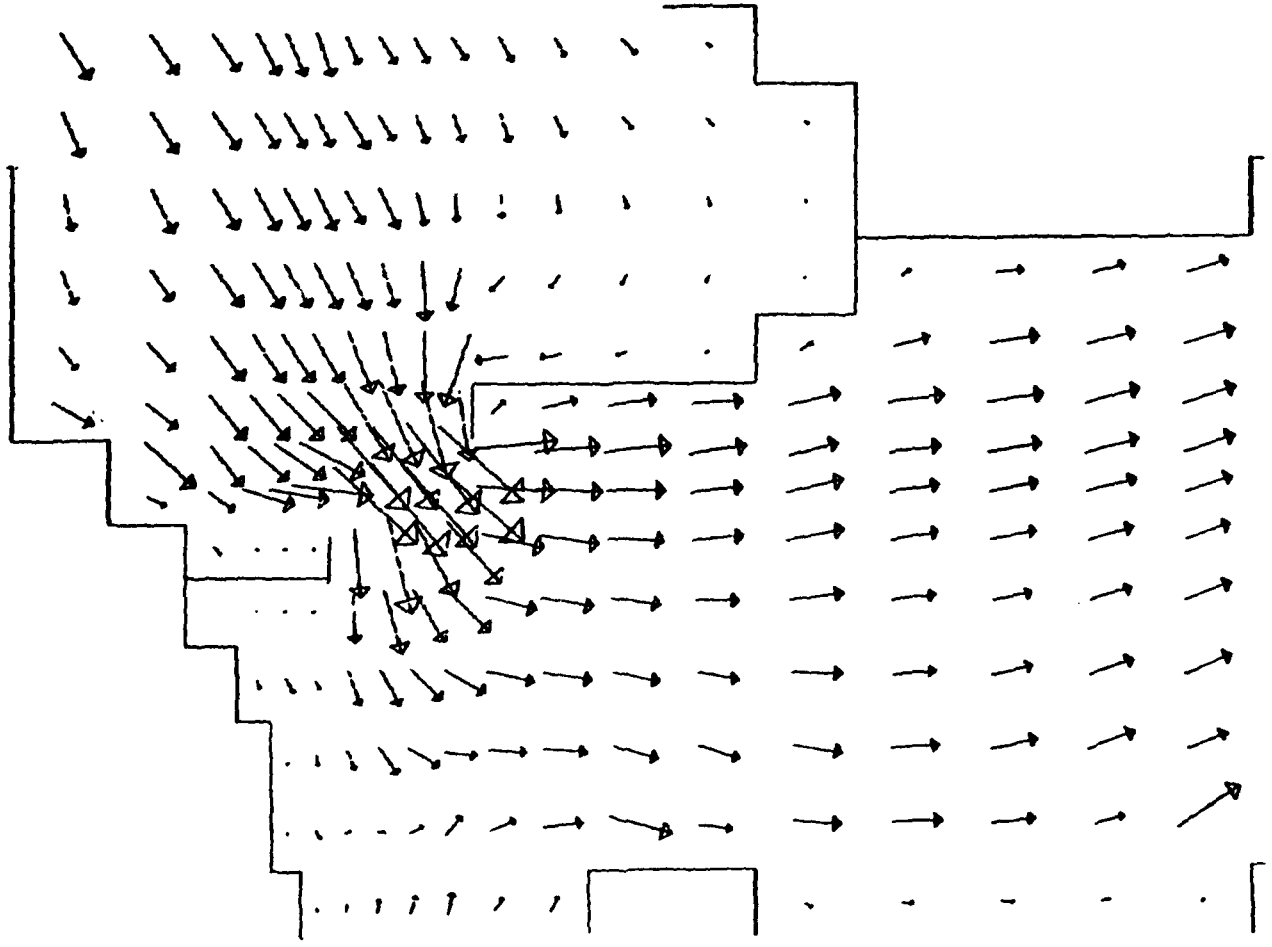

Figure 44. Enlargement of circulation pattern in the area of the proposed structure for The Rigolets, Plan 2A-1; maximum ebb flow

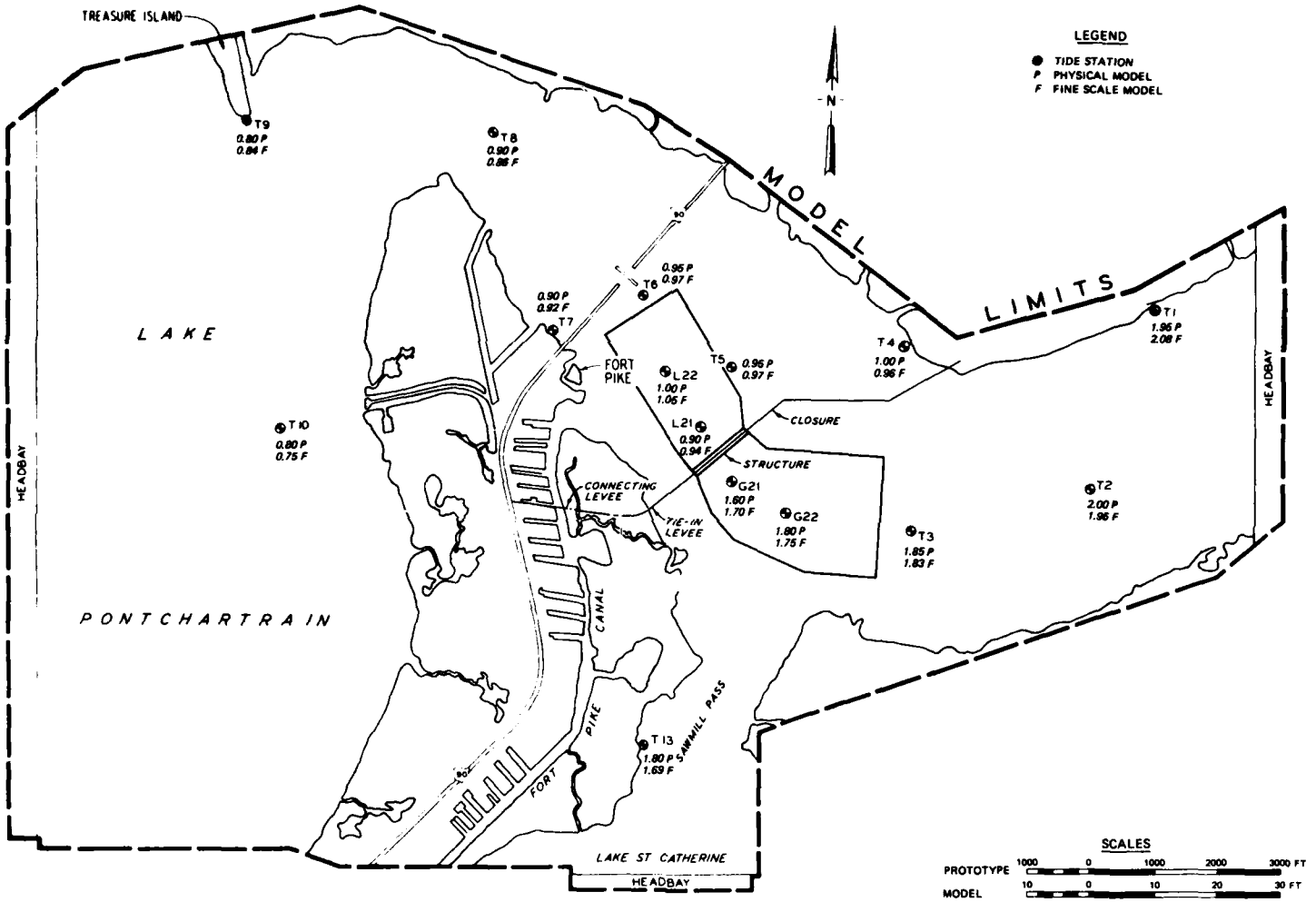

Figure 45. Surface elevation, ft NGVD, maximum flood flow with advective terms included; physical versus fine scale model for Plan 2A-1 in The Rigolets

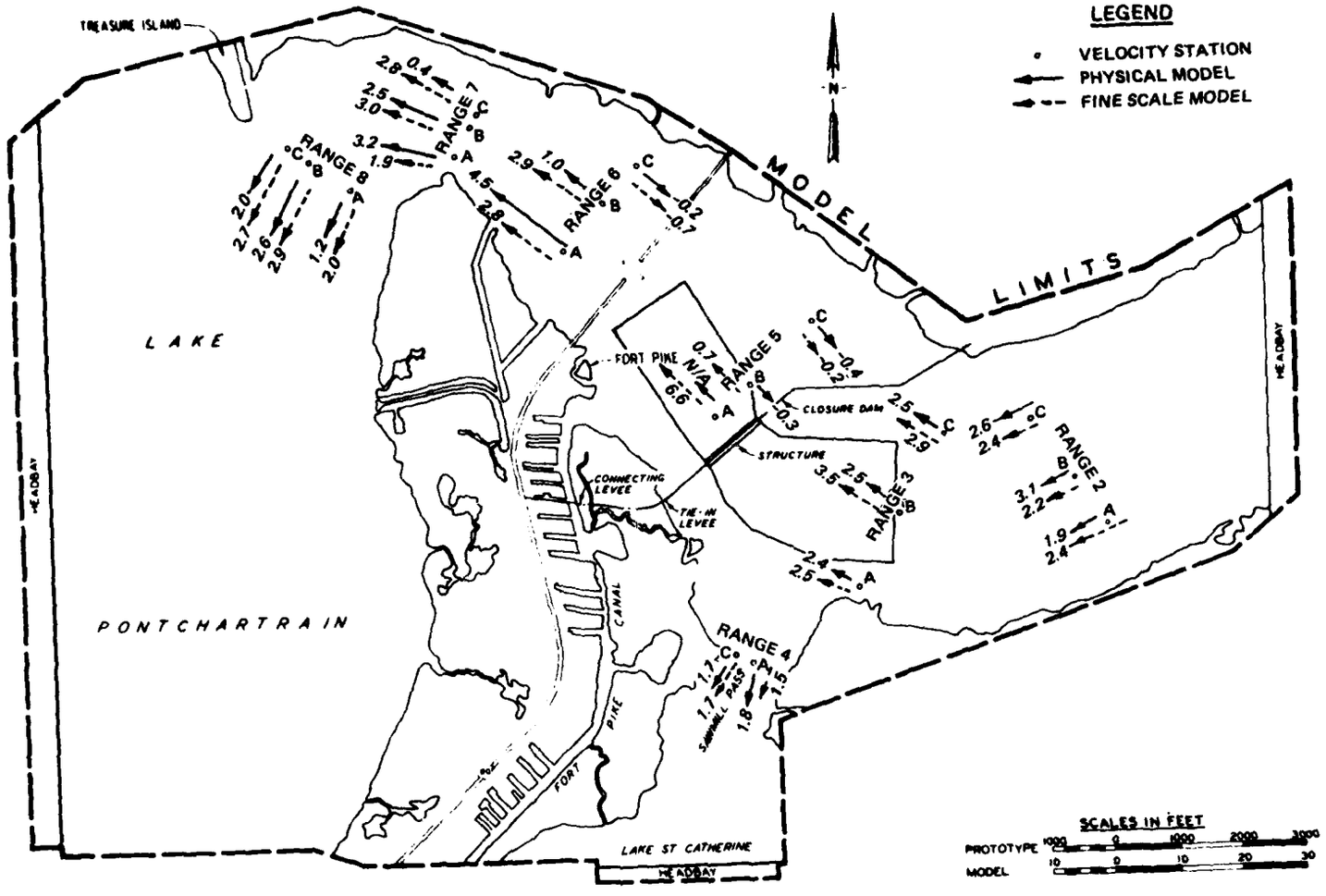

Figure 46. Velocities, fps, maximum flood flow with advective terms included; physical versus fine scale model for Plan 2A-1 in The Rigolets

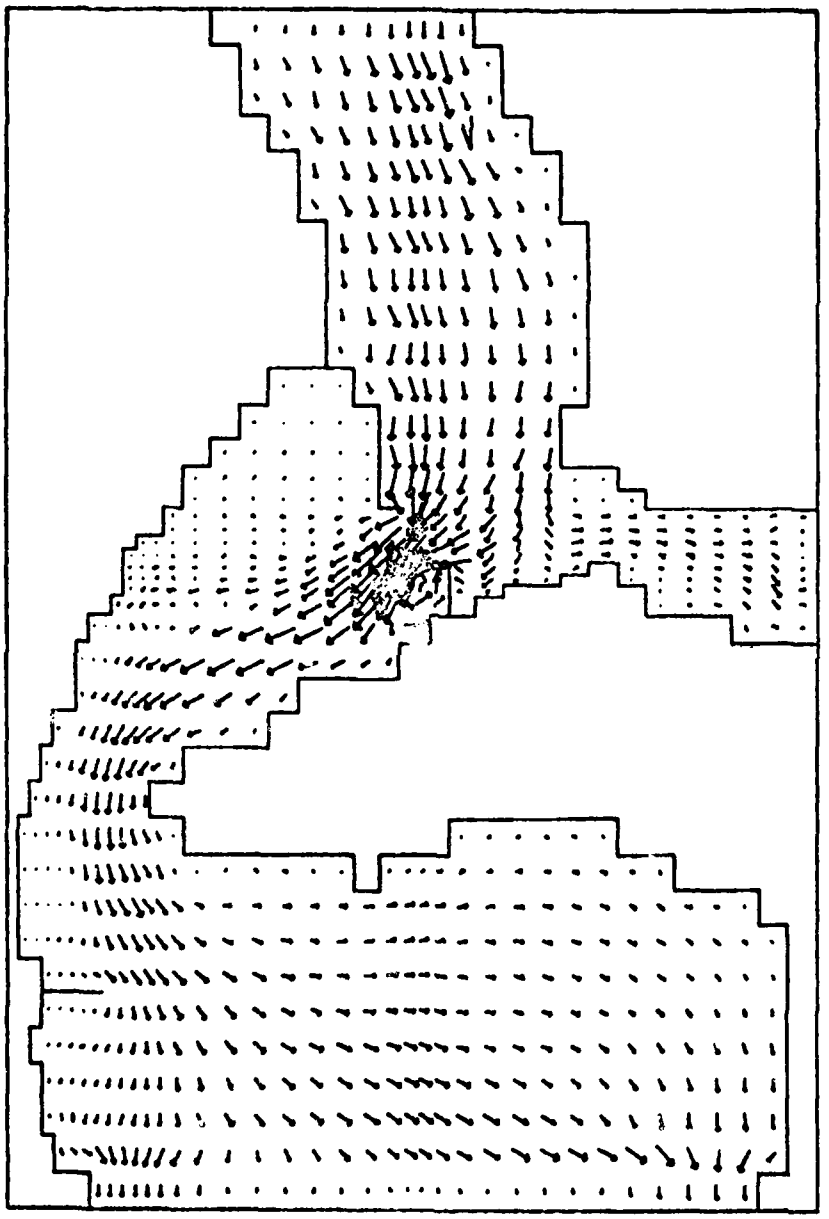

Figure 47. Circulation pattern for The Rigolets, Plan 2A-1; maximum flood flow with advective terms included

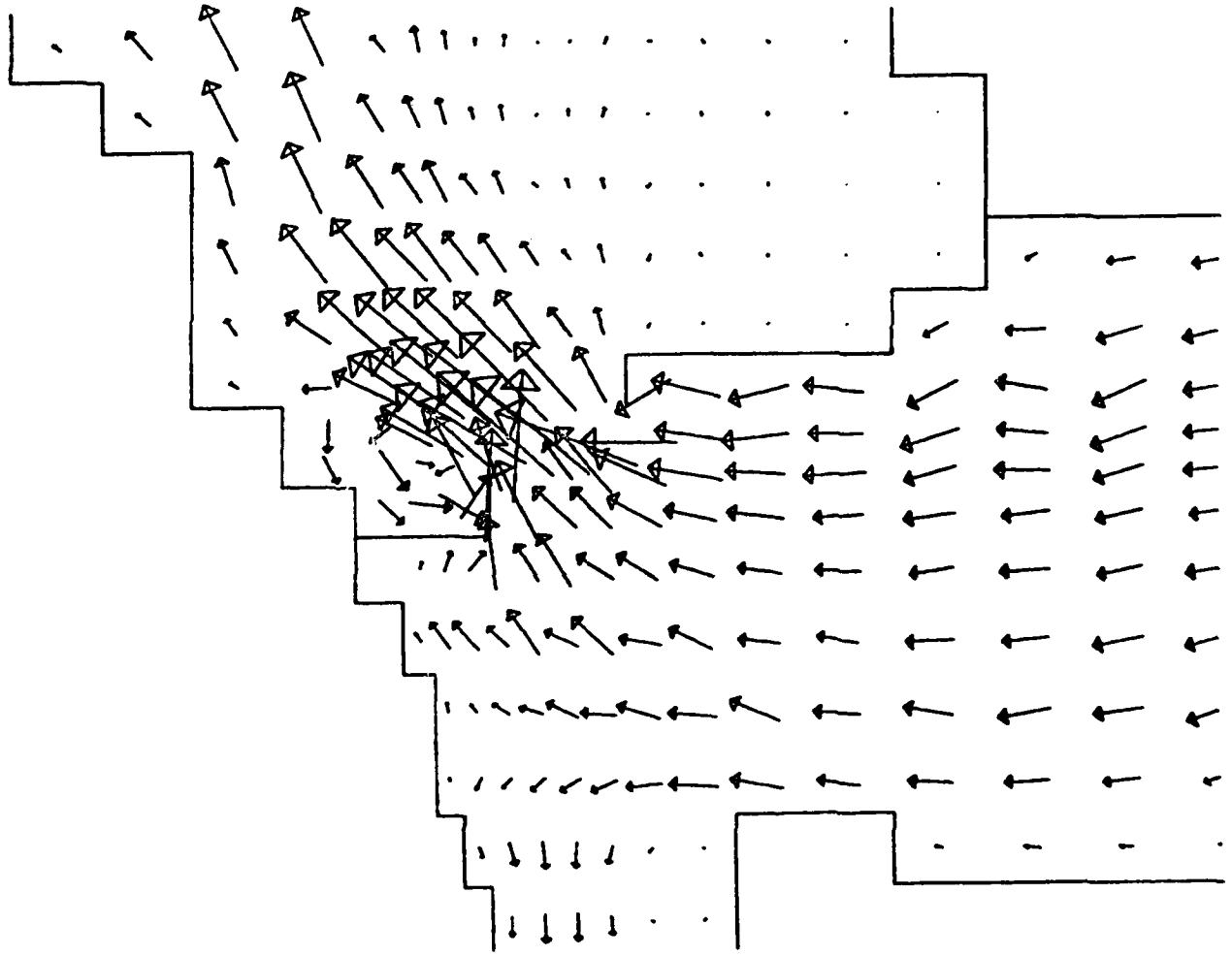

Figure 48. Enlargement of circulation pattern in the area of the proposed structure for The Rigolets, Plan 2A-1; maximum flood flow with advective terms included

conditions, and results were compared with physical model measurements for flows shown below:

Flow Condition	Discharge, cfs		Headwater Elevation ft NGVD
	Base	Plan	
Maximum	30,000	25,000	1.0
Medium	15,000	15,000	1.0
Minimum	5,000	5,000	1.0

In the calibration of the model for base conditions, the best comparisons were obtained for a uniform Manning's n of 0.025 except in the area of the constriction, guide wall pilings, and bridge piers. A high roughness was used in this area. The flow was forced into the center channel between the guide wall pilings and this roughness. It was further found necessary to use a different roughness factor for the flow in the ebb direction than in the flood direction to compensate for additional losses due to flow constriction. Manning's n values of 0.120 and 0.140 were used for the main channel area between the guide wall pilings for flood and ebb flows, respectively.

73. Results for base conditions are compared with physical model measurements in Figures 49-52 for maximum ebb and flood flows. Complete velocity and water-surface elevation data for the flow conditions tested are listed in Tables 1, 3, and 5. Circulation patterns for maximum flow conditions are presented in Figures 53-55. Figure 53 cannot be interpreted due to point density but is included to give the reader an overview of model extent and resolution. Additional circulation patterns for Seabrook Canal simulations only depict an enlargement of the proposed lock/structure location.

74. Comparison of numerical and physical model results is good. It can be readily observed that flow conditions are approaching limitations of the instrumentation for low flows.

75. In attempting to model maximum flow conditions through the lock and control structures as modeled by the physical model, it became obvious that WIFM could not represent the critical flows that were occurring in the physical model as the program was structured. Dynamic

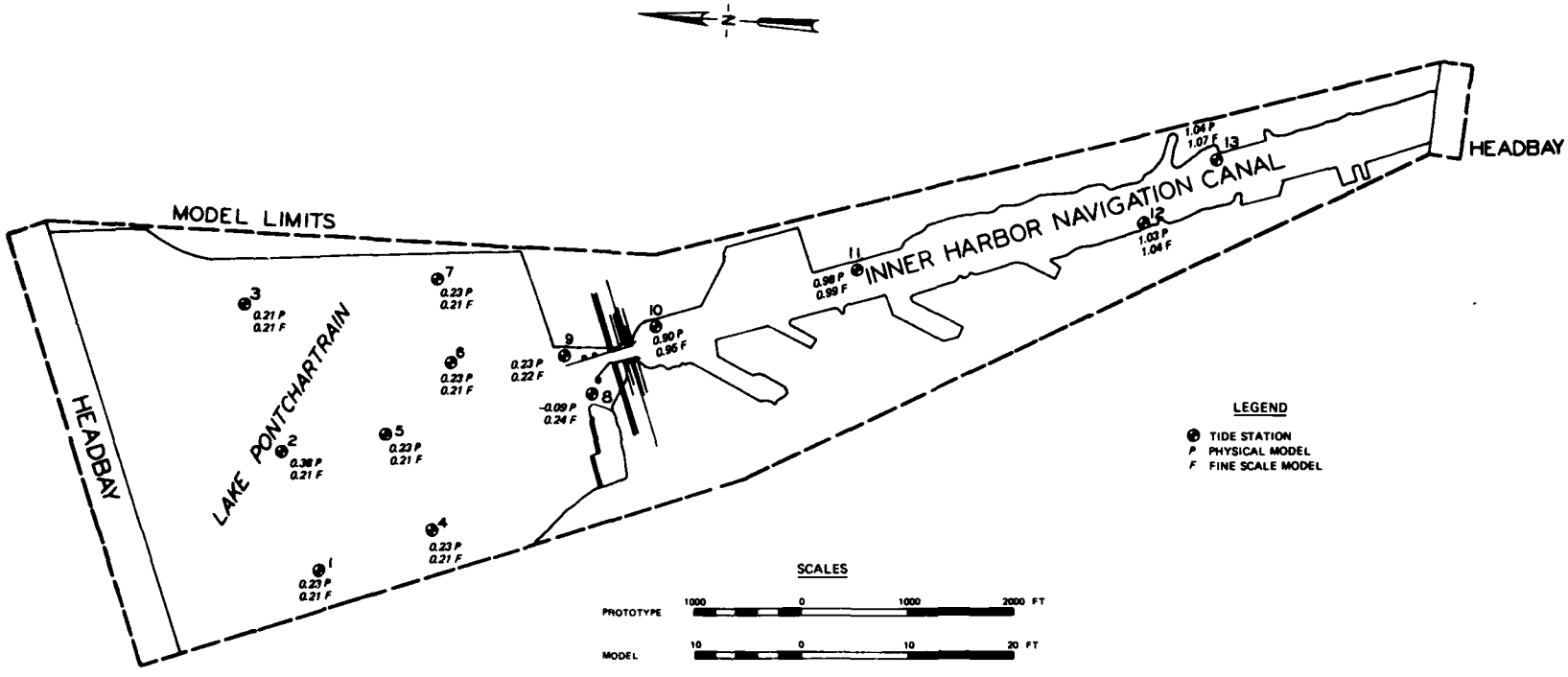

Figure 49. Surface elevation, ft NGVD, flood flow of 30,000 cfs; physical versus fine scale model for existing conditions in Seabrook Canal

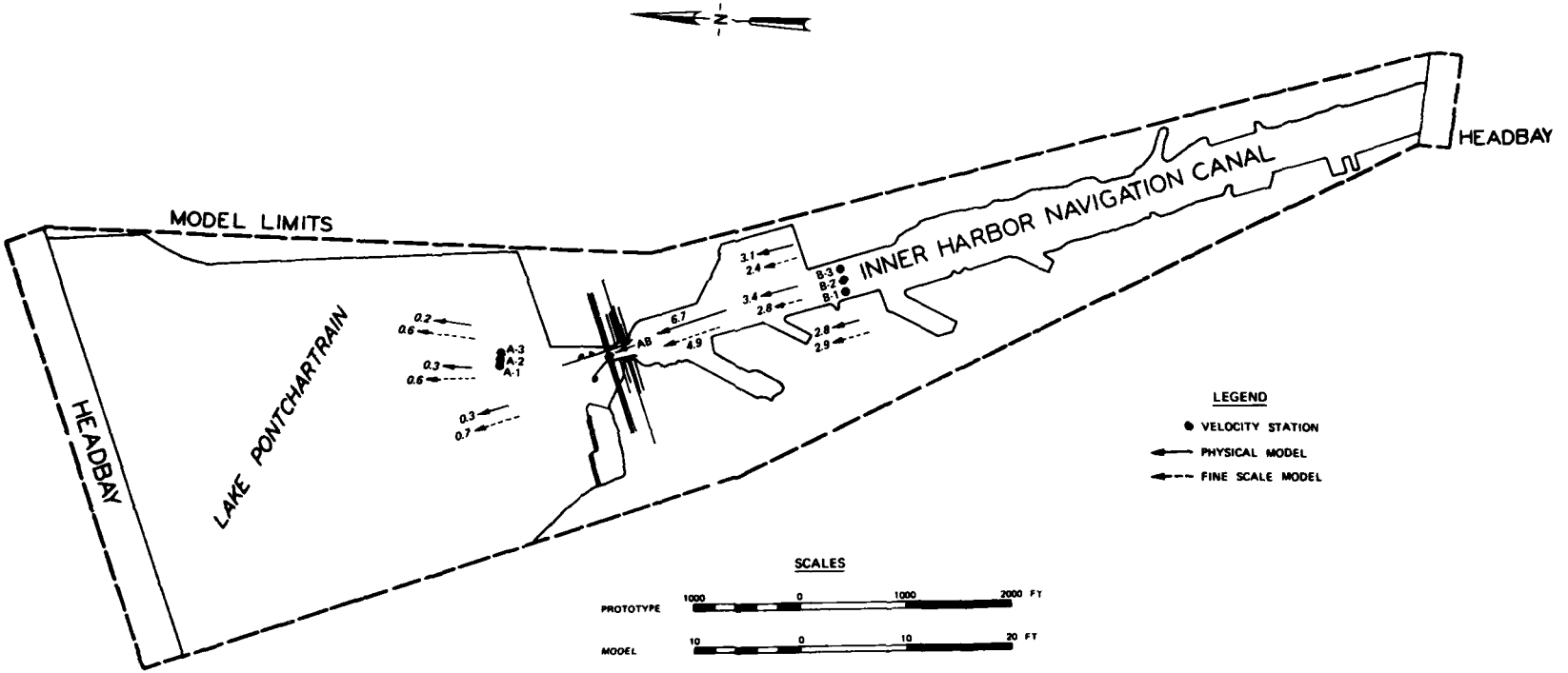

Figure 50. Velocities, fps, flood flow of 30,000 cfs; physical versus fine scale model for existing conditions in Seabrook Canal

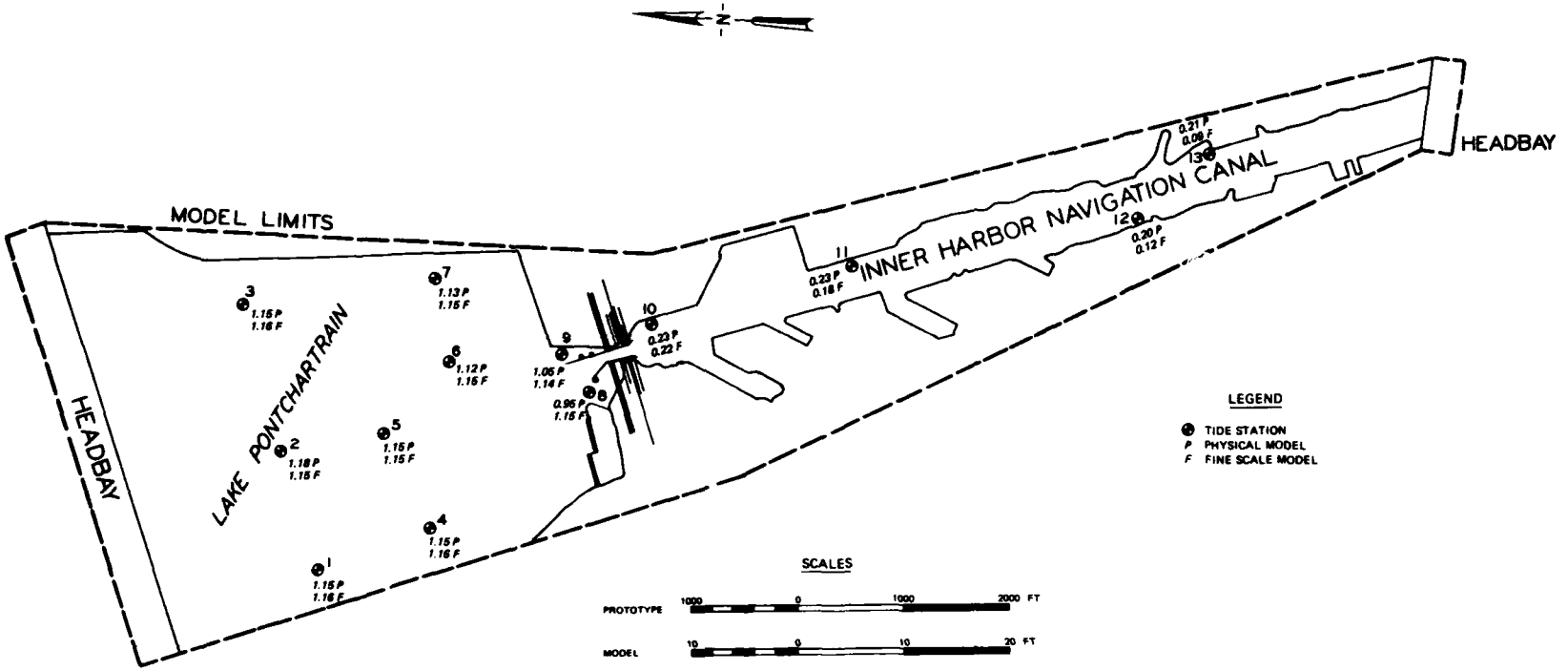

Figure 51. Surface elevation, ft NGVD, ebb flow of 30,000 cfs; physical versus fine scale model for existing conditions in Seabrook Canal

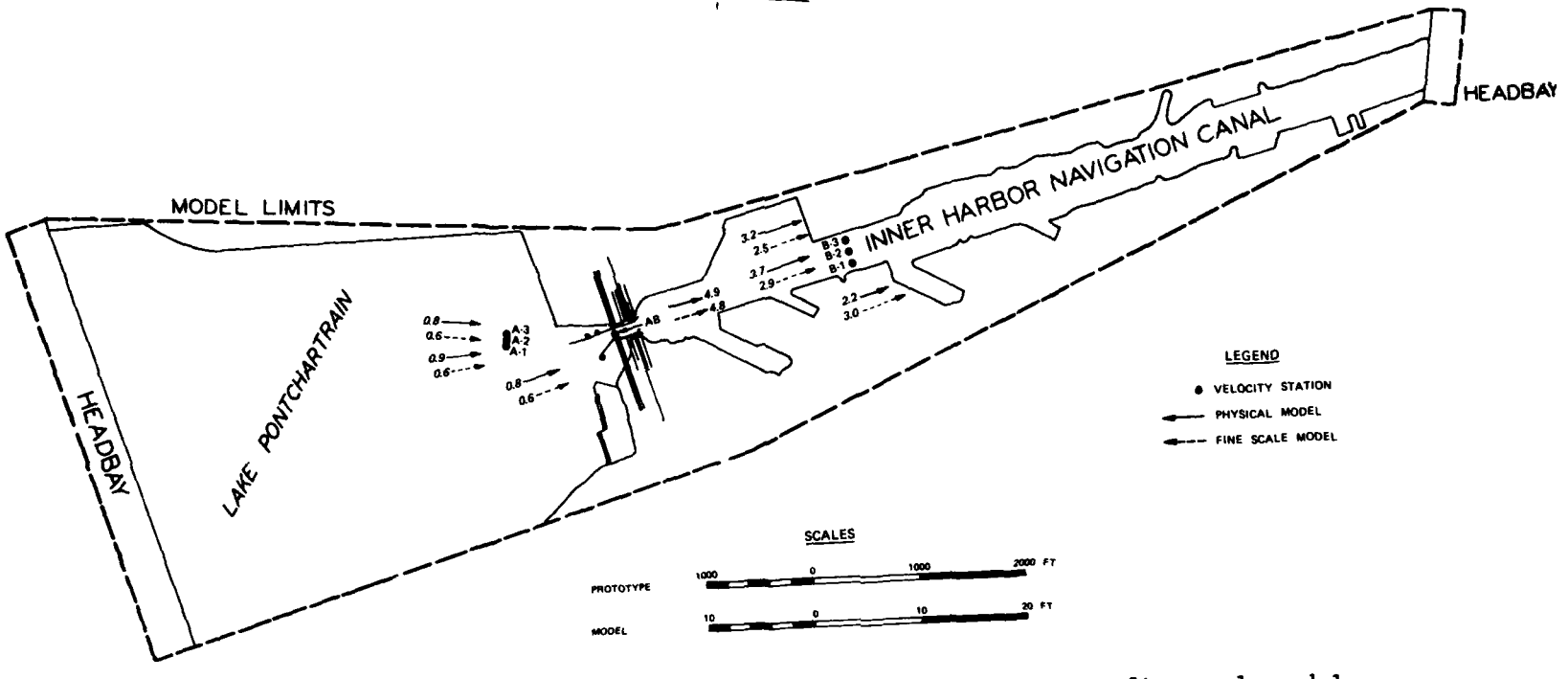

Figure 52. Velocities, fps, ebb flow of 30,000 cfs; physical versus fine scale model for existing conditions in Seabrook Canal

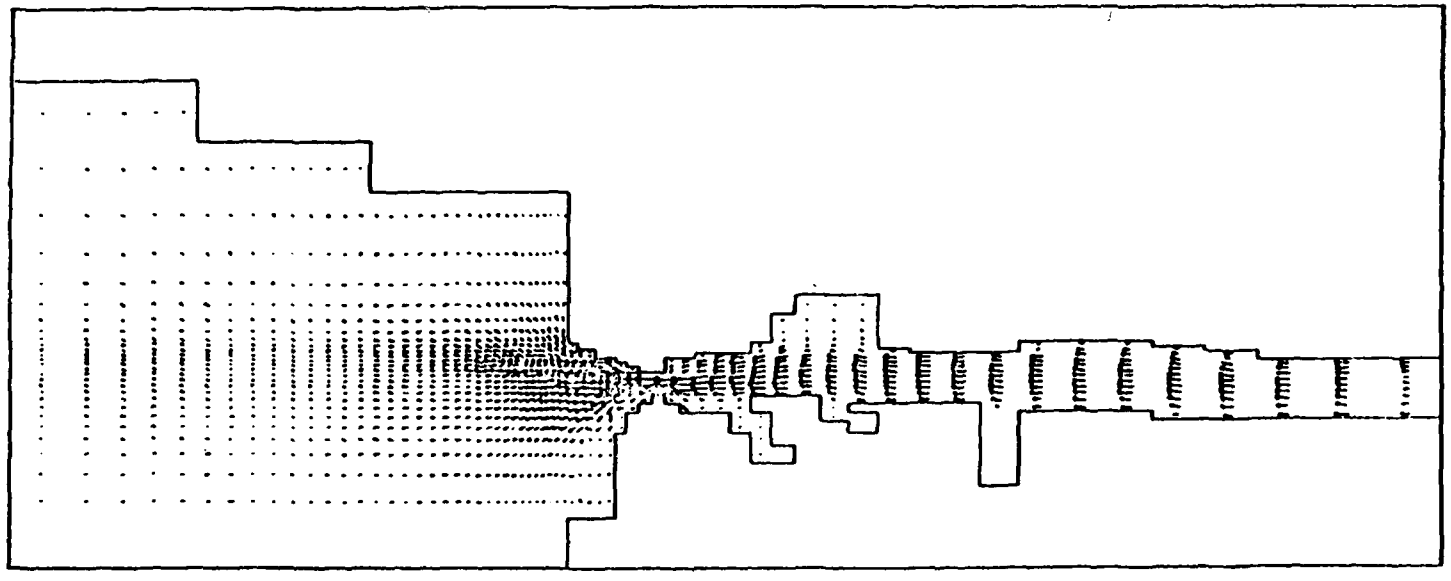

Figure 53. Circulation pattern for Seabrook Canal, existing conditions; flood flow 30,000 cfs

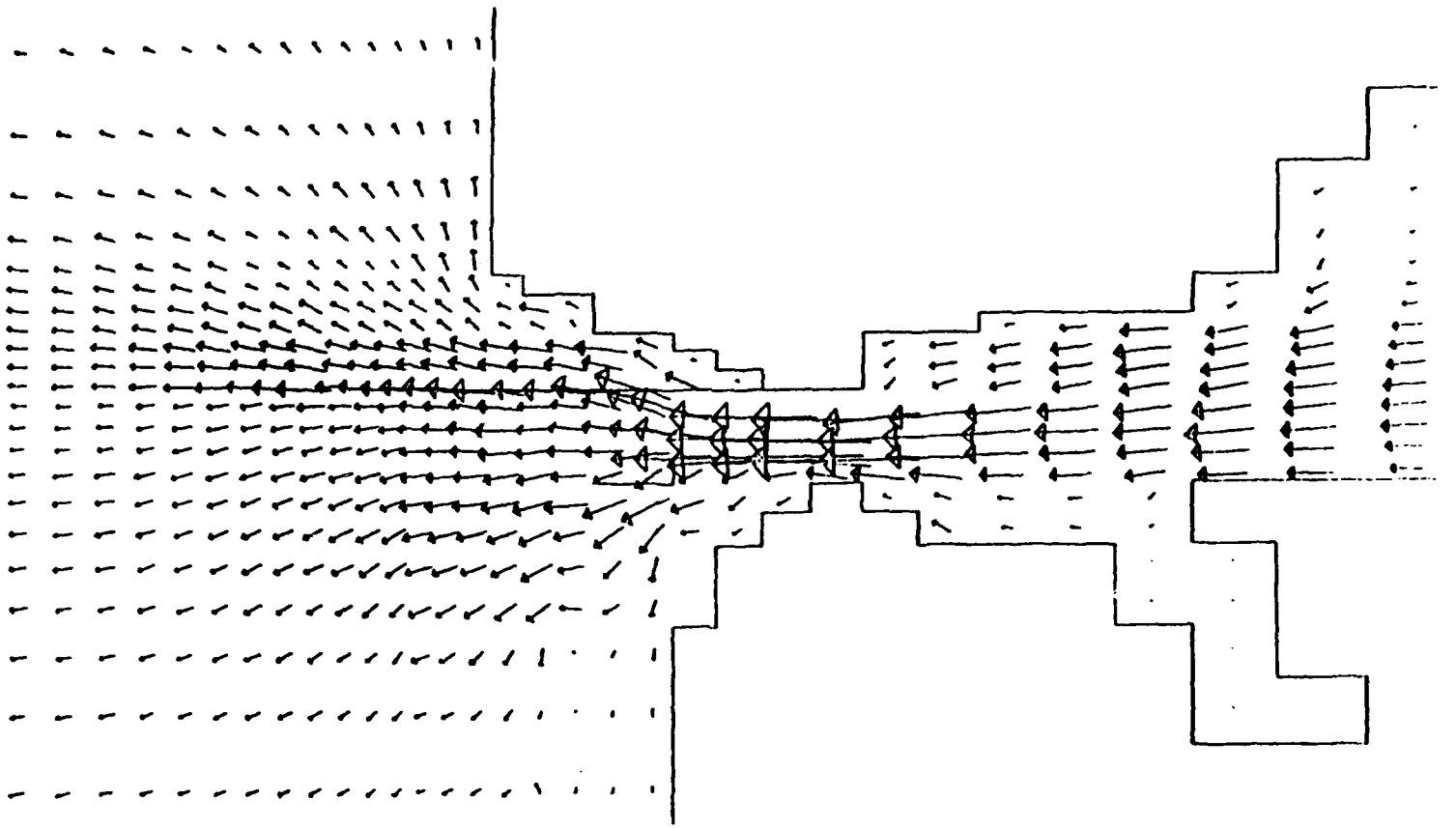

Figure 54. Enlargement of circulation pattern in the area of the proposed structure for Seabrook Canal, existing conditions; flood flow 30,000 cfs

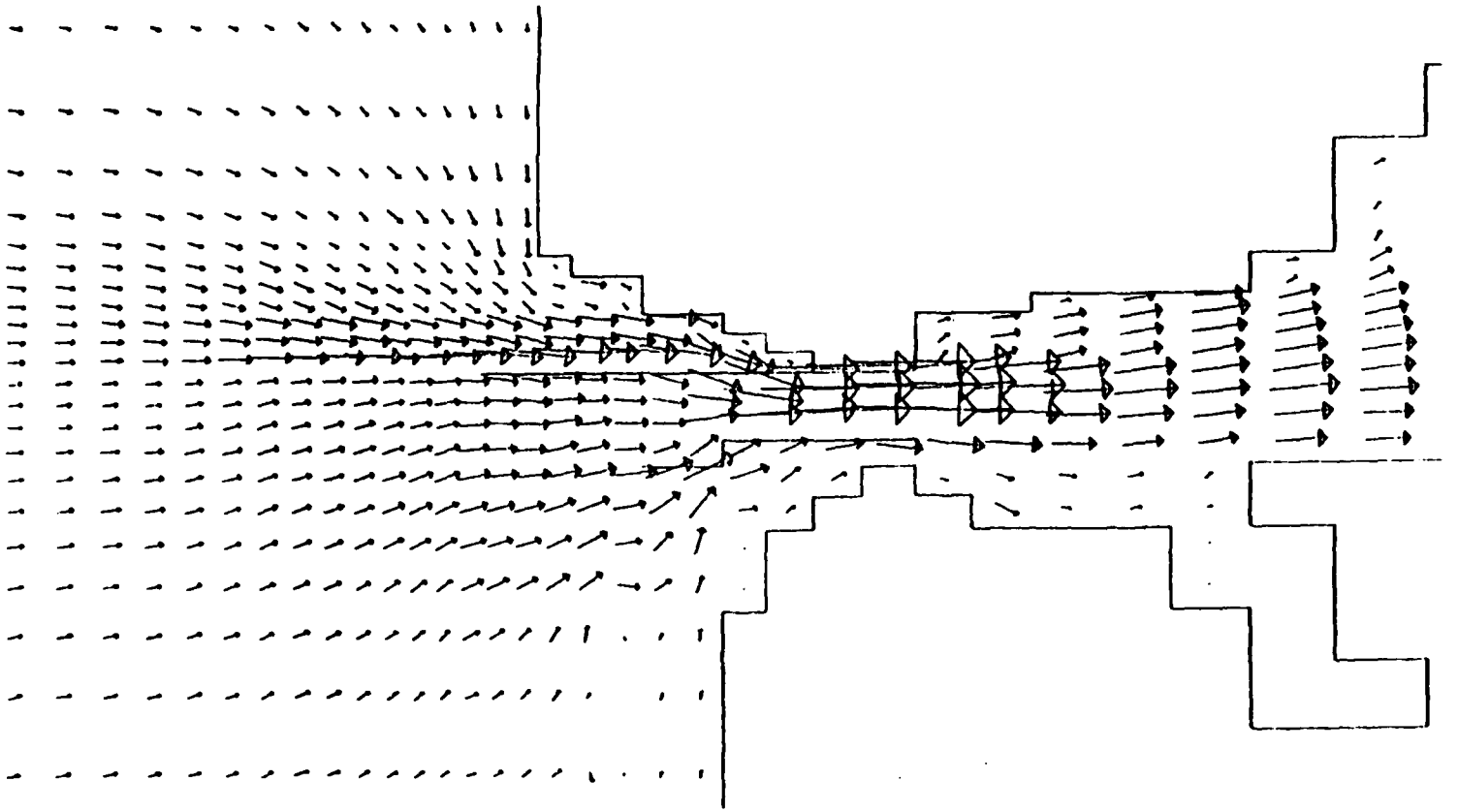

Figure 55. Enlargement of circulation pattern in the area of the proposed structure for Seabrook Canal, existing conditions; ebb flow 30,000 cfs

test runs of the larger scale numerical model of the Seabrook Lock and control structure demonstrated that the maximum flows through the structures that would be generated by tidal forces would be on the order of 10,000 cfs. Therefore, this was the maximum flow used in the fine grid model. Since all previous testing had demonstrated that the numerical model reproduced physical model results for the lower flow rates when the model was properly adjusted for modeling maximum flow rate, only the maximum flows were tested.

76. Results for the proposed lock and control structure are compared with the physical model water-surface elevations in Figures 56 and 57 for flood and ebb flows of 10,000 cfs. Complete water-surface elevation and velocity data are given in Table 18. Water-surface elevations are reproduced reasonably well. It can be observed that velocities on the Lake Pontchartrain side of the control structure for flood flows are not reproduced well since the flow does not remain concentrated in a jet-type flow but expands into the area around the structure as shown in Figure 58 showing the circulation pattern. This is the same situation observed in The Rigolets structure case. It could be expected that flow conditions around the structure could be more accurately reproduced by using the equations with the nonlinear advective terms included. However, for the purpose of this project, the simpler linear model adequately represents the head loss characteristics of the structures.

77. The velocity computed at gage AB is also low compared with that measured in the physical model. This is due to the contraction that takes place in the flow as it passes through the pilings in the bridge area. Again, since the main purpose of the physical model is to demonstrate the capability of the numerical model to reproduce the head loss and volume transport generated by the structure, this was not considered significant.

Chef Menteur Pass model

78. The Chef Menteur Pass was modeled for the maximum flow condition tested in the physical model, 125,000 cfs. It had been well demonstrated in testing the other structures that reproduction of conditions under maximum flows ensured reproduction of conditions for

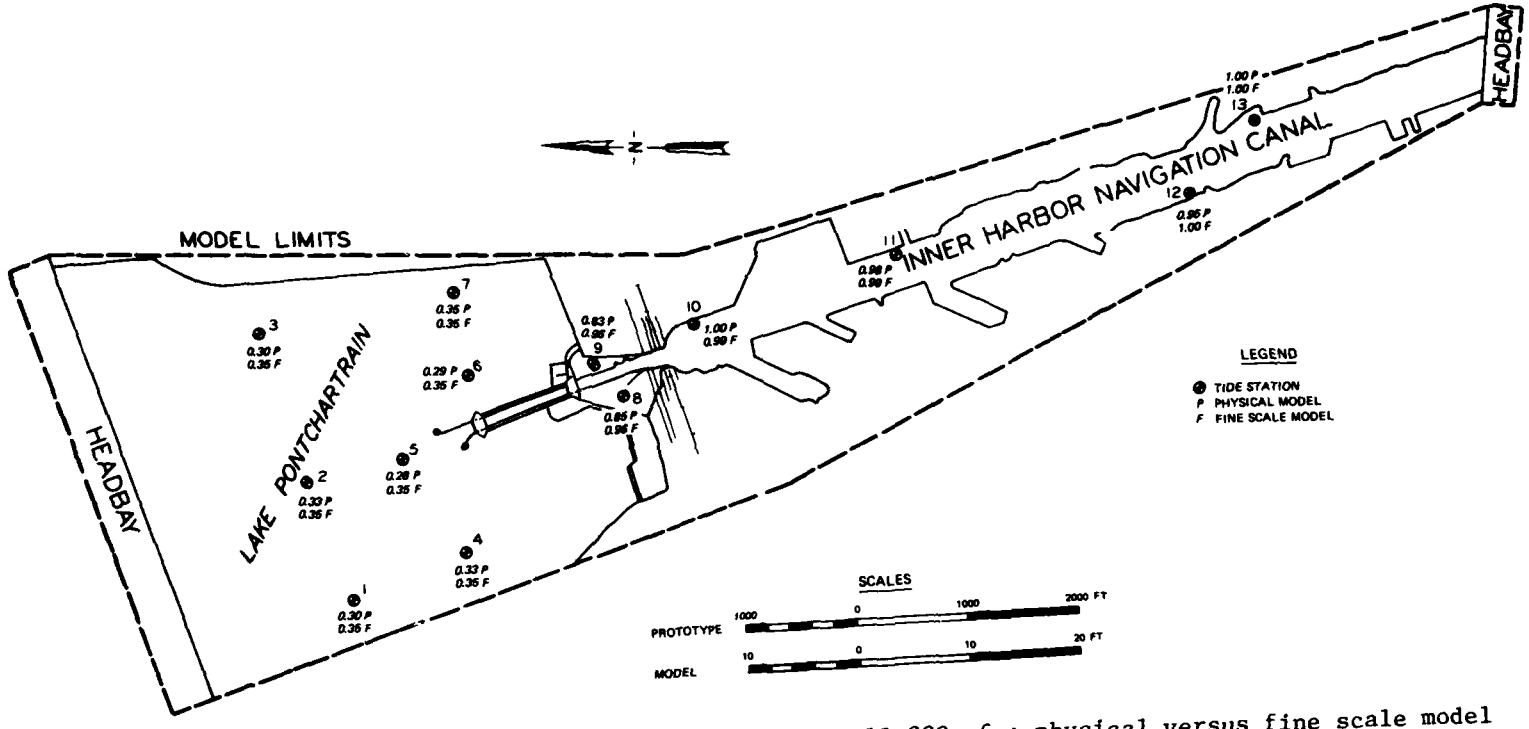

Figure 56. Surface elevation, ft NGVD, flood flow of 10,000 cfs; physical versus fine scale model for Plan 4 in Seabrook Canal

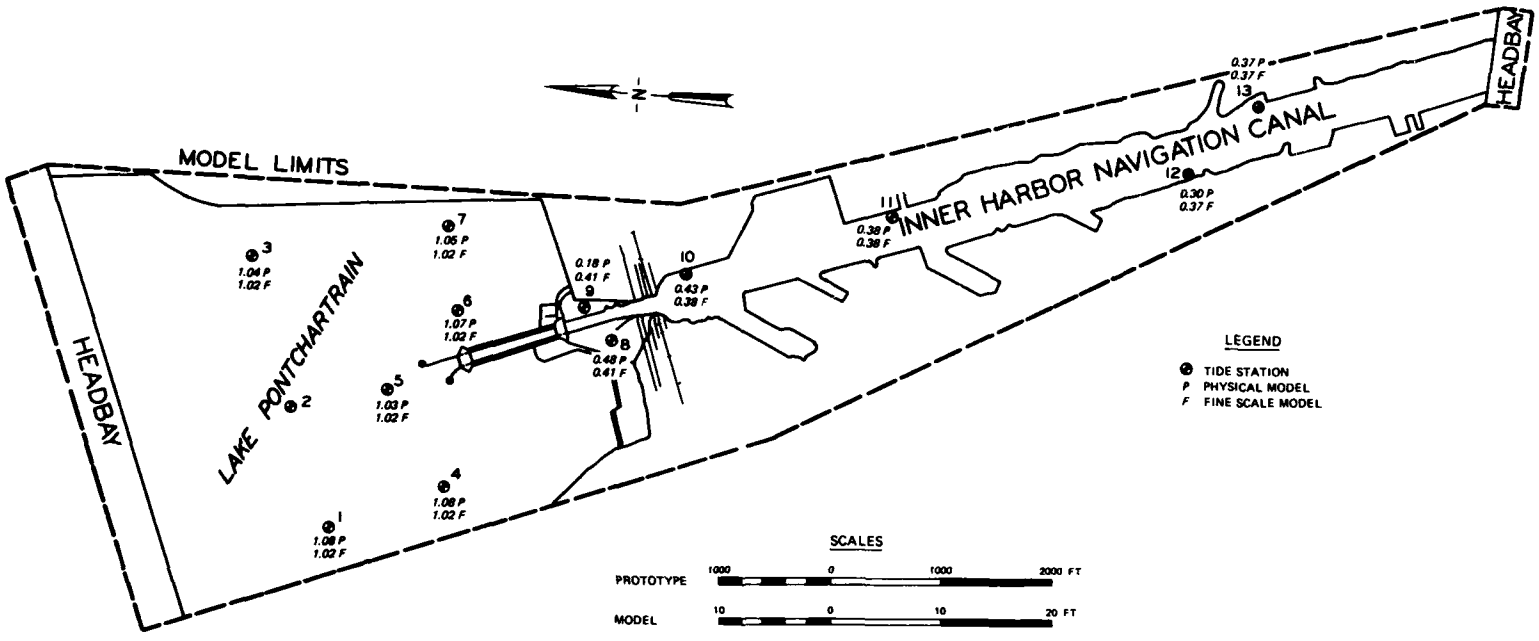

Figure 57. Surface elevation, ft NGVD, ebb flow of 10,000 cfs; physical versus fine scale model for Plan 4 in Seabrook Canal

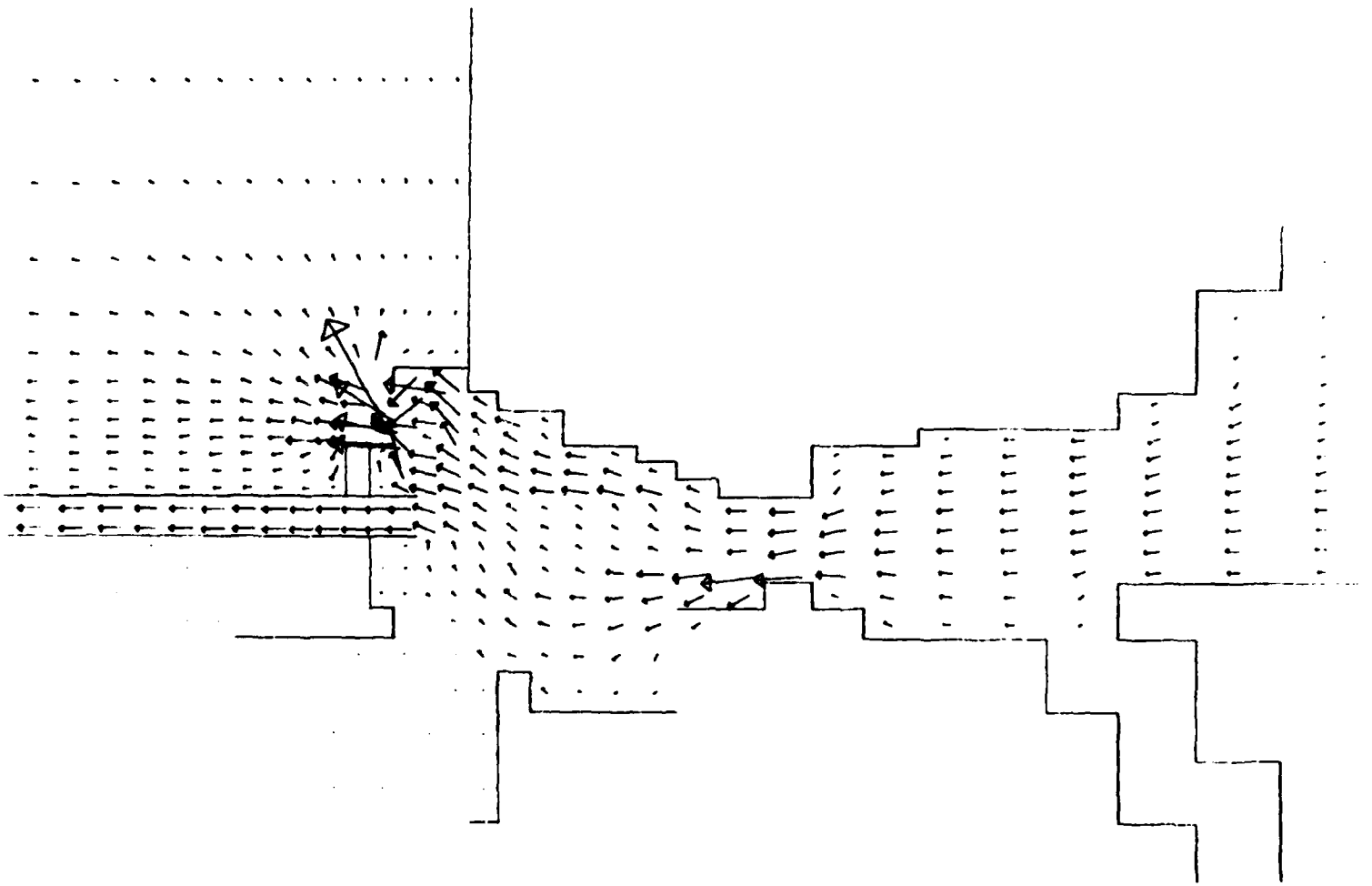

Figure 58. Enlargement of circulation pattern in the area of the proposed structure for Seabrook Canal, Plan 4; flood flow 10,000 cfs

AD-A120 162 ARMY ENGINEER WATERWAYS EXPERIMENT STATION VICKSBURG--ETC F/G 13/2
LAKE PONTCHARTRAIN AND VICINITY HURRICANE PROTECTION PLAN. REPO--ETC(U)
JUN 82 H L BUTLER, R C BERGER, L L DAGGETT

UNCLASSIFIED WES/TR/HL-82-2-2 NL

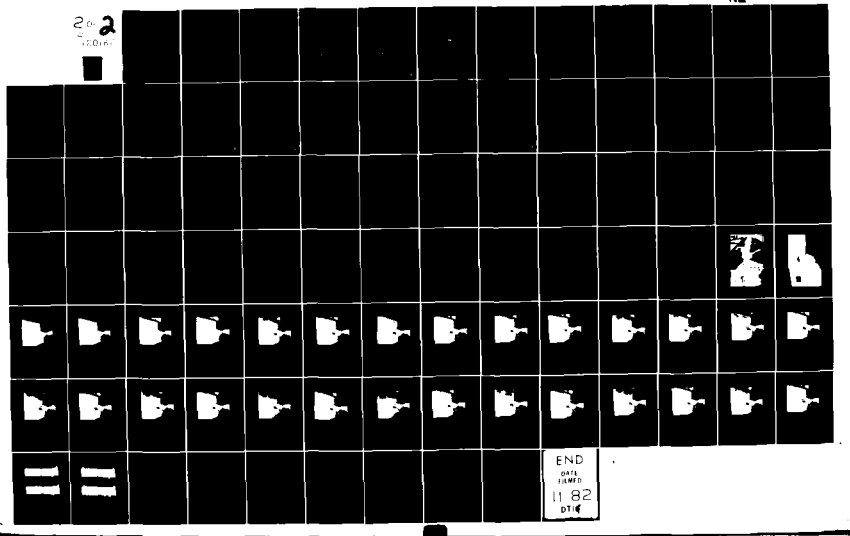

lesser magnitude flows. The best results were obtained for a uniform Manning's n of 0.025 in the canal and 0.050 in the marsh overflow areas surrounding the canal. The roughness of the submerged barriers representing the structure was 0.120 and 0.140 for the flood and ebb flows, respectively.

79. Results for these conditions are compared with physical model measurements in Figures 59-62 for the maximum flood and ebb flows. Water-surface elevation and velocity data for these flow conditions are presented in Tables 29 and 32. Circulation patterns for the maximum flood and ebb flows are represented in Figures 63-66 with closeup views of the structure area.

80. Results of these computations demonstrate that the numerical model can reproduce the overall head loss through the canal and control structure and that velocities are reasonably well reproduced on the average. However, the physical model demonstrated significant drops in water-surface elevations near the structure with a recovery of the water-surface elevations away from the structure. This appears to be due to an acceleration of the water. The flow of water also seems to be concentrated on one side of the channel in the physical model, whereas the flow in the numerical model is more uniform. It is anticipated that modeling this with the nonlinear advective terms would again improve details of the flow in the vicinity of the structure; however, since the linear model satisfies the study objective, no additional tests were run.

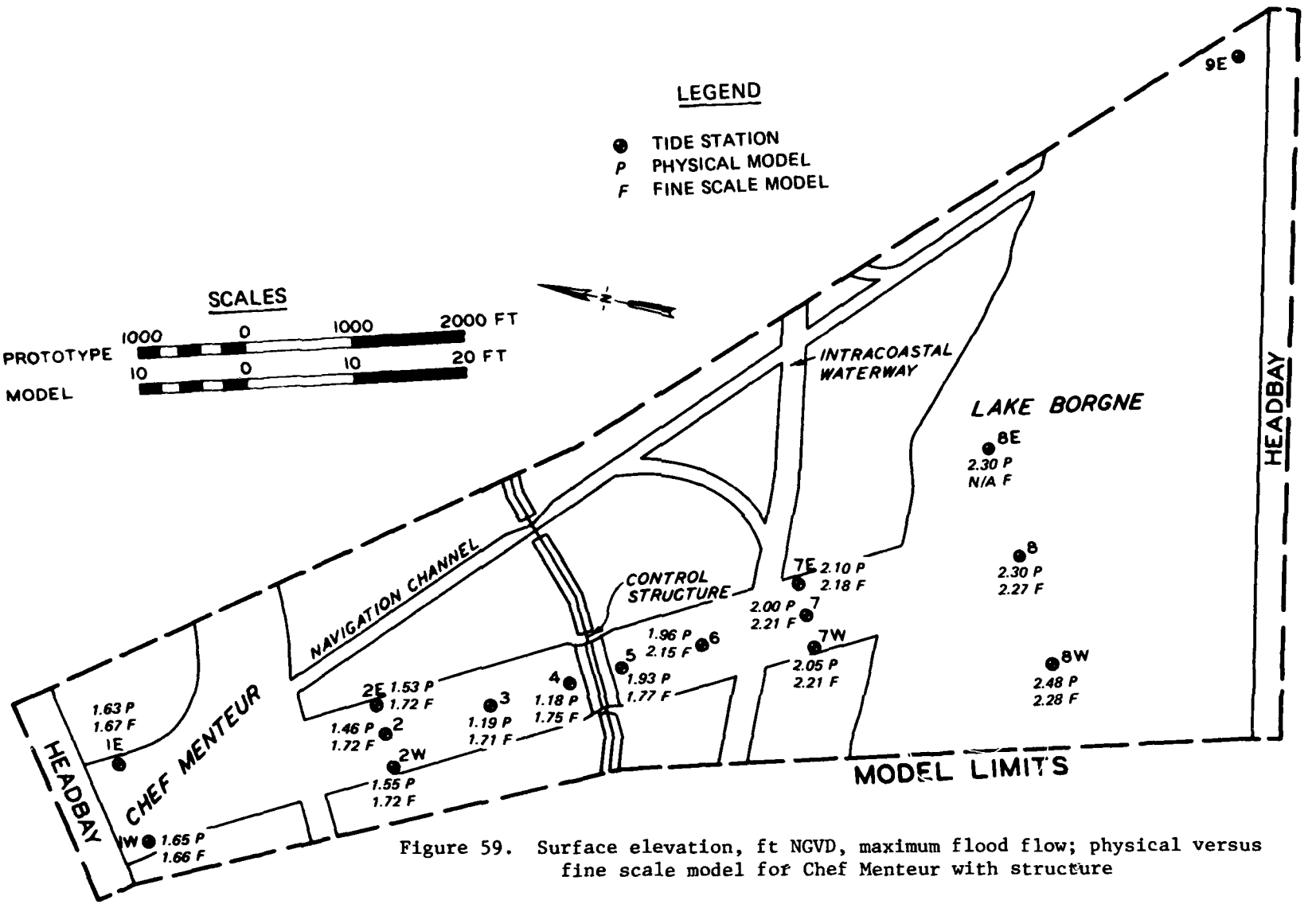

Figure 59. Surface elevation, ft NGVD, maximum flood flow; physical versus fine scale model for Chef Menteur with structure

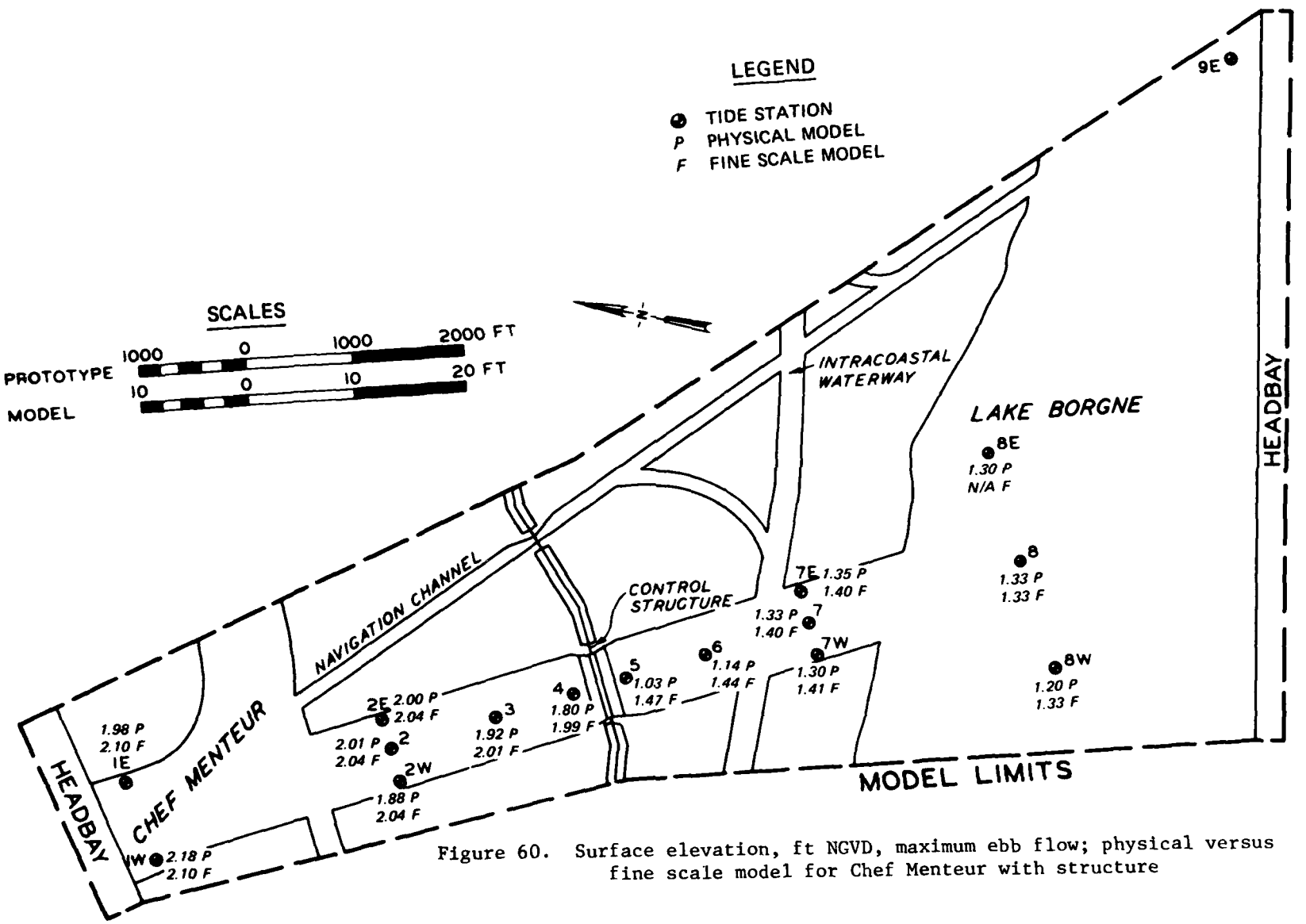

Figure 60. Surface elevation, ft NGVD, maximum ebb flow; physical versus fine scale model for Chef Menteur with structure

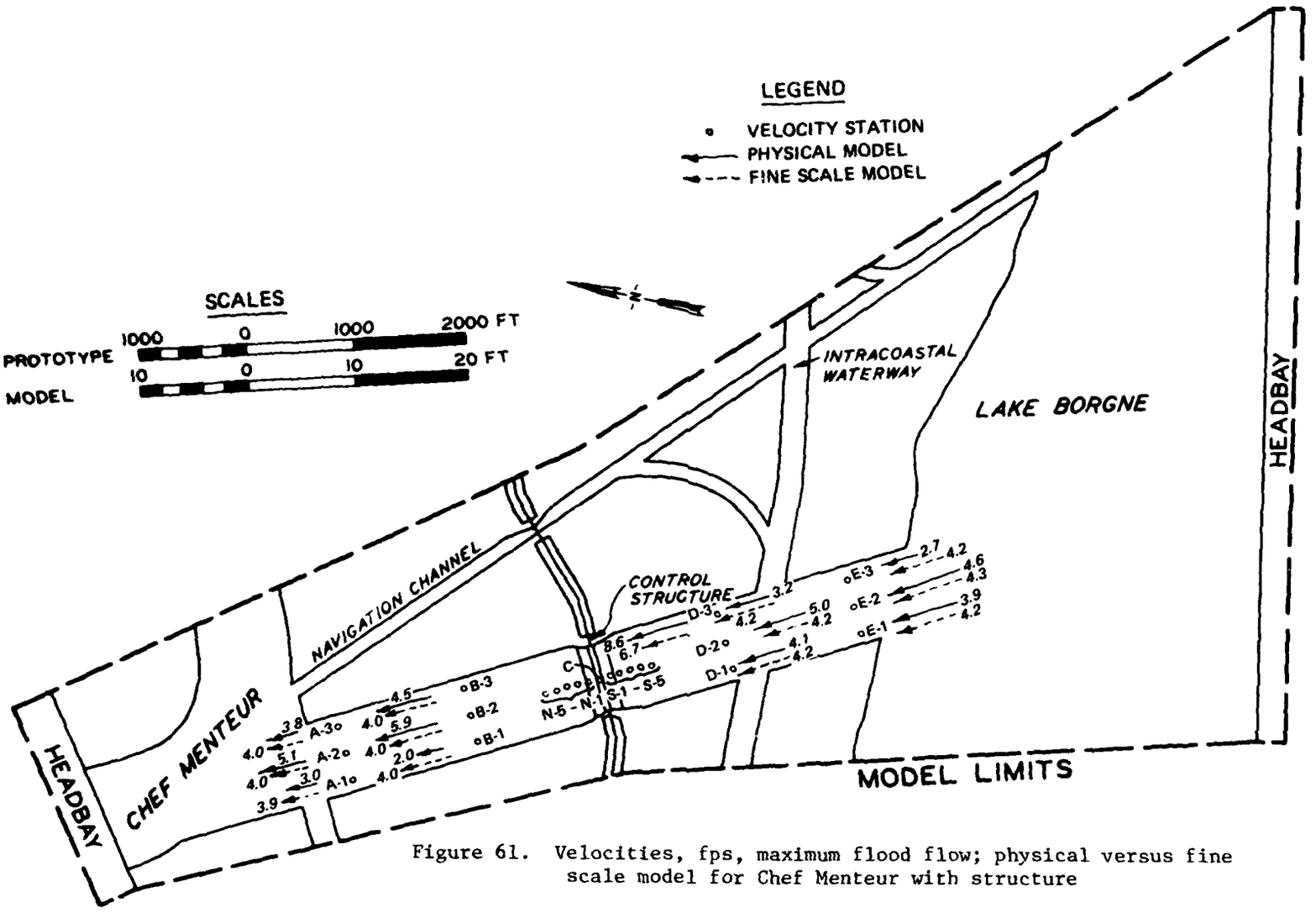

Figure 61. Velocities, fps, maximum flood flow; physical versus fine scale model for Chef Menteur with structure

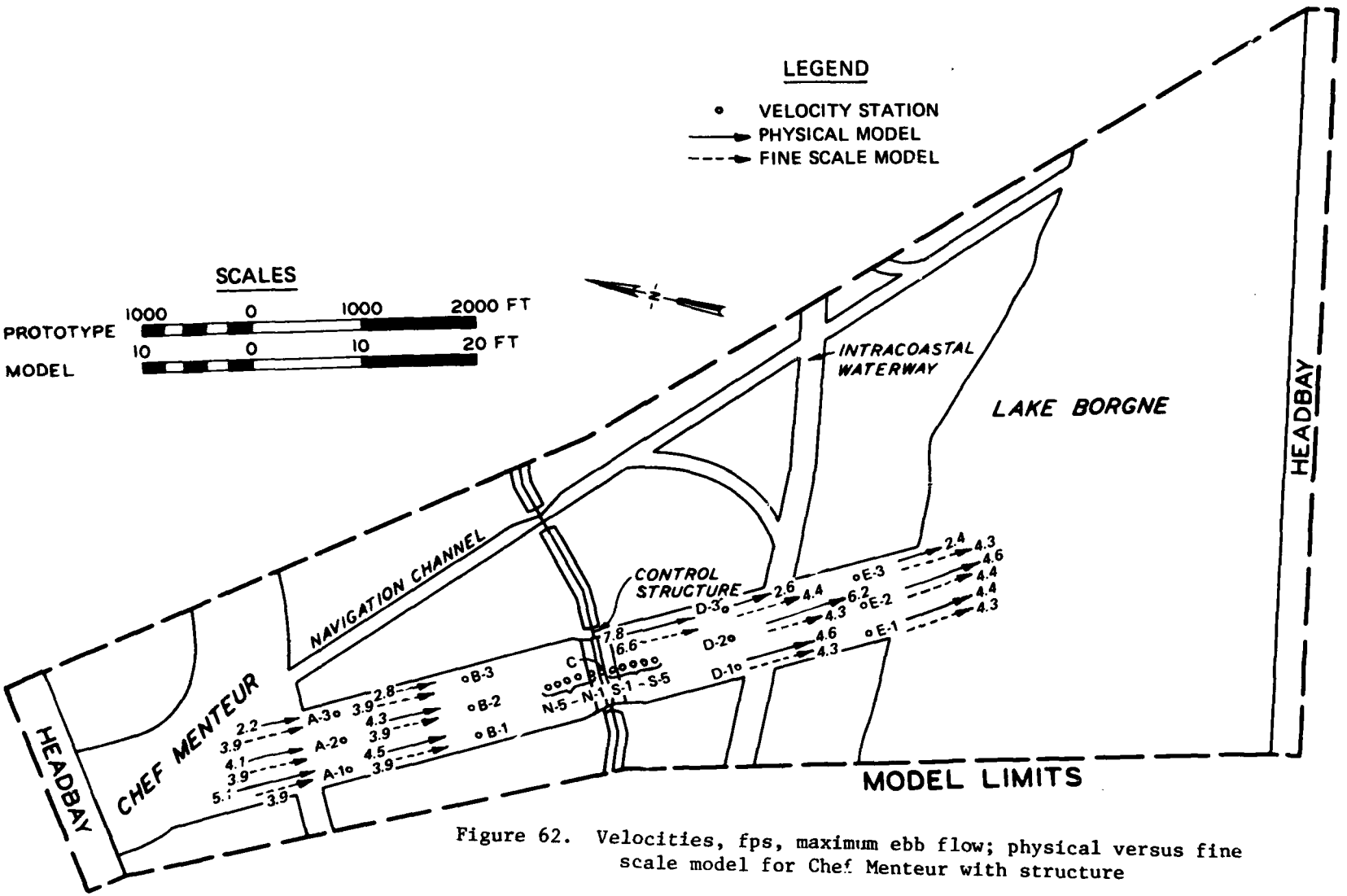

Figure 62. Velocities, fps, maximum ebb flow; physical versus fine scale model for Chef Menteur with structure

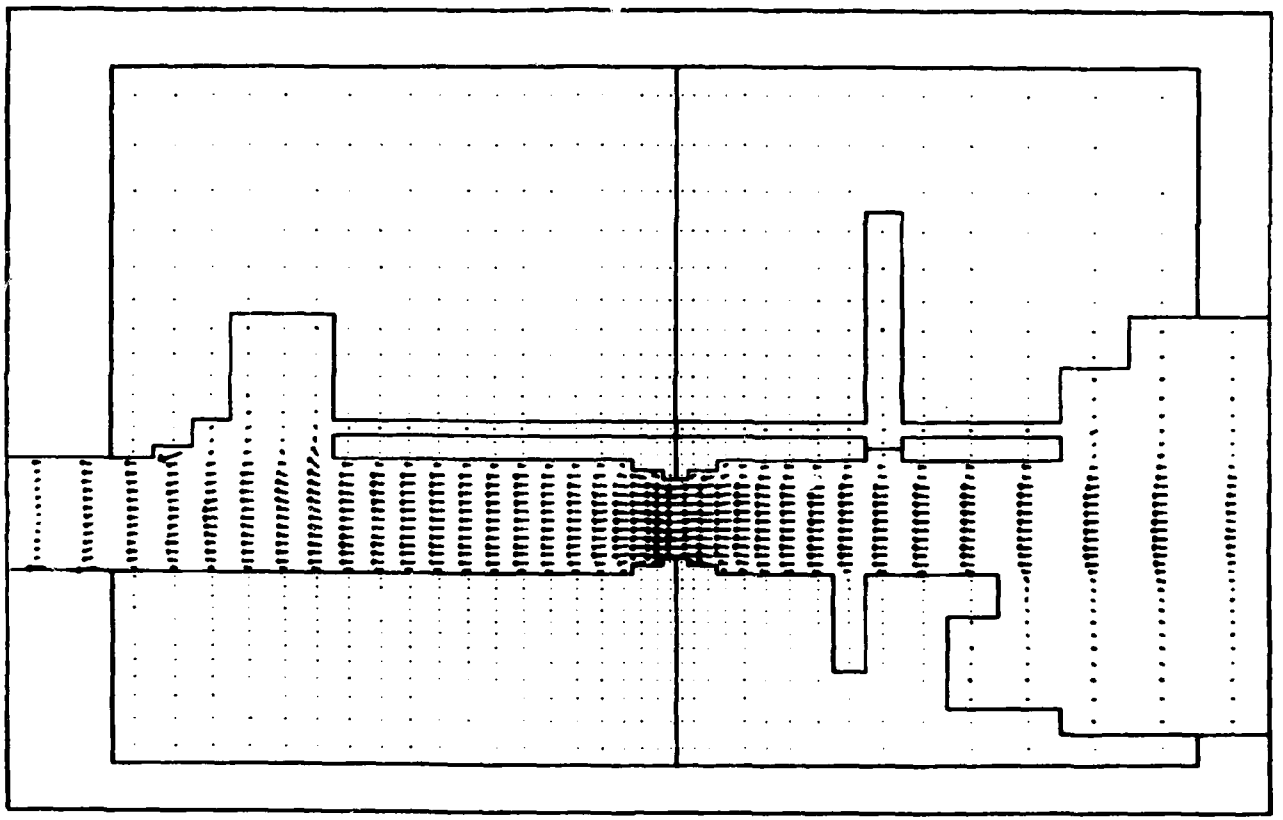

Figure 63. Circulation pattern for Chef Menteur with structure; maximum flood flow

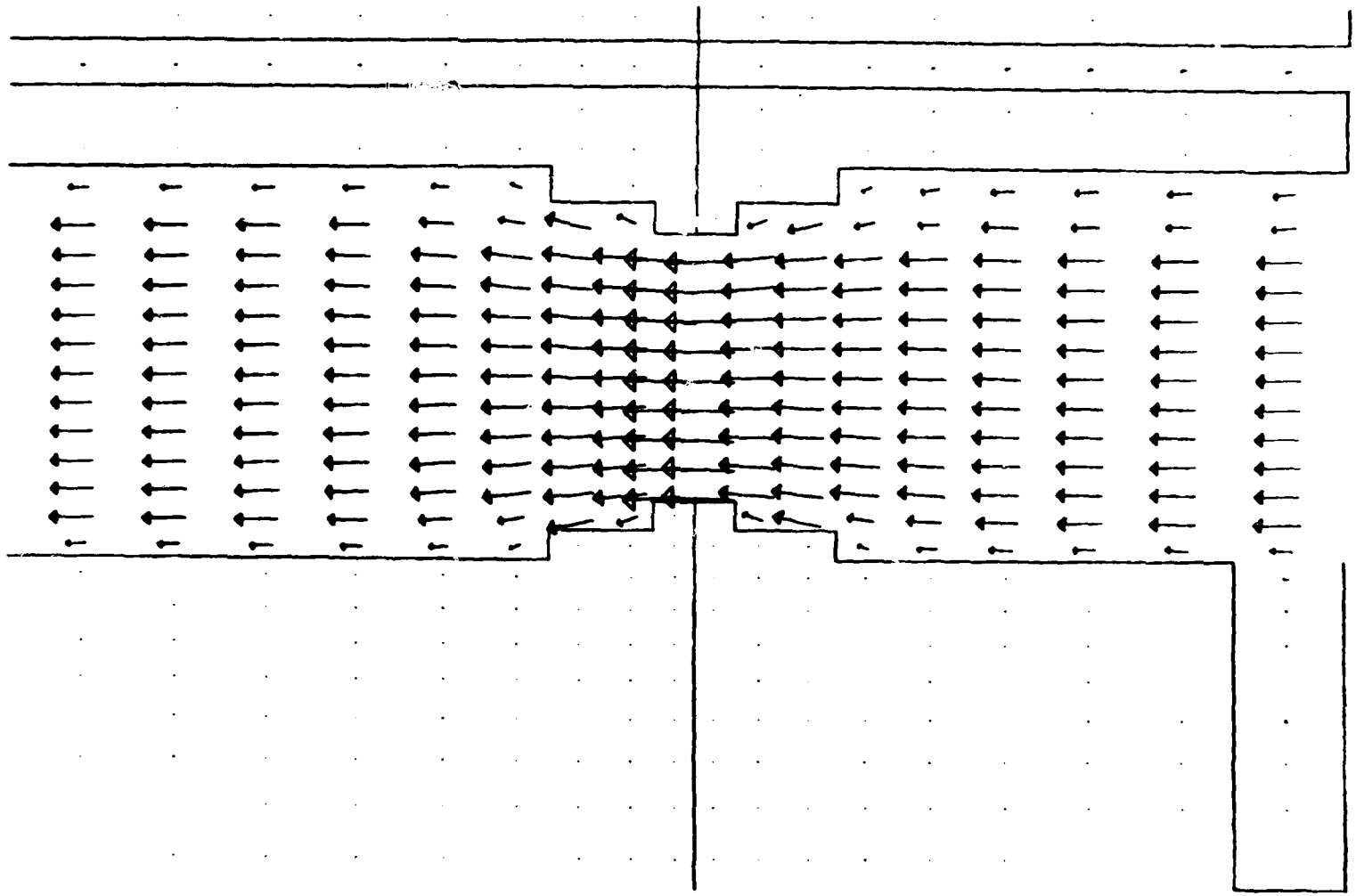

Figure 64. Enlargement of circulation pattern for Chef Menteur with structure; maximum flood flow

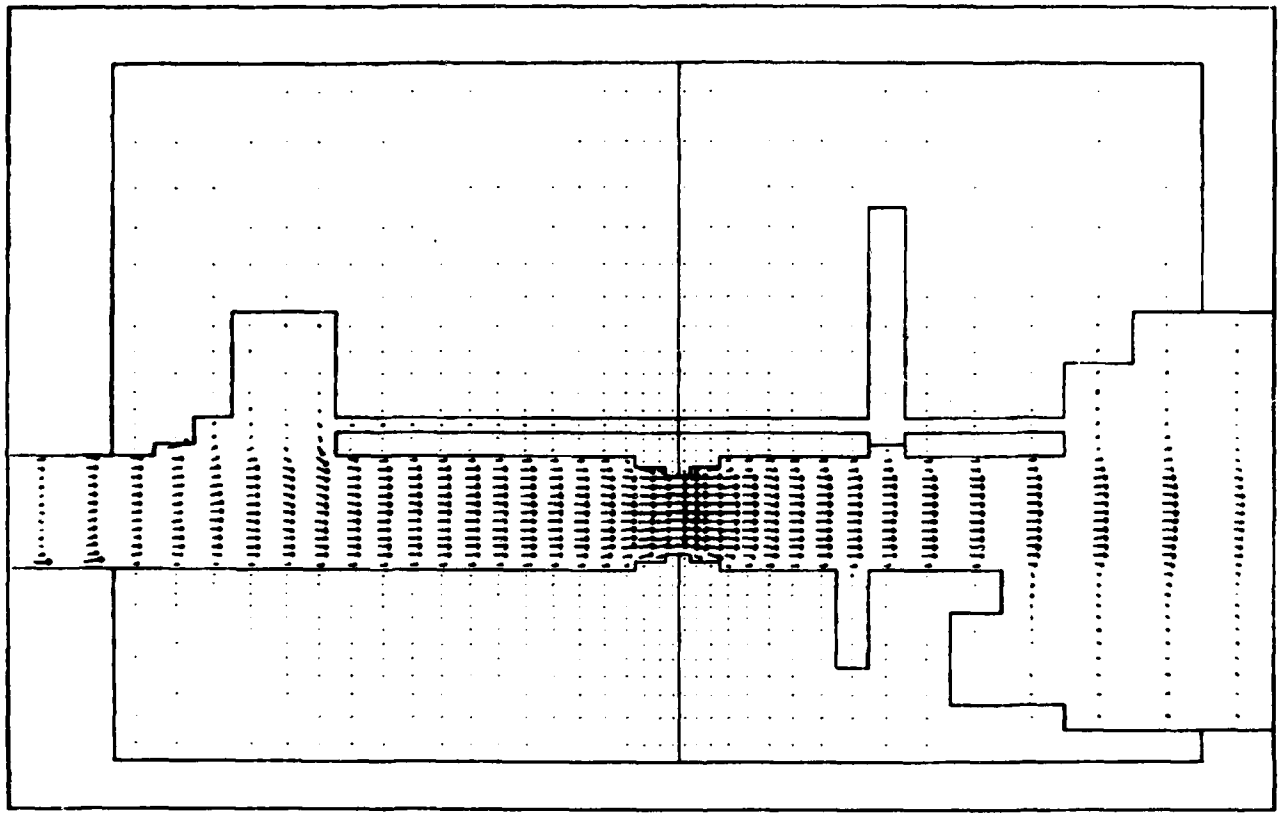

Figure 65. Circulation pattern for Chef Menteur with structure; maximum ebb flow

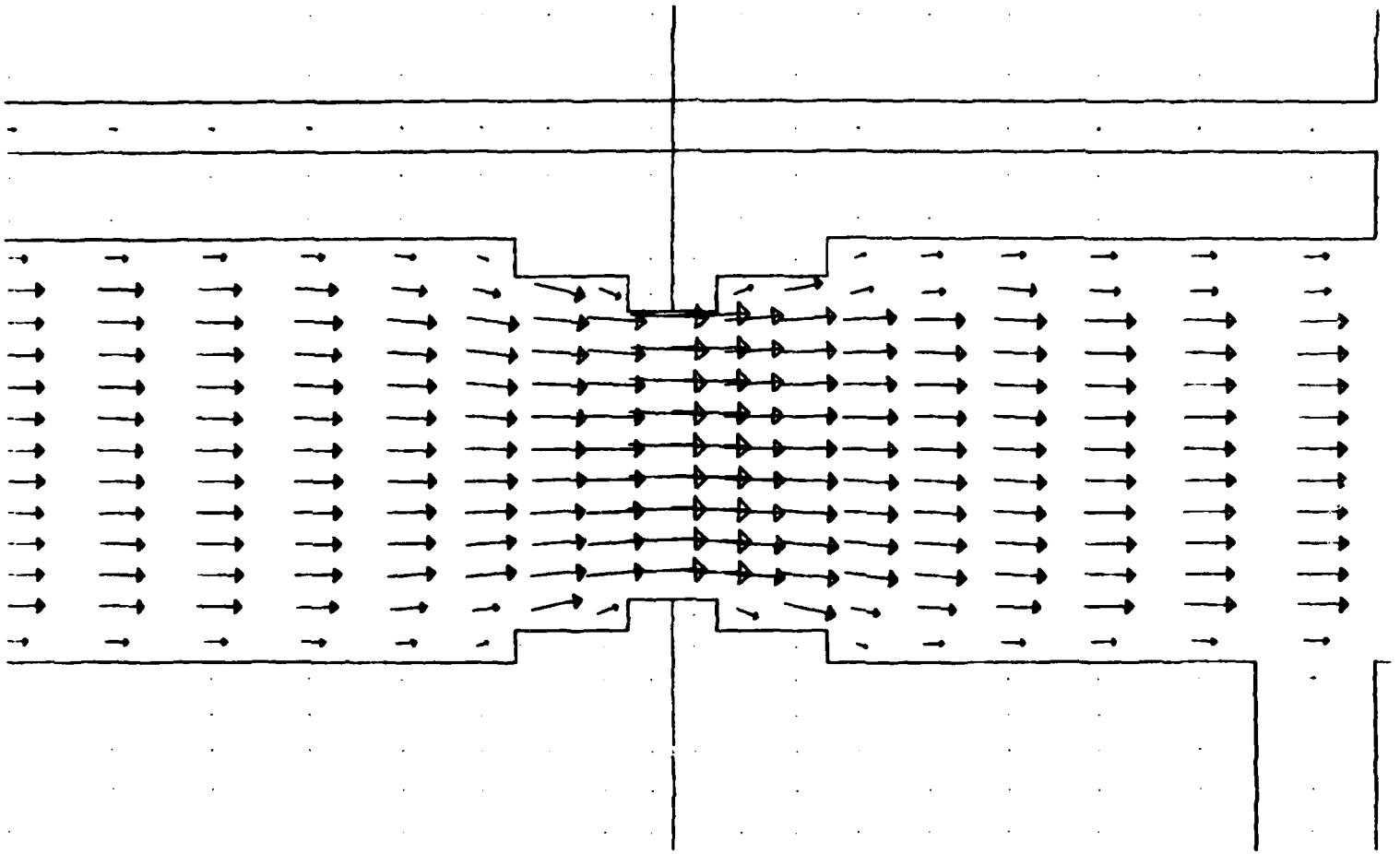

Figure 66. Enlargement of circulation pattern for Chef Menteur with structure; maximum ebb flow

PART V: SUMMARY AND CONCLUSIONS

81. Undistorted-scale physical models of the Seabrook Canal and Chef Menteur Pass were constructed and tested for the purpose of obtaining data to quantify the hydraulic characteristics of the various proposed structures in the hurricane barrier protection plan. Experimental data acquired from these models consisted of water-surface elevations for a range of flow rates and surface current patterns near the structures. Results from a previous model investigation of The Rigolets control structure were sufficient to define the characteristics of that structure.

82. Computational grid sectional models were developed, calibrated to define structure representation in each sectional model, and subsequently tested for various conditions simulated in the corresponding physical model. Fine scale numerical models were also constructed and tested as part of a grid sensitivity check and to supply a model for future detailed entrance pass studies.

83. For the computational grid models, single values of Manning's n were determined for each structure and found to adequately describe its characteristics for both flood and ebb conditions and for the entire range of flow rates tested. Results are summarized as

Structure	Manning's n
Rigolets	0.110
Chef Menteur	0.112
Seabrook Canal (bridge constriction)	0.190
Seabrook Canal (Plan 3)	0.400
Seabrook Canal (Plan 4)	0.230

Since the computational grid models are actually subgrids or windows of the global grid, the Manning's parameters can be used directly in the full lake simulations. Values obtained for the fine scale models differ from those determined for the computational grid models. This is expected since many unresolved geometric features of the passes in the computational grid are accurately described in the fine scale models.

The navigation channels in both Rigolets and Chef Menteur plans were omitted in the sectional modeling and analysis indicates an underestimation error of about 2% could occur in simulating the tidal prism of Lake Pontchartrain with the protection plan in place.

84. Test conditions for unsteady flow with each computational grid model will be discussed in a subsequent report in the Lake Pontchartrain series.

REFERENCES

Berger, R. G., and Boland, R. A. 1976 (Sep). "Hydraulic Charateristics of Rigolets Pass, Louisiana, Hurricane Surge Control Structures; Hydraulic Model Investigation," Technical Report H-76-16, U. S. Army Engineer Waterways Experiment Station, CE, Vicksburg, Miss.

Butler, H. L. 1980. "Evolution of a Numerical Model for Simulating Long-Period Wave Behavior in Ocean-Estuarine Systems," Estuarine and Wetland Processes with Emphasis on Modeling Marine Science Series, Vol. 11, Plenum Press, New York.

Butler, H. L. (In preparation). "Lake Pontchartrain and Vicinity Hurricane Protection Plan: Numerical Model Investigation of Plan Impact on the Tidal Prism of Lake Pontchartrain," Technical Report H-82-2, Report 3, U. S. Army Engineer Waterways Experiment Station, CE, Vicksburg, Miss.

Chow, Ven Te. 1959. "Open-Channel Hydraulics," McGraw-Hill Book Company, New York.

Keulegan, G. H. 1967 (Jul). "Tidal Flow in Entrances: Water-Level Fluctuations of Basins in Communication with Seas," Technical Bulletin No. 14, U. S. Army Corps of Engineers, Committee on Tidal Hydraulics, Vicksburg, Miss.

Outlaw, D. G. 1982 (Jan). "Lake Pontchartrain and Vicinity Hurricane Protection Plan; Prototype Data Acquisition and Analysis," Technical Report HL-82-2, Report 1, U. S. Army Engineer Waterways Experiment Station, CE, Vicksburg, Miss.

Table 1

Seabrook Model, Summary of Base Conditions for a Discharge of 5,000 cfs

	Water-Surface Elevation, ft NGVD									
	Flood					Ebb				
	Run 1	Run 2			Run 3	Run 1	Run 2			Run 3
Station	P	P	C	F	P	P	P	C	F	P
1	-1.10	1.00	--	0.92	1.95	-0.95	0.95	--	0.95	2.95
2	-1.00	1.10	--	0.92	2.05	-0.95	1.10	--	0.95	3.05
3	-1.12	0.92	--	0.92	1.86	-0.92	0.93	--	0.95	2.89
4	-1.10	0.95	--	0.92	1.90	-0.95	0.95	--	0.95	2.90
5	-1.10	1.00	0.97	0.92	1.90	-0.95	0.95	0.90	0.95	2.95
6	-1.12	0.94	--	0.92	1.88	-0.92	0.93	--	0.95	2.92
7	-1.10	0.95	--	0.92	1.90	-0.95	0.95	--	0.95	2.95
8	-1.16	0.89	--	0.92	1.84	-0.94	0.92	--	0.95	2.90
9	-1.15	0.95	--	0.92	1.90	-0.90	0.95	--	0.95	2.90
10	-0.95	1.10	--	0.94	2.05	-0.95	0.95	--	0.92	2.95
11	-0.95	1.10	--	0.94	2.00	-0.95	0.90	--	0.92	2.95
12	-1.00	1.05	--	0.94	2.00	-1.00	0.85	--	0.92	2.85
13	-1.01	1.01	1.01	0.95	1.92	-1.00	0.87	0.87	0.92	2.84

	Velocity, fps									
	Flood (Run 2)					Ebb (Run 2)				
	Surface	Mid	Bottom	Average		Surface	Mid	Bottom	Average	
	P	P	P	P	F	P	P	P	P	F
A1	0.3	0.3	0.3	0.3	0.1	0.2	0.2	0.3	0.2	0.1
A2	0.3	0.2	0.2	0.2	0.1	0.3	0.2	0.2	0.2	0.1
A3	0.2	0.2	0.2	0.2	0.1	0.2	0.2	0.2	0.2	0.1
AB	2.7	2.7	1.9	2.4	0.8	1.3	1.4	1.1	1.3	0.8
B1	1.3	1.5	1.0	1.3	0.5	0.4	0.5	0.5	0.5	0.5
B2	1.7	1.5	1.0	1.4	0.5	0.9	1.2	0.8	1.0	0.5
B3	1.1	1.1	0.6	0.9	0.4	0.7	0.4	0.4	0.5	0.4

Note: P = physical model; C = computational grid model; F = fine scale model.

Table 2

Seabrook Model, Summary of Base Conditions for a Discharge of 10,000 cfs

	Water-Surface Elevation, ft NGVD							
	Flood				Ebb			
	Run 1	Run 2		Run 3	Run 1	Run 2		Run 3
Station	P	P	C	P	P	P	C	P
1	1.93	0.98	--	-1.08	3.00	1.10	--	-0.88
2	2.00	1.10	--	-0.98	3.03	1.10	--	-0.85
3	1.86	0.92	--	-1.11	3.00	1.08	--	-0.85
4	1.85	0.95	--	-1.08	3.00	1.08	--	-0.85
5	1.93	0.98	0.90	-1.08	3.00	1.10	1.04	-0.85
6	1.86	0.93	--	-1.10	3.00	1.08	--	-0.86
7	1.88	0.98	--	-1.05	3.00	1.10	--	-0.85
8	1.82	0.89	--	-1.14	2.95	1.05	--	-0.91
9	1.85	0.95	--	-1.10	2.98	1.08	--	-0.88
10	2.03	1.13	--	-0.88	2.83	0.95	--	-1.00
11	2.00	1.10	--	-0.93	2.88	0.98	--	-1.00
12	2.00	1.08	--	-0.93	2.88	0.95	--	-1.05
13	1.96	1.03	1.03	-0.97	2.81	0.92	0.92	-0.98

	Velocity, fps							
	Flood (Run 2)				Ebb (Run 2)			
	Surface	Mid	Bottom	Average	Surface	Mid	Bottom	Average
	P	P	P	P	P	P	P	P
A1	0.3	0.4	0.3	0.3	0.4	0.4	0.2	0.3
A2	0.3	0.2	0.3	0.3	0.3	0.4	0.2	0.3
A3	0.2	0.2	0.2	0.2	0.2	0.4	0.2	0.3
AB	2.9	2.9	2.3	2.7	2.5	2.3	2.1	2.3
B1	1.4	1.4	1.0	1.3	1.2	1.4	1.3	1.3
B2	1.8	1.7	1.0	1.5	2.0	1.8	1.4	1.7
B3	1.0	1.2	0.6	0.9	0.8	1.1	0.5	0.8

Note: P = physical model; C = computational grid model.

Table 3

Seabrook Model, Summary of Base Conditions for a Discharge of 15,000 cfs

	Water-Surface Elevation, ft NGVD													
	Flood							Ebb						
	Run 1		Run 2			Run 3		Run 1		Run 2			Run 3	
Station	P	C	P	C	F	P	C	P	C	P	C	F	P	C
1	-1.30	--	0.73	--	0.71	1.70	--	-0.80	--	1.03	--	1.00	3.10	--
2	-1.20	--	0.83	--	0.71	1.80	--	-0.80	--	1.03	--	1.00	3.13	--
3	-1.29	--	0.71	--	0.71	1.68	--	-0.82	--	1.00	--	1.00	3.05	--
4	-1.30	--	0.73	--	0.71	1.68	--	-0.83	--	1.00	--	1.00	3.05	--
5	-1.30	-1.32	0.70	0.70	0.71	1.68	1.67	-0.83	-0.88	1.03	0.90	1.00	3.03	2.96
6	-1.31	--	0.70	--	0.71	1.68	--	-0.83	--	0.99	--	1.00	3.05	--
7	-1.30	--	0.70	--	0.71	1.70	--	-0.85	--	1.00	--	1.00	3.08	--
8	-1.38	--	0.65	--	0.72	1.64	--	-0.94	--	0.90	--	0.99	2.97	--
9	-1.33	--	0.68	--	0.72	1.68	--	-0.95	--	0.98	--	0.99	3.00	--
10	-1.00	--	0.98	--	0.90	1.95	--	-1.15	--	0.70	--	0.77	2.78	--
11	-0.98	--	0.98	--	0.90	1.93	--	-1.15	--	0.70	--	0.75	2.75	--
12	-1.00	--	0.95	--	0.92	1.93	--	-1.23	--	0.63	--	0.74	2.73	--
13	-0.98	-0.98	0.98	0.98	0.93	1.92	1.92	-1.22	-1.22	0.62	0.62	0.73	2.73	2.73

	Velocity, fps									
	Flood (Run 2)					Ebb (Run 2)				
	Surface	Mid	Bottom	Average		Surface	Mid	Bottom	Average	
	P	P	P	P	F	P	P	P	P	F
A1	0.3	0.3	0.3	0.3	0.3	0.3	0.5	0.3	0.4	0.3
A2	0.3	0.3	0.3	0.3	0.3	0.4	0.5	0.3	0.4	0.3
A3	0.2	0.2	0.2	0.2	0.3	0.4	0.4	0.2	0.3	0.3
AB	4.1	4.0	3.5	3.9	2.4	2.9	3.2	3.0	3.0	2.39
B1	1.6	1.8	1.5	1.6	1.5	1.2	1.2	0.6	1.0	1.5
B2	2.3	2.2	1.6	2.0	1.4	2.7	2.2	1.9	2.3	1.4
B3	1.9	1.9	1.3	1.7	1.2	2.3	2.0	1.9	2.1	1.2

Note: P = physical model; C = computational grid model; F = fine scale model.

Table 4

Seabrook Model, Summary of Base Conditions for a Discharge of 20,000 cfs

Station	Water-Surface Elevation, ft NGVD							
	Flood				Ebb			
	Run 1	Run 2		Run 3	Run 1	Run 2		Run 3
	P	P	C	P	P	P	C	P
1	1.58	0.65	--	-1.50	3.03	1.15	--	-0.78
2	1.70	0.73	--	-1.40	3.08	1.13	--	-0.73
3	1.59	0.60	--	-1.48	3.04	1.12	--	-0.76
4	1.58	0.63	--	-1.50	3.05	1.13	--	-0.75
5	1.60	0.63	0.53	-1.48	3.03	1.13	1.09	-0.73
6	1.58	0.61	--	-1.50	3.04	1.10	--	-0.76
7	1.58	0.63	--	-1.48	3.03	1.13	--	-0.75
8	1.49	0.51	--	-1.59	2.96	0.99	--	-0.91
9	1.58	0.65	--	-1.50	3.00	1.05	--	-0.80
10	1.93	1.00	--	-1.08	2.65	0.65	--	-1.28
11	1.98	1.03	--	-1.03	2.63	0.65	--	-1.30
12	1.98	1.05	--	-1.00	2.60	0.63	--	-1.35
13	1.98	1.03	1.03	-0.98	2.63	0.60	0.60	-1.41

	Velocity, fps							
	Flood (Run 2)				Ebb (Run 2)			
	Surface	Mid	Bottom	Average	Surface	Mid	Bottom	Average
	P	P	P	P	P	P	P	P
A1	0.5	0.3	0.3	0.4	0.5	0.6	0.4	0.5
A2	0.5	0.2	0.2	0.3	0.5	0.6	0.3	0.5
A3	0.2	0.2	0.2	0.2	0.5	0.6	0.3	0.5
AB	4.7	5.1	4.3	4.7	1.7	3.9	3.9	3.2
B1	2.4	2.0	1.9	2.1	1.4	1.6	2.0	1.7
B2	2.8	2.6	2.0	2.5	3.4	3.1	2.3	2.9
B3	2.4	2.4	1.9	2.2	2.6	2.2	1.1	2.0

Note: P = physical model; C = computational grid model.

Table 5

Seabrook Model, Summary of Base Conditions for a Discharge of 30,000 cfs

	Water Surface Elevation, ft NGVD									
	Flood					Ebb				
	Run 1	Run 2			Run 3	Run 1	Run 2			Run 3
Station	P	P	C	F	P	P	P	C	F	P
1	1.25	0.23	--	0.21	-1.93	3.23	1.15	--	1.16	-0.73
2	1.35	0.38	--	0.21	-1.80	3.23	1.18	--	1.15	-0.70
3	1.20	0.21	--	0.21	-1.97	3.23	1.15	--	1.16	-0.70
4	1.25	0.23	--	0.21	-1.95	3.23	1.15	--	1.16	-0.73
5	1.23	0.23	-0.05	0.21	-1.93	3.23	1.15	1.30	1.15	-0.70
6	1.23	0.23	--	0.21	-1.94	3.21	1.12	--	1.15	-0.75
7	1.25	0.23	--	0.21	-1.95	3.23	1.13	--	1.15	-0.75
8	0.99	-0.09	--	0.24	-2.34	3.07	0.95	--	1.15	-0.98
9	1.23	0.23	--	0.22	-1.95	3.15	1.05	--	1.14	-0.78
10	1.88	0.90	--	0.95	-1.18	2.45	0.23	--	0.22	-1.80
11	1.93	0.98	--	0.99	-1.08	2.43	0.23	--	0.18	-1.75
12	2.00	1.03	--	1.04	-1.00	2.45	0.20	--	0.12	-1.83
13	1.98	1.04	1.00	1.07	-0.97	2.45	0.21	0.20	0.09	-1.87

	Velocity, fps									
	Flood (Run 2)					Ebb (Run 2)				
	Surface	Mid	Bottom	Average		Surface	Mid	Bottom	Average	
	P	P	P	P	F	P	P	P	P	F
A1	0.3	0.3	0.2	0.3	0.7	0.9	1.0	0.5	0.8	0.6
A2	0.4	0.2	0.3	0.3	0.6	1.0	1.0	0.6	0.9	0.6
A3	0.2	0.2	0.2	0.2	0.6	0.9	0.9	0.7	0.8	0.6
AB	7.0	7.0	6.1	6.7	4.9	4.8	5.0	4.8	4.9	4.8
B1	3.2	2.8	2.3	2.8	2.9	2.0	2.0	2.5	2.2	3.0
B2	3.7	3.5	2.9	3.4	2.8	4.1	3.8	3.2	3.7	2.9
B3	3.5	3.2	2.6	3.1	2.4	4.1	3.3	2.1	3.2	2.5

Note: P = physical model; C = computational grid model; F = fine scale model.

Table 6

Seabrook Model, Plan 1

Discharge = 5000 cfs

Station*	Water-Surface Elevation, ft NGVD	
	Flood	Ebb
1	-5.60	3.35
2	-5.65	3.33
3	-5.59	3.33
4	-5.58	3.38
5	-5.68	3.33
6	-5.63	3.38
7	-5.23	3.33
8	3.17	-7.72
9	3.25	-9.00
10	3.20	-7.58
11	3.20	-7.63
12	3.18	-7.70
13	3.22	-7.60

* Gages 3, 6, 8, and 13 are electronic, the remainder are manual.

Table 7

Seabrook Model, Plan 2 Discharge = 5000 cfs

	Water-Surface Elevation, ft NGVD								
	Flood				Ebb				
Station*	Run 1	Run 2	Run 3	Run 4	Run 1	Run 2	Run 3	Run 4	Run 5
1	1.28	-0.08	-1.28	-2.35	-0.88	-0.05	1.03	2.00	2.93
2	1.30	-0.03	-1.23	-2.38	-0.90	-0.08	0.98	1.93	2.90
3	1.23	-0.07	-1.26	-2.36	-0.95	-0.13	0.95	2.02	2.90
4	1.30	0.00	-1.25	-2.33	-0.85	0.00	1.05	2.00	2.95
5	1.33	-0.05	-1.25	-2.40	-0.95	-0.03	1.00	1.95	2.90
6	1.28	-0.06	-1.27	-2.39	-0.89	-0.05	1.00	2.00	2.93
7	1.33	0.00	-1.20	-2.38	-0.93	-0.08	1.00	1.98	2.90
8	1.98	0.91	-0.12	-1.04	-2.20	-1.20	0.05	1.16	2.10
9	1.98	0.93	-0.20	-1.10	-2.45	-1.48	-0.20	0.88	2.00
10	2.05	1.00	-0.13	-1.05	-2.18	-1.15	0.10	1.15	2.08
11	2.05	0.95	-0.15	-1.00	-2.20	-1.20	0.03	1.15	2.08
12	2.00	0.98	-0.13	-1.03	-2.25	-1.25	0.15	1.28	2.00
13	2.03	0.96	-0.07	-0.98	-2.26	-1.26	-0.01	1.17	2.09

	Velocity, fps							
	Flood (Run 2)				Ebb (Run 3)			
	Surface	Mid	Bottom	Average	Surface	Mid	Bottom	Average
A1	2.9	2.9	2.6	2.8	0.6	1.0	0.3	0.6
A2	2.6	2.8	2.6	2.7	0.8	1.0	0.3	0.7
A3	0.3	0.7	0.8	0.6	0.7	1.0	0.4	0.7
AB	1.5	1.4	0.8	1.2	1.6	1.8	1.3	1.6
B1	0.5	0.9	0.6	0.7	0.4	0.8	1.1	0.8
B2	0.5	0.5	0.5	0.5	0.6	1.1	0.6	0.8
B3	0.3	0.4	0.3	0.3	0.3	0.7	0.6	0.4

* Gages 3, 6, 8, and 13 are electronic, the remainder are manual.

Table 8

Seabrook Model, Plan 2 Discharge = 6250 cfs

	Water-Surface Elevation, ft NGVD								
	Flood				Ebb				
Station*	Run 1	Run 2	Run 3	Run 4	Run 1	Run 2	Run 3	Run 4	Run 5
1	0.68	-0.58	-1.73	-3.10	3.00	2.00	1.05	0.03	-0.95
2	0.73	-0.53	-1.70	-3.10	3.00	2.05	1.10	0.08	-0.90
3	0.63	-0.61	-1.76	-3.16	2.99	1.98	1.03	0.03	-0.97
4	0.68	-0.55	-1.68	-3.10	3.03	2.03	1.08	0.05	-0.93
5	0.63	-0.60	-1.78	-3.13	3.03	2.05	1.08	0.08	-0.93
6	0.68	-0.58	-1.72	-3.14	3.05	2.04	1.09	0.07	-0.94
7	0.65	-0.58	-1.73	-3.13	3.00	2.08	1.10	0.08	-0.90
8	1.90	0.87	-0.03	-1.01	1.97	0.82	-0.36	-1.68	-3.21
9	1.88	0.85	-0.08	-1.05	1.98	0.73	-0.43	-1.75	-3.23
10	2.00	0.98	0.08	-0.88	1.98	0.73	-0.40	-1.73	-3.23
11	2.00	0.98	0.08	-0.93	1.93	0.78	-0.35	-1.73	-3.23
12	2.03	1.00	0.08	-0.85	2.00	0.80	-0.33	-1.73	-3.23
13	1.95	0.92	0.01	-0.95	1.89	0.72	-0.45	-1.77	-3.30

	Velocity, fps							
	Flood (Run 2)				Ebb (Run 3)			
	Surface	Mid	Bottom	Average	Surface	Mid	Bottom	Average
A1	4.1	4.1	3.3	3.8	0.9	1.1	0.2	0.7
A2	3.6	3.7	3.5	3.6	1.0	1.1	0.6	0.9
A3	0.7	1.5	1.4	1.2	0.9	1.1	0.5	0.8
AB	1.8	1.9	1.4	1.7	2.1	2.1	1.6	1.9
B1	0.8	1.1	0.7	0.9	0.4	1.3	1.1	0.9
B2	1.2	1.2	0.6	1.0	1.5	1.4	0.9	1.3
B3	0.3	0.8	0.3	0.5	0.3	0.4	0.4	0.4

* Gages 3, 6, 8, and 13 are electronic, the remainder are manual.

Table 9

Seabrook Model, Plan 2 Discharge = 7,500 cfs

	Water-Surface Elevation, ft NGVD								
	Flood				Ebb				
Station*	Run 1	Run 2	Run 3	Run 4	Run 1	Run 2	Run 3	Run 4	Run 5
1	0.05	-1.60	-3.88	-6.68	2.98	2.00	1.08	0.03	-0.45
2	0.10	-1.55	-3.83	-6.68	3.03	2.05	1.10	0.13	-0.45
3	-0.03	-1.59	-3.87	-6.63	2.92	1.94	1.03	0.01	-0.46
4	0.08	-1.55	-3.85	-6.63	3.00	2.00	1.10	0.10	-0.43
5	0.08	-1.58	-3.83	-6.63	3.03	2.05	1.10	0.10	-0.40
6	-0.04	-1.62	-3.92	-6.75	3.02	2.03	1.09	0.07	-0.45
7	0.03	-1.60	-3.90	-6.58	3.03	2.08	1.13	0.15	-0.40
8	1.98	0.90	-0.16	-0.25	1.51	0.31	-0.87	-2.39	-7.35
9	1.98	0.80	-0.28	-0.35	1.38	0.20	-1.00	-2.60	-8.33
10	2.10	1.00	-0.08	-0.13	1.48	0.23	-0.98	-2.48	-7.48
11	2.13	1.00	-0.05	-0.13	1.48	0.20	-0.98	-2.48	-7.45
12	2.15	0.98	-0.10	-0.20	1.45	0.25	-0.98	-2.48	-7.48
13	2.03	1.02	-0.04	-0.13	1.47	0.21	-0.97	-2.47	-7.47

	Velocity, fps							
	Flood (Run 2)				Ebb (Run 2)			
	Surface	Mid	Bottom	Average	Surface	Mid	Bottom	Average
A1	5.0	4.9	4.0	4.6	1.0	1.3	0.4	0.9
A2	4.2	4.4	4.0	4.2	1.1	1.3	0.6	1.0
A3	1.1	1.5	1.5	1.4	1.1	1.2	0.5	0.9
AB	2.3	2.4	2.0	2.2	2.6	2.6	1.7	2.3
B1	0.5	1.2	0.7	0.8	0.4	1.3	0.8	0.8
B2	1.6	1.4	1.0	1.3	1.9	1.5	1.2	1.5
B3	0.7	1.1	0.8	0.9	0.3	0.8	0.8	0.6

* Gages 3, 6, 8, and 13 are electronic, the remainder are manual.

Table 10

Seabrook Model, Plan 2 Discharge = 8,750 cfs

	Water-Surface Elevation, ft NGVD						
	Flood			Ebb			
Station*	Run 1	Run 2	Run 3	Run 1	Run 2	Run 3	Run 4
1	-1.03	-3.43	-7.63	2.90	2.03	0.95	0.48
2	-1.00	-3.38	-7.63	2.93	2.13	1.00	0.53
3	-1.05	-3.39	-7.60	2.89	2.06	0.93	0.43
4	-1.03	-3.40	-7.63	2.90	2.08	1.00	0.53
5	-1.00	-3.38	-7.63	2.93	2.13	1.00	0.53
6	-1.06	-3.41	-7.65	2.93	2.09	0.95	0.45
7	-1.05	-3.38	--	2.98	2.13	1.00	0.55
8	1.82	0.99	0.98	0.69	-0.49	-2.23	-7.44
9	1.73	0.88	0.88	0.53	-0.70	-3.03	-9.33
10	1.98	1.13	1.10	0.60	-0.60	-2.40	-7.60
11	1.98	1.10	1.05	0.63	-0.63	-2.38	-7.60
12	1.88	1.08	1.00	0.60	-0.60	-2.40	-7.60
13	1.92	1.10	1.11	0.58	-0.61	-2.36	-7.55

	Velocity, fps							
	Flood (Run 2)				Ebb (Run 3)			
	Surface	Mid	Bottom	Average	Surface	Mid	Bottom	Average
A1	4.7	6.2	5.6	5.5	1.3	0.8	0.2	0.8
A2	5.0	6.0	5.2	5.4	1.5	0.7	0.3	0.8
A3	1.2	2.1	2.0	1.8	1.3	1.5	0.6	1.1
AB	2.8	2.6	2.0	2.5	3.6	3.2	2.5	3.1
B1	1.2	1.4	1.1	1.2	1.0	1.6	1.1	1.2
B2	1.8	1.5	0.9	1.4	2.2	1.7	1.6	1.8
B3	1.1	1.2	0.6	1.0	1.5	0.8	0.4	0.9

* Gages 3, 6, 8, and 13 are electronic, the remainder are manual.

Table 11

Seabrook Model, Plan 2 Discharge = 10,000 cfs

	Water-Surface Elevation, ft NGVD		
		Ebb	
Station*	Flood	Run 1	Run 2
1	-4.98	3.08	2.25
2	-4.98	3.03	2.20
3	-5.00	3.05	2.16
4	-4.93	3.10	2.28
5	-5.00	3.03	2.23
6	-5.20	3.07	2.20
7	-4.88	3.05	2.23
8	2.08	0.00	-6.21
9	2.13	-0.48	-8.00
10	2.23	-0.05	-6.30
11	2.23	-0.03	-6.22
12	2.23	-0.18	-6.42
13	2.23	-0.06	-6.34

* Gages 3, 6, 8, and 13 are electronic, the remainder are manual.

Table 12

Seabrook Model, Plan 3 Discharge = 5000 cfs

	Water-Surface Elevation, ft NGVD								
	Flood				Ebb				
Station*	Run 1	Run 2	Run 3	Run 4	Run 1	Run 2	Run 3	Run 4	Run 5
1	-1.48	-0.45	0.48	1.65	3.08	1.93	1.08	0.08	-0.95
2	-1.48	-0.45	0.50	1.68	3.05	1.88	1.03	0.00	-1.00
3	-1.48	-0.42	0.48	1.60	3.04	1.83	1.02	0.00	-1.04
4	-1.43	-0.38	0.50	1.68	3.08	1.95	1.08	0.10	-0.93
5	-1.38	-0.43	0.45	1.70	3.03	1.90	1.03	0.05	-0.98
6	-1.47	-0.40	0.50	1.64	3.07	1.91	1.06	0.06	-0.98
7	-1.38	-0.40	0.60	1.73	3.05	1.90	1.00	0.05	-1.00
8	-1.02	0.03	0.88	1.92	2.71	1.50	0.64	-0.43	-1.52
9	-1.08	0.08	0.90	1.90	2.68	1.25	0.40	-0.70	-1.80
10	-0.98	0.05	0.98	2.00	2.70	1.55	0.65	-0.38	-1.50
11	-0.90	0.08	0.95	2.00	2.68	1.50	0.60	-0.40	-1.53
12	-0.98	0.03	0.93	1.98	2.60	1.45	0.60	-0.48	-1.60
13	-0.95	0.09	0.94	1.99	2.67	1.44	0.57	-0.49	-1.59

	Velocity, fps							
	Flood (Run 3)				Ebb (Run 3)			
	Surface	Mid	Bottom	Average	Surface	Mid	Bottom	Average
A1	1.6	1.7	1.8	1.7	0.7	0.9	0.2	0.6
A2	3.0	3.0	2.2	2.7	0.5	0.9	0.4	0.6
A3	0.8	1.7	1.2	1.2	0.6	0.9	0.2	0.6
AB	1.2	1.5	1.0	1.2	1.3	1.4	1.5	1.4
B1	0.4	0.9	0.5	0.6	0.7	1.1	0.4	0.7
B2	0.5	0.6	0.5	0.5	0.8	0.9	0.7	0.8
B3	0.3	0.7	0.3	0.4	0.3	0.4	0.7	0.5

* Gages 3, 6, 8, and 13 are electronic, the remainder are manual.

Table 13

Seabrook Model, Plan 3 Discharge = 7,500 cfs

	Water-Surface Elevation, ft NGVD								
	Flood				Ebb				
Station*	Run 1	Run 2	Run 3	Run 4	Run 1	Run 2	Run 3	Run 4	Run 5
1	-2.28	-1.03	0.03	1.18	2.98	1.83	1.00	-0.08	-1.05
2	-2.20	-1.00	0.08	1.20	3.00	1.93	1.05	-0.05	-0.98
3	-2.19	-1.04	0.07	1.15	2.97	1.82	0.94	-0.12	-1.04
4	-2.23	-1.03	0.08	1.15	3.00	1.90	1.03	-0.05	-1.00
5	-2.20	-1.03	0.08	1.18	3.00	1.93	1.03	0.00	-0.98
6	-2.26	-1.09	0.03	1.10	3.02	1.91	1.03	-0.06	-0.99
7	-2.23	-1.05	0.00	1.10	3.03	1.95	1.03	0.00	-0.93
8	-1.07	-0.07	0.91	1.89	2.40	1.22	0.24	-0.98	-2.04
9	-1.28	-0.20	0.78	1.78	2.30	1.10	0.13	-1.13	-2.23
10	-1.00	0.00	1.00	1.93	2.25	1.13	0.15	-1.05	-2.08
11	-1.00	0.00	1.00	1.95	2.30	1.13	0.18	-1.00	-2.08
12	-1.00	-0.05	0.95	1.90	2.33	1.18	0.20	-1.03	-2.10
13	-0.98	0.00	0.98	1.96	2.29	1.10	0.14	-1.07	-2.14

	Velocity, fps							
	Flood (Run 3)				Ebb (Run 3)			
	Surface	Mid	Bottom	Average	Surface	Mid	Bottom	Average
A1	2.8	3.1	2.7	2.9	1.1	1.3	0.2	0.9
A2	4.6	5.1	3.6	4.4	1.2	1.3	0.6	1.0
A3	2.6	3.5	2.3	2.8	1.1	1.3	0.6	1.0
AB	2.4	2.4	1.9	2.2	2.1	2.2	1.9	2.1
B1	1.2	1.2	1.0	1.1	0.4	0.9	1.0	0.8
B2	1.5	1.4	1.0	1.3	1.9	1.6	1.0	1.5
B3	1.1	1.1	0.7	1.0	1.2	0.7	0.7	0.9

* Gages 3, 6, 8, and 13 are electronic, the remainder are manual.

Table 14

Seabrook Model, Summary of Plan 3 for a Discharge of 10,000 cfs

	Water-Surface Elevation, ft NGVD										
	Flood					Ebb					
	Run 1	Run 2		Run 3	Run 4	Run 1	Run 2	Run 3		Run 4	Run 5
Station	P	P	C	P	P	P	P	P	C	P	P
1	0.60	-0.50	--	-1.78	-3.30	-0.90	-0.03	0.93	--	1.98	2.90
2	0.63	-0.48	--	-1.78	-3.30	-0.98	-0.03	0.90	--	1.95	2.88
3	0.62	-0.52	--	-1.80	-3.28	-0.95	-0.04	0.88	--	1.94	2.87
4	0.65	-0.48	--	-1.75	-3.25	-0.93	0.00	0.95	--	1.98	2.90
5	0.60	-0.55	-0.52	-1.80	-3.33	-0.93	-0.03	0.90	0.89	1.95	2.85
6	0.61	-0.62	--	-1.94	-3.47	-0.95	-0.02	0.90	--	1.97	2.90
7	0.73	-0.50	--	-1.73	-3.23	-0.96	-0.03	0.93	--	1.95	2.88
8	1.87	0.90	--	-0.11	-1.16	-3.30	-1.88	-0.64	--	0.66	1.78
9	1.85	0.88	0.94	-0.15	-1.23	-4.05	-2.30	-1.05	-0.51	0.25	1.65
10	2.00	1.05	--	0.05	-1.00	-3.35	-1.93	-0.68	--	0.60	1.73
11	2.00	1.08	--	0.05	-1.00	-3.38	-1.93	-0.62	--	0.60	1.73
12	1.98	1.03	--	0.00	-1.03	-3.45	-2.00	-0.75	--	0.50	1.65
13	2.01	1.05	1.05	0.06	-0.98	-3.41	-1.97	-0.73	-0.65	0.57	1.72

	Velocity, fps							
	Flood (Run 2)				Ebb (Run 3)			
	Surface	Mid	Bottom	Average	Surface	Mid	Bottom	Average
	P	P	P	P	P	P	P	P
A1	2.7	3.0	2.9	2.9	1.5	1.7	0.4	1.2
A2	5.5	6.3	5.0	5.6	1.4	1.8	0.8	1.3
A3	2.7	3.7	2.5	3.0	1.6	1.8	0.9	1.3
AB	3.1	3.0	2.6	2.9	2.9	2.8	2.6	2.8
B1	1.3	1.4	1.2	1.3	1.1	0.7	0.5	0.8
B2	1.6	1.6	1.1	1.4	2.2	2.0	1.6	1.9
B3	1.1	1.3	0.8	1.1	1.4	1.2	1.5	1.4

Note: P = physical model; C = computational grid model.

Table 15

Seabrook Model, Plan 3 Discharge = 12,500 cfs

	Water-Surface Elevation, ft NGVD								
	Flood				Ebb				
Station*	Run 1	Run 2	Run 3	Run 4	Run 1	Run 2	Run 3	Run 4	Run 5
1	-0.13	-1.68	-3.50	-7.38	2.95	1.90	1.03	0.05	-0.20
2	-0.08	-1.68	-3.48	-7.38	3.00	1.90	1.08	0.10	-0.13
3	-0.10	-1.67	-3.50	-7.37	2.86	1.82	0.98	0.07	-0.20
4	-0.10	-1.68	-3.45	-7.38	2.95	1.90	1.03	0.10	-0.13
5	-0.10	-1.70	-3.48	-7.33	2.93	1.90	1.08	0.10	-0.15
6	-0.28	-1.87	-3.75	-7.60	2.96	1.91	1.05	0.08	-0.19
7	-0.18	-1.70	-3.48	--	2.93	1.88	1.00	0.10	-0.13
8	1.77	0.74	-0.17	-0.28	1.21	-0.21	-1.50	-3.27	-8.98
9	1.60	0.50	-0.43	-0.53	1.08	-0.55	-1.95	-4.55	-10.55
10	1.93	0.90	-0.08	-0.10	1.13	-0.33	-1.68	-3.50	-9.40
11	1.98	0.90	0.00	-0.08	1.10	-0.35	-1.63	-3.48	-9.32
12	1.95	0.90	0.00	-0.10	1.08	-0.45	-1.78	-3.48	-9.50
13	1.96	0.94	0.05	-0.06	1.03	-0.40	-1.68	-3.48	-9.46

	Velocity, fps							
	Flood (Run 2)				Ebb (Run 3)			
	Surface	Mid	Bottom	Average	Surface	Mid	Bottom	Average
A1	4.2	4.5	4.5	4.4	2.0	1.9	0.3	1.4
A2	6.1	7.4	5.0	6.2	2.0	2.1	1.5	1.9
A3	3.9	5.4	3.9	4.4	2.0	2.0	0.8	1.6
AB	3.7	3.5	3.0	3.4	3.4	3.8	3.3	3.5
B1	1.4	1.6	1.5	1.5	2.0	1.4	1.4	1.6
B2	2.2	1.9	1.5	1.9	2.9	2.3	1.9	2.4
B3	1.5	1.6	1.3	1.5	2.0	1.6	1.3	1.6

* Gages 3, 6, 8, and 13 are electronic, the remainder are manual.

Table 16

Seabrook Model, Plan 3 Discharge = 15,000 cfs

	Water-Surface Elevation, ft NGVD				
	Flood		Ebb		
Station*	Run 1	Run 2	Run 1	Run 2	Run 3
1	-1.85	-3.58	3.05	2.03	1.25
2	-1.88	-3.60	3.03	2.00	1.23
3	-1.91	-3.48	2.94	1.96	1.18
4	-1.80	-3.48	3.08	2.05	1.28
5	-1.85	-3.55	3.00	2.03	1.23
6	-2.26	-3.92	3.02	2.02	1.21
7	-1.85	-3.53	3.00	2.00	1.23
8	1.68	1.43	0.55	-1.06	-5.73
9	1.38	1.10	0.23	-1.53	-7.78
10	1.90	1.63	0.38	-1.18	-5.98
11	1.93	1.65	0.43	-1.18	-6.03
12	1.90	1.65	0.38	-1.28	-6.08
13	1.95	1.70	0.34	-1.27	-6.04

* Gages 3, 6, 8, and 13 are electronic, the remainder are manual.

Table 17

Seabrook Model, Summary of Plan 4 for a Discharge of 5000 cfs

	Water-Surface Elevation, ft NGVD										
	Flood					Ebb					
	Run 1	Run 2		Run 3	Run 4	Run 1	Run 2		Run 3	Run 4	Run 5
Station	P	P	C	P	P	P	P	C	P	P	P
1	1.73	0.75	--	-0.15	-1.20	3.00	1.90	--	1.03	-0.05	-1.00
2	1.73	0.83	--	-0.13	-1.18	2.98	1.85	--	1.00	-0.10	-1.05
3	1.71	0.75	--	-0.18	-1.25	2.99	1.82	--	0.99	-0.12	-1.06
4	1.75	0.80	--	-0.10	-1.18	3.00	1.90	--	1.05	-0.03	-1.00
5	1.78	0.73	0.79	-0.18	-1.13	2.98	1.88	1.89	1.00	-0.10	-1.03
6	1.75	0.79	--	-0.13	-1.20	3.01	1.90	--	1.03	-0.08	-1.02
7	1.75	0.88	--	-0.08	-1.18	2.98	1.88	--	1.00	-0.10	-1.05
8	1.87	0.91	--	0.00	-1.02	2.84	1.69	--	0.81	-0.31	-1.29
9	1.83	0.98	0.95	0.10	-1.08	2.80	1.58	1.80	0.83	-0.28	-1.33
10	1.90	1.00	--	0.10	-0.98	2.80	1.70	--	0.83	-0.30	-1.28
11	1.90	0.95	--	0.05	-0.98	2.78	1.70	--	0.83	-0.33	-1.30
12	1.88	0.95	--	0.00	-1.00	2.73	1.63	--	0.75	-0.40	-1.43
13	1.90	0.96	0.97	0.06	-0.97	2.82	1.63	1.78	0.77	-0.37	-1.34

	Velocity, fps							
	Flood (Run 2)				Ebb (Run 3)			
	Surface	Mid	Bottom	Average	Surface	Mid	Bottom	Average
	P	P	P	P	P	P	P	P
A1	1.6	1.6	1.4	1.5	0.3	0.4	0.2	0.3
A2	1.2	1.6	1.3	1.4	0.3	0.6	0.2	0.4
A3	0.2	0.4	0.5	0.4	0.3	0.5	0.2	0.3
AB	1.1	1.5	1.2	1.3	1.1	1.3	1.2	1.2
B1	0.7	0.9	0.4	0.7	0.6	0.4	0.4	0.5
B2	0.5	0.7	0.5	0.6	0.8	1.0	0.6	0.8
B3	0.4	0.6	0.3	0.4	0.3	0.5	0.4	0.4

Note: P = physical model; C = computational grid model.

Table 18

Seabrook Model, Summary of Plan 4 for a Discharge of 10,000 cfs

	Water-Surface Elevation, ft NGVD												
	Flood						Ebb						
	Run 1	Run 2	Run 3			Run 4	Run 1	Run 2	Run 3			Run 4	Run 5
Station	P	P	P	C	F	P	P	P	P	C	F	P	P
1	-1.85	-0.80	0.30	--	0.35	1.30	2.95	1.95	1.08	--	1.02	0.10	-0.90
2	-1.80	-0.78	0.33	--	0.35	1.30	2.90	1.90	1.03	--	1.02	0.05	-0.93
3	-1.83	-0.79	0.30	--	0.35	1.29	2.87	1.91	1.04	--	1.02	0.06	-0.94
4	-1.80	-0.80	0.33	--	0.35	1.33	2.93	1.98	1.08	--	1.02	0.10	-0.90
5	-1.85	-0.83	0.28	0.30	0.35	1.28	2.88	1.93	1.03	1.04	1.02	0.05	-0.90
6	-1.88	-0.83	0.29	--	0.35	1.33	2.92	1.95	1.07	--	1.02	0.08	-0.92
7	-1.78	-0.73	0.35	--	0.35	1.35	2.90	1.93	1.05	--	1.02	0.05	-0.95
8	-1.07	-0.15	0.85	--	0.96	1.79	2.48	1.42	0.48	--	0.41	-0.61	-1.71
9	-1.10	-0.15	0.83	0.74	0.96	1.78	2.45	1.18	0.18	0.62	0.41	-0.88	-2.03
10	-0.98	-0.03	1.00	--	0.99	1.90	2.38	1.33	0.43	--	0.38	-0.68	-1.80
11	-0.98	-0.03	0.98	--	0.99	1.88	2.38	1.30	0.38	--	0.38	-0.70	-1.83
12	-0.98	-0.05	0.95	--	1.00	1.88	2.30	1.25	0.30	--	0.37	-0.80	-1.93
13	-0.90	0.02	1.00	0.86	1.00	1.92	2.36	1.30	0.37	0.50	0.37	-0.72	-1.85

	Velocity, fps									
	Flood (Run 3)					Ebb (Run 3)				
	Surface	Mid	Bottom	Average		Surface	Mid	Bottom	Average	
	P	P	P	P	F	P	P	P	P	F
A1	2.8	3.1	2.9	2.9	0.6	1.0	1.1	0.3	0.8	0.6
A2	3.0	3.1	3.3	3.1	0.5	0.9	1.1	0.4	0.8	0.5
A3	0.6	1.2	1.0	0.9	0.5	0.8	1.1	0.6	0.8	0.5
AB	1.8	2.9	2.6	2.4	0.9	2.5	2.5	2.3	2.4	0.9
B1	1.5	1.3	1.1	1.3	1.0	1.0	1.0	0.7	0.9	1.0
B2	1.7	1.6	1.2	1.5	0.9	1.8	1.9	1.3	1.7	1.0
B3	1.3	1.3	0.8	1.1	0.8	2.1	1.2	0.8	1.4	0.8

Note: P = physical model; C = computational grid model; F = fine scale model.

Table 19

Seabrook Model, Summary of Plan 4 for a Discharge of 15,000 cfs

	Water-Surface Elevation, ft NGVD										
	Flood					Ebb					
	Run 1	Run 2		Run 3	Run 4	Run 1	Run 2		Run 3	Run 4	Run 5
Station	P	P	C	P	P	P	P	C	P	P	P
1	-2.98	-1.73	--	-0.50	0.73	3.00	1.90	--	1.10	0.10	-0.90
2	-2.98	-1.73	--	-0.48	0.83	2.93	1.90	--	1.05	0.05	-0.93
3	-3.01	-1.76	--	-0.52	0.68	2.92	1.88	--	1.06	0.04	-0.93
4	-2.95	-1.70	--	-0.48	0.75	3.00	1.93	--	1.10	0.10	-0.90
5	-2.98	-1.78	-1.79	-0.55	0.65	2.93	1.90	1.89	1.05	0.05	-0.93
6	-3.10	-1.83	--	-0.51	0.73	2.96	1.92	--	1.09	0.07	-0.91
7	-2.95	-1.63	--	-0.48	0.80	2.95	1.85	--	1.03	0.08	-0.93
8	-1.35	-0.40	--	0.58	1.64	2.02	0.92	--	-0.05	-1.27	-2.53
9	-1.48	-0.43	-0.37	0.58	1.65	1.98	0.83	1.02	-0.23	-1.40	-2.70
10	-1.08	-0.10	--	0.83	1.90	1.90	0.73	--	-0.23	-1.48	-2.78
11	-1.05	-0.10	--	0.85	1.90	1.93	0.73	--	-0.23	-1.48	-2.73
12	-1.05	-0.10	--	0.88	1.90	1.83	0.65	--	-0.33	-1.58	-2.88
13	-1.02	-0.08	-0.08	0.89	1.91	1.84	0.70	0.77	-0.28	-1.53	-2.58

	Velocity, fps							
	Flood (Run 3)				Ebb (Run 3)			
	Surface	Mid	Bottom	Average	Surface	Mid	Bottom	Average
	P	P	P	P	P	P	P	P
A1	4.0	4.1	3.8	4.0	1.4	1.5	0.2	1.0
A2	4.0	3.6	4.2	3.9	1.4	1.5	0.8	1.2
A3	0.6	1.5	1.8	1.3	1.2	1.5	0.6	1.1
AB	4.2	4.1	3.5	3.9	3.4	3.4	3.3	3.4
B1	1.8	1.8	1.6	1.7	0.9	1.5	1.5	1.3
B2	2.3	2.2	1.6	2.0	2.6	2.7	2.3	2.5
B3	1.8	1.9	1.5	1.7	2.6	1.6	0.8	1.7

Note: P = physical model; C = computational grid model.

Table 20

Seabrook Model, Summary of Plan 4 for a Discharge of 20,000 cfs

	Water-Surface Elevation, ft NGVD										
	Flood					Ebb					
	Run 1	Run 2		Run 3	Run 4	Run 1	Run 2		Run 3	Run 4	Run 5
Station	P	P	C	P	P	P	P	C	P	P	P
1	0.05	-1.28	--	-2.85	-5.88	2.93	2.03	--	1.10	0.08	-0.88
2	0.00	-1.33	--	-2.88	-5.95	2.88	2.03	--	1.08	0.08	-0.90
3	0.05	-1.28	--	-2.89	-5.95	2.87	2.01	--	1.06	0.04	-0.95
4	0.08	-1.25	--	-2.85	-5.93	2.93	2.03	--	1.13	0.13	-0.88
5	-0.03	-1.33	-1.27	-2.90	-6.00	2.88	2.03	1.99	1.08	0.10	-0.90
6	0.08	-1.26	--	-2.88	-5.97	2.92	2.06	--	1.10	0.08	-0.92
7	0.03	-1.30	--	-2.88	-5.90	2.88	2.03	--	1.08	0.10	-0.93
8	1.64	0.59	--	-0.44	-1.40	1.44	0.37	--	-0.97	-2.49	-4.80
9	1.40	0.35	0.75	-0.73	-1.75	1.33	0.23	0.38	-1.25	-2.95	-6.20
10	2.00	1.00	--	0.00	-0.98	1.13	0.03	--	-1.28	-2.93	-5.15
11	2.00	1.00	--	0.00	-0.95	1.13	0.08	--	-1.28	-2.83	-5.13
12	2.03	1.00	--	0.00	-0.93	1.08	-0.05	--	-1.38	-3.00	-5.30
13	2.05	1.05	1.19	0.04	-0.88	1.09	-0.02	-0.10	-1.34	-2.94	-5.27

	Velocity, fps							
	Flood (Run 2)				Ebb (Run 3)			
	Surface	Mid	Bottom	Average	Surface	Mid	Bottom	Average
	P	P	P	P	P	P	P	P
A1	4.8	5.1	4.4	4.8	1.7	1.8	0.3	1.3
A2	5.2	6.6	5.2	5.7	1.6	1.6	1.3	1.5
A3	1.0	2.1	1.8	1.6	1.6	1.5	0.8	1.3
AB	4.2	5.0	4.4	4.5	4.4	4.3	4.2	4.3
B1	2.3	2.2	1.9	2.1	2.7	2.6	1.2	2.2
B2	2.8	2.6	1.9	2.4	3.3	3.2	2.3	2.9
B3	2.4	2.2	1.8	2.1	2.1	2.0	2.1	2.1

Note: P = physical model; C = computational grid model.

Table 21

Seabrook Model, Plan 4 Discharge = 25,000 cfs

	Water-Surface Elevations, ft NGVD						
	Flood			Ebb			
Station*	Run 1	Run 2	Run 3	Run 1	Run 2	Run 3	Run 4
1	-1.35	-3.45	-7.13	2.98	2.05	1.08	0.45
2	-1.35	-3.38	-7.00	3.00	2.05	1.08	0.50
3	-1.30	-3.35	-7.15	2.86	1.97	1.00	0.40
4	-1.30	-3.38	-7.13	2.98	2.03	1.08	0.50
5	-1.33	-3.43	-7.20	2.98	2.05	1.08	0.48
6	-1.27	-3.35	-7.44	2.96	2.04	1.05	0.44
7	-1.30	-3.43	--	3.00	2.00	1.00	0.43
8	1.35	0.49	0.17	0.65	-0.65	-2.52	-5.49
9	1.08	0.13	-0.18	0.35	-1.05	-3.13	-7.23
10	1.83	1.00	0.63	0.15	-1.18	-3.15	-6.10
11	1.90	1.08	0.73	0.18	-1.15	-3.08	-6.05
12	1.88	1.05	0.73	0.08	-1.33	-3.20	-6.48
13	1.92	1.10	0.84	0.18	-1.20	-3.15	-6.27

	Velocity, fps							
	Flood (Run 2)				Ebb (Run 3)			
	Surface	Mid	Bottom	Average	Surface	Mid	Bottom	Average
A1	5.3	6.2	6.1	5.9	2.2	2.2	0.9	1.8
A2	6.0	8.7	6.9	7.2	2.0	2.1	0.9	1.7
A3	2.3	3.7	3.2	3.1	1.9	2.0	0.7	1.5
AB	6.0	6.1	4.9	5.7	5.3	5.7	5.2	5.4
B1	2.9	2.5	2.0	2.5	3.1	1.4	2.3	2.3
B2	3.3	2.9	2.3	2.8	4.1	4.2	2.9	3.7
B3	2.9	2.7	2.1	2.6	3.6	2.7	3.0	3.1

* Gages 3, 6, 8, and 13 are electronic; the remainder are manual.

Table 22

Seabrook Model, Plan 4 Discharge = 30,000 cfs

	Water-Surface Elevation, ft NGVD		
		Ebb	
Station*	Flood	Run 1	Run 2
1	-7.93	3.10	2.10
2	-8.03	3.08	2.13
3	-8.04	3.00	2.02
4	-7.88	3.13	2.10
5	-8.00	3.03	2.13
6	-8.06	3.08	2.06
7	--	3.05	2.13
8	1.84	-0.55	-6.00
9	1.40	-2.00	-9.23
10	2.40	-1.20	-6.98
11	2.58	-1.18	-6.95
12	2.55	-1.28	-7.28
13	2.68	-1.30	-7.17

* Gages 3, 6, 8, and 13 are electronic; the remainder are manual.

Table 23

Seabrook Model, Plan 5 Discharge = 5000 cfs

Station*	Water-Surface Elevation, ft NGVD			
	Flood		Ebb	
	Run 1	Run 2	Run 1	Run 2
1	-0.28	2.13	1.00	3.00
2	-0.28	2.15	0.93	3.00
3	-0.36	2.09	0.91	2.80
4	-0.28	2.13	1.00	2.95
5	-0.33	2.03	0.98	2.93
6	-0.27	2.12	1.01	2.95
7	-0.28	2.10	1.00	2.93
8	1.02	3.03	-0.38	1.78
9	1.03	3.00	-0.35	1.83
10	1.05	3.00	-0.28	1.83
11	1.08	3.05	-0.28	1.93
12	1.15	3.10	-0.35	1.90
13	1.03	3.04	-0.34	1.78

	Velocity, fps							
	Flood (Run 1)				Ebb (Run 1)			
	Surface	Mid	Bottom	Average	Surface	Mid	Bottom	Average
L1	5.0	5.3	3.7	4.7	4.6	3.7	4.3	4.2
L2	5.7	5.7	3.9	5.1	6.9	6.1	4.1	5.7
L3	6.2	5.9	4.1	5.4	5.2	5.0	6.7	5.6
L4	4.7	5.0	4.0	4.6	5.4	5.4	4.3	5.0
L5	4.7	7.1	6.5	6.1	5.5	5.7	4.9	5.4
AB	1.6	1.6	1.2	1.5	3.2	3.4	3.0	3.2
B1	0.5	0.8	0.4	0.6	0.4	0.4	0.5	0.4
B2	1.0	1.1	0.6	0.9	0.9	1.2	0.9	1.0
B3	0.3	0.8	0.3	0.5	0.4	1.0	0.3	0.6
	Run (2)				Run (2)			
L1	4.7	4.7	6.5	5.3	4.9	4.2	3.7	4.3
L2	4.2	5.1	3.3	4.2	6.2	5.6	3.8	5.2
L3	5.1	4.4	3.3	4.3	5.1	3.9	2.8	3.9
L4	4.8	3.9	3.6	4.1	5.0	4.9	3.7	4.5
L5	5.3	6.0	5.3	5.5	5.7	5.3	3.9	5.0
AB	1.5	1.5	0.9	1.3	2.9	3.2	2.8	3.0
B1	0.4	1.0	0.7	0.7	0.4	1.3	0.5	0.7
B2	0.5	0.9	0.5	0.6	1.3	1.0	1.1	1.1
B3	0.3	0.4	0.3	0.3	0.3	0.3	0.9	0.5

* Gages 3, 6, 8, and 13 are electronic; the remainder are manual.

Table 24

Seabrook Model, Plan 5

Discharge = 10,000 cfs

Station*	Water-Surface Elevation, ft NGVD Flood	Ebb
1	-4.35	2.93
2	-4.28	2.98
3	-4.35	2.80
4	-4.28	2.95
5	-4.43	2.88
6	-4.32	2.92
7	-4.33	2.88
8	2.93	-2.80
9	2.98	-2.65
10	3.03	-2.38
11	3.10	-2.30
12	3.13	-2.33
13	3.02	-2.43

	Velocity, fps							
	Flood				Ebb			
	Surface	Mid	Bottom	Average	Surface	Mid	Bottom	Average
L1	7.2	11.0	7.8	8.7	8.6	9.9	7.7	8.7
L2	6.2	11.1	8.3	8.5	7.4	11.5	9.6	9.5
L3	6.8	10.8	8.6	8.7	8.0	9.4	7.6	8.3
L4	6.5	9.2	6.3	7.3	7.4	10.4	8.5	8.8
L5	9.8	14.1	12.8	12.2	7.1	11.1	8.2	8.8
AB	3.0	2.8	2.3	2.7	6.3	6.2	6.3	6.3
B1	1.1	1.4	0.9	1.1	1.9	0.8	1.1	1.3
B2	1.8	1.6	1.0	1.5	2.0	2.0	1.7	1.9
B3	0.3	1.2	0.7	0.7	1.6	1.6	0.7	1.3

* Gages 3, 6, 8, and 13 are electronic; the remainder are manual.

Table 25

Chef Menteur Model, Summary of Water-Surface Elevation, ft NGVD, for a Discharge of 25,000 cfs

	Flood					Ebb				
	Run 1		Run 2	Run 3	Run 4	Run 1		Run 2	Run 3	Run 4
Station	P	C	P	P	P	P	C	P	P	P
1W	2.00	2.000	0.95	-0.03	-0.98	2.13	2.077	1.00	0.08	-0.95
1E	1.98	--	0.93	-0.15	-1.03	2.08	--	0.98	0.03	-0.98
2W	1.98	--	0.95	-0.05	-1.00	2.10	--	0.98	0.08	-0.95
2	1.98	--	0.93	-0.05	-1.03	2.10	--	0.96	0.06	-0.96
2E	1.98	--	0.95	-0.05	-1.00	2.08	--	0.95	0.03	-0.95
3	1.97	2.005	0.92	-0.07	-1.05	2.11	2.076	0.97	0.05	-0.97
4	1.95	--	0.93	-0.10	-1.08	2.03	--	0.95	0.00	-0.98
5	2.03	--	0.98	0.00	-0.98	2.05	--	0.95	0.03	-1.00
6	2.01	2.024	0.96	-0.05	-1.03	2.06	2.056	0.92	0.01	-1.00
7W	2.00	--	0.98	0.00	-1.00	2.03	--	0.93	0.00	-1.00
7	2.01	--	0.97	-0.02	-0.99	2.07	--	0.93	0.01	-1.00
7E	2.00	--	1.00	0.00	-0.98	2.03	--	0.93	0.00	-1.00
8W	2.03	--	1.00	0.00	-1.00	2.05	--	0.93	0.00	-1.00
8	2.03	2.030	1.00	-0.03	-0.98	2.05	2.050	0.95	0.03	-1.00
8E	2.03	--	1.03	0.00	-0.98	2.05	--	0.93	0.00	--
9E	2.08	--	1.00	-0.15	-0.98	2.30	--	0.90	0.00	-1.05

Note: P = physical model; C = computational grid model.

Table 26

Water-Surface Elevations, Chef Menteur Structure Discharge = 50,000 cfs

	Water-Surface Elevation, ft NGVD							
	Flood				Ebb			
Station*	Run 1	Run 2	Run 3	Run 4	Run 1	Run 2	Run 3	Run 4
1W	2.08	0.83	-0.03	-1.00	2.00	1.03	0.03	-0.95
1E	2.00	0.80	-0.10	-1.10	1.95	1.00	0.00	-1.03
2W	2.03	0.83	-0.08	-1.05	2.03	1.03	0.03	-0.98
2	2.00	0.78	-0.11	-1.09	2.04	1.01	-0.02	-0.94
2E	2.03	0.83	-0.10	-1.05	2.03	1.03	0.03	-0.98
3	1.97	0.76	-0.14	-1.12	2.02	1.00	-0.03	-0.95
4	2.00	0.78	-0.10	-1.10	2.00	1.00	-0.03	-0.98
5	2.13	0.90	0.00	-0.98	1.93	0.83	-0.18	-1.10
6	2.08	0.88	-0.01	-0.99	1.89	0.86	-0.19	-1.12
7W	2.15	0.93	0.00	-0.98	1.93	0.90	-0.18	-1.03
7	2.11	0.90	0.01	-0.97	1.94	0.92	-0.13	-1.06
7E	2.15	0.93	0.03	-0.95	1.93	0.93	-0.10	-1.00
8W	2.20	1.00	0.10	-0.93	1.98	0.98	-0.10	--
8	2.18	0.95	0.03	-0.95	1.93	0.90	-0.15	-1.05
8E	2.20	0.93	0.08	-0.95	2.03	0.98	-0.13	--
9E	2.35	1.20	0.33	-0.63	2.03	1.03	-0.10	-1.00

* Gages 2, 3, 6, and 7 are electronic; the remainder are manual.

Table 27

Chef Menteur Model, Summary of Water-Surface Elevation, ft NGVD, for a Discharge of 75,000 cfs

Station	Flood					Ebb				
	Run 1		Run 2	Run 3	Run 4	Run 1		Run 2	Run 3	Run 4
	P	C	P	P	P	P	C	P	P	P
1W	1.88	1.945	0.90	-0.05	-1.10	2.18	2.073	1.23	0.18	-0.75
1E	1.93	--	0.80	-0.10	-1.10	2.10	--	1.13	0.13	-0.85
2W	1.88	--	0.80	-0.13	-1.10	2.05	--	1.08	0.03	-0.90
2	1.85	--	0.76	-0.16	-1.14	2.05	--	1.05	0.03	-0.91
2E	1.85	--	0.78	-0.15	-1.15	2.05	--	1.10	0.03	-0.88
3	1.74	1.957	0.66	-0.27	-1.27	2.02	2.061	1.01	-0.03	-0.97
4	1.73	--	0.65	-0.28	-1.28	1.93	--	1.00	-0.08	-1.00
5	2.05	--	0.95	0.03	-0.95	1.70	--	0.68	-0.40	-1.35
6	2.02	2.132	0.96	0.07	-0.91	1.73	1.883	0.72	-0.35	-1.33
7W	2.10	--	1.03	0.15	-0.88	1.80	--	0.83	-0.23	-1.23
7	2.05	--	0.97	0.08	-0.91	1.80	--	0.79	-0.25	-1.22
7E	2.10	--	1.03	0.15	-0.85	1.85	--	0.83	-0.18	-1.18
8W	2.28	--	1.20	0.33	-0.58	1.80	--	0.75	-0.40	--
8	2.18	2.180	1.10	0.15	-0.85	1.83	1.830	0.83	-0.28	-1.23
8E	2.23	--	1.13	0.23	-0.83	1.80	--	0.73	0.35	--
9E	2.55	--	1.38	0.80	0.03	1.68	--	0.58	-0.53	-1.37

Note: P = physical model; C = computational grid model.

Table 28

Water-Surface Elevation, Chef Menteur Structure Discharge = 100,000 cfs

	Water-Surface Elevation, ft NGVD							
	Flood				Ebb			
Station*	Run 1	Run 2	Run 3	Run 4	Run 1	Run 2	Run 3	Run 4
1W	1.78	0.80	-0.28	-1.28	2.20	1.20	0.23	-0.80
1E	1.93	1.80	-0.20	-1.20	2.05	1.08	0.13	-0.98
2W	1.75	0.65	-0.30	-1.25	1.95	0.98	0.03	-1.08
2	1.73	0.63	-0.39	-1.32	2.04	1.07	0.08	-1.01
2E	1.75	0.68	-0.35	-1.28	2.03	1.08	0.10	-0.98
3	1.59	0.49	-0.52	-1.52	1.96	0.98	-0.02	-1.12
4	1.63	0.53	-0.48	-1.45	1.93	0.98	0.00	-1.08
5	2.00	0.93	-0.08	-1.05	1.43	0.40	-0.60	-1.78
6	2.08	1.00	0.00	-0.97	1.49	0.47	-0.58	-1.71
7W	2.08	1.00	0.05	-0.90	1.55	0.53	-0.48	-1.58
7	2.09	1.00	0.00	-0.96	1.61	0.63	-0.39	-1.53
7E	2.10	1.05	0.10	-0.88	1.68	0.65	-0.33	-1.48
8W	2.35	1.33	0.40	-0.50	1.55	0.48	-0.65	--
8	2.20	1.13	0.08	-0.90	1.63	0.63	-0.40	-1.33
8E	2.23	1.18	0.20	-0.78	1.60	0.55	-0.50	--
9E	2.75	1.85	1.08	0.30	0.33	0.28	-0.98	-2.28

* Gages 2, 3, 6, and 7 are electronic; the remainder are manual.

Table 29

Chef Menteur Model, Summary of Water-Surface Elevation, ft NGVD, for a Discharge of 125,000 cfs

	Flood						Ebb					
	Run 1			Run 2	Run 3	Run 4	Run 1			Run 2	Run 3	Run 4
Station	P	C	F	P	P	P	P	C	F	P	P	P
1W	1.65	1.647	1.66	0.60	-0.35	-1.45	2.18	2.037	2.10	1.30	0.28	-0.68
1E	1.63	--	1.67	0.65	-0.40	-1.40	1.98	--	2.10	1.10	0.03	-0.88
2W	1.55	--	1.72	0.58	-0.45	-1.53	1.88	--	2.04	1.00	-0.08	-0.98
2	1.46	--	1.72	0.41	-0.57	-1.62	2.01	--	2.04	1.10	0.03	-0.80
2E	1.53	--	1.72	0.45	-0.53	-1.60	2.00	--	2.04	1.08	0.03	-0.83
3	1.19	1.682	1.71	0.13	-0.88	-1.92	1.92	2.003	2.01	1.01	-0.08	-1.01
4	1.18	--	1.75	0.15	-0.88	-1.85	1.80	--	1.99	0.90	-0.15	-1.03
5	1.93	--	1.77	0.85	-0.15	-1.15	1.03	--	1.47	0.13	-1.05	-2.08
6	1.96	2.170	2.15	0.94	-0.05	-1.05	1.14	1.495	1.44	0.22	-0.93	-2.00
7W	2.05	--	2.21	1.03	0.10	-0.90	1.30	--	1.41	0.33	-0.80	-1.73
7	2.00	--	2.21	0.99	-0.01	-1.00	1.33	--	1.40	0.42	-0.69	-1.71
7E	2.10	--	2.18	1.08	0.10	-0.85	1.35	--	1.40	0.48	-0.58	-1.55
8W	2.48	--	2.28	1.55	0.35	-0.20	1.20	--	1.33	0.23	-1.05	--
8	2.30	2.300	2.27	1.25	0.23	-0.88	1.33	1.330	1.33	0.45	-0.68	-1.70
8E	2.30	--	N/A	1.33	0.43	-0.50	1.30	--	N/A	0.38	-0.88	--
9E	3.23	--	--	2.43	1.63	0.92	1.00	--	--	-0.15	-1.53	-3.03

Note: P = physical model; C = computational grid model; F = fine scale model.

Table 30

Velocities, Chef Menteur Structure Discharge = 25,000 cfs

	Velocity, fps							
	Flood (Run 2)				Ebb (Run 2)			
Station	Surface	Mid	Bottom	Average	Surface	Mid	Bottom	Average
A1	0.4	0.9	0.6	0.6	0.8	1.0	0.6	0.8
A2	0.3	0.8	0.4	0.5	0.4	0.6	0.3	0.4
A3	0.9	1.2	0.8	1.0	0.5	0.9	0.5	0.6
B1	0.4	0.7	0.5	0.5	0.7	1.1	0.7	0.8
B2	0.5	1.1	0.7	0.8	0.3	0.4	0.3	0.3
B3	0.9	1.0	0.8	0.9	0.5	0.9	0.5	0.6
N5	1.1	1.2	0.6	1.0	0.8	0.8	0.4	0.7
N4	1.2	1.3	1.2	1.2	0.7	0.9	0.4	0.7
N3	1.4	1.3	0.9	1.2	0.7	1.0	0.5	0.7
N2	1.5	1.3	1.5	1.4	0.6	0.9	0.6	0.7
N1	1.2	1.6	0.5	1.1	1.0	1.1	0.9	1.0
C	1.8	1.9	1.7	1.8	0.9	1.8	0.9	1.2
S1	1.2	1.1	0.9	1.1	1.3	1.5	0.4	1.1
S2	1.0	1.0	0.4	0.8	1.1	1.3	0.6	1.0
S3	1.5	1.1	0.4	1.0	1.3	1.5	1.1	1.3
S4	1.1	1.1	0.8	1.0	1.1	1.4	1.1	1.2
S5	1.0	0.9	1.0	1.0	1.3	1.4	1.0	1.2
D1	0.4	0.9	0.4	0.6	0.8	1.1	0.8	0.9
D2	0.9	1.0	0.5	0.8	0.3	1.3	0.3	0.6
D3	0.7	0.9	0.6	0.7	0.5	0.5	0.6	0.5
E1	0.4	0.5	0.4	0.4	0.5	1.0	0.6	0.7
E2	0.9	1.1	0.3	0.8	0.4	0.9	0.6	0.6
E3	1.1	0.9	0.5	0.8	0.5	0.8	0.5	0.6

Table 31

Velocities, Chef Menteur Structure Discharge = 75,000

Station	Velocity, fps							
	Flood (Run 2)				Ebb (Run 2)			
	Surface	Mid	Bottom	Average	Surface	Mid	Bottom	Average
A1	1.0	1.7	1.6	1.4	3.4	2.8	2.1	2.8
A2	3.6	3.3	2.1	3.0	2.2	2.2	1.8	2.1
A3	2.9	3.0	2.2	2.7	2.5	2.3	1.9	2.2
B1	2.4	2.4	1.8	2.2	3.2	2.9	2.2	2.8
B2	3.7	3.7	3.2	3.5	2.9	2.8	2.1	2.6
B3	3.3	2.9	2.1	2.8	2.8	2.4	1.9	2.4
N5	4.2	4.1	4.0	4.1	3.0	2.6	2.1	2.6
N4	4.6	4.2	2.3	3.5	2.8	2.5	1.9	2.4
N3	4.0	4.4	3.4	3.9	3.2	2.8	2.2	2.7
N2	3.1	4.5	2.8	3.5	2.9	3.0	2.1	2.7
N1	5.0	5.0	3.1	4.4	3.9	3.4	2.8	3.3
C	6.3	6.1	5.7	6.0	5.6	5.7	5.3	5.4
S1	1.4	3.7	3.1	2.7	5.2	4.8	5.2	5.1
S2	2.2	3.3	2.4	2.6	4.3	4.0	3.2	3.8
S3	3.0	3.0	2.3	2.8	3.8	3.7	3.5	3.7
S4	3.4	1.4	2.5	2.4	3.7	3.9	3.3	3.6
S5	3.7	3.0	2.4	3.0	3.8	4.1	3.4	3.8
D1	2.9	2.6	1.9	2.5	3.2	3.5	2.5	3.0
D2	3.0	2.9	2.3	2.7	3.8	3.2	2.5	3.2
D3	3.0	2.6	1.9	2.5	3.1	2.9	1.9	2.6
E1	1.5	1.5	1.5	1.5	2.4	4.2	2.0	2.9
E2	3.5	3.7	2.6	3.3	3.4	2.8	2.0	2.7
E3	2.6	2.5	1.9	2.3	2.9	2.6	1.5	2.3

Table 32

Chef Menteur Model, Summary of Velocity, fps, for a Discharge of 125,000 cfs

Station	Flood (Run 1) Surface P	Mid P	Bottom P	Average P	F	Ebb (Run 1) Surface P	Mid P	Bottom P	Average P	F
A1	3.7	3.2	2.1	3.0	3.9	5.6	5.7	4.0	5.1	3.9
A2	6.0	4.9	4.3	5.1	4.0	4.5	4.6	3.3	4.1	3.9
A3	4.6	4.1	2.8	3.8	4.0	2.4	2.3	1.9	2.2	3.9
B1	2.3	2.3	1.3	2.0	4.0	5.2	4.5	3.7	4.5	3.9
B2	6.3	6.5	5.0	5.9	4.0	4.[illegible]	4.5	3.9	4.3	3.9
B3	5.2	4.5	3.8	4.5	4.0	3.0	3.2	2.3	2.8	3.9
N5	6.6	6.9	6.6	6.7	--	4.4	4.5	3.1	4.0	--
N4	6.0	7.5	5.6	6.4	--	4.0	4.3	3.1	3.8	--
N3	4.6	6.9	4.4	5.3	--	4.8	4.5	3.6	4.3	--
N2	5.0	7.5	4.8	5.8	--	4.4	4.6	3.1	4.0	--
N1	5.1	7.3	4.7	5.7	--	5.4	5.3	4.5	5.1	--
C	6.2	10.3	9.3	8.6	6.7	6.7	7.7	8.9	7.8	6.6
S1	5.3	5.7	4.7	5.2	--	6.4	7.9	5.2	6.5	--
S2	5.2	5.4	4.1	4.9	--	6.5	6.8	4.7	6.0	--
S3	4.6	4.9	3.4	4.3	--	5.8	6.1	5.0	5.6	--
S4	5.1	5.3	3.6	4.7	--	5.9	6.8	5.3	6.0	--
S5	4.7	4.8	3.7	4.4	--	5.6	6.4	4.8	5.6	--
D1	4.5	4.3	3.4	4.1	4.2	4.9	4.6	4.3	4.6	4.3
D2	6.0	5.0	4.1	5.0	4.2	6.5	6.3	5.7	6.2	4.3
D3	3.3	3.7	2.7	3.2	4.2	2.8	2.7	2.3	2.6	4.4
E1	3.9	4.5	3.2	3.9	4.2	4.5	4.9	3.8	4.4	4.3
E2	4.4	5.5	4.0	4.6	4.3	5.1	5.3	3.5	4.6	4.4
E3	2.7	2.8	2.5	2.7	4.2	2.4	2.4	2.4	2.4	4.3

Note: P = physical model; F = fine scale model.

Table 33

Rigolets Model, Summary of Water-Surface Elevation, ft NGVD, for Base Conditions

Tide Gage	Flood Conditions								
	Max*			Med**			Min†		
	P	C	F	P	C	F	P	C	F
T-1	1.95	2.02	2.06	1.20	1.19	1.30	1.00	1.00	1.00
T-2	1.95	1.93	1.95	1.25	1.15	1.25	1.00	0.99	0.98
T-3	1.90	1.85	1.86	1.20	1.11	1.20	1.00	0.98	0.97
T-4	1.70	1.72	1.81	1.10	1.06	1.18	0.95	0.97	0.97
T-5	1.70	1.67	1.72	1.10	1.03	1.14	0.95	0.96	0.95
T-6	1.75	1.63	1.65	1.10	1.00	1.10	0.95	0.95	0.94
T-7	1.70	1.63	1.63	1.10	1.00	1.09	0.95	0.95	0.94
T-8	1.60	1.57	1.57	1.05	0.98	1.06	0.95	0.94	0.93
T-9	1.55	1.51	1.52	1.00	0.95	1.03	0.90	0.94	0.92
T-10	1.50	1.51	1.45	1.00	0.95	0.99	0.90	0.94	0.91
T-13	1.70	1.74	1.73	1.10	1.09	1.14	0.90	0.97	0.95

(Continued)

Note: P = physical model; C = computational grid model; F = fine scale model.

* 216,000 cfs into Lake Pontchartrain.

** 143,000 cfs into Lake Pontchartrain.

† 69,000 cfs into Lake Pontchartrain.

Table 33 (Continued)

Velocity Range	Velocity, fps					
	Max		Med		Min	
	P	F	P	F	P	F
2A	1.8	1.9	1.3	1.3	0.5	0.6
2B	2.7	2.3	1.9	1.6	1.0	0.9
2C	2.9	2.8	1.7	1.9	0.8	0.9
3A	1.9	1.6	1.4	1.0	0.9	0.4
3B	1.9	2.1	1.5	1.4	0.9	0.7
3C	3.0	2.7	1.9	1.8	1.1	0.9
4A	1.9	1.0	1.2	0.6	0.4	0.2
4B	2.1	1.5	1.7	1.0	0.7	0.5
4C	2.1	1.1	1.7	0.7	0.5	0.3
5A	1.9	2.5	1.5	1.6	0.9	0.8
5B	2.5	2.1	1.6	1.5	0.9	0.8
5C	1.7	2.0	1.2	1.4	0.7	0.7
6A	2.4	2.0	1.6	1.3	0.9	0.6
6B	1.9	2.5	1.4	1.8	0.6	0.9
6C	1.6	1.8	1.2	1.3	0.5	0.8
7A	2.5	2.7	1.9	1.9	0.7	1.0
7B	1.8	2.2	1.3	1.4	0.4	0.6
7C	1.7	2.3	1.3	1.5	0.5	0.7
8A	0.8	1.7	0.3	1.1	0.4	0.5
8B	2.6	2.2	1.7	1.4	1.0	0.6
8C	2.4	1.9	1.6	1.3	0.9	0.7

Note: P = physical model; F = fine scale model.

Table 34

Rigolets Model, Summary of Water-Surface Elevation, ft NGVD, for Base Conditions

Tide Gage	Ebb Conditions								
	Max*			Med**			Min†		
	P	C	F	P	C	F	P	C	F
T-1	1.15	1.12	1.18	0.70	0.71	0.64	0.95	1.00	1.00
T-2	1.30	1.28	1.31	0.70	0.76	0.70	1.00	1.02	1.02
T-3	1.50	1.40	1.41	0.75	0.81	0.75	1.00	1.03	1.04
T-4	1.50	1.39	1.47	0.75	0.81	0.77	1.00	1.03	1.04
T-5	1.55	1.45	1.57	0.80	0.84	0.82	1.00	1.04	1.05
T-6	1.60	1.57	1.65	0.80	0.89	0.86	1.05	1.06	1.06
T-7	1.60	1.61	1.67	0.85	0.91	0.87	1.00	1.06	1.07
T-8	1.65	1.66	1.74	0.90	0.93	0.90	1.05	1.06	1.07
T-9	1.75	1.73	1.79	0.95	0.96	0.92	1.00	1.07	1.08
T-10	1.85	1.87	1.86	0.95	1.02	0.96	1.00	1.09	1.09
T-13	1.55	1.52	1.54	0.85	0.86	0.82	0.95	1.04	1.07

(Continued)

Note: P = physical model; C = computational grid model; F = fine scale model.

* 223,000 cfs from Lake Pontchartrain.

** 143,000 cfs from Lake Pontchartrain.

† 75,000 cfs from Lake Pontchartrain.

Table 34 (Continued)

Velocity Range	Velocity, fps					
	Max		Med		Min	
	P	F	P	F	P	F
2A	2.3	2.1	1.8	1.3	0.7	0.6
2B	2.2	2.4	1.4	1.7	0.6	1.0
2C	3.1	3.0	1.9	2.0	0.9	1.0
3A	1.5	1.6	0.9	1.0	0.3	0.5
3B	2.4	2.2	1.6	1.5	1.0	0.8
3C	2.6	2.9	1.7	1.9	1.0	0.9
4A	1.6	0.9	1.4	0.8	0.8	0.6
4B	1.2	1.3	1.2	1.2	0.5	1.1
4C	1.0	1.0	1.0	0.9	1.0	0.8
5A	1.8	2.6	1.5	1.6	0.8	0.7
5B	2.3	2.2	1.4	1.5	0.8	0.8
5C	2.8	2.1	1.9	1.4	1.1	0.7
6A	2.1	2.1	1.5	1.3	0.9	0.5
6B	2.5	2.6	1.7	1.8	0.9	0.9
6C	2.3	1.9	1.4	1.3	0.9	0.8
7A	1.8	2.8	1.1	1.8	0.7	0.9
7B	2.3	2.3	1.4	1.4	0.6	0.6
7C	2.3	2.4	1.4	1.4	0.6	0.7
8A	1.9	1.8	1.1	1.1	0.7	0.5
8B	2.4	2.3	1.2	1.5	0.3	0.6
8C	1.2	2.0	0.2	1.3	0.1	0.6

Note: P = physical model; F = fine scale model.

Table 35

Rigolets Model, Summary of Water-Surface Elevation, ft NGVD, for Plan 2A

Tide Gage	Flood Conditions					
	Max*		Med**		Min†	
	P	C	P	C	P	C
T-1	1.95	1.96	2.00	1.99	1.95	1.95
T-2	2.00	1.86	2.05	1.95	1.95	1.94
T-3	1.85	1.76	1.95	1.91	1.90	1.93
T-4	1.00	1.02	1.60	1.62	1.85	1.86
T-5	0.95	1.02	1.60	1.62	1.80	1.86
T-6	0.95	1.00	1.55	1.61	1.75	1.86
T-7	0.90	0.99	1.55	1.61	1.75	1.86
T-8	0.90	0.93	1.55	1.59	1.85	1.85
T-9	0.80	0.87	1.45	1.56	1.75	1.85
T-10	0.80	0.87	1.45	1.56	1.65	1.85
T-13	1.80	1.68	1.95	1.88	1.85	1.92

	Ebb Conditions					
	Max††		Med‡		Min‡‡	
	P	C	P	C	P	C
T-1	0.50	0.51	1.50	1.46	1.85	1.83
T-2	0.80	0.68	1.55	1.52	1.90	1.85
T-3	0.65	0.81	1.50	1.57	1.85	1.87
T-4	2.00	1.74	2.05	1.93	2.10	1.96
T-5	1.90	1.62	2.05	1.88	2.05	1.95
T-6	1.90	1.80	2.00	1.96	2.00	1.97
T-7	1.90	1.84	2.00	1.97	2.05	1.98
T-8	1.95	1.89	2.00	1.99	2.00	1.98
T-9	2.00	1.96	2.05	2.02	2.00	1.99
T-10	2.00	2.10	2.05	2.07	2.00	2.00
T-13	1.15	0.96	1.70	1.62	1.95	1.88

Note: P = physical model; C = computational grid model.
* 216,000 cfs into Lake Pontchartrain.
** 143,000 cfs into Lake Pontchartrain.
† 69,000 cfs into Lake Pontchartrain.
†† 223,000 cfs from Lake Pontchartrain.
‡ 143,000 cfs from Lake Pontchartrain.
‡‡ 75,000 cfs from Lake Pontchartrain.

Table 36

Rigolets Model, Summary of Water-Surface Elevation, ft NGVD,

for Plans 2A and 2A-1

	Flood Conditions									
	Max*				Med**			Min†		
Gage Tide	P	F 2A	F 2A-1	F†† 2A-1	P	F 2A	F 2A-1	P	F 2A	F 2A-1
T-1	1.95	2.11	2.11	2.08	0.90	1.00	1.00	0.90	1.00	1.00
T-2	2.00	2.00	2.00	1.96	0.95	0.95	0.94	0.95	0.98	0.98
T-3	1.85	1.90	1.90	1.83	0.85	0.89	0.89	0.80	0.97	0.97
T-4	1.00	1.09	1.11	0.96	0.45	0.50	0.50	0.80	0.87	0.87
T-5	0.95	1.09	1.09	0.97	0.40	0.50	0.50	0.70	0.87	0.87
T-6	0.95	1.03	1.03	0.97	0.35	0.50	0.47	0.75	0.86	0.86
T-7	0.90	1.01	1.02	0.92	0.35	0.45	0.46	0.75	0.86	0.86
T-8	0.90	0.94	0.95	0.86	0.40	0.42	0.42	0.75	0.86	0.86
T-9	0.80	0.88	0.89	0.84	0.35	0.40	0.40	0.75	0.85	0.85
T-10	0.80	0.80	0.81	0.75	0.35	0.35	0.35	0.60	0.83	0.83
T-13	1.80	1.76	1.77	1.69	0.85	0.82	0.83	0.85	0.95	0.95
ΔH_{2-10}	1.20	1.20	1.19	1.21	0.60	0.60	0.59	0.35	0.15	0.15

	Ebb Conditions								
	Max‡			Med‡‡			Min§		
	P	F 2A	F 2A-1	P	F 2A	F 2A-1	P	F 2A	F 2A-1
T-1	0.50	0.63	0.63	0.35	0.48	0.48	0.85	0.93	0.93
T-2	0.80	0.77	0.77	0.55	0.54	0.54	0.95	0.95	0.95
T-3	0.65	0.90	0.99	0.50	0.60	0.60	0.90	0.97	0.97
T-4	2.00	1.79	1.78	1.10	0.97	0.97	1.05	1.06	1.06
T-5	1.90	1.79	1.79	1.10	0.98	0.98	1.05	1.06	1.06
T-6	1.90	1.85	1.85	1.10	1.01	1.00	1.05	1.07	1.07
T-7	1.90	1.88	1.87	1.05	1.02	1.02	1.05	1.07	1.09
T-8	1.95	1.95	1.94	1.10	1.05	1.04	1.05	1.08	1.08
T-9	2.00	2.00	2.00	1.10	1.07	1.07	1.05	1.08	1.08
T-10	2.00	2.08	2.07	1.10	1.11	1.11	1.05	1.10	1.10
T-13	1.15	1.05	1.04	0.70	0.68	0.67	1.00	1.00	1.00
ΔH_{2-10}	1.20	1.31	1.30	0.55	0.57	0.57	0.10	0.15	0.15

Note: P = physical model; F = fine scale model.
* 216,000 cfs into Lake Pontchartrain.
** 143,000 cfs into Lake Pontchartrain.
† 69,000 cfs into Lake Pontchartrain.
†† Advective terms included in momentum equations.
‡ 223,000 cfs from Lake Pontchartrain.
‡‡ 143,000 cfs from Lake Pontchartrain.
§ 75,000 cfs from Lake Pontchartrain.

Table 37

Rigolets Model, Summary of Average Velocity, fps, for Flood Conditions

Velocity Range	Flood Conditions: Max* P	Max* F 2A	Max* F 2A-1	Max* F†† 2A-1	Med** P	Med** F 2A	Med** F 2A-1	Min† P	Min† F 2A	Min† F 2A-1
2A	1.9	1.9	1.9	2.4	1.5	1.3	1.3	0.8	0.6	0.6
2B	3.1	2.4	2.4	2.2	2.1	1.6	1.6	1.3	0.9	0.9
2C	2.6	2.7	2.8	2.4	1.9	1.9	1.9	1.1	0.9	0.9
3A	2.4	1.7	1.6	2.5	1.7	1.1	1.1	1.0	0.5	0.5
3B	2.5	2.5	2.5	3.5	1.7	1.7	1.7	1.0	0.9	0.9
3C	2.5	2.6	2.5	2.9	1.8	1.8	1.8	1.2	0.8	0.9
4A	1.8	1.1	1.0	1.5	1.4	0.6	0.6	0.8	0.2	0.2
4B	1.7	1.5	1.5	1.6	1.4	1.0	1.0	1.0	0.5	0.5
4C	1.7	1.1	1.1	1.7	1.4	0.8	0.8	1.2	0.4	0.3
5A	--	3.4	2.9	6.6	--	2.3	2.0	--	1.1	0.9
5B	-0.3	2.9	4.0	0.7	-0.3	2.0	2.8	-0.3	1.1	1.4
5C	-0.4	1.1	1.2	-0.2	-0.3	0.8	0.7	-0.3	0.3	0.3
6A	4.5	2.0	2.0	2.8	3.1	1.3	1.3	1.7	0.6	0.6
6B	1.0	2.6	2.6	2.9	0.6	1.8	1.8	0.3	0.9	0.9
6C	-0.2	1.8	1.9	-0.7	-0.1	1.3	1.3	0.2	0.7	0.7
7A	3.2	2.7	2.7	1.9	2.2	1.9	1.9	1.1	1.0	1.0
7B	2.5	2.2	2.2	3.0	1.3	1.4	1.4	0.7	0.7	0.7
7C	0.4	2.3	2.3	2.8	0.3	1.5	1.5	-0.2	0.7	0.7
8A	1.2	1.7	1.7	2.0	0.6	1.2	1.2	-0.4	0.5	0.5
8B	2.6	2.2	2.2	2.9	2.0	1.4	1.4	1.1	0.6	0.6
8C	2.7	2.0	2.0	2.0	1.8	1.4	1.4	1.2	0.7	0.7

Note: P = physical model; F = fine scale model.
* 216,000 cfs into Lake Pontchartrain.
** 143,000 cfs into Lake Pontchartrain.
† 69,000 cfs into Lake Pontchartrain.
†† Advective terms included in momentum equations.

Table 38

Rigolets Model, Summary of Average Velocities, fps, for Ebb Conditions

Velocity Range	Max*			Med**			Min†		
	P	F 2A	F 2A-1	P	F 2A	F 2A-1	P	F 2A	F 2A-1
2A	3.1	2.1	2.1	1.9	1.3	1.3	1.0	0.6	0.6
2B	2.5	2.5	2.5	1.5	1.7	1.7	0.8	0.9	0.9
2C	2.5	3.0	3.0	1.8	1.9	2.0	1.1	1.0	1.0
3A	2.2	1.8	1.7	1.4	1.1	1.1	0.5	0.5	0.5
3B	5.5	2.7	2.7	3.8	1.8	1.8	1.6	1.0	1.0
3C	0.9	2.8	2.8	0.6	1.8	1.8	0.2	0.9	0.9
4A	1.2	1.0	1.0	1.0	0.8	0.8	1.1	0.7	0.7
4B	0.6	1.4	1.3	0.8	1.2	1.2	0.6	1.1	1.1
4C	1.1	1.0	1.0	0.5	0.9	0.8	0.2	0.8	0.8
5A	--	3.5	3.0	--	2.2	1.9	--	1.0	0.9
5B	2.5	3.0	4.1	1.8	2.0	2.7	0.8	1.1	1.4
5C	0.8	1.1	1.2	1.0	0.7	0.7	0.2	0.3	0.3
6A	2.2	2.0	2.0	1.6	1.3	1.3	0.6	0.6	0.6
6B	2.0	2.7	2.7	1.3	1.8	1.8	0.7	0.9	0.9
6C	2.2	1.9	1.9	1.5	1.3	1.3	0.9	0.7	0.7
7A	2.1	2.8	2.8	1.4	1.8	1.8	0.6	0.9	0.9
7B	2.2	2.2	2.2	1.5	1.4	1.4	0.7	0.6	0.6
7C	2.4	2.3	2.3	1.2	1.5	1.5	0.6	0.7	0.7
8A	1.7	1.8	1.8	1.3	1.1	1.1	0.8	0.5	0.5
8B	2.0	2.2	2.2	1.3	1.4	1.4	0.5	0.6	0.6
8C	1.5	2.0	2.0	0.8	1.3	1.3	0.4	0.6	0.6

Note: P = physical model; F = fine scale model.
* 223,000 cfs from Lake Pontchartrain.
** 143,000 cfs from Lake Pontchartrain.
† 75,000 cfs from Lake Pontchartrain.

SEABROOK PASS PHOTO 1

PHOTO 2

CHIEF MENTEUR PASS

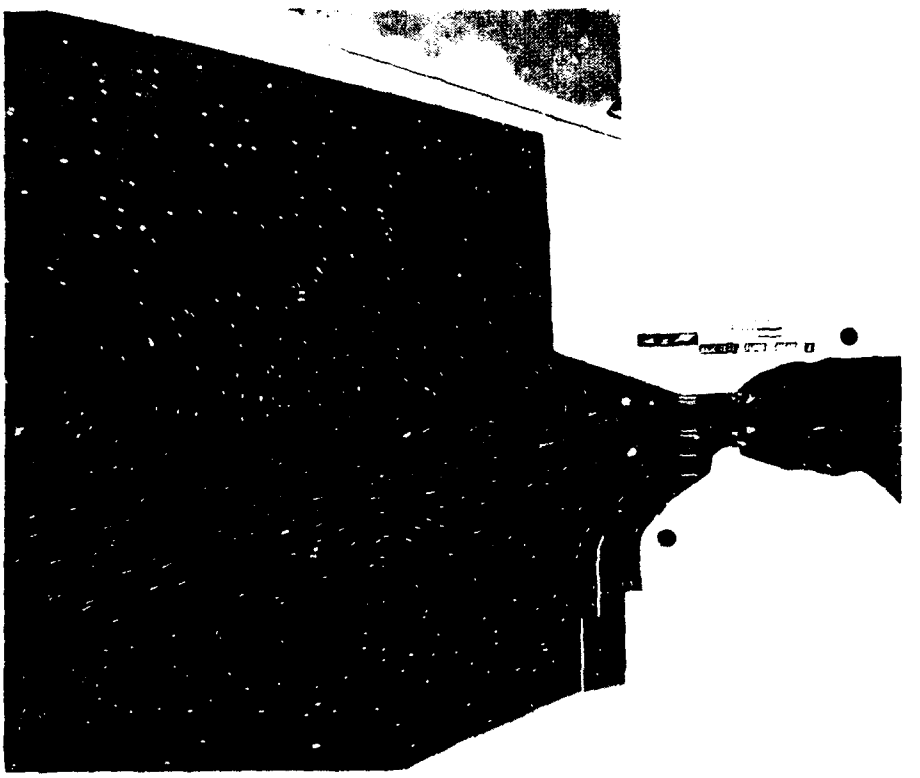

VELOCITY
SCALE

0 5 10 20

BASE
FLOOD DISCHARGE = 15,000 CFS
EXPOSURE TIME = 3 SEC

PHOTO 3

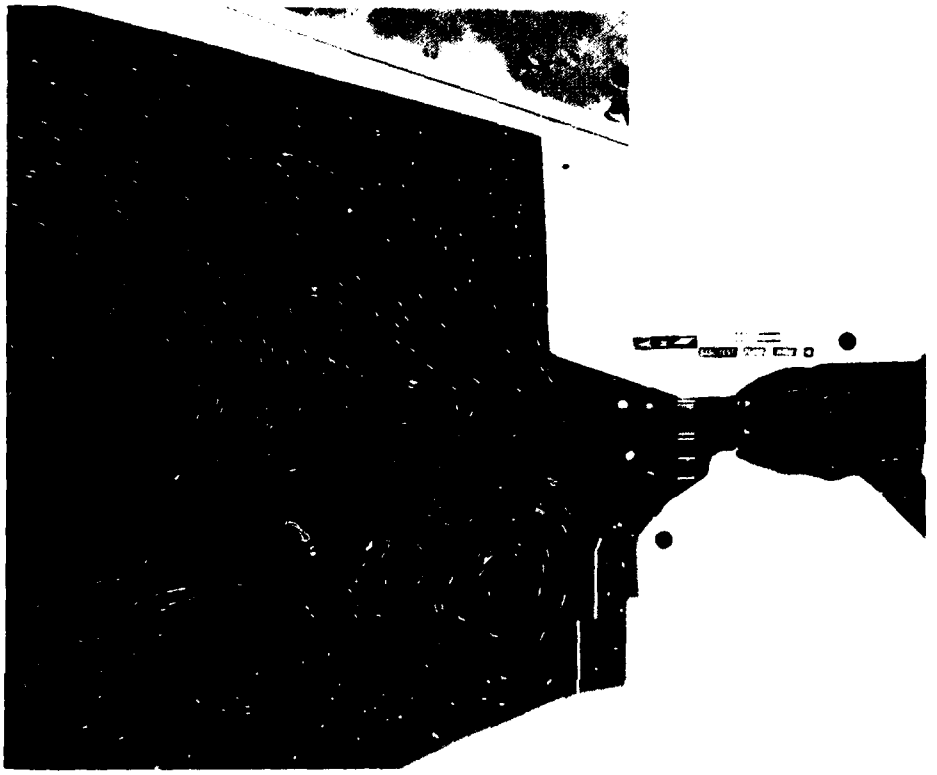

VELOCITY
SCALE

0 5 10 20

BASE
FLOOD DISCHARGE = 30,000 CFS
EXPOSURE TIME = 3 SEC

PHOTO 4

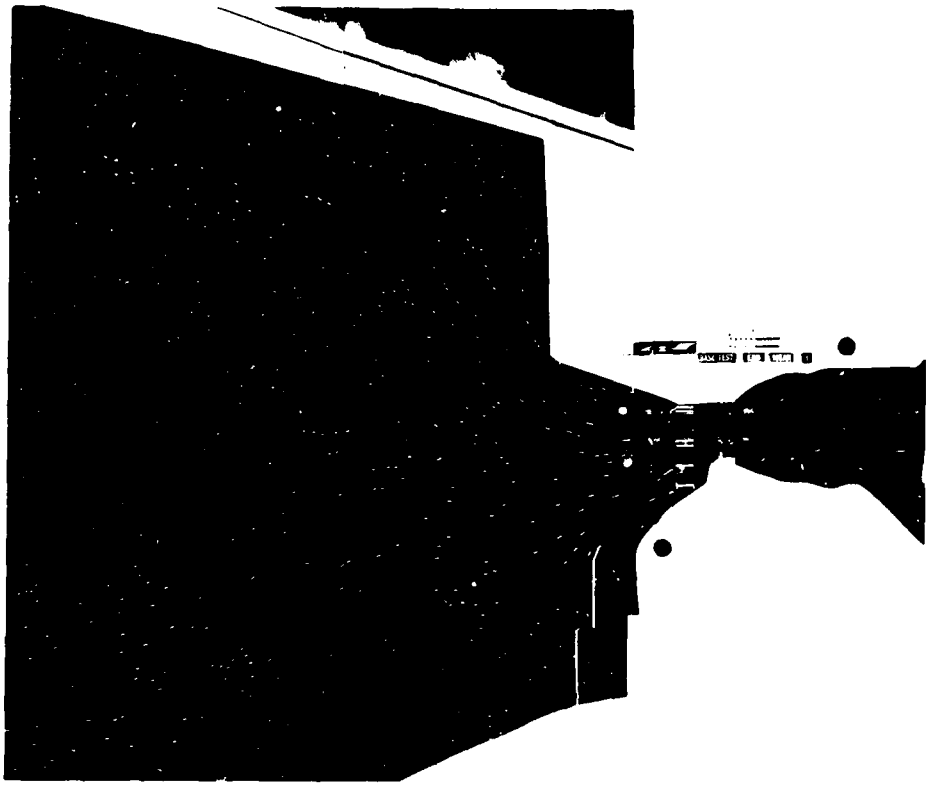

VELOCITY
SCALE

0 5 10 20

BASE
EBB DISCHARGE = 15,000 CFS
EXPOSURE TIME = 3 SEC

PHOTO 5

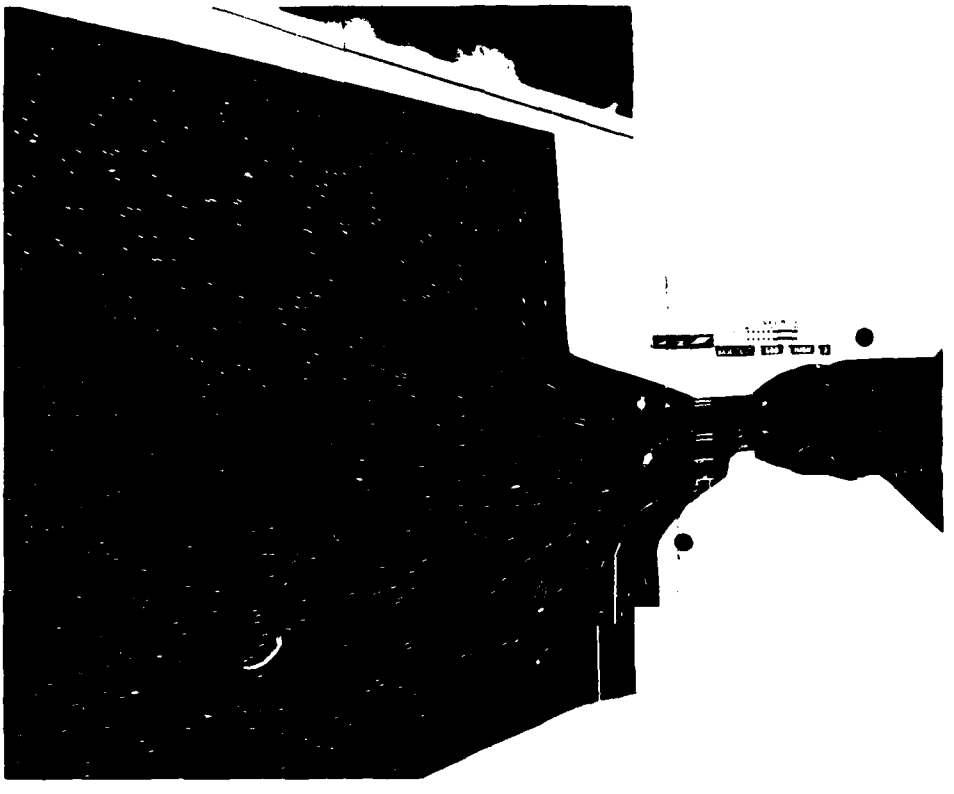

VELOCITY
SCALE

0 5 10 20

BASE
EBB DISCHARGE = 30,000 CFS
EXPOSURE TIME = 3 SEC

PHOTO 6

VELOCITY
SCALE

0 5 10 20

PLAN 2
FLOOD DISCHARGE = 5,000 CFS
EXPOSURE TIME = 9 SEC

PHOTO 7

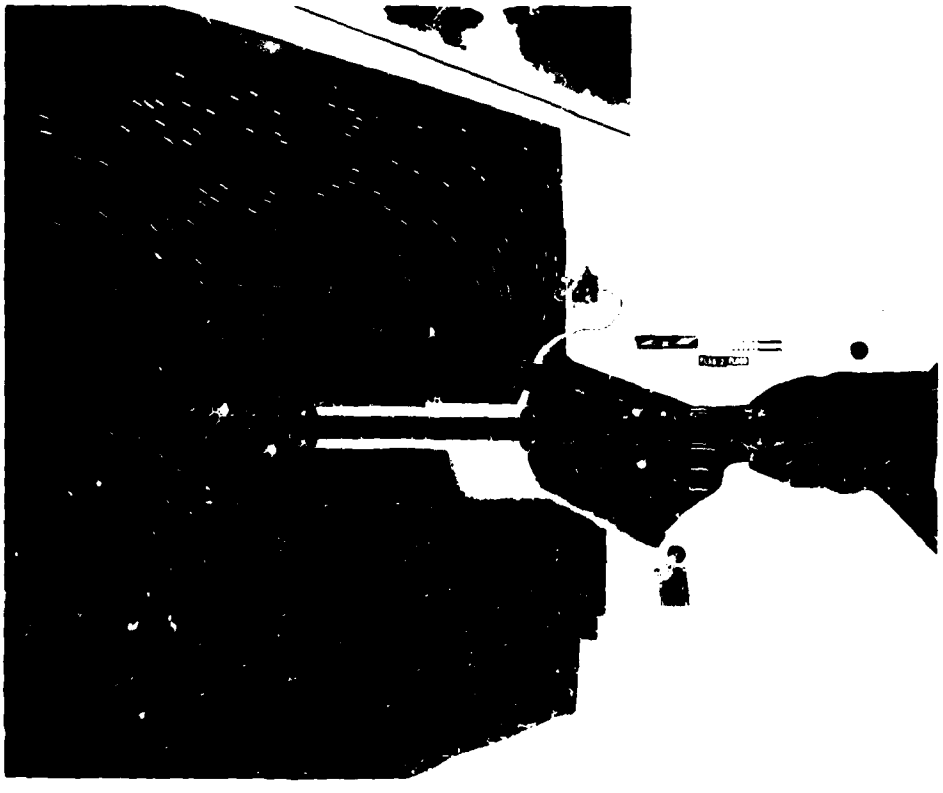

VELOCITY SCALE

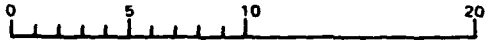

PLAN 2
FLOOD DISCHARGE = 5,000 CFS
EXPOSURE TIME = 9 SEC

PHOTO 8

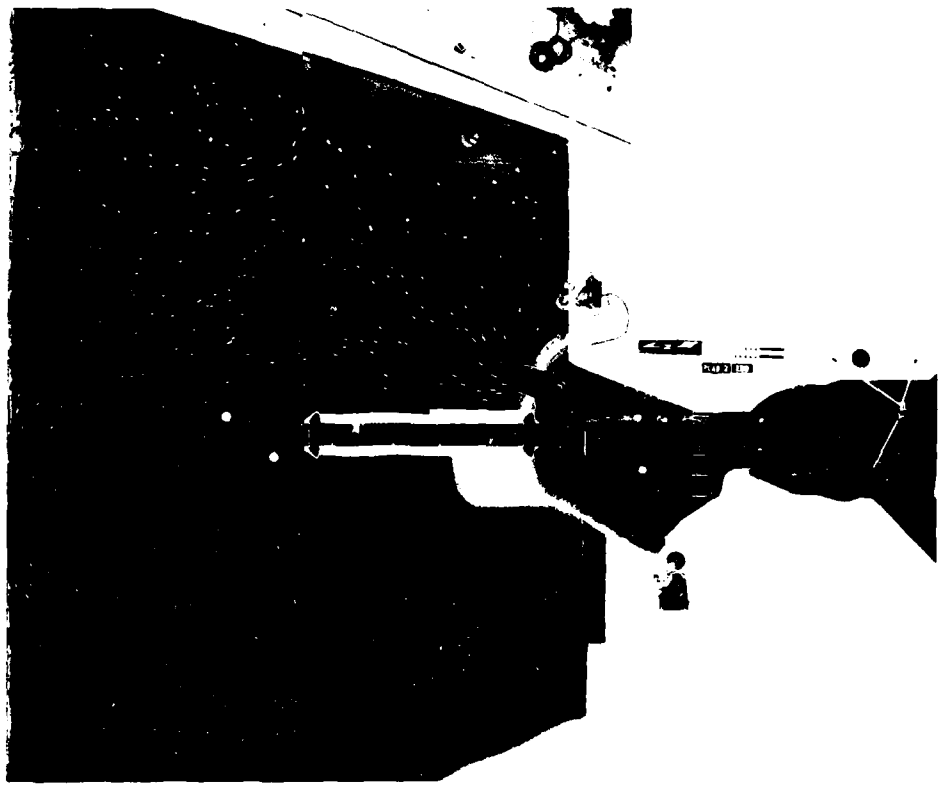

VELOCITY
SCALE

0 5 10 20

PLAN 2
EBB DISCHARGE = 5,000 CFS
EXPOSURE TIME = 3 SEC

PHOTO 9

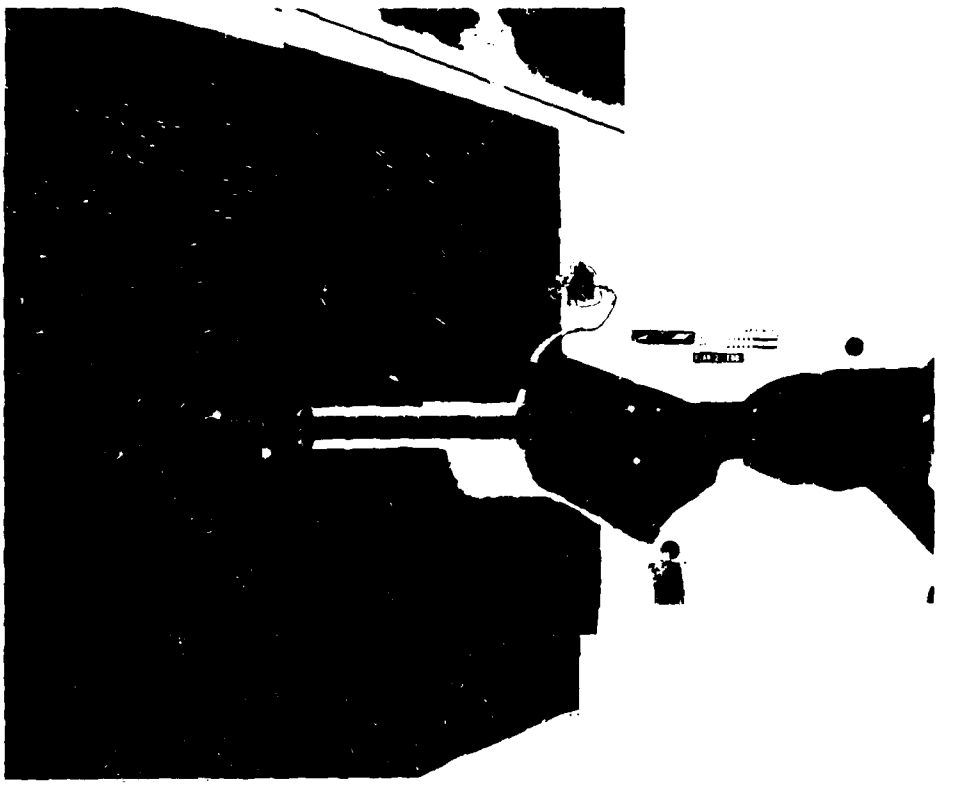

VELOCITY SCALE

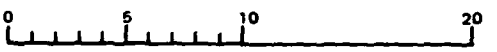

PLAN 2
EBB DISCHARGE = 5,000 CFS
EXPOSURE TIME = 9 SEC

PHOTO 10

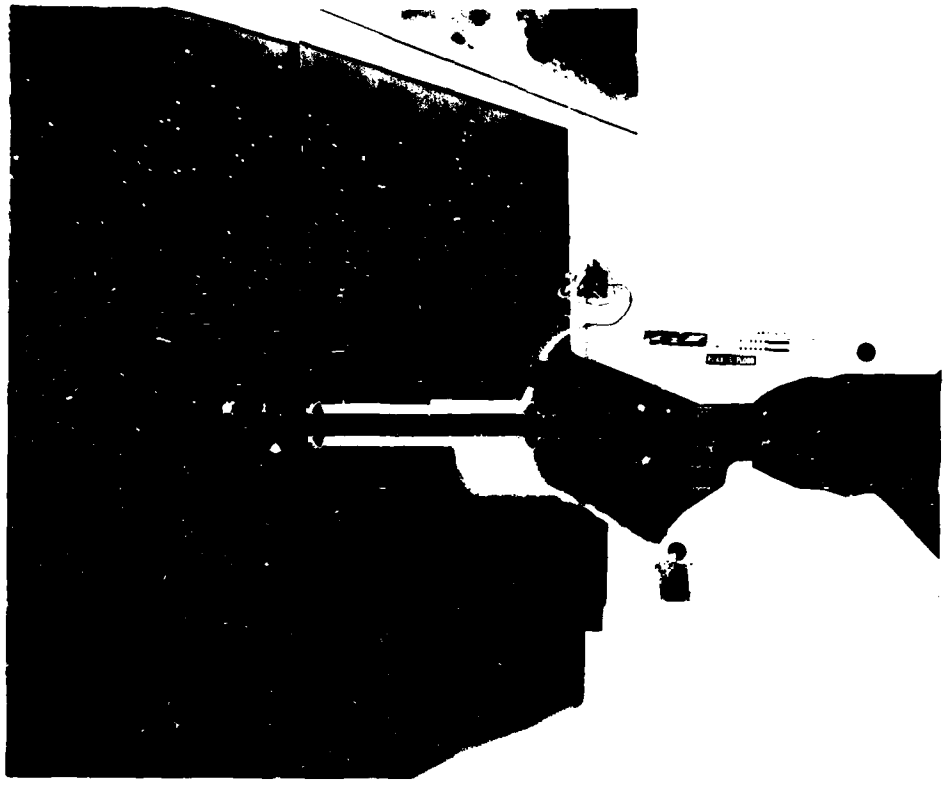

VELOCITY
SCALE

0 5 10 20

PLAN 3
FLOOD DISCHARGE = 5,000 CFS
EXPOSURE TIME = 3 SEC

PHOTO 11

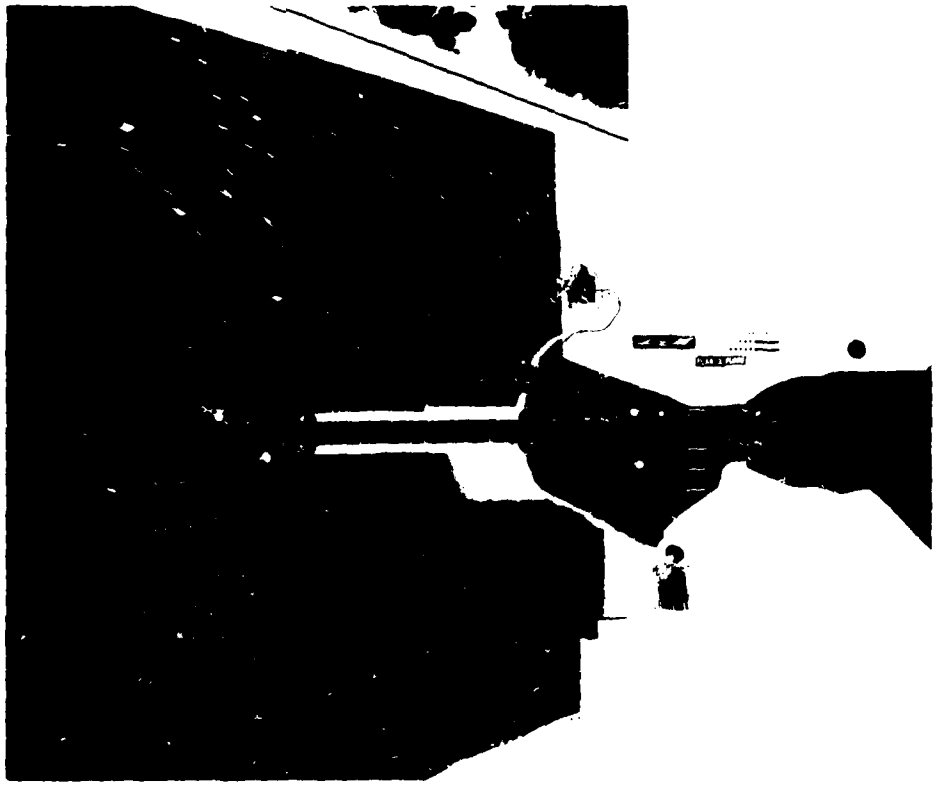

VELOCITY SCALE

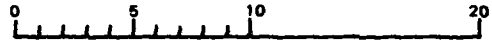

PLAN 3
FLOOD DISCHARGE = 5,000 CFS
EXPOSURE TIME = 9 SEC

PHOTO 12

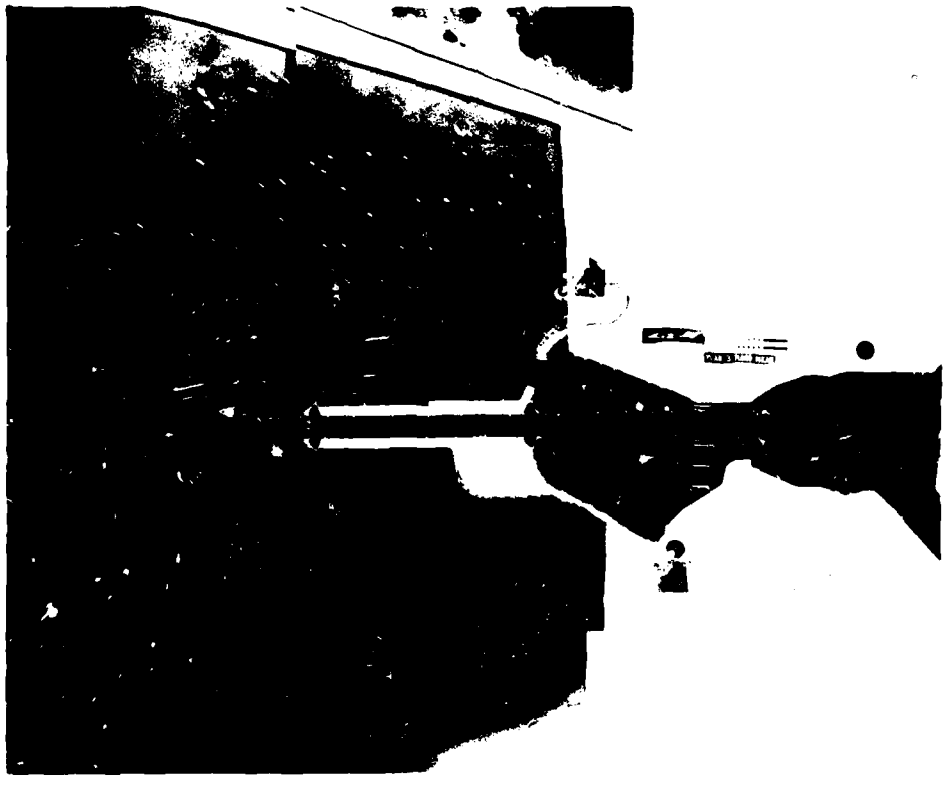

VELOCITY
SCALE

0 5 10 20

PLAN 3
FLOOD DISCHARGE = 10,000 CFS
EXPOSURE TIME = 3 SEC

PHOTO 13

VELOCITY SCALE

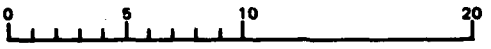

PLAN 3
FLOOD DISCHARGE = 10,000 CFS
EXPOSURE TIME = 9 SEC

PHOTO 14

VELOCITY
SCALE

0 5 10 20

PLAN 3
EBB DISCHARGE = 5,000 CFS
EXPOSURE TIME = 3 SEC

PHOTO 15

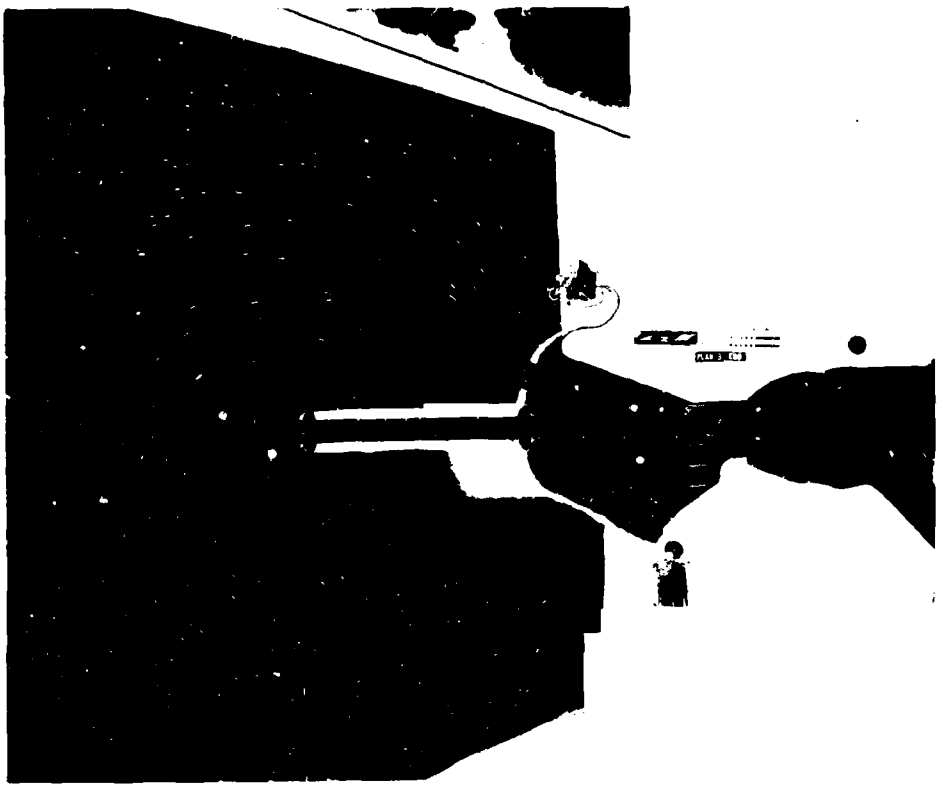

VELOCITY SCALE

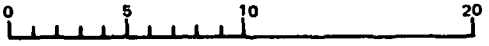

PLAN 3
EBB DISCHARGE = 5,000 CFS
EXPOSURE TIME = 9 SEC

PHOTO 16

VELOCITY
SCALE

0 5 10 20

PLAN
EBB DISCHARGE = 10,000 CFS
EXPOSURE TIME = 3 SEC

PHOTO 17

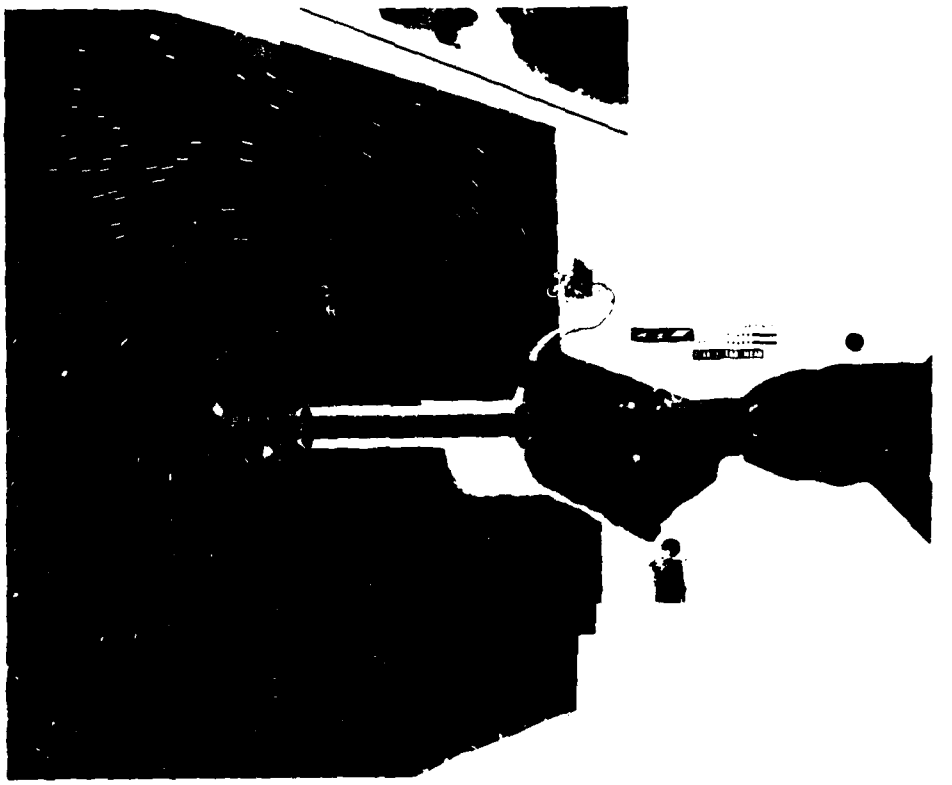

VELOCITY SCALE

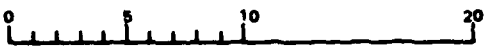

PLAN 3
EBB DISCHARGE = 10,000 CFS
EXPOSURE TIME = 9 SEC

PHOTO 18

VELOCITY
SCALE

0 5 10 20

PLAN 4
FLOOD DISCHARGE = 5,000 CFS
EXPOSURE TIME = 3 SEC

PHOTO 19

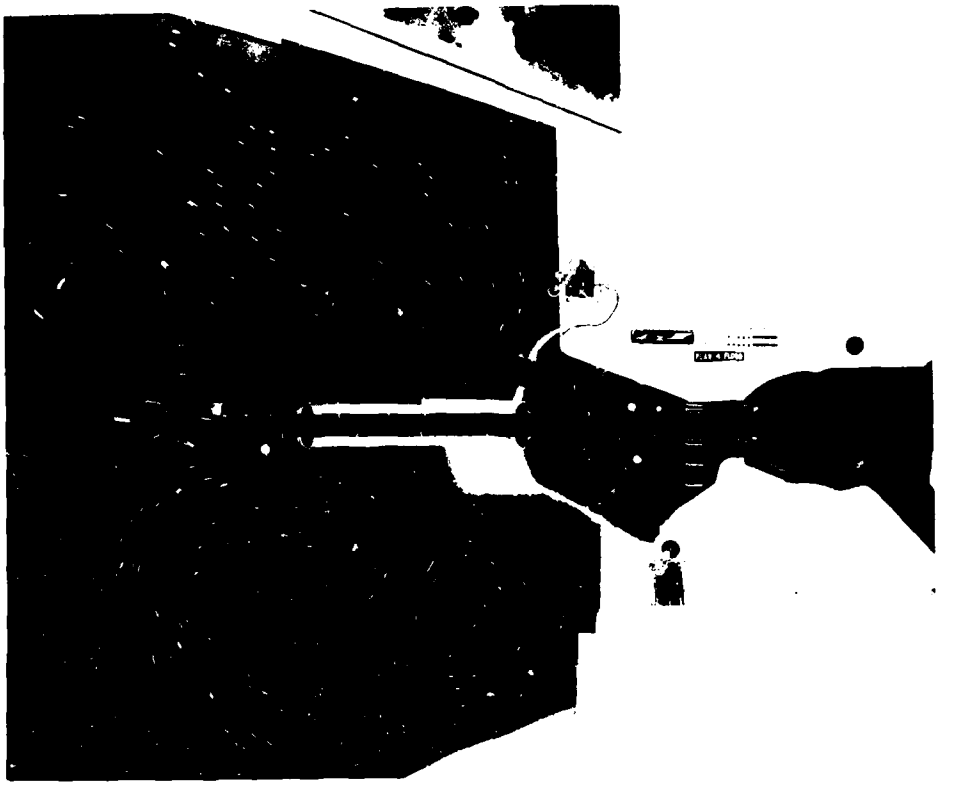

VELOCITY SCALE

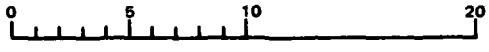

PLAN 4
FLOOD DISCHARGE = 5,000 CFS
EXPOSURE TIME = 9 SEC

PHOTO 20

VELOCITY
SCALE

0 5 10 20

PLAN 4
FLOOD DISCHARGE = 10,000 CFS
EXPOSURE TIME = 3 SEC

PHOTO 21

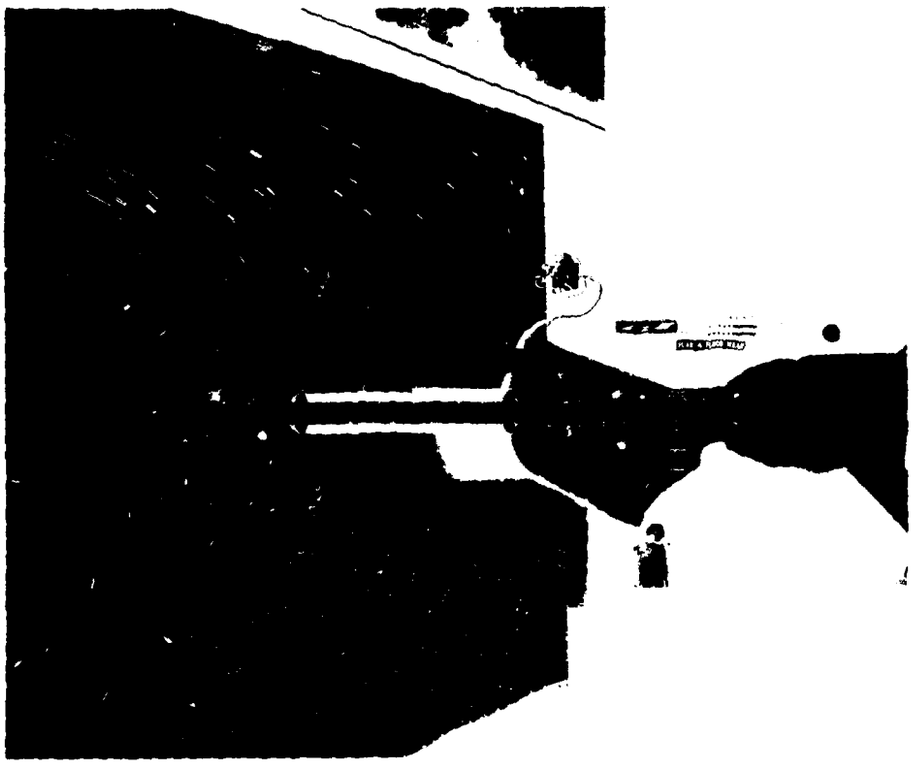

VELOCITY SCALE

0 5 10 20

PLAN 4
FLOOD DISCHARGE = 10,000 CFS
EXPOSURE TIME = 9 SEC

PHOTO 22

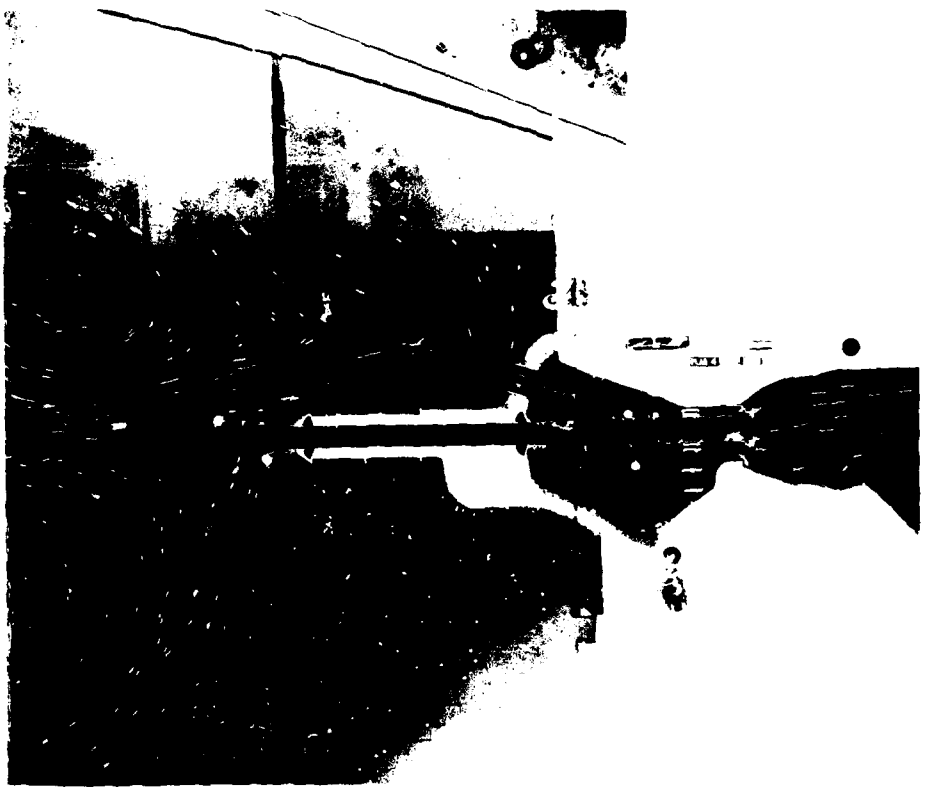

VELOCITY
SCALE

0 5 10 20

PLAN 4
FLOOD DISCHARGE = 15,000 CFS
EXPOSURE TIME = 3 SEC

PHOTO 23

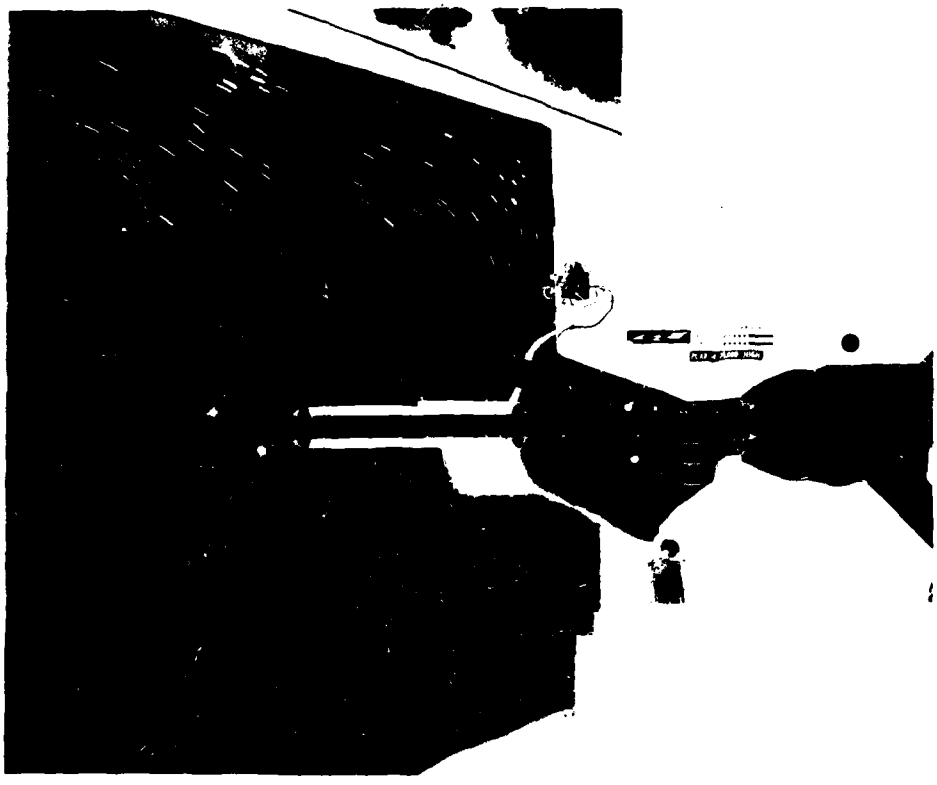

VELOCITY SCALE

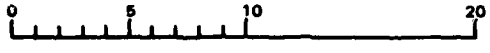

PLAN 4
FLOOD DISCHARGE = 15,000 CFS
EXPOSURE TIME = 9 SEC

PHOTO 24

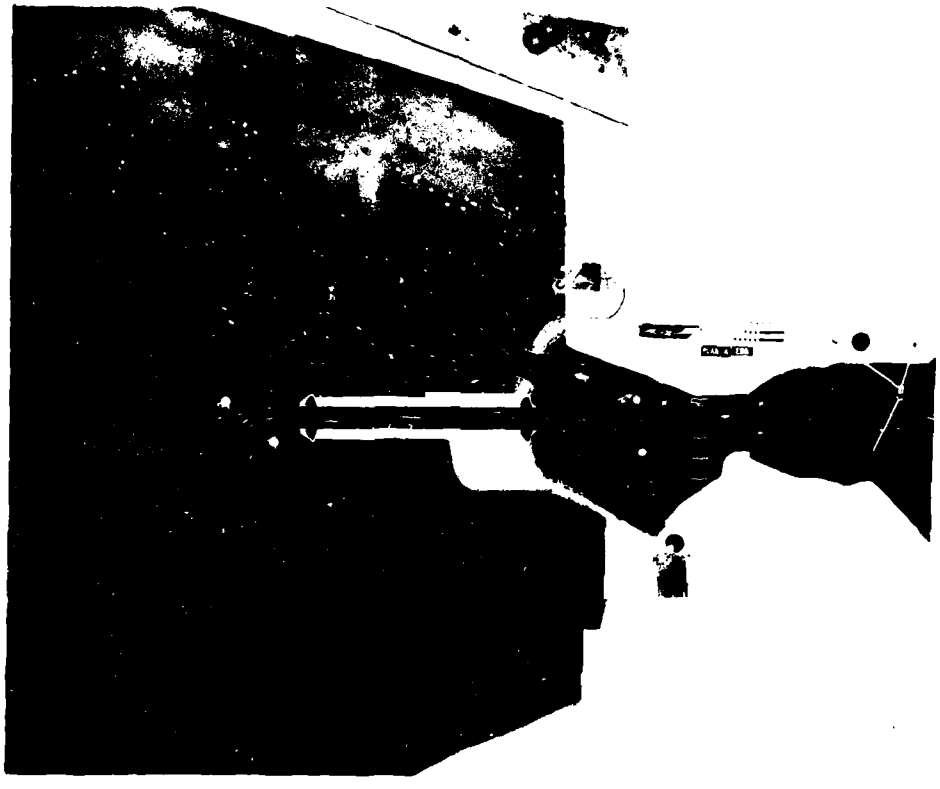

VELOCITY
SCALE

0 5 10 20

PLAN 4
EBB DISCHARGE = 5,000 CFS
EXPOSURE TIME = 3 SEC

PHOTO 25

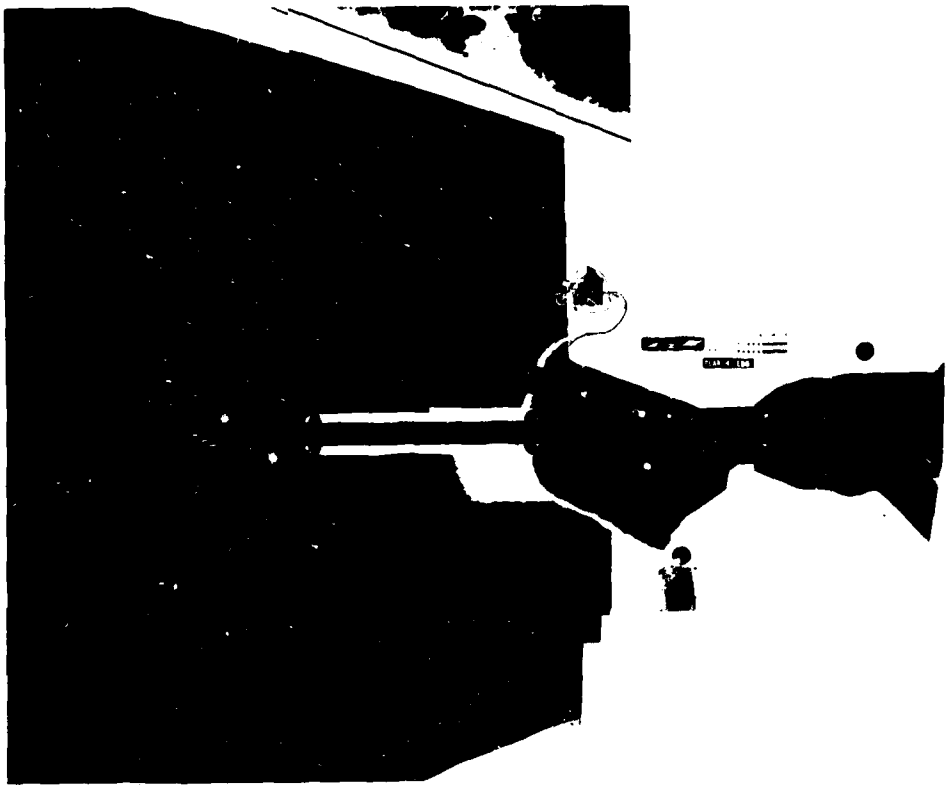

VELOCITY SCALE

0 5 10 20

PLAN 4
EBB DISCHARGE = 5,000 CFS
EXPOSURE TIME = 9 SEC

PHOTO 26

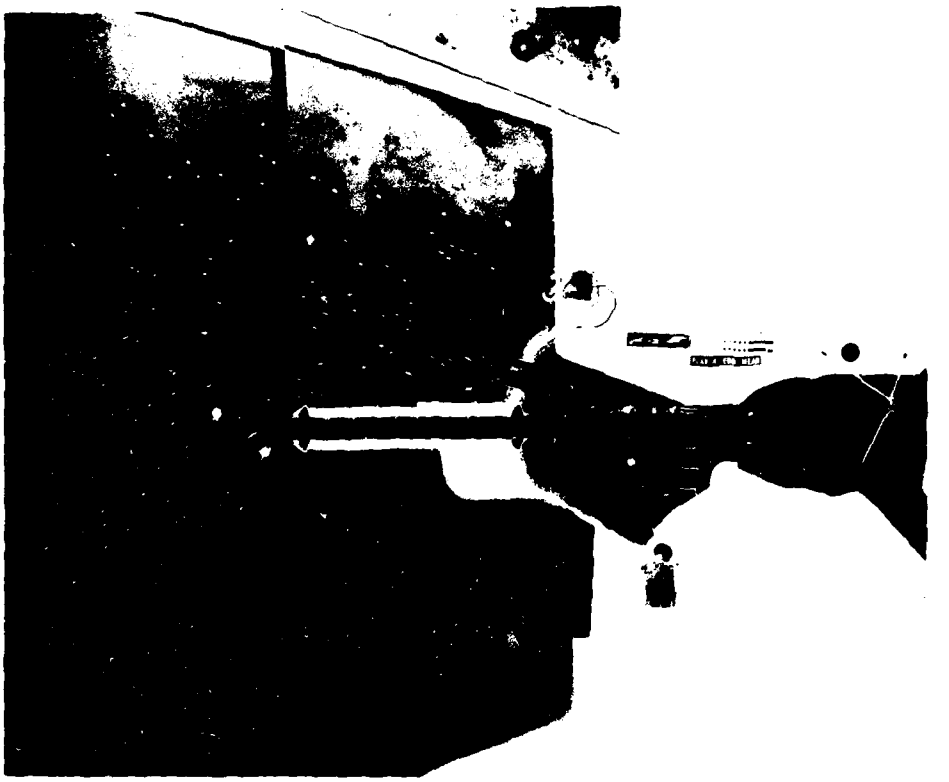

VELOCITY
SCALE

0 5 10 20

PLAN 4
EBB DISCHARGE = 10,000 CFS
EXPOSURE TIME = 3 SEC

PHOTO 27

VELOCITY SCALE

0 5 10 20

PLAN 4
EBB DISCHARGE = 10,000 CFS
EXPOSURE TIME = 9 SEC

PHOTO 28

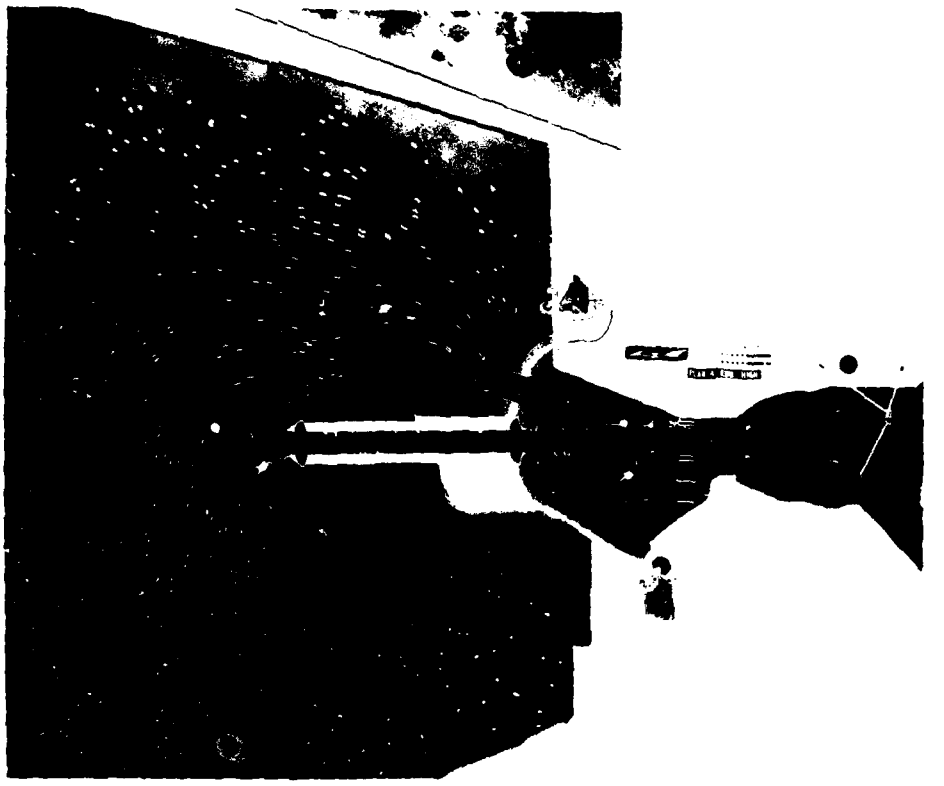

VELOCITY
SCALE

0 5 10 20

PLAN 4
EBB DISCHARGE = 15,000 CFS
EXPOSURE TIME = 3 SEC

PHOTO 29

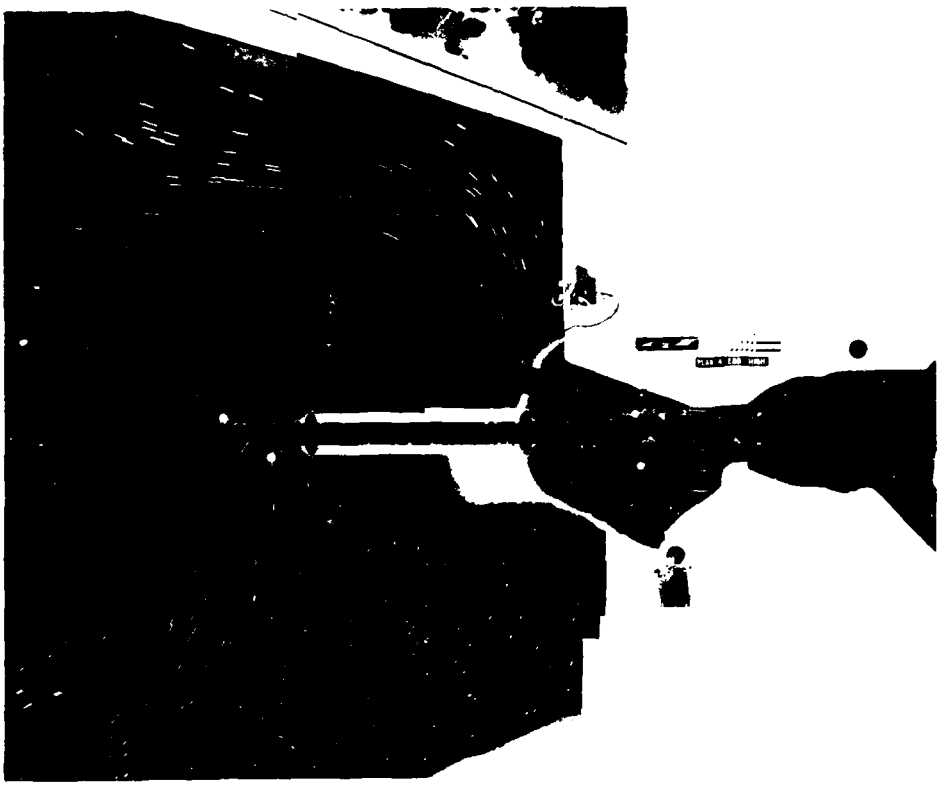

VELOCITY SCALE

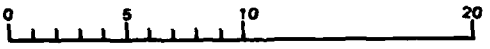

PLAN 4
EBB DISCHARGE = 15,000 CFS
EXPOSURE TIME = 9 SEC

PHOTO 30

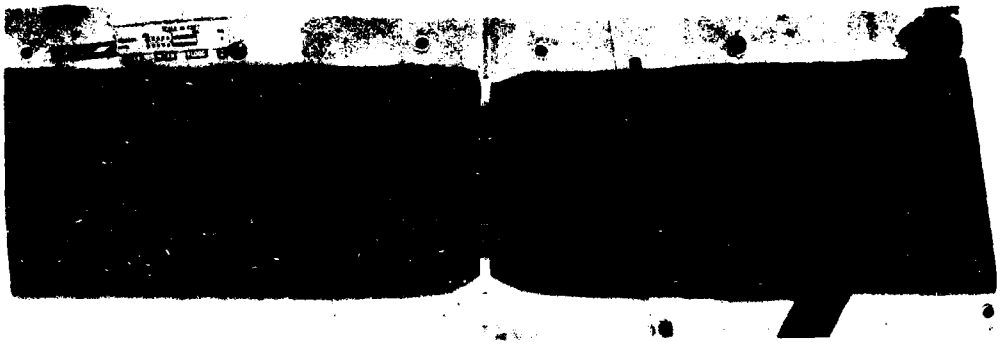

DISHARGE 75,000 CFS

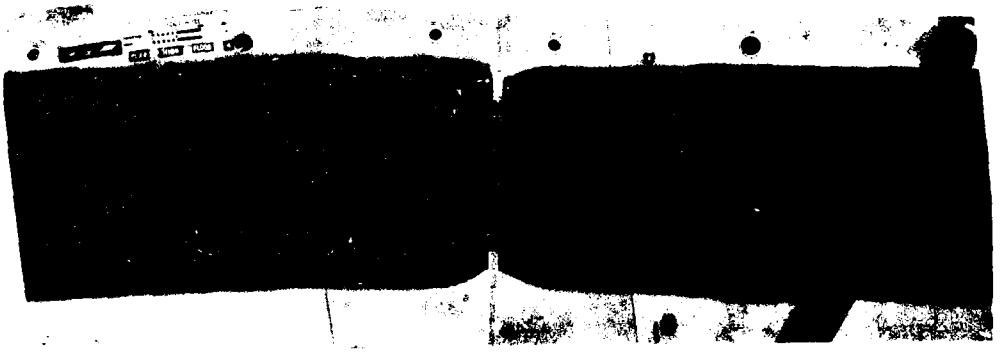

DISCHARGE 125,000 CFS

VELOCITY SCALE

5 0 5 10 15 FPS

SURFACE CURRENT PATTERNS

FLOOD FLOW

PHOTO 31

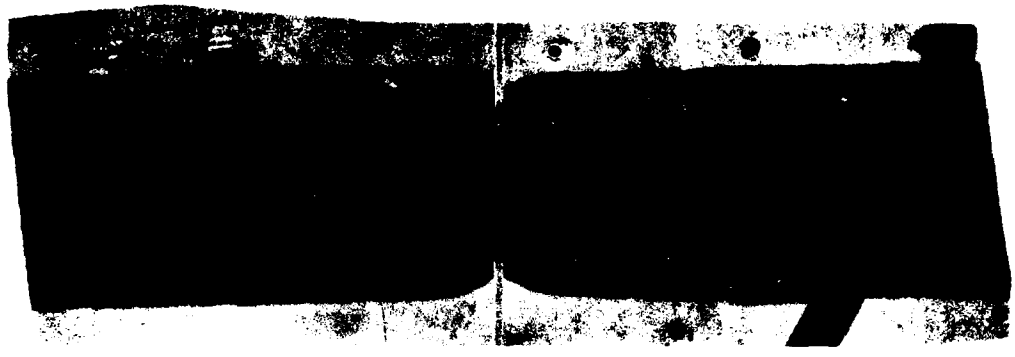

DISCHARGE 75,000 CFS

DISCHARGE 125,000 CFS

VELOCITY SCALE

5 0 5 10 15 FPS

SURFACE CURRENT PATTERNS
EBB FLOW

PHOTO 32

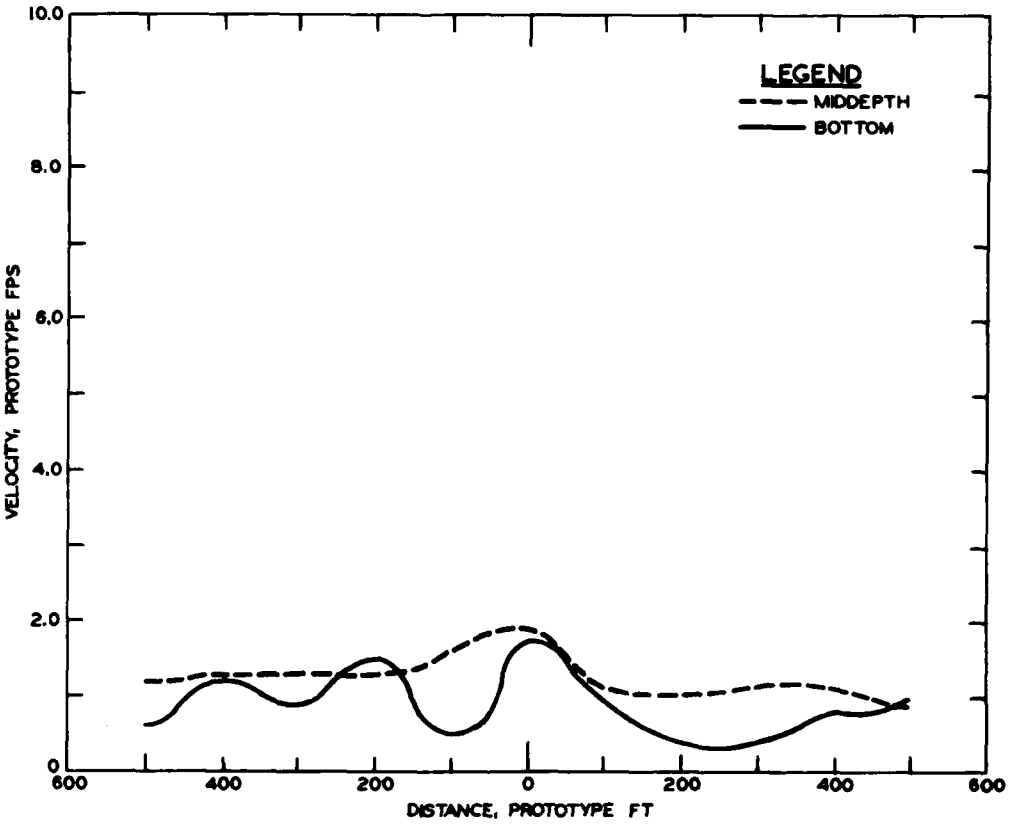

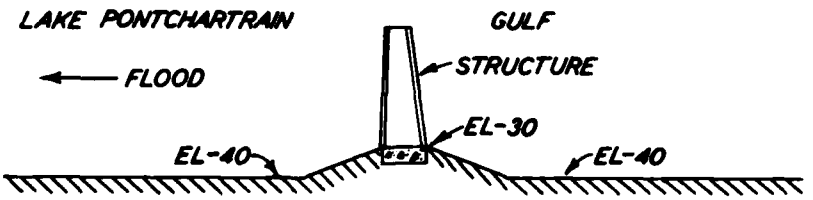

NOTE: ELEVATIONS ARE IN FEET REFERRED TO NGVD.

FLOOD FLOW 25,000 CFS

PLATE 1

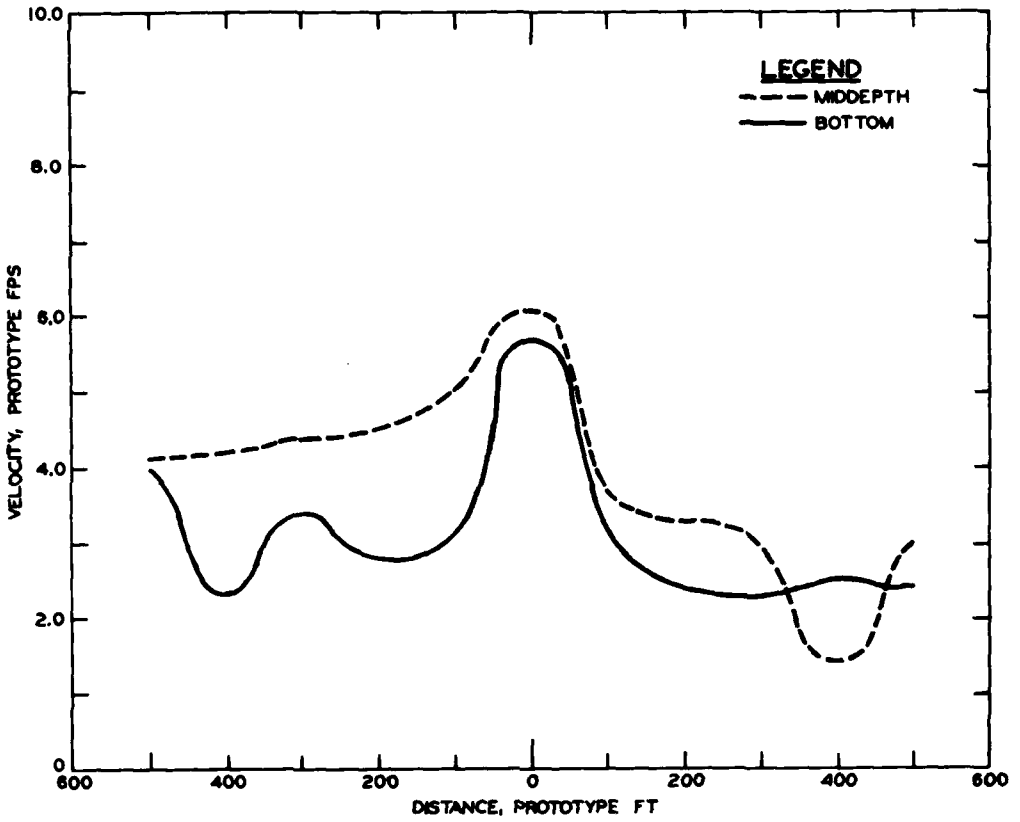

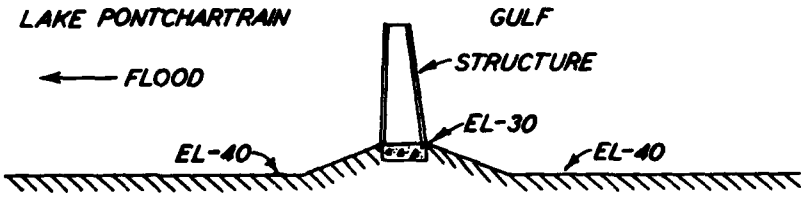

NOTE: ELEVATIONS ARE IN FEET REFERRED TO NGVD.

FLOOD FLOW 75,000 CFS

PLATE 2

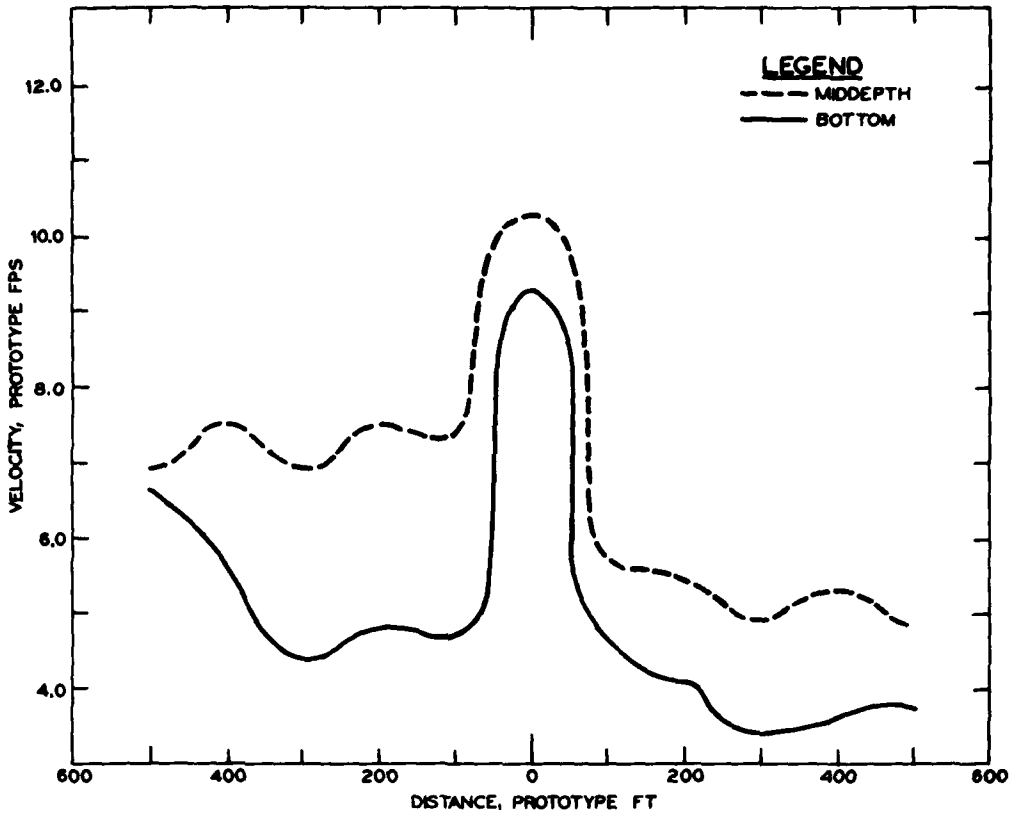

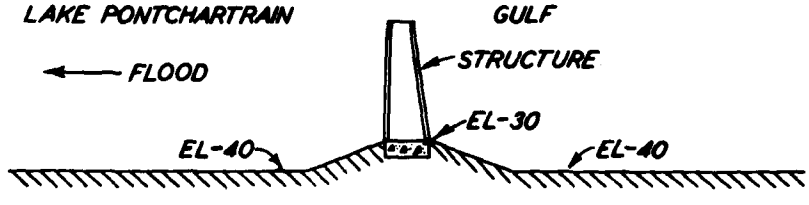

NOTE: ELEVATIONS ARE IN FEET REFERRED TO NGVD.

FLOOD FLOW 125,000 CFS

PLATE 3

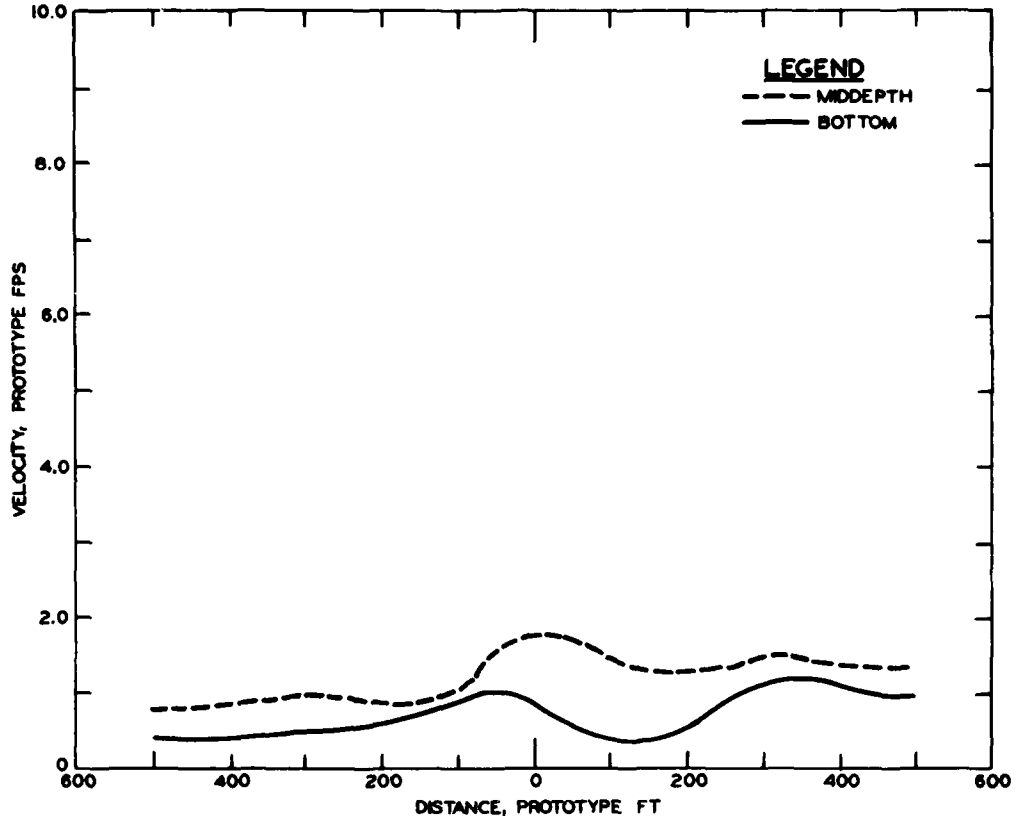

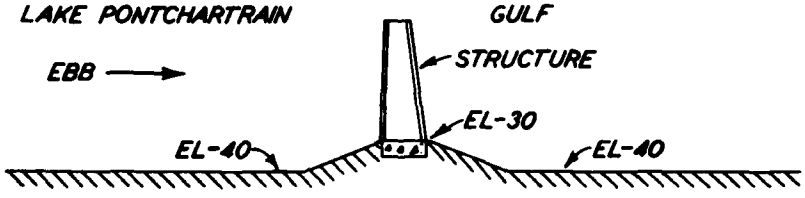

NOTE: ELEVATIONS ARE IN FEET REFERRED TO NGVD.

EBB FLOW 25,000 CFS

PLATE 4

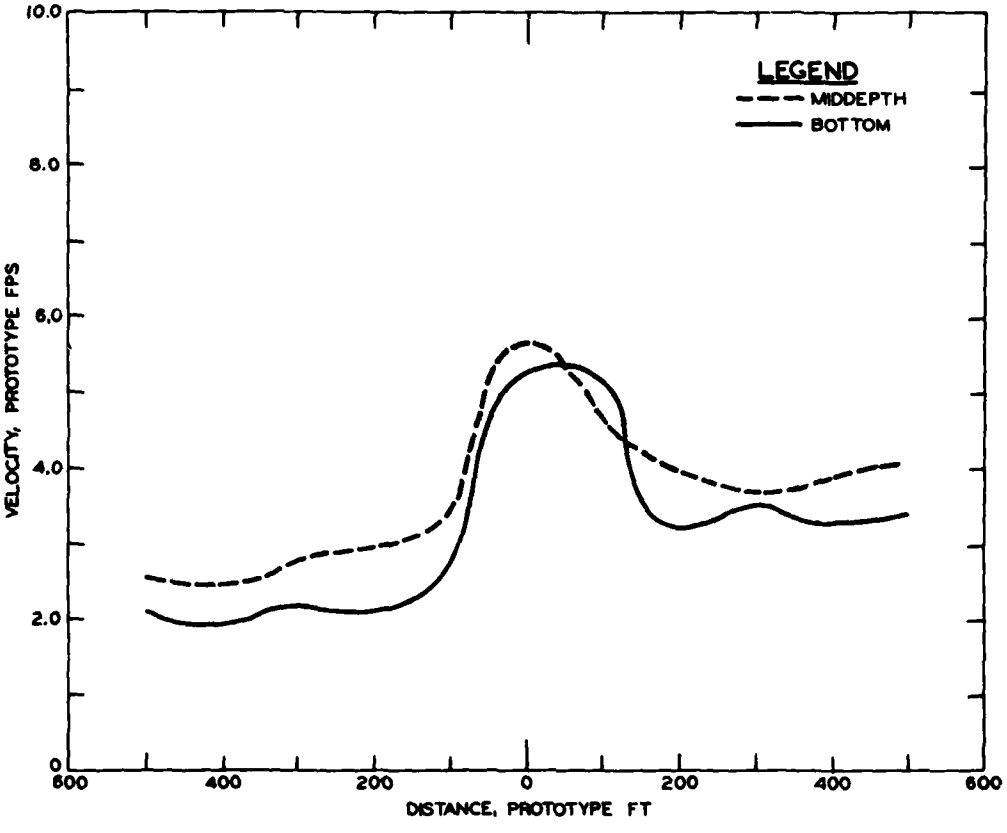

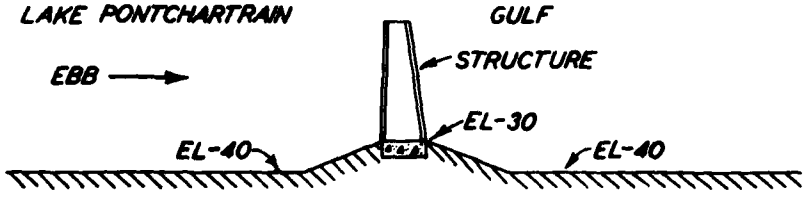

NOTE: ELEVATIONS ARE IN FEET REFERRED TO NGVD.

EBB FLOW 75,000 CFS

PLATE 5

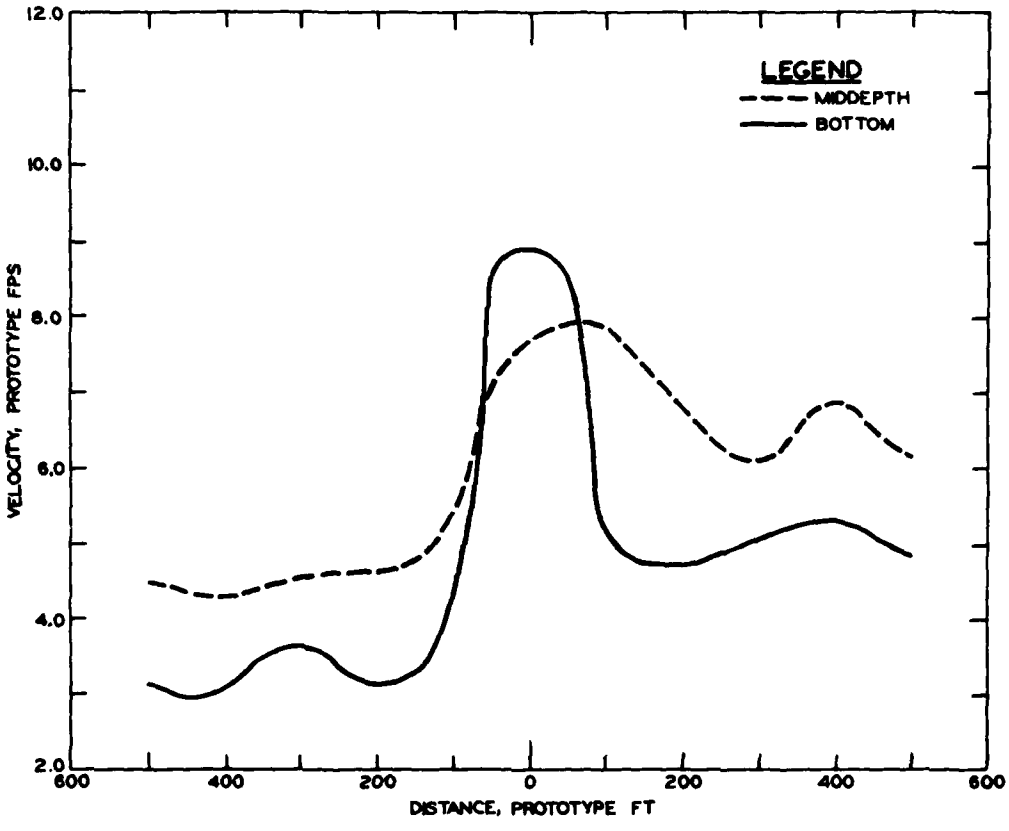

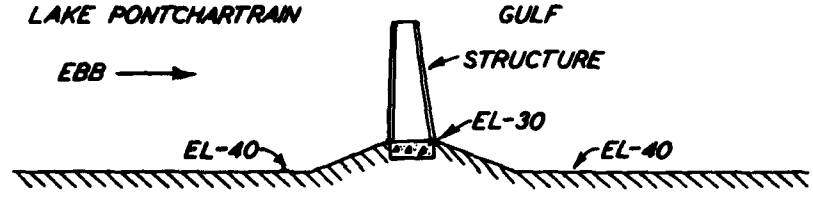

NOTE: ELEVATIONS ARE IN FEET REFERRED TO NGVD.

EBB FLOW 125,000 CFS

PLATE 6

In accordance with letter from DAEN-RDC, DAEN-ASI dated 22 July 1977, Subject: Facsimile Catalog Cards for Laboratory Technical Publications, a facsimile catalog card in Library of Congress MARC format is reproduced below.

Lake Pontchartrain and vicinity hurricane protection plan : Report 2 : Physical and numerical model investigation of control structures and the Seabrook Lock : Hydraulic and Mathematical Model Investigation / by H. Lee Butler ... [et al.] (Hydraulics Laboratory, U.S. Army Engineer Waterways Experiment Station). -- Vicksburg, Miss. : The Station ; Springfield, Va. : available from NTIS, 1982.
176 p. in various pagings, 6 p. of plates ; ill. ; 27 cm. -- (Technical report ; HL-82-2, Report 2)
Cover title.
"June 1982."
"Prepared for U.S. Army Engineer District, New Orleans.
Bibliography: p. 104.

1. Difference equations. 2. Hurricane protection. 3. Hydraulic models. 4. Mathematical models. 5. Pontchartrain, Lake (La.) I. Butler, H. Lee. II. United States. Army. Corps of Engineers. New

Lake Pontchartrain and vicinity hurricane : ... 1982. (Card 2)

Orleans District. III. U.S. Army Engineer Waterways Experiment Station. Hydraulics Laboratory. III. Series: Technical report (U.S. Army Engineer Waterways Experiment Station) ; HL-82-2, Report 2.
TA7.W34 no.HL-82-2 Report 2

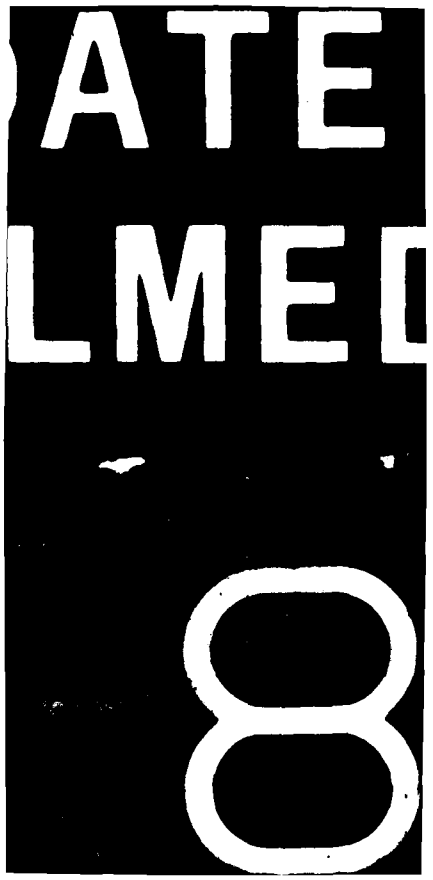
ATE
LMED
8